REVIEW ON EXISTING DATA ON UNDERWATER SOUNDS PRODUCED BY THE OIL AND GAS INDUSTRY

A report prepared by Seiche Ltd
for the Joint Industry Programme (JIP)
on E&P Sound and Marine Life

JIP Topic - Sound source characterisation and propagation

E&P **SOUND**
& MARINE LIFE
PROGRAMME

September 2020

About the E&P Sound & Marine Life Programme

The ocean is filled with a wide variety of natural and anthropogenic sounds. Since the early 1990s, there has been increasing environmental and regulatory focus on anthropogenic sounds in the sea and on the effects these sounds may have on marine life. There are now many national and international regimes that regulate how we introduce sound to the marine environment. We believe that effective policies and regulations should be firmly rooted in sound independent science. This allows regulators to make consistent and reasonable regulations while also allowing industries that use or introduce sound to develop effective mitigation strategies.

In 2005, a broad group of international oil and gas companies and the International Association of Geophysical Contractors (IAGC) committed to form a Joint Industry Programme under the auspices of the International Association of Oil and Gas Producers (IOGP) to identify and conduct a research programme that improves understanding of the potential impact of exploration and production sound on marine life. The Objectives of the programme were (and remain):

1. To support planning of exploration and production (E&P) operations and risk assessments
2. To provide the basis for appropriate operational measures that are protective of marine life
3. To inform policy and regulation.

The members of the JIP are committed to ensuring that wherever possible the results of the studies it commissions are submitted for scrutiny through publication in peer-reviewed journals. The research papers are drawn from data and information in the contract research report series. Both contract reports and research paper abstracts (and in many cases full papers) are available from the Programme's web site at www.soundandmarinelife.org.

Seiche Ltd
Bradworthy Industrial Estate
Langdon Road, Bradworthy
Holsworthy, Devon EX22 7SF
United Kingdom
Tel: +44 (0) 1409 404050
Email: info@seiche.com
Web: www.seiche.com

Seiche Measurements LLC
10355 Centre park Dr
Suite 240
Houston TX77043
United States of America
Tel: +1 713 201 5726
Email: info@seiche.com
Web: www.seiche.com

Review on Existing Data on Underwater Sounds Produced by the Oil and Gas Industry

Guillermo Jiménez-Arranz, Nikhil Banda, Stephen Cook and Roy Wyatt

June 2020

Prepared by:
Seiche Ltd.

Submitted to:
E&P Sound & Marine Life (JIP)

Document Control

Project Reference	P783		
Client	E & P Sound & Marine Life, Joint Industry Programme	Client Reference	
		Revision	Date
Prime Author(s)	Guillermo Jiménez-Arranz	5.1	15 June 2020
Reviewed by	Nikhil Banda, Stephen Cook		
Authorised for release	Mark Burnett		

Disclaimer

Copyright Notice

Executive Summary

The soundscape in the oceans results from the combination of natural, biological and anthropogenic acoustic sources. Sounds generated by human activity include shipping, seismic exploration, active sonar, offshore drilling, pile driving and dredging. A significant proportion of that noise is generated during the exploration, development, production and decommissioning phases in the oil and gas industry.

The purpose of this report is to provide an updated catalogue of measurements from intentional or unintentional sounds introduced in the sea by activities carried out by the oil and gas industry. This report is conceived as a support tool for the assessment of the impact in the marine environment of industrial acoustic sources. Each relevant sound source has a dedicated chapter, which includes general information about its characteristics, operation and acoustic behaviour, followed by a table that compiles sound levels and additional information from measurements published in the literature. This report reviews and incorporates the findings of a previous JIP report written by Wyatt (2008). Some of the acoustic sources covered in the report are air gun arrays, marine vibrator, acoustic deterrent devices, sonar, vessels, dredging, drilling, production, decommissioning and aircrafts.

Few measurements have been made on underwater noise sources and those available are often limited in their scope. Measurements from different projects can be difficult to compare due to the dynamic conditions of the ocean, the lack of a standard method for measuring, processing and analysing the sound, and often an incomplete description of that method and the acoustic properties of the environment at the time the measurements were made.

Since sound level measurements can be taken at any range, a common way of normalising these levels for comparison is to estimate the source level, or sound level at 1 m from the source. Local geographic, geological, oceanographic and meteorological conditions have a very substantial impact on the way sound propagates in the sea; these conditions should be considered to make a good estimate of the source level. Analytical and numerical sound propagation models can incorporate this information, but frequently source levels are estimated from simple experimental curves, fitted to the measured data. The latter approach tends to overestimate source levels, and these values should be used as a guideline only. For a correct interpretation and comparison of results, as much information as possible should be provided about the environment and the measuring, processing and analysis approach. This report considers only literature with a detailed description of measuring procedures, data processing and metrics; secondary sources and grey literature have not been included, except when information is scarce.

The information in this report has been extracted from journal articles, technical reports, disclosed military reports, product specifications, and books.

Symbols and Acronyms

$ADCP$	Acoustic Doppler Current Profiler
ADD	Acoustic Deterrent Device
AHD	Acoustic Harassment Device
$ACCOBAMS$	Agreement on the Conservation of Cetaceans of the Black Sea, Mediterranean Sea and Contiguous Atlantic Area
$ASCOBANS$	Agreement on the Conservation of Small Cetaceans of the Baltic and North Seas
AF	Attenuation Factor [dB/km]
$avg, \bar{}$	Average (subscript, accent)
α	Constant (= 0.55)
@	"At", used to indicate measured distance of a source level (e.g. 180 dB re 1µPa@50m)
BLD	Bucket Ladder Dredge
BHD	Back Hoe Dredge
BW	Band Width
B	Number of propeller blades
BC	Bulk Carrier
BW_{-6dB}, BW_{-10dB}	Bandwidth calculated at 6 or 10 dB below maximum spectral value [Hz]
CBB	Concrete Basic Brick
CC	Cabin Cruiser
CDU	Concrete Drilling Unit
$CIDS$	Concrete Island Drilling System
CPA	Closest Point of Approach
CR	Cruise Ship
CRI	Caisson Retained Island
CS	Container Ship
CSD	Cutter Suction Dredge
CT	Chemical Tanker
CTD	Conductivity, Temperature, Depth
c	Speed of sound in water (≈1500 m/s) [m/s]; explosive charge subscript
DC	Duty Cycle [%], Direct Current (0 Hz)
DT	Displacement Ton
DWT	Deadweight Tonnage
E	Sound exposure magnitude subscript

$Eq.$	Equation
FFT	Fast Fourier Transform
$Fig.$	Figure
FPS	Floating Production System
$FPSO$	Floating, Production, Storage and Offloading
FR	Frequency Range
FR_{-6dB}, FR_{-10dB}	Frequency range at 6 or 10 dB below maximum spectral value [Hz]
FSO	Floating, Storage and Offloading
FSU	Floating Storage Unit
FT	Fishing Trawler
f	Frequency, operating frequency [Hz]
f_b	Fundamental frequency of propeller blade [Hz]
f_e	Fundamental frequency of piston engine [Hz]
GD	Grab Dredge (a.k.a. bucket dredge or clamshell dredge)
GRT	Gross Register Tonnage
GT	Gross Tonnage
g	Acceleration of gravity (≈ 9.81 m/s^2) [m/s^2]; air gun subscript
$HELCOM$	Helsinki Commission
h_w	Depth of water column [m]
IB	Ice Breaker
IDU	Integrated Drilling Unit
k	Constant
LC	Landing Craft
LBL	Long Base Line
LNG	Liquified Natural Gas
LPG	Liquified Petroleum Gas
L_E	Sound exposure level [dB re 1 µPa^2·s or dB$_E$]
$L_{p(,rms)}$	Root-mean-square sound pressure level [dB re 1 µPa$_{(rms)}$ or dB$_{(rms)}$]
$L_{p,pk}$	Peak sound pressure level [dB re 1 µPa$_{pk}$ or dB$_{pk}$]
$L_{p,pk-pk}$	Peak-to-peak sound pressure level [dB re 1 µPa$_{pk\text{-}pk}$ or dB$_{pk\text{-}pk}$]
$L_{E,f}$	Sound exposure spectral density level [dB re 1 µPa^2·s/Hz]
$L_{p,f}$	Mean-square sound pressure spectral density level [dB re 1 µPa^2/Hz]
λ	Wavelength [m]
$MBES$	Multi-Beam Echo Sounder
$MSDF$	Marine Strategy Framework Directive
M	Number of revolutions per cylinder and firing in the piston engine
m_c	Mass of explosive charge [kg]

max	Maximum subscript
N	Number of cylinders in the piston engine
n	Positive integer (1,2,3…)
OH	Open Hatch
OT	Oil Tanker
$OSPAR$	Oslo/Paris Convention for the Protection of the Marine Environment of the North-East Atlantic
oct	Octave
$PIES$	Pressure Inverted Echo Sounder
PT	Product Tanker
$p_{(rms)}$	Root-mean-square sound pressure [$Pa_{(rms)}$]
p_{pk}	Peak sound pressure [Pa_{pk}]
p_{pk-pk}	Peak-to-peak sound pressure [Pa_{pk}]
$p_{pk,unconf}$	Shock wave peak sound pressure in unconfined explosive charges [Pa]
$p_{pk,conf}$	Shock wave peak sound pressure in confined explosive charges [Pa]
P_{atm}	Atmospheric pressure (≈101,325 Pa) [Pa]
P_g	Air gun chamber pressure [psi]
P_w	Hydrostatic pressure [Pa]
pk	Peak magnitude subscript
RMS	Root-mean-square
$RO-RO$	Roll-On, Roll-Off
Rx	Reception, receiver
r	Range [m]
r_0	Maximum range of applicability of shock wave theory for unconfined charges [m]
RL	Received Level [$dB_{(rms)}$, dB_{pk}, dB_E]
r_{max}	Maximum range [m]
rpm	Turning rate of the piston engine [rpm]
ρ_w	Density of water (≈1025 kg/m^3) [kg/m^3]
rms	Root-mean square magnitude subscript
$SBES$	Single-Beam Echo Sounder
SBL	Short Base Line
SBP	Sub-Bottom Profiler
SEL	Sound exposure level
SL	Source Level [$dB_{(rms)}$, dB_{pk}, dB_E]
SLF	Spreading Loss Factor
SMB	Steel Mud Base
$SOFAR$	Sound Fixing and Ranging

SPL	Sound Pressure Level
SPT	Standard Penetration Testing
$SSDC$	Single-Steel Drilling Caisson
$SSDG$	Ship's Service Diesel Generator
SSS	Side-Scan Sonar
ST	Super Tanker
seq	Sequence subscript (for acoustic deterrents)
$Tab.$	Table
TEU	Twenty-foot Equivalent Unit
$TSHD$	Trailing Suction Hopper Dredge
T	Repetition period [s]
T_0	Reference temperature (= 273.15 K) [K]
T_b	Bubble period
TL	Transmission Loss [dB]
T_w	Water temperature [K]
Tx	Transmission, transmitter
τ	Pulse duration [s]
τ_c	Time constant for the pressure decay of an unconfined explosive charge [µs]
typ	Typical
$ULCC$	Ultra Large Crude Carrier
$USBL$	Ultra-Short Base Line
u_c	Critical velocity of water jet from a water gun [m/s]
VC	Vehicle Carrier
$VLCC$	Very Large Crude Carrier
V_g	Air or water gun chamber volume [in^3]
$V_{g,tot}$	Total volume of the air gun array [in^3]
w	Water subscript
WI	Waveform Integration
z	Depth below water surface [m]
z_c	Depth of explosive charge below water surface [m]
z_g	Air gun depth below water surface [m]
z_{max}	Maximum depth below water surface [m]
z_r	Receiver depth below water surface [m]
z_s	Source depth below water surface [m]

Units

atm	Atmosphere (= 101325 Pa)
bps	Bits per second
°C	Celsius
dB	Decibel
ft	Foot (= 0.3048 m)
G	Giga (10^9)
Hz	Hertz
hp	Horsepower (= 745.7 W)
in	Inch (= 0.0254 m)
J	Joule [$\mathrm{kg\ m^2\ s^{-2}}$]
K	Kelvin
k	Kilo (10^3)
kg	Kilogram
kn	Knot (= 0.514 m/s)
M	Mega (10^6)
m	Metre, Milli (10^{-3})
µ	Micro (10^{-6})
Pa	Pascal [$\mathrm{kg\ m^{-1}\ s^{-2}}$]
ppt	Parts per thousand
psi	Pound per square inch (= 6894.76 Pa)
rpm	Revolutions per minute
s	Second
TEU	Twenty-foot equivalent unit (6.1 m container length)
t	Tonne or metric ton (= 10^3 kg)
V	Volt
W	Watt [$\mathrm{kg\ m^2\ s^{-3}}$]

Terminology

Air Gun Array: combination of air gun sub-arrays.

Air Gun String: set of aligned air guns or air-gun clusters.

Air Gun Subarray: group of air gun strings.

Attenuation Factor: level of attenuation with range. The attenuation factor depends on the reflection coefficient of the seabed, scattering of the sea surface and absorption of sea water. This factor dominates in shallow waters and at long distances from the source.

Bandwidth: difference between the upper and lower frequency of a frequency band.

Cavitation: phenomenon consisting in the formation of vapor cavities in a liquid as a result of a fast change in pressure. The cavitation can generate considerable noise due to the collapse of the bubbles formed. The propeller in a vessel is a common source of cavitation.

Continuous Sound: acoustic signal of long or undetermined duration.

Cumulative Energy Curve: representation of the accumulated energy of a sound event with time. This curve is typically used for the calculation of the *RMS sound pressure* or the *sound exposure* of a transitory signal.

Decibel: unit equal to ten times the logarithm of a power ratio. The decibel is used to quantify variables characterised by a large dynamic range, such as the acoustic pressure. The decibel can be used to express an absolute quantity by using a reference value. Quantities express in decibels are referred to as *levels*. The factor that accompanies the logarithm is 10 for acoustic power and intensity, and 10 for acoustic pressure. The decibel is denoted by the letters dB.

Deghosting: signal processing technique consisting in removing the *ghost* or surface reflection from a measured air gun pulse. The ghost produces a comb-filter effect in the frequency spectrum of the pulse, and by eliminating it a better resolution and quality image of the seabed stratigraphy can be obtained.

Density: mass per unit volume. Its unit is kilograms per cubic metre (kg/m^3). The density of sea water is a function of temperature, salinity and hydrostatic pressure, and has a value of 1022 kg/m^3 for 25 °C, 33 ppt and 1 atm.

Directivity: directional signature of a sound source. A source is more *directive* when its directivity pattern diverts from a perfect sphere or *omnidirectional pattern*. At wavelengths that are comparable to or lower than the dimensions of a source, the directional behaviour is more pronounced.

Far Field: region of the sound field in which the sound waves originated in different parts of the source arrive practically in phase. In this region, the irregular wavefront at the source becomes virtually spherical, resulting in a sound pressure attenuation proportional to range. The far field occurs at an approximate range of L^2/λ, with L the largest dimension of the source.

Frequency: number of cycles of a periodic or harmonic wave per unit time. Reciprocal of the *period*. Denoted by letter *f*. Its unit is the Hertz (Hz).

Frequency Band: region of the frequency spectrum delimited by a lower and upper frequency. The frequency spectrum is divided into frequency bands, which can be *constant*, as is the case in a narrowband spectrum calculated with the DFT (see PSD), or with a *bandwidth* proportional to the band's central frequency. Octave and third-octave band spectra a examples of the latter. In an octave band spectrum, consecutive central frequencies are spaced by a factor of 2, and in a third-octave band spectrum, by a factor of $2^{1/3}$.

Frequency Spectrum: distribution of amplitudes and phases of a time signal in the frequency domain. The conversion between the time and frequency domains is achieved with the Fourier Transform. The complex frequency spectrum of a discrete time signal is calculated with the Discrete Fourier Transform (DFT).

Ghost: sound pressure wave reflected in the sea surface. The ghost is characterised by being a inverted-phase version of the direct, incident sound. In rough seas and at high frequencies part of the incident energy is scattered in multiple directions, reducing the amplitude of the ghost.

Harmonics: integer multiples of a fundamental frequency.

Impulsive Sound: transitory sound characterised by high pressure and short rise time.

Lloyd Mirror: acoustic phenomenon produced by the combination of the direct sound wave and the sea surface reflection or *ghost*. The Lloyd mirror is characterised by a pattern of constructive and destructive interferences, followed by a rapid decay of sound pressure with distance.

Near Field: region of the sound field in which different vibrating parts of the source behave as individual emitters. In this region, the difference in the travelled distance of the sound waves generated by each of these emitters is comparable to or higher than the wavelength, which results in a pressure pattern of constructive and destructive interferences. In the near field, the wavefront is irregular (non-spherical).

Pulse Length: effective duration of a transitory signal or pulsed sound event. The pulse length is generally calculated as the time between the 5 % and 95 % energy on the cumulative energy curve of the event.

Peak Pressure: also referred to as zero-to-peak pressure, is the maximum absolute value of the pressure waveform. This metric is preferred for impulsive sounds. The unit of the peak acoustic pressure is the pascal (Pa) peak. The metric descriptor (i.e. peak) should always accompany the units for this metric. The peak acoustic pressure is calculated as follows:

$$p_{0-p} = \max\{|p(t)|\}$$

Peak-to-Peak Pressure: difference between the maximum and minimum values of the pressure waveform. Along with the peak pressure, this metric is preferred for impulsive sounds. The unit of the peak-to-peak acoustic pressure is the pascal (Pa) peak-to-peak. The metric descriptor (i.e. peak-to-peak) should always accompany the units for this metric. The peak-to-peak acoustic pressure is calculated as follows:

$$p_{p-p} = \max\{p(t)\} - \min\{p(t)\}$$

Peak Sound Pressure Level: decibel representation of the peak acoustic pressure. The peak sound pressure level uses a logarithmic factor of 20 and a reference value of 1 µPa.

$$SPL_{0-p} = 20\log\left(\frac{p_{0-p}}{1\ \mu\text{Pa}}\right)$$

Peak-to-Peak Sound Pressure Level: decibel representation of the peak-to-peak acoustic pressure. The peak sound pressure level uses a logarithmic factor of 20 and a reference value of 1 µPa.

$$SPL_{p-p} = 20\log\left(\frac{p_{p-p}}{1\ \mu\text{Pa}}\right)$$

Percentile: value below which a given percentage of observations falls.

Period: duration of one cycle of a periodic or harmonic wave. Reciprocal of the *frequency*. Denoted by letter *T*. Its unit is the second (s).

Pressure: force per unit area. There are three types of pressure that are interesting in underwater acoustics: the atmospheric, which results from the weight of the column of air at the sea surface; the hydrostatic, which is the combination of the weight of the water column per unit area at a given depth and the atmospheric pressure; and acoustic, which represents pressure fluctuations with respect to the hydrostatic pressure. Atmospheric and hydrostatic pressures are time-invariant, at least for the time scales considered in acoustic measurements, whereas the acoustic pressure is time-dependent. Their unit is the Pascal (Pa).

Power Spectral Density: frequency spectrum of the power of a signal, computed in constant-width bands of 1 Hz. For a sound pressure waveform, the amplitude of the spectrum is given in Pa^2/Hz. To calculate the power spectral density

of a N-sample discrete (digital) time signal, the magnitude of the Discrete Fourier transform (DFT) is divided by the number of samples, squared and then multiplied by the signal duration (T = N/f_s). The PSD of a discrete signal $x[n]$, with frequency spectrum $X[k]$, is given by:

$$s_{xx}[k] = \left(\frac{|X[k]|}{N}\right)^2 \cdot T \quad [\mathrm{Pa}^2/\mathrm{Hz}]$$

Power Spectral Density Level: logarithmic representation of the power spectral density. The unit is dB re. 1 µPa^2/Hz.

$$S_{xx}[k] = 10\log(s_{xx}[k]) \quad [\mathrm{dB\ re.\ 1\ \mu Pa}^2/\mathrm{Hz}]$$

Range: distance from the sound source to the receiver.

Received Level: sound level at a given range. The received level is related to the source and transmission levels by the following equation:

$$RL = SL - TL$$

Regression Equation: equation that establishes a relationship between two variables by minimising the error between its solution and a set of observations. A simple regression equation of the form $RL = SL - SLF \cdot \log(r) - AF \cdot r$ is used in underwater acoustics to estimate the source level SL from measurements. In the previous equation RL is the received level, r the range or distance from the source, SLF the spreading loss factor and AF the attenuation factor. Compared to a sound propagation model, this approach is simpler but has the disadvantage of being only applicable at ranges that are long enough for late reflections to dominate.

RMS Pressure: root-mean square acoustic pressure, that is the square root of the squared pressure averaged over time. This is the most common acoustic metric and is particularly useful in the characterisation of the amplitude of *continuous sounds*. However, the RMS pressure has been widely used in underwater acoustics to characterise *impulsive sounds*, for which this metric is not best suited as pulses of different energy and duration could result in similar RMS values. The *cumulative energy curve* with a 90% energy interval is typically used for the estimation of the pulse length, necessary for the calculation of the RMS pressure. The unit of the RMS acoustic pressure is the pascal (Pa) RMS. If a pressure value is given in Pa, without a metric descriptor, it will be assumed to be of RMS type. The RMS acoustic pressure is calculated as follows:

$$p_{rms} = \sqrt{\frac{1}{\tau}\int_{\tau} p^2(t)\,dt}$$

Specific Acoustic Impedance: ratio of *acoustic pressure* to *particle velocity*. The specific acoustic impedance is a property of the medium and indicates the opposition of that medium to the motion of a longitudinal wave. Denoted by letter Z_0. Its unit is the pascal second per metre (Pa·s/m) or rayl. The specific acoustic impedance of an homogeneous medium is related to its density and sound speed by:

$$Z_0 = \rho c$$

Speed of Sound: distance per unit time. Its units are metres per second (m/s). The speed of sound in water is a function of temperature, salinity, hydrostatic pressure and acidity, and has a value of 1532 m/s for 25 °C, 33 ppt and 1 atm. It is related to the wavelength and frequency of a propagating sound wave by:

$$c = \lambda f$$

Sound Exposure: integral of the square pressure. The sound exposure is related to the energy contained in the acoustic signal. As such, the sound exposure is suitable for both continuous and transitory signals, in particular for dose or noise impact assessment. Its unit is the pascal square second (Pa^2·s). The sound exposure is related to the RMS pressure and is calculated as follows:

$$p_{0-p} = \int_{\tau} p^2(t)\, dt = p_{rms}^2 \cdot \tau$$

Sound Exposure Level: decibel representation of the *sound exposure*. The sound exposure level uses a logarithmic factor of 10 and a reference value of 1 $\mu Pa^2 \cdot s$.

$$SEL = 10 \log\left(\frac{p_{rms}^2 \cdot \tau}{1\ \mu Pa^2 s}\right) = SPL_{rms} + 10 \log \tau$$

Sound Level: any acoustic metric expressed in decibels. This includes sound pressure level (rms, peak, peak-to-peak) and sound exposure level.

Sound Pressure Level: decibel representation of the *RMS acoustic pressure*. The sound pressure level uses a logarithmic factor of 20 and a reference RMS pressure of 1 µPa.

$$SPL_{rms} = 20 \log\left(\frac{p_{rms}}{1\ \mu Pa}\right)$$

Sound Propagation Model: mathematical algorithm that uses a numerical approximation to predict the transmission loss experienced by the sound emitted by an acoustic source as it propagates in a given underwater environment. Some of the most widely used propagation modelling theories and examples of algorithms are raytracing (Bellhop), parabolic equation (RAMGeo), normal modes (Kraken) and wavenumber integration (OASES).

Source Level: sound level produced at one metre from a point source. The source level of a real source is an hypothetical value, obtained from back-propagating measurements taken in the far-field of the source using a sound propagation model or an empirical regression equation. The source level must not be interpreted as a true representation of the sound level at one metre from the source, but as an intermediate metric necessary for the estimation of sound levels in the source's far field.

Spreading Loss Factor: level of attenuation per ten-times distance increase. A factor of 20 indicates spherical propagation of sound, associated with free-field (i.e. unbounded) conditions, and a factor of 10 indicates cylindrical propagation, associated with long-range propagation in-between two parallel, perfectly rigid, semi-infinite planes i.e. waveguide). The spreading loss factor can be lower than 10 or higher than 20, specially at ranges where the direct sound or early reflections dominate.

Streamer: surface cable consisting in an array of hydrophones used to record seismic data. Various streamers are towed by a seismic vessel during seismic exploration. The recorded data is used to generate an image of the seabed stratigraphy through specialised signal processing techniques.

Transitory Sound: acoustic signal of limited or determined duration.

Transmission Loss: sound attenuation level at a given range, referenced to one metre. The transmission loss can be calculated with a sound propagation model or estimated with a regression equation fitted to sound level measurements.

Wavelength: distance of a cycle in a propagating periodic or harmonic wave. Denoted by Greek letter λ. Its unit is the metre (m).

Content

1 Introduction

Ocean sounds result from natural, biological and anthropogenic acoustic sources. Natural sources include earthquakes, lightning, wind, rainfall and swell patterns. Shipping, seismic exploration, active sonar, offshore drilling, pile driving and dredging are some sources of human origin.

The general ambient noise in the oceans is a continuous, well characterised sound dominated by distant shipping (< 200 Hz), wind and rainfall (0.2- 50 kHz), and thermal agitation of water molecules (> 50 kHz) (Urick, 1983). In shallow temperate waters the crackling sound produced by the claw snap of a multitude of snapping shrimps can be the dominant noise source in the mid-frequency range; whereas in polar regions, sounds from ice cracking may be the main source of mid-frequency noise. Anthropogenic sounds contribute to raise these ambient noise levels during periods of activity and in localised areas, but some of them can propagate over long distances, particularly low frequency sounds produced by large ships and air gun arrays.

Low frequency noise has increased in the North-East Pacific at a rate of approximately 3 dB per decade in the period from 1950 to 1998 (McDonald et al., 2006). This increase is explained by the growth in number and size of propeller-driven vessels, caused by the expanding world economy. Working along these lines, a simple relationship between the increment of gross domestic product of a country and the increment of low frequency ocean noise was shown by Frisk (2012). The rise in low frequency sound levels does not occur at a global scale and in some cases, such as in the Equatorial Pacific since 2010 or in the South Atlantic, the trend becomes negative (Miksis-Olds & Nichols, 2016). Industrial activities are also an important contributor to ambient noise levels, generally during limited periods and in a regional scale. Low-frequency ambient noise may be dominated by different acoustic sources depending on the region; for example, in the South Atlantic seismic air gun signals are the primary source, while shipping and biological sources are the major contributors in the Equatorial Pacific (Miksis-Olds & Nichols, 2016). Small vessels, although not contributing to the global background levels, may be important localised sound sources.

It has been suggested that a significant proportion of the ambient noise is due to activities of the oil and gas industries during the exploration, development, production and decommissioning phases. The transport of oil and gas related products accounts for nearly 50% of the gross shipping tonnage, despite using only 19% of the total number of vessels in the world's commercial fleet (McDonald et al., 2006; Hildebrand, 2005).

Marine animals, and marine mammals in particular, rely on their auditory system for communication, mating and social interaction, navigation, foraging, prey detection and predator avoidance. Background noise can mask these vital sounds and cause stress reactions, behavioural changes or even physical damage on individuals, which may result in population impacts in the long term. The increasing evidence of the negative effects of anthropogenic noise on marine life has motivated environmental organisations, regulatory agencies and governments to look for solutions. Widely signed international agreements related to underwater noise include MSFD, HELCOM, OSPAR, ASCOBANS, ACCOBAMS, and the International Convention on Migratory Species (Erbe, 2013).

1.1 General Notes on Underwater Acoustics

The propagation of sound underwater is very complex and may travel through several different paths before reaching the receiver. Sound can either travel directly through the water, be reflected and scattered off the sea surface and seabed, or even travel along the seabed and emerge in the water column at some distance from the source. It then becomes evident that the environment will have a strong effect on the sound field. The characteristics of the received sound depend on the acoustic properties of the source, the nature of the propagation environment and the relative position between source, receiver and boundary surfaces. The received level of the source signal at a specific point in the water column is dependent on many variables, including source and receiver depths, salinity and temperature gradients in the water column, sea bed properties, sea state and bathymetry. Many of the environmental variables exhibit important differences depending on the geographical location and time scale (with day-night, seasonal and long term changes).

The propagation in the water is mainly governed by its sound speed, which varies with depth and range, and gives rise to focusing, channelling and shadowing effects (Coats, 2006; Lurton, 2010; Urick, 1983). Complex vertical variations in temperature and salinity in the water column allow for occurrence of acoustic channels at certain depths, where sound might get trapped by effect of vertical sound speed gradients of opposite sign. Except for long ranges, shallow waters and regions with oceanic fronts, the sound speed can be considered *horizontally stratified* (i.e. strong depth dependence, weak range dependence).

The ocean is a dynamic medium, with tides, internal and surface waves, eddies, turbulences, mixtures of water bodies of different temperature and densities, and temperature and salinity varying throughout the water body. These phenomena introduce a degree of variability into the sound speed profiles of the ocean, resulting in space and time variations on the sound propagation conditions and sound levels. These variations dominate near the sea surface, and despite being relatively small they have a significant effect on long range propagation.

The *transmission loss* or sound level attenuation between source and receiver depends on four main factors: geometric spreading, acoustic impedance of the seabed, absorption in water, and scattering from sea surface and seabed. The spherical wave front of an acoustic wave results in a 6 dB sound pressure attenuation per doubling of distance in free field or deep waters; in shallow waters this wave front can be shaped into cylindrical form, reducing the attenuation to 3 dB per doubling of distance. Low-frequency signals, such as those produced by seismic air guns, can easily penetrate the seabed and experience an attenuation with distance potentially higher than that from spherical spreading. The sea surface returns a phase-inverted version of the incident sound wave, producing a dipole effect which brings about a maximum attenuation at constant depth of 12 dB per doubling of distance. In shallow waters or at long distances the acoustic impedance of the seabed has an important effect on the transmission loss. The absorption in sea water depends on its temperature, salinity, acidity and hydrostatic pressure, and is particularly high for high frequency sounds (Fisher & Simmons, 1977; Francois & Garrison,1982a; Francois & Garrison,1982b). With the appropriate propagation conditions, a 100 Hz sound signal may be detectable after travelling in deep waters tens of kilometres from the source, or even hundreds if trapped in the so-called SOFAR channel, whereas a 100 kHz sound signal may be completely attenuated in only a few kilometres from the source. The typical attenuation characteristics of different acoustic frequencies in seawater with distance from the source are given in Appendix II.

The *received level* equals the source level minus the transmission losses (RL = SL – TL). The *source level* is the sound pressure level that a *point source*, an infinitesimally small version of the original acoustic source, would generate at one metre. The source level is a theoretical value used by those sound propagation algorithms that base their calculations on the assumption of a point source.

Real sources exhibit a complex sound pressure distribution in their proximity, in the so-called near field region. In the near field, the dimensions of the individual vibrating elements that integrate the source are comparable to the radiated wavelength, resulting in complex pressure and phase patterns. The distance below which the near field occurs depends on the overall dimensions of the source and the radiating frequency; for larger sources and higher frequencies the near field extends to larger distances. Beyond that critical distance, the source starts to behave as a single radiating element and the complex amplitude and phase fluctuations stabilise as the *wavefront* or area of constant phase becomes spherical; this region is known as the *far field*.

The size of the source and operational constraints make it impractical or impossible to measure the sound pressure level at 1 m from the source, leading in most cases to measurements in the far field region. The far field is an acoustically stable region where the source behaves as a monopole and the point source assumption becomes valid, as the spherical wave front is fully developed. Measuring in the far field is not just simpler or practicable, but also allows better comparison of results from various sources.

However, to make a good estimate of the source level, an appropriate sound propagation algorithm and realistic values for the acoustic parameters of the environment are needed. In general, information about properties of the environment is limited, especially seabed composition. In many cases, this difficulty leads to using oversimplified models or simple regression equations fitted to a limited set of range dependent measurements. A range dependent transmission loss generated with a validated numerical sound propagation algorithm is the most desirable method to calculate source levels. Source levels should be taken carefully, especially when empirical regression equations are used to estimate them. The transmission loss curve should always be provided to aid in the comparison and interpretation of source levels, whether it comes from full sound propagation modelling or simple empirical curve fitting.

1.2 Outline of Review

This report aims to be a quick reference guide to the characteristics and acoustic properties of underwater sound sources used in the oil and gas industry. There is a chapter dedicated to each relevant sound source, which includes general information about its characteristics, operation and acoustic behaviour, followed by a table that compiles sound levels and additional information from measurements published in the literature. The information has been extracted from journal papers, technical reports, disclosed military reports, product specifications, and books.

A detailed explanation of what is included in the tables and the approach followed to build them is given in the next section, "Notes on Tables". Gathering meaningful and representative measurements is especially challenging due to the complexity of the underwater environment. It is then essential for the comparison and interpretation of data included in this report to consider only literature giving a detailed description of measuring procedures, data processing and metrics. Secondary sources and grey literature, i.e. literature with insufficient or irrelevant information, have not been included, except when there is a scarcity of information.

The broadband or single band levels are included in the tables. The band levels of the spectra of various sources are not tabulated: instead, these spectra are shown in figures to make interpretation and comparisons easier.

It is assumed that the reader has a general knowledge of the activities related to the oil and gas industry. In case the reader is not familiar with it, a useful review of these activities is given by the Department of Trade and Industry (DTI, 2001).

1.3 Notes on Tables

The tables presented in this report include all or some of the following fields: source type and model, source characteristics, water depth, sediment, measurement, source level, signal characteristics, regression equation, description and reference. For simplicity, in those cases where the data is scarce some of the fields are omitted and any relevant information is added to the *description* column.

In the first column of the tables, the type of source is indicated in bold letters, with the model in brackets and italic letters. Sometimes the data refers to a type of source in general and not to a particular model: in that case, the word 'General' is shown in brackets. Instead of the model, the name of the source is indicated for shipping, dredging, drilling, pipe/cable laying and production sources. The name of a vessel or platform works as a unique identifier, and including it is especially important as these sources are prone to be measured in different projects; the data can then be related and compared, and the changes in the noise emission pattern can be tracked. Photos of the vessels in the tables are included in Appendix III to aid in the understanding and interpretation of the tabulated data.

The characteristics of the source are essential to interpret the measured sound levels. This information helps to compare sources of the same type which differ in their configuration and output power. The source characteristics may be included in the *source type and model* column, to distinguish between sources, or in the *description* column, as additional information.

Water depth and sediment play a critical role in the transmission of sound. In shallow waters, the seabed properties have an important contribution to the transmission loss pattern; also, low frequencies attenuate rapidly due to the impossibility of acoustic modes to be formed below a certain cut-off frequency. In deep water, the spherical spreading is the main cause of attenuation, but sound may experience low attenuation if it becomes trapped in the deep-sea acoustic channel (SOFAR), which typically occurs at depths of around 1000 m. It is much easier for the sound to couple with the deep-sea acoustic channel and travel long distances if the source is located at high latitudes and near the continental slope (Etter, 2013). Sound channels can also be formed in shallow water, but are generally transitory due to the high variability of temperature and salinity conditions. For the sound to travel long distances, the source must be placed within the channel, the wavelength must be shorter than the channel's width and the channel must be stable along the propagation path.

In the *measurement* column, the broadband sound level measured at a certain range from the source is quoted. In some cases, a single band or single frequency value is given. Multiple sound levels at different ranges might be provided if the data is clear and considered relevant, but generally the closest to the source is quoted in the tables, as the direct sound from the source is predominant in these conditions and this is likely to provide a better representation of its acoustic behaviour. The distances quoted by the authors are generally far enough from the source to be unaffected by the complexity of the near field interactions. The tabulated sound levels can be peak, peak-to-peak, RMS or SEL. No measured cumulative sound exposure levels or *cSEL* have been found in the literature, thus all the quoted sound levels refer to single acoustic events.

In the *source level* column the sound level at 1 m is quoted. It is common practice in the literature to provide a source level for each measured level at range. In those rare occasions where a source level is not given by the author of a paper or report, but a simple set of measurements at various ranges is available, we fitted a simple regression equation of the form $RL = SL - SLF \cdot \log r$ (see paragraph below about *regression equation*) to provide a source level. For some of the measurements included in the tables, the quoted source levels are unrealistically large; those values are highlighted in *red*.

The *regression equation* column contains, whenever given by the author, the curve fitted to the experimental data, the percentile used (95%, 90%, or 50% or *median*) and the range of validity, which

corresponds to the range covered by the measurements. Except for a few exceptions where sound propagation modelling is used, the source level quoted in the tables is obtained from the regression equation. In the case that two regression equations are provided, each covering a different set of distances, the source level in the curve for the closest range is quoted.

In the reviewed literature, rarely a source level is estimated using an analytical or numerical sound propagation model: instead, a simple regression equation in the form $RL = SL - SLF \cdot \log r - AF \cdot r$ is used, where SLF is the *spreading loss factor*, AF the *absorption factor*, and r the range. These regression equations are simple fitting curves and do not account for the propagation characteristics of the environment to determine the source level, so their accuracy beyond the measured ranges is limited. Source levels estimated in this way, and not through a calibrated propagation model, must be used carefully.

In general, exceptional care must be taken when using the source level as a metric to characterise the acoustic output of a source. Near the source, at ranges of less than a few hundred meters, the sound field is dominated by the direct signal and a series of discrete, early reflections. This results in a particularly complex sound field, highly dependent on the characteristics of the adjacent environment and source directivity. Further away from the source the combination of multiple high order reflections results in a more stable decay of acoustic energy with range. Therefore, in a sound field consisting of at least two regions with highly distinctive sound patterns, the limitations of a three-parameters empirical equation become apparent. The empirical regression equations are useful as a summary of a large set of sound level measurements. However, these equations should not be used as a tool for predicting sound levels beyond the limits of the fitted measurements. This is particularly true for sound level estimates in the proximity of the source, where the average spreading loss factor tends to be considerably lower than at larger distances. For an in-depth discussion about source levels, regression equations and their validity at closer distances from the source, see Section 1.4.

The *signal characteristics* column includes information such as pulse duration, period, duty cycle, frequency range, maximum energy bands, bandwidth, tonal frequencies, temporal characteristics of the signal or mechanism generating the noise.

The *description* column contains any additional information that can be useful for interpreting the measurements and does not fit in any of the other columns. In general, things like the context of the measurements, the location, source and receiver depth, source characteristics, and notes on the values presented in the other columns are shown in the description column.

The *reference* column simply cites the author and year of the document in which the data included in the table was presented originally.

The conditions within which measurements are made by different authors are diverse, as the environment, source and receiver locations, characteristics of the target source, activity and characteristics of non-target sources, measurement equipment or processing techniques will be unique for each project and deployment. An effort have been made to compile as much relevant information as possible, presenting it in a way that is clear and allows the reader to easily extract, compare and interpret data from different acoustic sources, and environmental and operational conditions. Not all authors report their results in the same way, so in order to provide clear and complete information the tables in this report have been populated with data coming from text, tables and figures. Simple calculations were made on data from the literature to report values in units that were consistent throughout the tables. Broadband and spectral sound levels were extracted from figures in those cases where these levels were not explicitly given in tables or text; in the tables included in this report, data extracted from figures is highlighted in *blue*. In a few cases, more complex calculations were necessary for completeness or to interpret or refute some of the results; in those cases, it was clearly stated that the values or analysis came from “the reviewer”.

1.4 Source Level and Far Field

The source level is the sound level that an infinitesimally small version of a real source, known as *point source*, will produce at a distance of one metre in a given direction when placed in a homogenous infinite propagation medium (*free-field* condition). The source level is typically used to report the intrinsic acoustic output of a source at a given angle of emission. By definition, the source level depends on direction but is independent of the propagation medium. The source level is a parameter that not only allows for simple comparison of acoustic outputs from different sources, it is also an essential piece of information that propagation models based on the point-source approximation use for sound field simulations. These are the two main reasons that lead the authors of this report to add tables that contained a thorough list of source levels for a variety of sources, environments and operational conditions.

The concept of source level is better understood after explaining two essential concepts: the *near field* and *far field* of a source. These two concepts refer to two regions of the space, relative to a source, with distinctive acoustic properties. Let first consider a real source that can be modelled as a combination of multiple small individual emitters or *point sources*. The pressure waves produced by those individual emitters add up with their own particular phase at a given point in the space. In the near field, the relative phase of these interfering waves is strongly dependent on receiver location, which results in a series of constructive and destructive interferences along any direction from the source. In the far field, the relative phase of the interfering acoustic waves from the individual emitters becomes virtually independent of travelled distance. In that region, the pressure attenuation is inversely proportional to distance ($TL = 20 \log r$) and the directional behaviour of the source stabilises, becoming distance-independent. In other words, in the far field a real source can be approximated to a *directional point source*. The far-field distance depends on the dimensions of the source and the frequency of the emitted signal, and is approximated by a^2/λ, with a the maximum source dimension and λ the wavelength (Foote, 2014).

A source level does not represent the sound level at 1 m from a real source, as at 1 m the point source condition is not met and the source appears as a multi-element distributed emitter. In that sense, a source level is not a real sound level, but a means to calculate sound levels in the far field (i.e. at distances where the point source approximation is valid) using a known range-dependent transmission loss. In the nearfield, sound levels predicted from a known source level will tend to overestimate measurements. Whether predicted sound levels from a point source approximation overestimate the real sound levels in the nearfield will depend on the dimensions and shape of the source, frequency content of the emitted signal, and receiver location. Nonetheless, the point source assumption will lead eventually to overestimated sound levels at close proximity of the source, where distances are comparable to the separation between individual emitters.

There are three main ways of obtaining source levels for an acoustic source, 1) from an acoustic source model (e.g. Gundalf or Nucleus for air guns), 2) a range-dependent transmission loss from a calibrated sound propagation model fitted to the measurements, or 3) a range-dependent empirical regression equation of the form $RL = SL - SLF \cdot \log r - AF \cdot r$ fitted to the measurements. Some *source models* provide a way of calculating source levels that account for the source directional behaviour and are fully independent of the environment (e.g. air gun array models); other models are intrinsically linked to the environment and cannot produce source levels that accurately characterise the sound source for all possible environments (e.g. pile driving models). Measurement-fitting of a range-dependent transmission loss obtained from a calibrated *sound propagation model* will provide a single-figure source level that integrates the acoustic output from all vertical angles of emission (angle-independent), but which does not dependent on the environment if done with an adequate measurement sample. The *empirical regression* method is simpler than using a calibrated sound propagation model and provides a fair representation of the sound level attenuation with range. However, simple regression curves are more sensitive to the

measured sample, and will tend to produce biased results outside the ranges within which measurements were taken and fitting was applied. For this reason, source levels calculated with a simple empirical regression may only be appropriate for sound field simulations within the ranges used for the curve fitting. It is for that reason that regression equations and their range of validity are included in the tables. The vast majority of source levels reported in the literature that have been added to this report were calculated with the empirical regression method; only a few used sound propagation models, not all of them calibrated. Source levels from acoustic source models were not included. In some instances, regression equations can lead to source level values that largely overestimate those expected for sources of similar characteristics; those values are highlighted in red in the tables.

There are various reasons why source levels calculated from measurements can sometimes be larger than expected. They can be caused by an *uncalibrated model* or *by limited sound level data over range*, which result in source levels holding certain dependency with the propagation path and environment. Measurements that do not correspond to a *unique operational phase* of the source can also lead to inaccurate source levels (bias) and increased variance (uncertainty); whether the source levels have higher bias or uncertainty will depend on the curve fitting method and the quality of the measured sample. Additionally, when backpropagating sound level measurements to 1 m it is important that the measured *sounds originate from a single source*. Unique localised sources are not always the norm, as certain activities such as dredging or drilling are typically accompanied by vessels that operate closely to the source. In those cases where there is no opportunity to measure the target source alone or vessels are considered another component of the distributed source, statistically-representative measurements will be key to avoid localised high variability due to unusual periods of vessel activity.

Some of the largest source levels found in the literature came from basic spreading-loss and attenuation equations fitted to measurements taken in waters just a few meters deep. Under such conditions the seabed will be expected to have a significant impact on the sound attenuation with range and spreading loss factors greater than 40 will not be uncommon at longer ranges. Figure 1.1 shows a measurement from an air gun array in waters 2 m deep (see Table 2.1, part 4; data from McPherson et al., 2012). This is a clear example of how limited data over range can compromise the accuracy of the empirical regression equation.

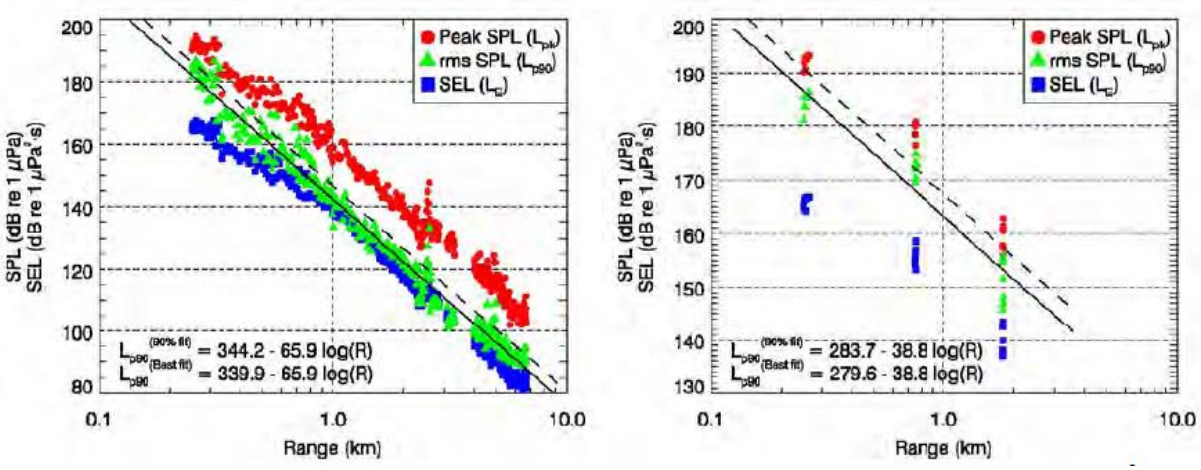

Figure 1.1 Sound levels (peak, RMS and SEL) measured from a 320 in^3 air-gun array during a seismic survey in the Beaufort Sea, Alaska in waters ~2 m deep (from McPherson et al, 2012). The 90th and 50th (best-fit) percentile regression equations are included for the endfire (left) and broadside (right) directions. Source levels as high as the ones shown here may occur when using a simple spreading-loss and attenuation equation, but are infrequent and not representative of the sound levels near the source.

1.5 Report Structure

This report is structured in one introductory chapter, the main body consisting of five chapters, each dealing with a different group of acoustic sources, and the appendices.

Chapter 1, i.e. the current chapter, contains background information about noise in the oceans from natural, biological and anthropogenic sources and their potential impact on marine life. Highlights on underwater acoustics and sound propagation are also given to help with interpreting the results and understanding some of the concepts referred to in the main body. A brief outline of this review and detailed comments about the content of the tables and the approach taken to build them are also included.

Chapter 2 deals with low frequency sources used by oil and gas industry for seismic exploration and shallow hazard assessment. It includes four sections for the most common or relevant acoustic sources (air gun array, sparker, boomer and marine vibrator) and two additional sections for historical or rarely used sources (water gun and sleeve exploder). The air gun array is the most widely used acoustic source in the oil and gas industry and is described in more detail. A table of measurements is included at the end of each section for the corresponding type of seismic source.

Chapter 3 presents information about a set of medium to high frequency active sources, classified under the title of engineering sources. It includes acoustic deterrent and harassment devices (ADD, AHD), single and multibeam echo sounders (SBES, MBES), sub-bottom profilers (SBP), side-scan sonars (SSS), underwater communication systems, underwater positioning systems and acoustic doppler current profilers (ADCP). Many of these devices are types of sonar. The boomer and sparker are considered engineering sources, but since already described in Chapter 2, these sources are covered briefly in the chapter. A table of measurements is added at the end of each section for the corresponding type of engineering source.

Chapter 4 deals with noise produced by different types of vessels. The chapter is structured in various sections including general background, individual sources of sound in a ship, vessel types and their acoustic characteristics, and a summary of sound produced by shipping activity. One table is added at the end of sections 4.2-4.5 with measurements from four groups of vessels: *large* (e.g. supertankers, tankers and cruise ships), *icebreakers*, *medium* (e.g. research and support vessels, tugs) and *small* (e.g. boats and hovercrafts).

Chapter 5 presents information about sounds produced by exploration, construction, production and decommissioning activities carried out by oil and gas industry that have not been covered in previous chapters. The chapter contains the following sections: dredging, drilling, production, pipe laying and decommissioning. A table of measurements is added at the end of each section. A large amount of literature on pile driving noise has been published since the publication of the last JIP report (Wyatt, 2008), and it has been considered appropriate to produce a separate report with detailed information about published data on sounds from pile driving activities (Jiménez-Arranz et al., 2017).

Chapter 6 presents data of noise transmitted underwater by overflying aircrafts, including fixed and rotary wing models. A table of measurements is included at the end of the chapter.

Appendix I includes some additional information about underwater acoustic sources not related to oil and gas industry. The chapter contains three tables with information about sounds produced by industrial, military, natural and biological sources. The idea of this chapter is to provide a general picture of the sound in the oceans to allow industry, regulators and scientific community to gain a better understanding of the relative contribution of sounds produced by oil and gas industry. *Appendix II* includes two figures: one describing ambient noise levels as a function of shipping traffic and sea state, and the other showing the sound level attenuation with frequency due to absorption in sea water. *Appendix III* shows pictures of the vessels included in the tables. These images are expected to aid the reader in interpreting the measurements.

2 Seismic Sources

Seismic surveying is intended to study the composition of the upper crust of the seafloor. These surveys are conducted for a variety of reasons; checking foundations for roads or large structures or detecting resources like groundwater or minerals are some of them, but most of commercial seismic surveys are conducted for detection (exploration) and monitoring (production) of oil and gas (OGP, 2011). The seismic sources are primarily used by the oil and gas industry to investigate shallow subsoil structures before engineering site work, or deeper layers in the search for fossil fuels.

Every marine surveying technique uses a particular configuration of source and receivers to send sound waves into the earth and capture the reflected energy. The strength of the reflected wave and the time it takes to travel through the different layers in the seafloor and back to the sensor are processed to get a stratigraphic image of the earth's crust (see Figure 2.1).

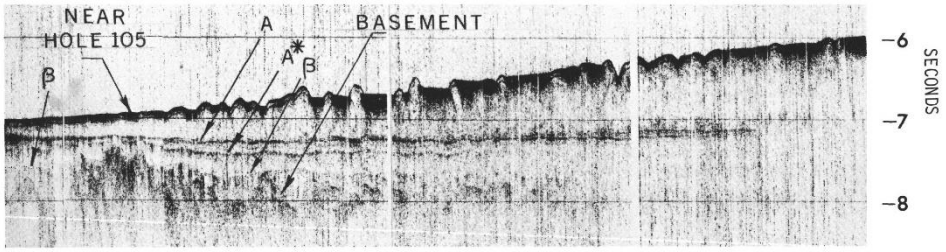

Figure 2.1 Example of a reflection seismogram (DSDP Initial Reports, Vol. 11, Ch. 6, 1972, deepseadrilling.org/i_reports.htm)

The selection of the seismic source is based on survey requirements. The acoustic energy emitted by low frequency sources, such as air guns, is concentrated below 250 Hz, making its signal capable of penetrating the deeper layers of the seabed. Seismic sources with a higher frequency output, such as sparkers or boomers, do not penetrate so deep into the seabed. These can only reach depths in the order of hundreds of metres, however they can generate higher resolution images. High resolution surveys are aimed for shallow hazard assessment, whereas deep penetration surveys are common in oil exploration and production.

Offshore oil and gas exploration, development and production activities typically take place in continental margins. Operations have traditionally been conducted in shallow waters on the continental shelf, but the need for new resources moved the operations to deeper waters. The relatively high activity of seismic exploration, along with the displacement of the operations into deeper waters, where low frequencies propagate better, could have an important effect on background noise levels in the oceans. The average number of seismic surveys conducted per month and recorded from 1994 to 2005 is represented in Figure 2.2 for different regions of

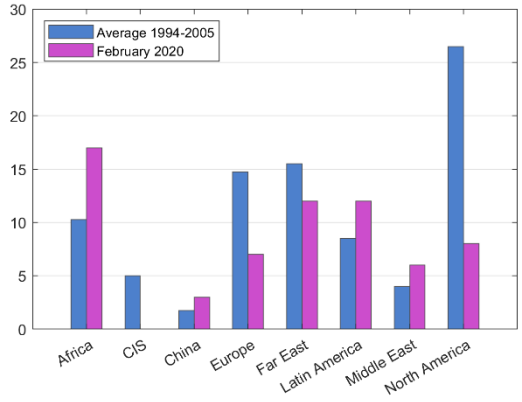

Figure 2.2 Average number of offshore seismic exploration operations per month from 1994 to 2005 (blue bars, Hildebrand 2009), and snapshot of total number of operative geophysical survey vessels on 27th Feb 2020 (purple, Searcher Seismic app). Results shown by region.

world, along with a snapshot of the number of active geophysical survey vessels (seismic and geotechnical) on the 27th February 2020. The number of active seismic surveys has certainly diminished since the financial crisis in 2008. On 2015, the worldwide fleet comprised at least 168 seismic vessels (Paganie, 2015).

A summary of the most commonly used seismic sources by the oil and gas industry is presented in the next sections. A table including measured sound levels from different seismic sources, along with location, source characteristics and some additional data, is presented at the end of each section.

2.1 The Air Gun

Air guns produce high levels of low frequency sound, most of it below 250 Hz, by releasing a volume of highly pressurised air into the water, which produces 90 percent of its energy in the band 70 to 140 Hz (van de Sman, 1998). Air guns are generally combined in an array to produce a low frequency acoustic beam aimed toward the sea floor. The acoustic emission of the air gun array is not limited to low frequencies and to the vertical downward direction: frequencies up to 20 kHz and significant lateral acoustic energy can be emitted into the surrounding water (Tashmukhambetov et al., 2008; Landrø et al, 2013).

The *air gun* is the most common and most powerful frequency source used by the oil and gas industry. The compressed air enclosed in the pneumatic chamber of an air gun is released rapidly into the water, generating a high-level acoustic pulse. The bubble formed by the released mass of air produces a series of amplitude oscillations, which attenuate with each expansion and collapse of the bubble until it reaches the equilibrium state (see Figure 2.3, left).

The defining properties of an air gun are the *pressure* and *volume* of the chamber; typical volumes for a single air gun vary from 20 to 800 in^3, with 2000 psi being the most commonly used chamber pressure. Air guns with higher volume, higher chamber pressure or placed at shallower depths produce bubbles with lower dominant frequency (Landrø & Amundsen, 2010). The relation of the bubble frequency to the water temperature and the volume, chamber pressure and depth of the air gun is described by Eq. 2.1 (Landrø, 2014). This equation accounts for the effect of water temperature, not included in the original Rayleigh-Willis equation; the approximate term on the right is the Rayleigh-Willis equation (Willis, 1941).

$$f = k\frac{\left(P_{atm}+\rho_w g z_g\right)^{\frac{5}{6}}}{\sqrt[3]{P_g V_g}}\left(1+\alpha\frac{T_w-T_0}{T_0}\right)^{-1} \approx k\frac{\left(10+z_g\right)^{\frac{5}{6}}}{\sqrt[3]{P_g V_g}} \qquad (2.1)$$

where P_{atm} is the atmospheric pressure in Pa (P_{atm} = 101325 Pa), ρ_w the density of sea water in kg/m^3 (ρ_w = 1025 kg/m^3 at water surface, 20°C and 35 ppt salinity), g the acceleration of gravity in m/s, z_g the depth of the air gun below sea surface in m, P_g the chamber pressure in Pa, V_g the air gun volume in m^3, T_w the water temperature in K, T_0 the reference temperature (T_0 = 273.15 K), and k and α constants (α = 0.55, with k a constant of proportionality).

Beyond a certain distance, which depends on the dimensions and maximum wavelength of interest, any source in free field can be modelled as a monopole. This distance is known as the *far-field*. A typical example of the far-field acoustic signature produced by a single air gun is shown in Figure 2.3. A primary sharp peak, a number of secondary peaks of decaying amplitude associated with damped bubble oscillations, and the phase-inverted copy or *ghost* that follows each positive peak, are the primary features of the time source signature of an air gun (see Figure 2.3, left).

The air above the sea surface acts as a mirror for any incoming underwater acoustic wave, reflecting most of its energy with an inverted phase. This phase-inverted copy of the acoustic pulse is known as *ghost reflection* and is of key importance from the point of view of seismic data processing. A destructive interference is produced when the ghost signal blends with the original downward travelling pulse,

introducing a comb filter effect in the spectrum that reduces the effective bandwidth (see Figure 2.3, right). The low-frequency harmonics that appear in the first 100 Hz of the signature's frequency response are caused by the stable oscillation period of the air bubble.

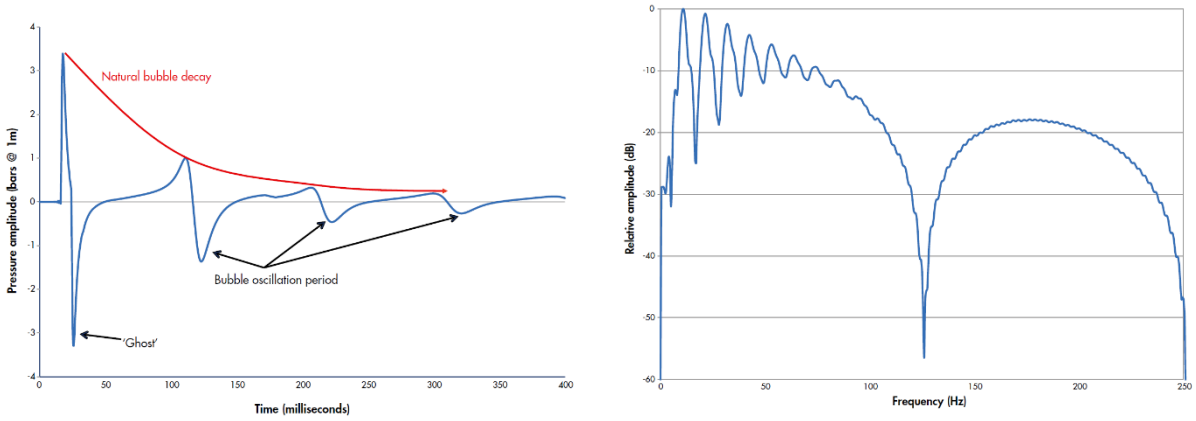

Figure 2.3 Source signature of a 150 in^3 air gun in bars (left) and its normalised amplitude spectrum in dB (right). From OGP (2011)

The depth of the source selected for the survey is a decisive parameter, as it will determine the maximum depth of penetration and resolution of the seismic image – deeper sources result in better penetration and shallower sources provide better resolution –. The useful band of an air gun pulse is between the first notch (DC) and second notch in the spectrum. High resolution, shallow subsurface surveys require *shallower depths*, i.e. second ghost notch at higher frequencies; and low resolution, deep penetration surveys require *deeper depths*, i.e. second ghost notch at lower frequencies. The normal operating depth for air guns is between 5 and 7 m (Gausland, 1998). However, deeper source operation have become more common since the introduction of the GeoStreamer in 2007, which facilitates deghosting of measurements through dual-sensors (hydrophone, accelerometer) installed in the streamer.

Not only the depth of the air gun, but also the depth of the receiver, affects the received level. Sound levels closer to the sea surface are lower than away from it. The greatest attenuation gradient occurs in the first few metres from the surface. This is explained by the so-called *Lloyd's mirror* effect, a dipole-type spatial sound pressure pattern that results from the high reflectivity of the water-air boundary.

In deep waters or close to the source, where the direct signal and surface reflection dominate and seabed contribution is minimal, the source can be reasonably approximated to a dipole, provided that the receiver is placed in the far field. This dipole consists in the original monopole (the air gun array) and an imaginary monopole of opposite phase (the *ghost source*), placed symmetrically with respect to the sea surface. This dipole or Lloyd's mirror produces a spatial interference pattern, creates a spectral comb-filter and enhances the vertical directivity of the source, especially in the low end of the spectrum, for which the sea surface is effectively flat. No relevant examples of air gun arrays measured at multiple receiver depths have been found in the literature to illustrate the influence of the *Lloyd's mirror* on received sound levels.

The energy of the primary pulse of an air gun is concentrated between 10 and 200 Hz, which is the typical range of interest in seismic surveying. Frequencies up to 20 kHz can be emitted by the air gun (Tashmukhambetov et al., 2008; Landrø et al, 2013; Khodabandeloo & Landrø, 2017), but their amplitude is generally small compared to the lower end of the spectrum, below 1 kHz. According to Landrø et al. (2013), the high frequency content of the measured acoustic signal varies with size and total volume of the air gun array, and is believed to be caused by ghost cavitation in the space between air gun strings. For a 2730 in^3 air gun array consisting of three strings separated by 6 m and deployed at 5 m depth, the peak amplitude of the high frequency event appears to be 15-30 times lower than the amplitude of the primary peak (i.e. 24 – 30 dB difference).

The *air gun array* is the source used in marine seismic exploration. It typically consists of a few groups of 6-8 aligned air guns or air gun clusters, each called a string. An air gun array is made up of one or more sub-arrays, with 1-6 strings each (see Figure 2.4 and Figure 2.5). The volume of an air gun array is the sum of the volumes of the individual guns, and is typically in the range of 3000-8000 in^3, although air gun arrays with larger or smaller total volumes are not uncommon. The air guns hang beneath floats, between 3 and 10 m below the sea surface and generally at 6 m (see Figure 2.4). During a survey the air guns are activated at regularly spaced source-point intervals, every 10-15 s depending on vessel speed. The activation interval depends on the source-point distance and the speed of the source vessel.

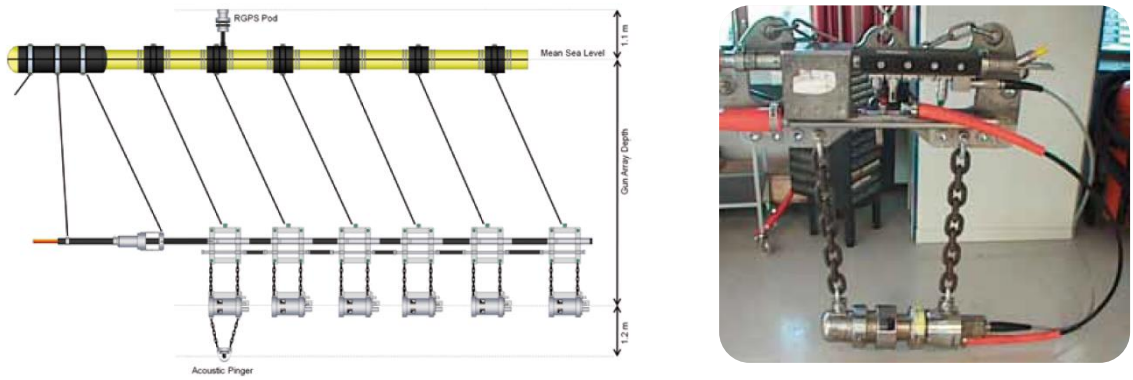

Figure 2.4 Side view of a string of air guns. There are 12-guns arranged in 2-gun clusters. The yellow tube provides floatation and the guns are hung below at the desired depth. Precise positioning is provided by combining information from the RGPS in the float and the acoustic pingers under the guns (left). Suspended single air gun (right). From OGP (2011)

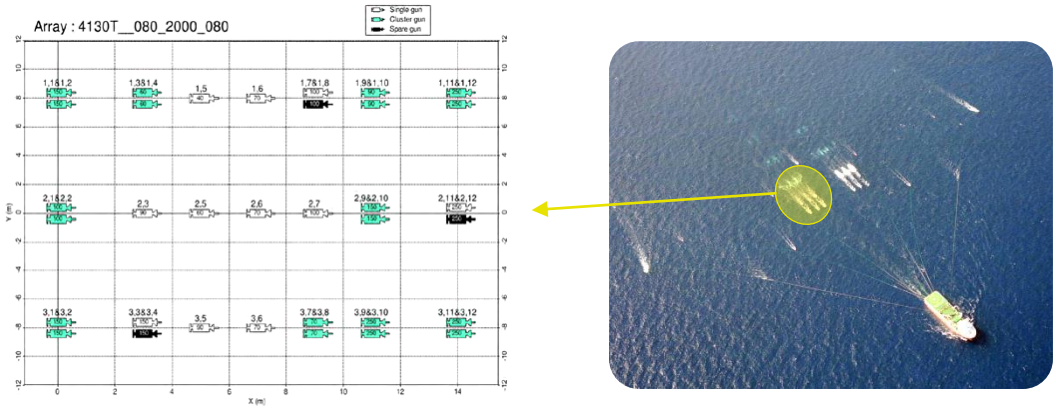

Figure 2.5 Air gun array layout from NUCLEUS+ (left) and deployment example (right). The source vessel is towing two arrays.

There are two main reasons for deploying air guns in arrays: The first is to increase the power of the source. The second is to minimize the bubble oscillations by tuning the array; air guns with different volumes will have different bubble periods, leading to a constructive summation of the first (primary) peak and destructive summation of the bubble amplitudes.

The basic idea behind the increase of source strength in an array when compared to a single air gun is that a source array of n single sources produces n times the acoustic pressure of the single source. Neither the chamber pressure nor the total volume of the array have a crucial influence on its strength. The *strength* or peak-to-peak amplitude of the pulse generated by the array in the vertical direction is in the range of 10-100 bar-m (240-260 dB re µPa@1m). The *strength* of an air gun array is: 1) linearly proportional to the number of air guns in the array; close to linearly proportional to the firing pressure of the array; and roughly proportional to the cube root of its volume (Caldwell & Dragoset, 2000). This is summarised in the following expression:

$$p_{pk} \propto n P_g V_g^{1/3} \tag{2.2}$$

where p_{pk} is the peak pressure emitted by the air gun array in free field, n is the number of air guns in the array, P_g the chamber pressure and V_g the total volume of the array. A comparison between measured peak source levels from Table 2.1 and peak levels calculated with Eq. 2.2 is shown in Figure 2.6. The difference in decibels between peak and rms source levels is assumed to be constant with distance, so that the rms levels in the tables and the levels calculated with Eq. 2.2 can be directly compared. Fig. 2.6 shows a good agreement between measurements and calculations, highlighting the rapid increase and then the stabilisation of the output pressure as the number of air guns and the total volume increases. The high variability in the measured source levels can be attributed to the limited accuracy of experimental regression equations to estimate the sound level at 1 m from the source.

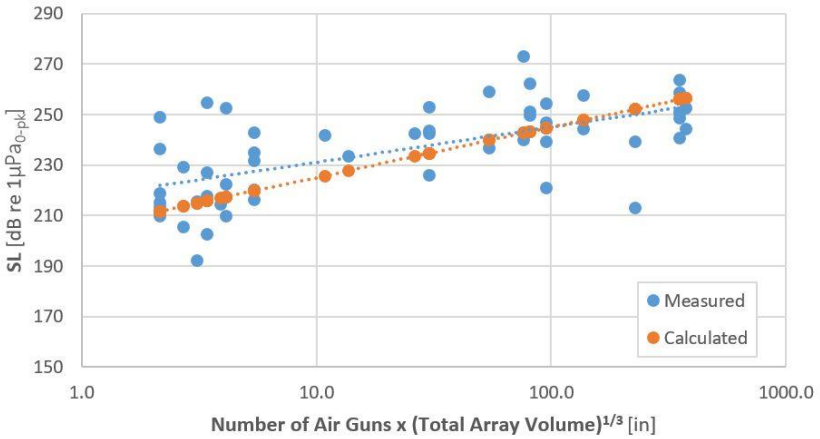

Figure 2.6 Peak source level of an air gun array as a function of the number of air guns and its total volume. Comparison between measurements (blue, see Tab. 2.1) and approximate equation (orange, see Eq. 2.2).

The *pressure signature of an air gun array* is measured in the far-field (200-250 m beneath the array), where the array behaves as a point-source, and is then normalized to a distance of 1 m. Due to the constructive interference achieved far away from the source through the synchronisation of air gun firing times, the pressure level at 1 m tends to be considerably lower than the far-field level normalised to 1 m (~20 dB difference). The time it takes for an air gun signal to reach the maximum amplitude once triggered depends on its chamber volume; for the peaks to merge in the far field, air guns with different volumes are activated at different times. The main parameters used to characterise the signature of the array are the strength of the primary pulse (i.e. peak amplitude) and the *primary-to-bubble ratio* (PBR). The higher the PBR the closer is the signature to a single pulse (see Figure 2.7, left). It can be noticed how the bubble oscillations are drastically reduced in the array (compare with Figure 2.3, left). Two other important features of the array's signature are the rise time of the primary peak and the length of the bubble pulse.

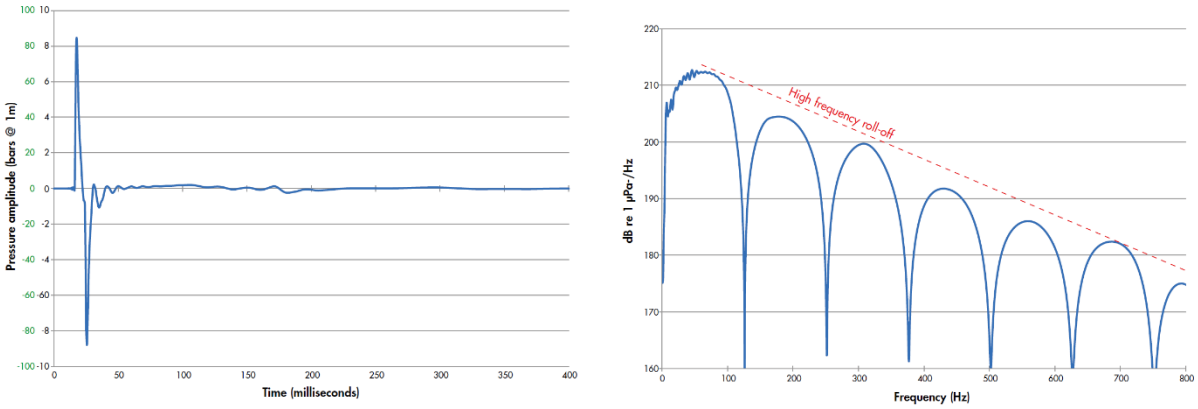

Figure 2.7 Source signature from a 4450 in^3 array with 33 guns (left) and its normalised amplitude spectrum in decibels (right). From OGP (2011).

The acoustic energy emitted by an air gun array is not the same in all directions; the array is designed to project most of its energy vertically downwards, and as a result pressure levels emitted horizontally are 15-24 dB lower. Factors that contribute to this directional radiation are the arrangement of the sources in a horizontal plane, the dimensions of the array, the distribution of the air gun volumes within the array, the synchronised activation of the individual air guns and the proximity of the array to the water surface. Figure 2.8 shows that most of the energy between 20 and 180 Hz is projected downwards, low frequency radiation tends to be more omnidirectional, high frequency radiation presents secondary lobes and the array is more directive in the cross-line direction. The latter is explained by the number of air guns per subarray, which is larger than the number of subarrays. Figure 2.9 shows the broadband acoustic field created by the array in the horizontal and vertical planes.

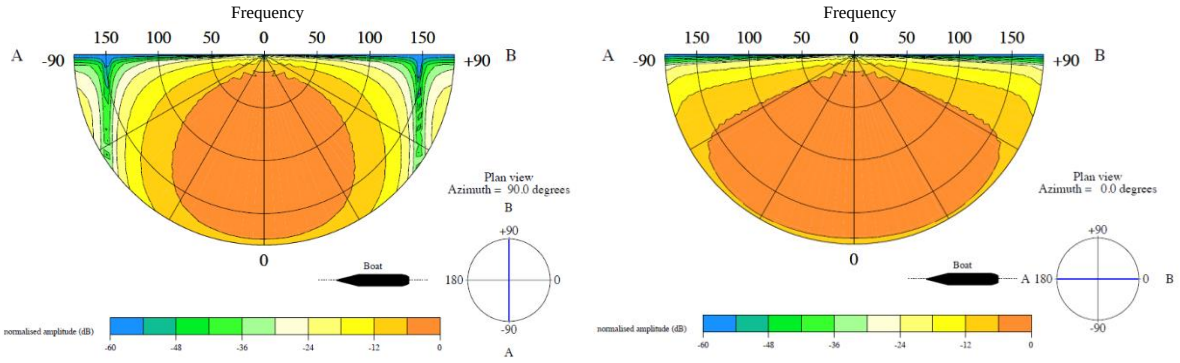

Figure 2.8 Modelled sound pressure level emitted by a 1760 in^3 air gun array in a vertical plane in cross-line (left) and in-line (right) directions. The vertical angle of emission is represented by the radial lines and the frequencies (0-180 Hz) are shown in concentric circles. The coloured pattern represents the sound pressure levels. The array has two identical strings with three paired air guns each, which leads to an asymmetry in the horizontal directivity pattern. Models from Gundalf™.

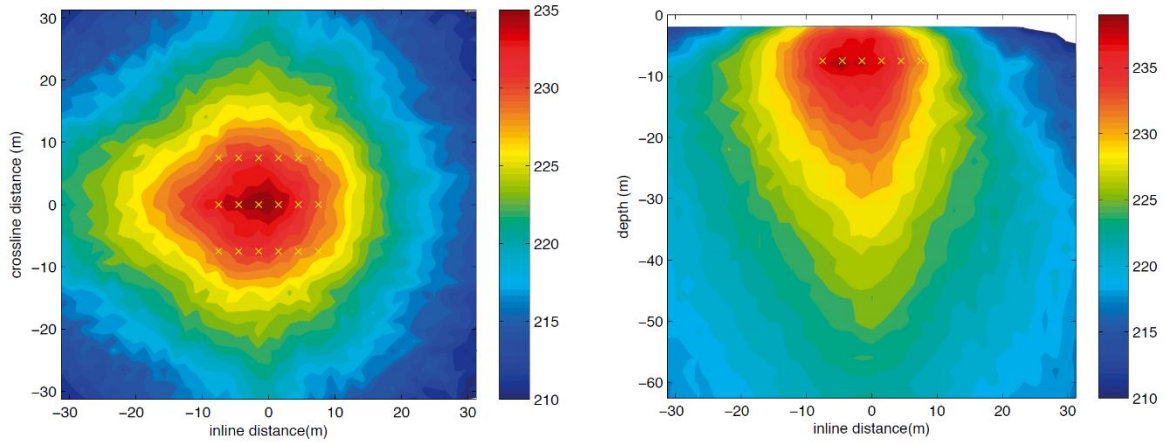

Figure 2.9 Modelled broadband (0-400 Hz) peak sound pressure level emitted by a 5205 in^3 air-gun array at 7.5 m depth in the horizontal plane (left) and in the vertical plane (right). The yellow crosses show the position of individual guns. From OGP (2011).

An air gun array is designed to direct as much energy as possible towards the seabed. However, most of the acoustic measurements are taken at a distance from the source, away from the main vertical beam. Characterising the sound field under the array is also important to gain a full understanding of the potential impact in the marine environment.

The horizontal directivity certainly exists, but may be difficult to identify from the values in the tables due to the influence of the environmental conditions and the limited accuracy of the method used in the literature to estimate the sound levels at 1 m.

2.1.1 Sound Levels with Range

Overall sound levels decrease as the distance from the source increases, as a result of geometric spreading, absorption losses in water and seabed, and scattering in seabed and sea surface. The attenuation rate of the SPL with distance at a predetermined source and receiver depth is somewhere between a cylindrical and a hyper-spherical spreading law (1/r and $1/r^4$, i.e. 3-12 dB per doubling of distance), and primarily depends on water depth, bathymetry and seabed geology along the propagation path. The transmission loss is not a simple function of range, and a single spreading loss curve may not be sufficient to describe the different attenuation patterns that occur at different ranges. The sound levels produced by a 3147 in^3 air gun array at two sets of ranges are shown in Figure 2.10. Note that two regression equations had to be calculated to cover all distances.

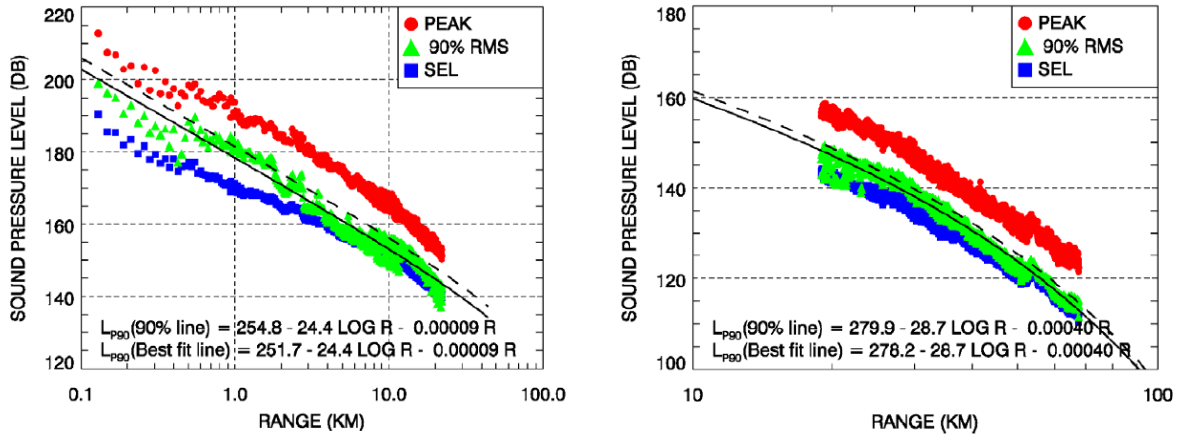

Figure 2.10 Sound levels (peak, RMS and SEL) measured from a 3147 in^3 air-gun array during a seismic survey in the Chukchi Sea, Alaska (from Funk et al., 2008). The measured sound levels and the 90th and 50th (best-fit) percentile regression equations are included for two sets of distances: 100 m to 20 km (left) and 20 to 80 km (right).

Far field simulations of air gun array signatures indicate that peak sound levels are of the order of 265 dB for some of the largest air gun arrays (~4000 in^3). Source levels with peak and rms values larger than 270 and 250 dB should be treated with suspicion, as those values will suggest a flaw in the approach followed to back-propagate measured sound levels to 1 m (see Section 1.4 for possible causes for inaccurate source levels).

In the nearfield, sound levels predicted with the point source assumption will tend to overestimate levels measured in practice. Fontana and Boukhanfra (2018) reported measurements on a 2-string air gun array with an active volume of 3,090 in^3 (10 active clusters) made with the 36 array's near-field hydrophones at distances from 4 to 56 m from the centre of the array. The sound level measured at the closest distance of ~4 m was 144.5 dB, ~6 dB lower than the predicted far-field signature back-projected to 4 m using spherical spreading loss. The predicted far-field signature was 6-12 dB higher than the maximum near-field sound levels at the measured ranges of 4, 22, 29, 48 and 56 m from the centre of the array.

2.1.2 Pulse Duration with Range

The duration of the recorded sound event produced by a seismic source tends to increase with range (Green and Richardson, 1988). The loss of high frequency energy with distance results in a smearing effect that affects the individual reflections contained in the event. This along with the higher number of reflections that reach the receiver as the range increases contribute to extend the duration of the event.

A report written by Beland et al. (2013) regarding the monitoring and mitigation of marine mammals during a seismic survey in 2012 contains a detailed analysis of the duration of pulses produced by a 70 in^3 air gun and a 4380 in^3 air gun array, both measured in shallow and deep water locations. The pulse duration was calculated as the duration of the window containing 90% of the signal energy. The pulse duration is

shown to increase with distance, for both sources and at both locations, and varies from 0.1 to 2 s between 300 m to 80 km range. Figure 2.11 shows some of the results presented in the report: It is worth noting that as the pulse duration changes with range, so does the relationship between SPL_{rms} and SEL.

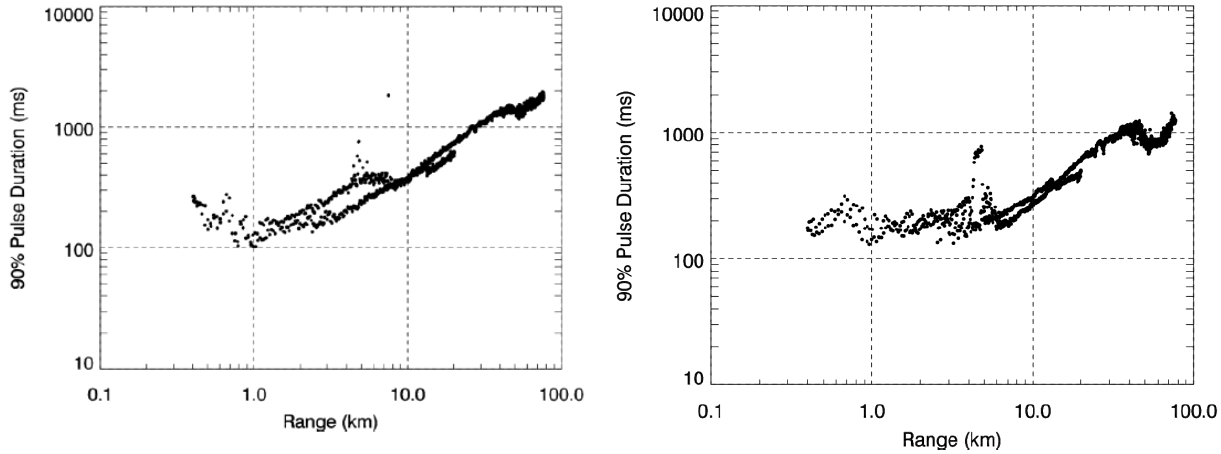

Figure 2.11 90% energy pulse duration from a 70 in^3 air-gun (left) and a 4380 in^3 air-gun array (right), measured in a shallow water site (50 m water depth) during a marine seismic survey in the Beaufort Sea (from Beland et al., 2013)

2.1.3 Pulse Spectra in Dispersive Media

In the same study from Greene & Richardson (1988) it is shown that the frequency characteristics of the received signal varied with range and water depth. The higher frequency components of the pulse arrived before the lower frequencies. This downward frequency sweep is characteristic of long range pulse propagation. Hauser et al. (2008) make a detailed analysis of the effect of range on the frequency characteristics of the signal generated by an 880 in^3 air gun array during a marine seismic survey in the Colville River Delta, in very shallow waters (< 15 m). The drift of the pulse with time toward low frequencies is likely the result of the combined effect of the low-frequency components associated with bubble oscillations and the dispersive characteristics of the shallow water medium (see Figure 2.12, left). The wave transmitted into the seafloor can return to the water column after travelling along shallow geological layers (*head wave*) and then be detected before the direct pulse, as low frequencies that penetrate the seabed travel faster than the sound in water. (see Figure 2.12, right). Both phenomena, *head waves* and *frequency dispersion*, contribute to build air gun pulses of longer duration at longer distances from the source. This same behaviour for the received air gun pulses has been highlighted in other reports (Beland et al., 2013).

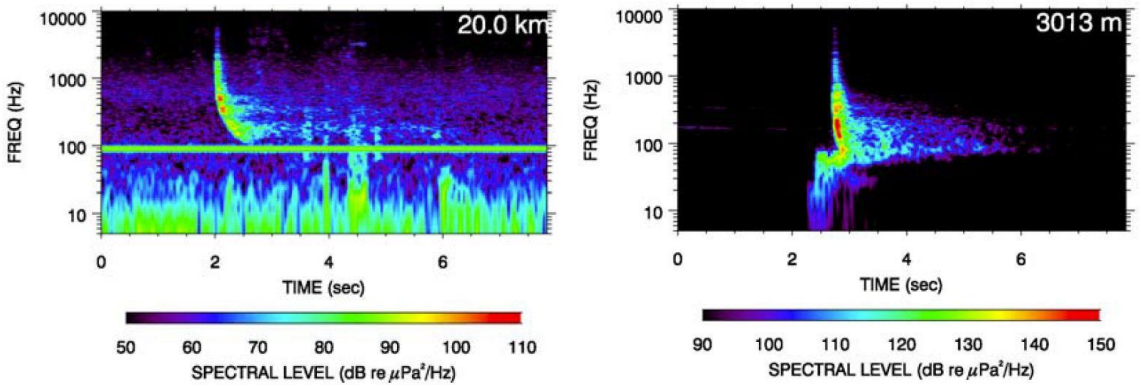

Figure 2.12 Spectrogram of 880 in^3 an air-gun pulse measured during a marine seismic survey in the Colville River Delta (from Hauser et al., 2008), in very shallow waters (< 15 m). The figures show the downward chirp effect caused by frequency dispersion (left) and the early arrival of the low frequency head wave (right).

Table 2.1 Sounds produced by single air guns and air gun arrays

Source (Configuration)	$V_{g,tot}$ [in^3]	h_w [m]	Characterised Direction	Measurement [dB re 1µPa]	SL [dB re 1µPa@1m]	Regression Equation	Signal Characteristics	Description	Reference
Single Air Gun	10	~35	All aspects combined	N/A	200.8 dB_{rms}	RL_{rms} = 200.8 - 16.6log_{10}r - 7.2·10^{-4}r, range of validity 100 m to 15 km. 90th percentile regression equation	T = 2 - 5 s	z_s = 1.5 m z_r = 1 m above seafloor Towed by vessel *Henry C.* Camden Bay, Beaufort Sea Broadband (f_s = 48 kHz)	Ireland et al., 2009
Single Air Gun	10	~35	All aspects combined	N/A	239.8 dB_{rms}	RL_{rms} = 239.8 - 28.8log_{10}r, range of validity 200 m to 15 km. 90th percentile regression equation	T = 4 s	z_s = 1.5 m z_r = 1 m above seafloor Towed by vessel *Alpha H.*. Camden Bay, Beaufort Sea Broadband (fs = 48 kHz)	Ireland et al., 2009
Single Air Gun	10	~40	All aspects combined	N/A	206.1 dB_{rms}	RL_{rms} = 206.1 - 17.3log_{10}r - 8.1·10^{-4}r, range of validity 200 m to 15 km. 90th percentile regression equation	T = 6 s	z_s = 2 m z_r = 1 m above seafloor Chukchi Sea Broadband (fs = 48 kHz)	Ireland et al., 2009
Single Air Gun	10	22	All aspects combined	N/A	209.8 dB_{rms}	RL_{rms} = 209.8 - 17.7log_{10}r - 2.62·10^{-3}r, range of validity 200 m to 10 km. 90th percentile regression equation	T = 3 s	z_s = 2.25 m z_r = 3 m above seafloor Beechey Point, Beaufort Sea, sandy sediment Broadband (fs = 16.4 kHz)	Funk et al., 2010
Single Air Gun	10	~45	All aspects combined	N/A	227.3 dB_{rms}	RL_{rms} = 227.3 - 27.5log_{10}r, range of validity 200 m to 20 km. 90th percentile regression equation	T ~ 18 s	z_s = 2 m z_r = 1 m above seafloor Chukchi Sea (~71N,168W) Broadband (fs = 48 kHz)	Reiser et al., 2010
Single Air Gun	10	~45	All aspects combined	N/A	204.4 dB_{rms}	RL_{rms} = 204.4 - 16log_{10}r - 8.2·10^{-4}r, range of validity 200 m to 20 km. 90th percentile regression equation	T ~ 6 s	z_s = 2 m z_r = 1 m above seafloor Chukchi Sea (~70.5N,164W) Broadband (fs = 48 kHz)	Reiser et al., 2010
Single Air Gun	10	15	NA	178.2 dB_{pk-pk} @ 120 m[a] 182.5 dB_{pk-pk} @ 120 m[b] 160 dB_{rms} @ 120 m[a] 161.7 dB_{rms} @ 120 m[b] 152.5 dB_{sel} @ 120 m[a] 152.5 dB_{sel} @ 120 m[b] Four-values averages	[a]213 dB_{pk-pk} [b]216 dB_{pk-pk} [a]186 dB_{rms} [b]186 dB_{rms} [a]195 dB_{sel} [b]195 dB_{sel}	RL_{pk-pk} = 213 -18log_{10}r RL_{pk-pk} = 216 -17log_{10}r RL_{rms} = 186 -19log_{10}r RL_{rms} = 186 -17log_{10}r RL_{sel} = 195 -19log_{10}r RL_{sel} = 195 -17log_{10}r Range of validity 6-1,300 m (all)	T = 10 s τ = 19-167 ms Peak frequency [a]37, [b]5, [b]113 Hz BW_{-10dB} = [a]64, [b]240 Hz	*Context*: impulsive source study for small mammal EIA *Area*: Aarhus Bay, Denmark *Seabed*: sandy, flat *Source*: HGS Sleeve Gun I z_s = 7.5 m, z_r = 7.5 m RMS 125 ms, SEL 1 s windows Broadband 5 Hz - 200 kHz Pressure [a]1700 psi, [b]790 psi	Hermannsen et al, 2015
Single Air Gun	20	10	All aspects combined	N/A	241.2 dB_{rms}	RL_{rms} = 241.2 - 26.3log_{10}r - 1.18·10^{-3}r, range of validity 40 m to 20 km. 90th percentile regression equation	T = 13 - 22 s (33.5 m)	z_s = 2 m z_r = 3 m above seafloor Colville River, Beaufort Sea Seismic vessel *Wiley Gunner* Broadband (fs = 48 kHz)	Hauser et al., 2008
		2		N/A	220.2 dB_{rms}	RL_{rms} = 220.2 - 21log_{10}r - 8.8·10^{-4}r, range of validity 80 - 800 m. 90th percentile regression equation RL_{rms} = 158.4 - 30.5log_{10}(r/800) - 1.7·10^{-2}(r-800), range of validity 0.8 - 2.5 km. 90th percentile regression equation	T = 13 - 22 s (33.5 m)	z_s = 2 m z_r ~ 1.5 m above seafloor Colville River, Beaufort Sea Seismic vessel *Wiley Gunner* Broadband (fs = 48 kHz)	

Table 2.1 Sounds produced by single air guns and air gun arrays (cont., part 2)

Source (Configuration)	$V_{g,tot}$ [in^3]	h_w [m]	Characterised Direction	Measurement [dB re 1µPa]	SL [dB re 1µPa@1m]	Regression Equation	Signal Characteristics	Description	Reference
Single Air Gun	20	10	All aspects combined	N/A	245.3 dB_{rms}	RL_{rms} = 245.3 - 29.7log_{10}r - 7.8·10^{-4}r, range of validity 200 m to 20 km. 90th percentile regression equation	T = 13 - 22 s (33.5 m)	z_s = 2 m z_r = 3 m above seafloor Colville River, Beaufort Sea Seismic vessel *Shirley V* Broadband (fs = 48 kHz)	Hauser et al., 2008
		2		N/A	196.3 dB_{rms}	RL_{rms} = 196.3 - 8.2log_{10}r - 2.09·10^{-2}r, range of validity 15 m to 3 km. 90th percentile regression equation	T = 13 - 22 s (33.5 m)	z_s = 2 m z_r ~ 1.5 m above seafloor Colville River, Beaufort Sea Seismic vessel *Shirley V* Broadband (fs = 48 kHz)	
Air Gun Cluster 2 Guns	20	22	All aspects combined	N/A	233.9 dB_{rms}	RL_{rms} = 233.9 - 25log_{10}r - 1.39·10^{-3}r, range of valuidity 200 m to 10 km. 90th percentile regression equation	T = 3 s	z_s = 2.25 m z_r = 3 m above seafloor Beechey Point, Beaufort Sea, sandy sediment Broadband (fs = 16.4 kHz)	Funk et al., 2010
Air Gun Cluster 2 Guns	20	30 - 40	All aspects combined	N/A	222.6 dB_{rms}	RL_{rms} = 222.6 - 21.1log_{10}r - 4.3·10^{-4}r, range of validity 200 m to 20 km. 90th percentile regression equation	T = 3 s	z_s = 2.25 m z_r = 3 m above seafloor Camden Bay, Beaufort Sea Sandy sediment Broadband (fs = 16.4 kHz)	Funk et al., 2010
Air Gun Cluster 2 Guns	20	~40	All aspects combined	N/A	211.1 dB_{rms}	RL_{rms} = 211.1 - 17.3log_{10}r - 6.1·10^{-4}r, range of validity 200 m to 15 km. 90th percentile regression equation	T = 6 s	z_s = 2 m z_r = 1 m above seafloor Chukchi Sea Broadband (fs = 48 kHz)	Ireland et al., 2009
Air Gun Cluster 2 Guns	20	~35	All aspects combined	N/A	207.3 dB_{rms}	RL_{rms} = 207.3 - 17.4log_{10}r - 8.5·10^{-4}r, range of validity 100 m to 15 km. 90th percentile regression equation	T = 2 - 5 s	z_s = 1.5 m z_r = 1 m above seafloor Towed by vessel *Henry C.* Camden Bay, Beaufort Sea Broadband (fs = 48 kHz)	Ireland et al., 2009
Air Gun Cluster 2 Guns	20	~35	All aspects combined	N/A	225.8 dB_{rms}	RL_{rms} = 225.8 - 23.4log_{10}r - 5.1·10^{-4}r, range of validity 200 m to 15 km. 90th percentile regression equation	T = 4 s	z_s = 1.5 m z_r = 1 m above seafloor Towed by vessel *Alpha H.* Camden Bay, Beaufort Sea Broadband (fs = 48 kHz)	Ireland et al., 2009
Air Gun Array 2 Guns in 1 x Sub Array	20	~45	All aspects combined	N/A	232.6 dB_{rms}	RL_{rms} = 232.6 - 27.2log_{10}r, range of validity 200 m to 20 km. 90th percentile regression equation	T ~ 18 s	z_s = 2 m z_r = 1 m above seafloor Chukchi Sea (~71N,168W) Broadband (fs = 48 kHz)	Reiser et al., 2010
Single Air Gun	25	15	N/A	178.5 dB_{pk-pk} @ 120 m[a] 183.7 dB_{pk-pk} @ 120 m[b] 159.7 dB_{rms} @ 120 m[a] 163.7 dB_{rms} @ 120 m[b] 151 dB_{sel} @ 120 m[a] 155 dB_{sel} @ 120 m[b] Four-values averages	[a]212 dB_{pk-pk} [b]214 dB_{pk-pk} [a]186 dB_{rms} [b]186 dB_{rms} [a]195 dB_{sel} [b]195 dB_{sel}	RL_{pk-pk} = 212 -18log_{10}r RL_{pk-pk} = 214 -16log_{10}r RL_{rms} = 186 -19log_{10}r RL_{rms} = 186 -17log_{10}r RL_{sel} = 195 -18log_{10}r RL_{sel} = 195 -16log_{10}r Range of validity 6-1,300 m (all)	T = 10 s τ = 20-100 ms Peak frequency [a]90, [b]6, [b]44 Hz BW_{-10dB} = [a]173, [b]178 Hz	*Context*: impulsive source study for small mammal EIA *Area*: Aarhus Bay, Denmark *Seabed*: sandy, flat *Source*: HGS Sleeve Gun I z_s = 7.5 m, z_r = 7.5 m RMS 125 ms, SEL 1 s windows Broadband 5 Hz - 200 kHz Pressure [a]1700 psi, [b]790 psi	Hermannsen et al, 2015

Table 2.1 Sounds produced by single air guns and air gun arrays (cont., part 3)

Source (Configuration)	$V_{g,tot}$ [in^3]	h_w [m]	Characterised Direction	Measurement [dB re 1µPa]	SL [dB re 1µPa@1m]	Regression Equation	Signal Characteristics	Description	Reference
Single Air Gun	30	~40	All aspects combined	N/A	253.1 dB_{rms}	RL_{rms} = 253.1 - 28.5$\log_{10}$r, range of validity 8 - 40 km. 90th percentile regression equation	T ~ 20 s	z_s = 6 m z_r = 1 m above seafloor Towing distance 276 m Chukchi Sea Broadband (fs = 48 kHz)	Ireland et al., 2009
		~20	All aspects combined	N/A	206.4 dB_{rms}	RL_{rms} = 206.4 - 14.9$\log_{10}$r, range of validity 80 m to 80 km. 90th percentile regression equation	T ~ 20 s	z_s = 6 m z_r = 1 m above seafloor Towing distance 276 m Harrison Bay, Beaufort Sea Broadband (fs = 48 kHz)	
Single Air Gun	30	~50	All aspects combined	N/A	183.2 dB_{rms}	RL_{rms} = 183.2 - 7.1$\log_{10}$r, range of validity 80 m to 1 km. 90th percentile regression equation RL_{rms} = 226.6 - 21.2$\log_{10}$r - 2.2·10^{-4}r, range of validity 1 - 50 km. 90th percentile regression equation	T ~ 10 s	z_s = 6 m z_r = 3 m above seafloor Towing distance 276 m Chukchi Sea Sandy sediment Broadband (fs = 16.4 kHz)	Funk et al., 2010
		~30	All aspects combined	N/A	188.2 dB_{rms}	RL_{rms} = 188.2 - 5.8$\log_{10}$r - 5.57·10^{-3}r, range of validity 200 m to 1.2 km. 90th percentile regression equation RL_{rms} = 239.3 - 24.9$\log_{10}$r - 4·10^{-4}r, range of validity 600 m to 50 km. 90th percentile regression equation	T ~ 10 s	z_s = 6 m z_r = 3 m above seafloor Towing distance 276 m Camden Bay, Beaufort Sea, sandy sediment Broadband (fs = 16.4 kHz)	
Single Air Gun	40	15	N/A	132 dB_{pk} @ 5 km	222 dB_{pk}	N/A	τ = 0.3 s Main energy at 100 Hz	z_s = 1 m Broadband 20 Hz - 1 kHz	Greene & Richardson, 1988
Single Air Gun (*Bolt 1900B*)	40	< 20	N/A	N/A	191 dB_{rms} [a] 193.5 dB_{rms} [b]	N/A	N/A	Broadband 1 Hz - 125 kHz Chamber [a]1500 psi, [b]2000 psi	Nedwell & Edwards, 2004
Single Air Gun	40	~2	Endfire (bow, stern)	N/A	245.6 dB_{rms}	RL_{rms} = 245.6 - 25.2$\log_{10}$r - 1.14·10^{-2}r, range of validity 200 m to 3 km. 90th percentile regression equation	N/A	z_s = 2 m z_r = 1 m above seafloor Prudhoe Bay, Beaufort Sea (inside island barrier) Broadband (fs = 96 kHz)	McPherson et al., 2012
Single Air Gun	40	~15	Endfire (bow, stern)	N/A	208.8 dB_{rms}	RL_{rms} = 208.8 - 13.6$\log_{10}$r - 4.39·10^{-3}r, range of validity 100 m to 8 km. 90th percentile regression equation	N/A	z_s = 2 m z_r = 1 m above seafloor Prudhoe Bay, Beaufort Sea (outside island barrier) Broadband (fs = 96 kHz)	McPherson et al., 2012
Single Air Gun	40	15	N/A	182 dB_{pk-pk} @ 120 m[a] 187.7 dB_{pk-pk} @ 120 m[b] 162 dB_{rms} @ 120 m[a] 167.7 dB_{rms} @ 120 m[b] 153.7 dB_{sel} @ 120 m[a] 159.7 dB_{sel} @ 120 m[b] Four-values averages	[a]213 dB_{pk-pk} [b]216 dB_{pk-pk} [a]186 dB_{rms} [b]186 dB_{rms} [a]195 dB_{sel} [b]195 dB_{sel}	RL_{pk-pk} = 217 -18$\log_{10}$r RL_{pk-pk} = 221 -17$\log_{10}$r RL_{rms} = 188 -18$\log_{10}$r RL_{rms} = 192 -18$\log_{10}$r RL_{sel} = 197 -18$\log_{10}$r RL_{sel} = 200 -17$\log_{10}$r Range of validity 6-1,300 m (all)	T = 10 s τ = 21-50 ms Peak frequency [a]6, [a]79, [b]40 Hz BW_{-10dB} = [a]185, [b]154 Hz	*Context*: impulsive source study for small mammal EIA *Area*: Aarhus Bay, Denmark *Seabed*: sandy, flat *Source*: HGS Sleeve Gun I z_s = 7.5 m, z_r = 7.5 m RMS 125 ms, SEL 1 s windows Broadband 5 Hz - 200 kHz Chamber [a]1700 psi, [b]790 psi	Hermannsen et al, 2015
Air Gun Array 4 Guns in 2 x Clusters	40	~40	All aspects combined	N/A	224.6 dB_{rms}	RL_{rms} = 224.6 - 20.2$\log_{10}$r - 6.8·10^{-4}r, range of validity 200 m to 15 km. 90th percentile regression equation	T = 6 s	z_s = 2 m z_r = 1 m above seafloor Chukchi Sea Broadband (fs = 48 kHz)	Ireland et al., 2009
Air Gun Array 4 Guns in 2 x Sub Arrays	40	~45	All aspects combined	N/A	218 dB_{rms}	RL_{rms} = 218 - 17.5$\log_{10}$r - 6.1·10^{-4}r, range of validity 200 m to 20 km. 90th percentile regression equation	T ~ 6 s	z_s = 2 m z_r = 1 m above seafloor Chukchi Sea (~70.5N,164W) Broadband (fs = 48 kHz)	Reiser et al., 2010

Table 2.1 Sounds produced by single air guns and air gun arrays (cont., part 4)

Source (Configuration)	$V_{g,tot}$ [in^3]	h_w [m]	Characterised Direction	Measurement [dB re 1µPa]	SL [dB re 1µPa@1m]	Regression Equation	Signal Characteristics	Description	Reference
Air Gun Array 4 Guns in 2 x Sub Arrays	40	~45	All aspects combined	N/A	231.3 dB_{rms}	RL_{rms} = 231.3 - 25.7log_{10}r, range of validity 200 m to 20 km. 90th percentile regression equation	T ~ 18 s	z_s = 2 m z_r = 1 m above seafloor Chukchi Sea (~71N,168W) Broadband (fs = 48 kHz)	Reiser et al., 2010
Single Air Gun	60	38	All aspects combined	N/A	205.6 dB_{rms}	RL_{rms} = 205.6 - 13.9og_{10}r - 9.3·10^{-4}r, range of validity 30 m to 10 km. 90th percentile regression equation	T ~ 4 s Main energy at 100 Hz	z_s = 6 m z_r = 3 m above seafloor Towing distance 394 m Chukchi Sea, West Barrow Sandy sediment Broadband (fs = 48 kHz)	Blees et al., 2010
Single Air Gun	70	< 8	Fwd. Endfire and broadside (bow, port, starboard combined)	N/A	243.4 dB_{rms}	RL_{rms} = 243.4 - 31.4log_{10}r - 8·10^{-4}r, range of validity 20 m to 8 km. 50th percentile regression equation (mean)	T = 12 s	z_s = 1.1 m z_r ~ 0.3 m above seafloor Prudhoe Bay, Beaufort Sea Sandy sediment Broadband (fs = 44.1 kHz)	Aerts et al., 2008
			Bwd. Endfire (stern)	N/A	200.9 dB_{rms}	RL_{rms} = 200.9 - 11.3log_{10}r - 7.2·10^{-3}r, range of validity 20 m to 8 km. 50th percentile regression equation (mean)			
Single Air Gun	70	55	Fwd. Endfire (bow)	N/A	213.5 dB_{rms}	RL_{rms} = 213.5 - 17log_{10}r - 2.6·10^{-4}r, range of validity 0.4 - 80 km. 90th percentile regression equation	T = 18-20 s	z_s = 8.5 m z_r = 50 m Chukchi Sea, cont. shelf Sandy sediment Broadband (fs = 96 kHz)	Beland et al., 2013
		550	Fwd. Endfire (bow)	N/A	230.8 dB_{rms}	RL_{rms} = 230.8 - 24.5log_{10}r, range of validity 2 - 8 km. 90th percentile regression equation		z_s = 8.5 m z_r = 50 m Beaufort Sea, cont. slope Sandy sediment Broadband (fs = 96 kHz)	
Air Gun Array 4 x 70 in^3 Guns	280	~ 30	Endfire (bow, stern combined)	N/A	233.4 dB_{rms} 242.7 dB_{pk} 203.9 dB_E	RL_{rms} = 233.4 - 22.2log_{10}r - 7.58·10^{-4}r RL_{pk} = 242.7 - 21.7log_{10}r - 6.31·10^{-4}r RL_E = 203.9 - 15.7log_{10}r - 7.47·10^{-4}r Range of validity 60 m to 20.5 km	T ~ 4 s Main energy at 100 Hz	z_s = 2.5 m z_r = 3 m above seafloor Towing distance 245 m 2000 psi chamber Broadband (fs = 44.1 kHz)	Patterson et al, 2007
Air Gun Array 8 Guns in 1 x Sub Array	320	~2	Endfire (bow, stern)	N/A	344.2 dB_{rms}	RL_{rms} = 344.2 - 65.9log_{10}r, range of validity 100 m to 7 km. 90th percentile regression equation	N/A	z_s = 1 m z_r = 1 m above seafloor *Flip flop* firing (2 x 320 in^3 sub arrays) Prudhoe Bay, Beaufort Sea (inside island barrier) Broadband (fs = 96 kHz)	McPherson et al., 2012
			Broadside (port, starboard)	N/A	283.7 dB_{rms}	RL_{rms} = 283.7 - 38.8log_{10}r, range of validity 200 m to 2 km. 90th percentile regression equation			
		~15	Endfire (bow, stern)	N/A	249.9 dB_{rms}	RL_{rms} = 249.9 - 23.6log_{10}r - 2.44·10^{-3}r, range of validity 100 m to 10 km. 90th percentile regression equation	N/A	z_s = 2 m z_r = 1 m above seafloor Flip flop firing (2 x 320 in3 sub arrays) Prudhoe Bay, Beaufort Sea (outside island barrier) Broadband (fs = 96 kHz)	
			Broadside (port, starboard)	N/A	227.6 dB_{rms}	RL_{rms} = 227.6 - 14.2log_{10}r - 3.78·10^{-3}r, range of validity 100 m to 6 km. 90th percentile regression equation			
Air Gun Array 3 Guns	330	34	N/A	135-161 dB_{rms} @ 3-10 km[a] 143-167 dB_{rms} @ 3-10 km[b] 146-158 dB_{rms} @ 3-10 km[c]	195.3 dB_{rms}	RL_{rms} = 195.3 - 10log_{10}r - 9·10^{-4}r, range of validity 2 to 25 km.	N/A	z_r = [a]3, [b]9, [c]18 m Broadband 20 Hz - 1 kHz	Greene & Richardson, 1988

Table 2.1 Sounds produced by single air guns and air gun arrays (cont., part 5)

Source (Configuration)	$V_{g,tot}$ [in^3]	h_w [m]	Characterised Direction	Measurement [dB re 1µPa]	SL [dB re 1µPa@1m]	Regression Equation	Signal Characteristics	Description	Reference
Air Gun Array 8 Guns in 2 x Sub-Arrays (*1 Sub-Array*)	440	< 8	Bwd. Endfire and broadside (stern, port, starboard combined)	N/A	233.3 dB_{rms}	RL_{rms} = 233.3 - 27.6log_{10}r - 2.4·10^{-3}r, range of validity 100 m to 8 km. 50th percentile regression equation (mean)	T = 12 s (6 s ping pong)	z_s = 1.8 m z_r ~ 0.3 m Towing distance 8-10 m Prudhoe Bay, Beaufort Sea Sandy sediment Broadband (fs = 44.1 kHz)	Aerts et al., 2008
			Fwd. Endfire (bow)	N/A	234.6 dB_{rms}	RL_{rms} = 234.6 - 20.8log_{10}r - 7.3·10^{-3}r, range of validity 40 m to 1.5 km. 50th percentile regression equation (mean)			
Air Gun Array 4 Guns in 2 x Sub-Arrays	440	< 8	Bwd. Endfire and broadside (stern, port, starboard combined)	N/A	243.8 dB_{rms}	RL_{rms} = 243.4 - 33.8og_{10}r, range of validity 100 m to 6 km. 50th percentile regression equation (mean)	T = 12 s (6 s *ping pong*)	z_s = 1.1 m z_r ~ 0.3 m above seafloor Prudhoe Bay, Beaufort Sea Sandy sediment Broadband (fs = 44.1 kHz)	Aerts et al., 2008
			Fwd. Endfire (bow)	N/A	216.9 dB_{rms}	RL_{rms} = 216.9 - 19.3log_{10}r - 4.6·10^{-3}r, range of validity 20 m to 8 km. 50th percentile regression equation (mean)			
Air Gun Array 16 Guns in 2 x Sub Arrays	640	~15	Endfire (bow, stern)	N/A	248.7 dB_{rms}	RL_{rms} = 248.7 - 21.2log_{10}r - 2.87·10^{-3}r, range of validity 400 m to 40 km. 90th percentile regression equation	N/A	z_s = 2 m z_r = 1 m above seafloor *Simultaneous* firing (2 x 320 in^3 sub arrays) Prudhoe Bay, Beaufort Sea (outside island barrier) Broadband (fs = 96 kHz)	McPherson et al., 2012
			Broadside (port, starboard)	N/A	235.2 dB_{rms}	RL_{rms} = 235.2 - 16log_{10}r - 3.61·10^{-3}r, range of validity 100 m to 5 km. 90th percentile regression equation			
Air Gun Array 8 Guns in 2 x Sub-Arrays (*Full Array*)	880	< 8	Fwd. Endfire and broadside (bow, port, starboard combined)	N/A	264 dB_{rms}	RL_{rms} = 264 - 36.7log_{10}r - 7·10^{-4}r, range of validity 40 m to 9 km. 50th percentile regression equation (mean)	T = 12 s	z_s = 1.8 m z_r ~ 0.3 m above seafloor Towing distance 8-10 m Prudhoe Bay, Beaufort Sea Sandy sediment Broadband (fs = 44.1 kHz)	Aerts et al., 2008
			Bwd. Endfire (stern)	N/A	230.9 dB_{rms}	RL_{rms} = 230.9 - 18.0log_{10}r - 4.7·10^{-3}r, range of validity 40 m to 1.5 km. 50th percentile regression equation (mean)			
Air Gun Array 10 Guns in 2 x Sub-Arrays [*1]	880	10	Fwd. Endfire (bow)	N/A	237.6 dB_{rms}	RL_{rms} = 237.6 - 23.7log_{10}r - 1.16·10^{-3}r, range of validity 40 m to 25 km. 90th percentile regression equation	T = 13 - 22 s (33.5 m)	z_s = 2 m z_r = 3 m above seafloor Colville River, Beaufort Sea Broadband (fs = 48 kHz). Subarrays installed at both sides of the stern, 1.5 m from port and starboard. Source model Bolt 600 C. Pressure of operation 1900 psi. Installed in the *Wiley Gunner* vessel	Hauser et al., 2008
			Broadside (port, starboard)	N/A	245.4 dB_{rms}	RL_{rms} = 245.4 - 24.7log_{10}r - 8.7·10^{-4}r, range of validity 200 m to 20 km. 90th percentile regression equation			
		2	Fwd. Endfire (bow)	N/A	317.0 dB_{rms}	RL_{rms} = 317.0 - 54.1log_{10}r, range of validity 200 m to 5 km. 90th percentile regression equation	T = 13 - 22 s (33.5 m)	z_s = 2 m z_r ~1.5 m above seafloor Colville River, Beaufort Sea Broadband (fs = 48 kHz). Subarrays installed at both sides of the stern, 1.5 m from port and starboard. Source model Bolt 600 C. Pressure of operation 1900 psi. Installed in the *Wiley Gunner* vessel	
			Broadside (port, starboard)	N/A	245.4 dB_{rms}	RL_{rms} = 245.4 - 24.7log_{10}r - 8.7·10^{-4}r, range of validity 200 m to 20 km. 90th percentile regression equation			

Table 2.1 Sounds produced by single air guns and air gun arrays (cont., part 6)

Source (Configuration)	$V_{g,tot}$ [in^3]	h_w [m]	Characterised Direction	Measurement [dB re 1µPa]	SL [dB re 1µPa@1m]	Regression Equation	Signal Characteristics	Description	Reference
Air Gun Array 10 Guns in 2 x Sub-Arrays[*1]	880	10	Fwd. Endfire (bow)	N/A	211.9 dB_{rms}	RL_{rms} = 211.9 - 11.8log_{10}r - 7.8·10^{-3}r, range of validity 20 m to 1 km. 90th percentile regression equation RL_{rms} = 168.8 - 42.7log_{10}(r/10^3) - 4.1·10^{-4}(r-10^3), range of validity 1 - 25 km. 90th percentile regression equation	T = 13 - 22 s (33.5 m)	z_s = 2 m z_r = 3 m above seafloor Colville River, Beaufort Sea Broadband (fs = 48 kHz). Subarrays installed at both sides of the stern, 1.5 m from port and starboard. Source model Bolt 600 C. Pressure of operation 1900 psi. Installed in vessel *Shirley V*	Hauser et al., 2008
			Broadside (port, starboard)	N/A	230.3 dB_{rms}	RL_{rms} = 230.3 - 18.1log_{10}r - 1.46·10^{-3}r, range of validity 200 m to 20 km. 90th percentile regression equation			
		2	Fwd. Endfire (bow)	N/A	322.2 dB_{rms}	RL_{rms} = 322.2 - 54.3log_{10}r, range of validity 80 - 800 m. 90th percentile regression equation	T = 13 - 22 s (33.5 m)	z_s = 2 m z_r ~1.5 m above seafloor Colville River, Beaufort Sea Broadband (fs = 48 kHz). Subarrays installed at both sides of the stern, 1.5 m from port and starboard. Source model Bolt 600 C. Pressure of operation 1900 psi. Installed in vessel *Shirley V*	
			Broadside (port, starboard)	N/A	255.4 dB_{rms}	RL_{rms} = 255.4 - 28.1log_{10}r - 3.3·10^{-3}r, range of validity 100 m to 10 km. 90th percentile regression equation			
Air Gun Array 8 Guns in 1 x Sub-Array	1049	~ 40	Fwd. Endfire (bow)	N/A	253.1 dB_{rms} 260.4 dB_{pk} 222.2 dB_E	RL_{rms} = 253.1 - 26.0log_{10}r RL_{pk} = 260.4 - 25.0log_{10}r RL_E = 222.2 - 17.9log_{10}r Range of validity 300 m to 30 km	T ~ 19 s	z_s = 6 m z_r = 3 m above seafloor Towing distance 245 m 2000 psi chamber Broadband (fs = 44.1 kHz)	Patterson et al, 2007
			Bwd. Endfire (stern)	N/A	240.6 dB_{rms} 245.7 dB_{pk} 216.9 dB_E	RL_{rms} = 240.6 - 22.8log_{10}r - 1.87·10^{-4}r RL_{pk} = 245.7 - 20.9log_{10}r - 2.25·10^{-4}r RL_E = 216.9 - 16.5log_{10}r - 3.06·10^{-4}r Range of validity 300 m to 30 km			
			Broadside (port, starboard combined)	N/A	242.2 dB_{rms} 247.2 dB_{pk} 210.7 dB_E	RL_{rms} = 242.2 - 19.9log_{10}r RL_{pk} = 247.2 - 17.7log_{10}r RL_E = 210.7 - 11.6log_{10}r Range of validity 200 m to 1.2 km			
Air Gun Array 3 Guns	1150	150-3,500	Multiple	185.5 dB_{pk} @ 300 m 191.5 dB_{pk-pk} @ 300 m	235 dB_{pk} 241 dB_{pk-pk}	TL = 20log_{10}r	τ = 0.02 s Main energy < 1 kHz	Context: airgun measurement experiment in Aug 2009 *Area:* Beaufort Sea z_r = 150 m Broadband 10 Hz - 1 kHz	Keen et al., 2018
		330-3,500	Multiple	110 dB_{rms} @ 290 km 128 dB_{pk-pk} @ 290 km 116 dB_E @ 290 km	223.4 dB_{rms} 235 dB_{pk-pk} 179.8 dB_E	RL_{rms} = 223.4 - 20.4log_{10}r RL_{pk-pk} = 235 - 19.2log_{10}r RL_E = 279.8 - 11.5log_{10}r Range of validity 290 m to 750 km	τ = 4-9 s Upward frequency sweep (dispersion)	*Context*: geophysical survey in Sep-Oct 2007 *Area*: Point Barrow (AK) Receiver in Chukchi Shelf (h_w=328 m), source in Beaufort Sea (h_w=2-3 km) z_r = 10 m above seafloor Broadband 10 Hz - 1 kHz	
Air Gun Array	1403	110 - 130	N/A	119 dB_{rms} @ 52 km 110 dB_{rms} @ 73 km	201.8 dB_{rms}	RL_{rms} = 201.8 - 10log_{10}r - 6.1·10^{-4}r Range of validity 8 to 80 km. Equation from combined 1403 and 2868 in^3 array data	N/A	z_r = 18 Broadband 20 Hz - 1 kHz	Greene & Richardson, 1988
Air Gun Array	1709	20	N/A	179 dB_{rms} @ 1.9 km 150 dB_{rms} @ 11.1 km	239.9 dB_{rms}	RL_{rms} = 239.9 - 20log_{10}r - 9.7·10^{-4}r Range of validity 1 to 15 km	τ = 0.2 s	z_r = 18 m Broadband 20 Hz - 1 kHz	Greene & Richardson, 1988
Air Gun Array 12 Guns	2868	20	All aspects combined	143 - 160 dB_{rms} @ 12-17 km	201.8 dB_{rms}	RL_{rms} = 201.8 - 10log_{10}r - 6.1·10^{-4}r Range of validity 8 to 80 km . Equation from combined 1403 and 2868 in^3 array data	N/A	Broadband 20 Hz - 1 kHz	Greene & Richardson, 1988
		44		147 - 157 dB_{rms} @ 9-20 km					

Table 2.1 Sounds produced by single air guns and air gun arrays (cont., part 7)

Source (Configuration)	$V_{g,tot}$ [in^3]	h_w [m]	Characterised Direction	Measurement [dB re 1µPa]	SL [dB re 1µPa@1m]	Regression Equation	Signal Characteristics	Description	Reference
Air Gun Array 26 Guns in 3 x Sub-Arrays	3000	~40	Endfire (bow, stern)	N/A	235.1 dB_{rms}	RL_{rms} = 235.1 - 17.5log_{10}r - 5.1·10^{-4}r, range of validity 100 m to 6 km. 90th percentile regression equation	T ~ 10 s (*ping pong with 2 x 3000 in^3 arrays*)	z_s = 6 m z_r = 3 m above seafloor Broadband (fs = 48 kHz)	Blees et al., 2010
			Broadside (port, starboard)	N/A	243.7 dB_{rms}	RL_{rms} = 243.7 - 19.7log_{10}r - 1.7·10^{-4}r, range of validity 100 m to 6 km. 90th percentile regression equation			
Air Gun Array 24 Guns in 3 x Sub-Arrays	3147	~ 40	Fwd. Endfire (bow)	N/A	249.5 dB_{rms} 266.4 dB_{pk} 224.6 dB_E	RL_{rms} = 249.5 - 22.3log_{10}r - 3.25·10^{-4}r RL_{pk} = 266.4 - 24.3log_{10}r - 9.45·10^{-5}r RL_E = 224.6 - 16.1log_{10}r - 3.54·10^{-4}r Range of validity 300 m to 30 km	T ~ 19 s	z_s = 6 m z_r = 3 m above seafloor Towing distance 245 m 2000 psi chamber Broadband (fs = 44.1 kHz)	Patterson et al, 2007
			Bwd. Endfire (stern)	N/A	247.2 dB_{rms} 249.8 dB_{pk} 221.0 dB_E	RL_{rms} = 247.2 - 22.4log_{10}r - 2.05·10^{-4}r RL_{pk} = 249.8 - 19.9log_{10}r - 2.24·10^{-4}r RL_E = 221.0 - 15.4log_{10}r - 3.55·10^{-4}r Range of valuidity 300 m to 30 km			
			Broadside (port, starboard combined)	N/A	239.7 dB_{rms} 249.8 dB_{pk} 222.9 dB_E	RL_{rms} = 239.7 - 19.0log_{10}r RL_{pk} = 249.8 - 19.7log_{10}r RL_E = 222.9 - 15.4log_{10}r Range of valuidity 500 m to 5 km			
Air Gun Array 24 Guns in 3 x Sub-Arrays	3147	~50	Endfire (bow, stern)	N/A	254.8 dB_{rms}	RL_{rms} = 254.8 - 24.4log_{10}r - 9·10^{-5}r, range of validity 100 m to 20 km. 90th percentile regression equation. Receiver 95 km offseted from source track RL_{rms} = 279.9 - 28.7log_{10}r - 4·10^{-4}r, range of validity 18 - 70 km. 90th percentile regression equation. Receiver aligned with source track	T ~ 10 s	z_s = 6 m z_r = 3 m above seafloor Towing distance 276 m Chukchi Sea Sandy sediment Broadband (f_s = 48 kHz)	Funk et al., 2008
			Broadside (port, starboard)	N/A	231.8 dB_{rms}	RL_{rms} = 231.8 - 14.9log_{10}r, range of validity 100 m to 2 km. 90th percentile regression equation RL_{rms} = 327 - 43log_{10}r, range of validity 2-100 km. 90th percentile regression equation			
		~30	Fwd. Endfire (bow)	N/A	247.6 dB_{rms}	RL_{rms} = 247.6 - 19.9log_{10}r - 4.1·10^{-4}r, range of validity 600 m to 60 km. 90th percentile regression equation	T ~ 10 s	z_s = 6 m z_r = 3 m above seafloor Towing distance 276 m Camdem Bay, Beaufort Sea, sandy sediment Broadband (f_s = 48 kHz)	
			Broadside (port, stern)	N/A	262.5 dB_{rms}	RL_{rms} = 262.5 - 24.6log_{10}r - 4·10^{-4}r, range of validity 500 m to 50 km. 90th percentile regression equation			
Air Gun Array 24 Guns in 3 x Sub-Arrays	3147	~40	Endfire (bow, stern)	N/A	241.6 dB_{rms}	RL_{rms} = 241.6 - 20log_{10}r - 4.4·10^{-4}r, range of validity 400 m to 10 km. 90th percentile regression equation RL_{rms} = 157.2 - 35.3log_{10}(r/10^4) - 6.4·10^{-6}(r-10^4), range of validity 10 - 100 km. 90th percentile regression equation	T ~ 10 s (2 x arrays in *flip flop* mode)	z_s = 6 m z_r = 1 m above seafloor Towing distance 276 m Chukchi Sea Broadband (f_s = 48 kHz)	Ireland et al., 2009
			Broadside (port, starboard)	N/A	241.9 dB_{rms}	RL_{rms} = 241.9 - 18.5log_{10}r - 4.1·10^{-4}r, range of validity 400 m to 40 km. 90th percentile regression equation			
		~20	Endfire (bow, stern)	N/A	207 dB_{rms}	RL_{rms} = 207 - 10.2log_{10}r - 6.6·10^{-4}r, range of validity 1 - 50 km. 90th percentile regression equation	T ~ 10 s (2 x arrays in *flip flop* mode)	z_s = 6 m z_r = 1 m above seafloor Towing distance 276 m Harrison Bay, Beaufort Sea Broadband (f_s = 48 kHz)	
			Broadside (port, starboard)	N/A	228 dB_{rms}	RL_{rms} = 228.0 - 12.2log_{10}r - 2.054·10^{-3}r, range of valuidity 500 m to 10 km. 90th percentile regression equation			

Table 2.1 Sounds produced by single air guns and air gun arrays (cont., part 8)

Source (Configuration)	$V_{g,tot}$ [in^3]	h_w [m]	Characterised Direction	Measurement [dB re 1µPa]	SL [dB re 1µPa@1m]	Regression Equation	Signal Characteristics	Description	Reference
Air Gun Array 40 Guns (26 Active)	3280 (active)	55-70	Multiple	135 dB_{rms} @ 35 km 151 dB_{pk-pk} @ 35 km 135 dB_E @ 35 km	374.3 dB_{rms} 363.6 dB_{pk-pk} 356.9 dB_E	$RL_{rms} = 374.3 - 51.8\log_{10}r$ $RL_{pk-pk} = 363.6 - 45.9\log_{10}r$ $RL_E = 356.9 - 47.9\log_{10}r$ Range of validity 35 to 100 km	τ = 1-3 s Downward frequency sweep (dispersion)	*Context*: seismic survey in Aug-Oct 2013 *Area*: Chukchi Sea (AK) z_r = 10 m above seafloor Broadband 10 Hz - 1 kHz NOTE: Excessive source level and transmission loss. Independent concurrent report from Cate et al. (2014) gives $RL_{rms} = 244.9 - 21.3\log_{10}r - 2.6{\cdot}10^{-4}$, range of validity 0.5-100 km	Keen et al., 2018
Air Gun Array 36 Guns in 4x Sub-Arrays	3320	~40	Endfire (bow, stern)	N/A	262.6 dB_{rms}	$RL_{rms} = 262.6 - 25.9\log_{10}r - 3.3{\cdot}10^{-4}r$, range of validity 0 to 55 km. 90th percentile regression equation	T ~ 18-22 s (46 m)	z_s = 8.5 m z_r = 1.5 m above seafloor Towing distance 50 m Chukchi Sea Broadband (fs = 32 kHz)	Ireland et al., 2007
			Broadside (port, starboard)	N/A	232.8 dB_{rms}	$RL_{rms} = 232.8 - 15.8\log_{10}r - 8.1{\cdot}10^{-4}r$, range of validity 0.5 to 20 km. 90th percentile regression equation			
Air Gun Array	3955	100	N/A	N/A	262.9 dB_{rms} [a]	N/A	N/A	Broadband 1 Hz - 125 kHz [a]The author mentions that this high level could be the result of an error in the TL calculation	Nedwell & Edwards, 2004
Air Gun Array	3960	50 - 200	Broadside	193.6 dB_{rms} @ 180 m	246.4 dB_{rms}	$RL_{rms} = 246.4 - 24.8\log_{10}r$	T = 10 s	N/A	LePage et al., 1995
Air Gun Array 14 Guns in 2 x Sub-Arrays	4380	55	Fwd. Endfire (bow)	N/A	230.2 dB_{rms}	$RL_{rms} = 230.2 - 16.3\log_{10}r - 2.6{\cdot}10^{-4}r$, range of validity 1 - 80 km. 90th percentile regression equation	T = 18-20 s	z_s = 8.5 m z_r = 3 m above seafloor Chukchi Sea, cont. shelf Sandy sediment Ice covered waters (>80%) Broadband (fs = 96 kHz)	Beland et al., 2013
			Broadside (port, starboard)	N/A	204.7 dB_{rms}	$RL_{rms} = 204.7 - 6.8\log_{10}r - 8.4{\cdot}10^{-4}r$, range of validity 0.4 - 20 km. 90th percentile regression equation			
		550	Fwd. Endfire (bow)	N/A	209.9 dB_{rms}	$RL_{rms} = 209.9 - 14.7\log_{10}r - 1.9{\cdot}10^{-4}r$, range of validity 3 - 30 km. 90th percentile regression equation		z_s = 8.5 m z_r = 3 m above seafloor Beaufort Sea, cont. slope Sandy sediment Ice covered waters (>80%) Broadband (fs = 96 kHz)	
			Broadside (port, starboard)	N/A	275.1 dB_{rms}	$RL_{rms} = 275.1 - 30.3\log_{10}r$, range of validity 3 - 30 km. 90th percentile regression equation			

2.2 The Sparker

The plasma sound source, more commonly known as *sparker*, is a relatively high powered, low-frequency acoustic source which produces an intense acoustic pulse by an electrical discharge. The pulse covers a relative broad frequency band, from 50 to 4,000 kHz, with source levels typically in the range of 210-220 dB_{rms}. It can only operate in salt water, in order to meet the conductivity requirements of the system. The sparker provides good vertical resolution (0.5 – 10 m) and reasonable sea floor penetration (< 1 km).

A large electrical charge is stored in a capacitor bank, which when released, generates an electrical arc between two electrodes in the conductive fluid (salt water). A vapour bubble is formed, which grows and collapses until the equilibrium state is reached. The implosion of the bubbles creates the shock wave (Duchesne & Bellefleur, 2007).

Sparkers were very popular during the 1960s before being replaced by small-volume air guns (Trabant, 1984). The lower penetration of sparkers compared to air guns, the complexity of the acoustic signature, the danger associated to the high voltages and electrical charges necessary to generate the spark or the disruption or damage of nearby equipment by the powerful electromagnetic interference produced by the spark are some of the drawbacks associated to this source (Duchesne & Bellefleur, 2007; Trabant, 1984; Nedwell, 1994). However, since the 1990s the sparker technology has regained popularity because of the low cost and simple deployment, but also because it still can be used in certain areas where air guns are restricted due to environmental concerns (Duchesne & Bellefleur, 2007).

The acoustic signature of the sparker is long and complex. The electric discharge creates a series of secondary bubbles that extend the duration of the pulse (25 – 50 ms) and attenuate frequencies of interest, by the effect of their destructive interference. The variable discharge paths associated with the array of electrodes add more complexity to the signature (Duchesne & Bellefleur, 2007). Figure 2.13 shows a typical spark signature, with arrows pointing to the secondary bubble pulses.

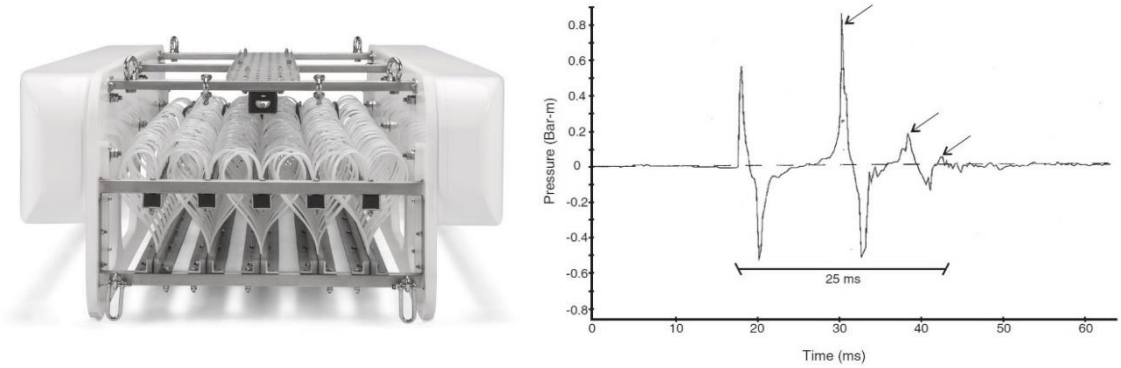

Figure 2.13 Sparker Dura-Spark (left, from www.appliedacoustics.com) and acoustic signature of an 8 kJ sparker array; arrows point to the secondary pulses (from Duchesne & Bellefleur, 2007).

2.2.1 Tables

Table 2.2 Sounds produced by sparkers

Source (*Model*)	h_w [m]	Measurement [dB re 1µPa]	SL [dB re 1µPa@1m]	Signal Characteristics	Description	Reference
Sparker (General)	N/A	N/A	216-222 dB_{pk}	Pulsed τ = 1-5 ms	N/A	Cluster Maritime Français, 2014
Sparker single	N/A	212 dB_{pk}@ 0.25 m[a]	200 dB_{pk}	Pulsed τ = 0.2 ms (3 µs main peak)	8 kV sparker, 1 mm electrode gap Tested in tank [a] TL = 20·log$_{10}$r	Nedwell, 1994
Sparker single	N/A	N/A	221 dB_{pk}	N/A	30 kJ sparker	Richardson et al, 1995
Sparker single (*Squid 500*)	N/A	N/A	216 dB_{rms}	τ = 1-5 ms	Maximum energy output 1200 J	Applied Acoustics, 2008
Sparker single (*Squid 2000*)	N/A	N/A	222 dB_{rms}	τ = 1-5 ms	Maximum energy output 2500 J	Applied Acoustics, 2008
Minisparker single (*Squid*)	< 200 m	N/A	209 dB_{rms}	Pulsed T = 4-6 s τ = 0.8 ms Frequency range 150-1700 Hz Main energy at 900 Hz	Towed close to surface (< 1 m) Energy input 1.5 kJ	USGS, 2000

2.3 The Boomer

The boomer is an electro-mechanical acoustic source, which produces a short-duration, broadband pulse by sending an electrical impulse to two spring-loaded plates. Boomers consist of an electrical coil magnetically coupled to a metallic plate and attached on the other side to a moving diaphragm. The energy contained in the capacitors is discharged into the coil, so the induced magnetic field causes the diaphragm to vibrate, radiating sound into the water. The higher energy transmitted into the plate will result in a longer and lower frequency pulse (Applied Acoustics, 2013).

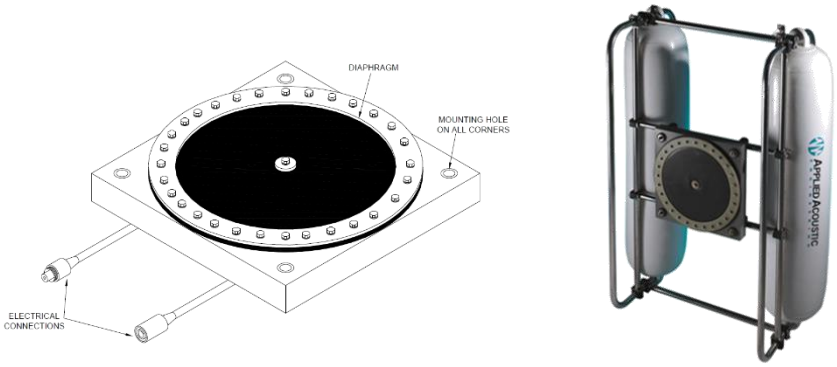

Figure 2.14 Sketch of an AA2xx boomer plate (left) and photo of the A200 system (from www.appliedacoustics.com)

The source operates in a frequency range from 0.3 to 6 kHz, with the dominant frequency between 1.5 and 3 kHz (see Figure 2.15). Source levels are in the range of 205-225 dB_{rms}. The frequency response of the boomer is in the higher end of the spectrum for seismic sources, and is characterised by vertical resolutions of 0.5 to 1 m and penetration of 25 to 50 m. The system is commonly mounted on a sled and towed behind the boat. Boomer systems have similar resolution and penetration capabilities to chirp sonar (see subsection 3.4.1); the magnitude of the acoustic output and frequency range provide boomers with greater penetration depths, but rather lower horizontal and vertical resolutions (Dix et al; Genesis, 2011).

Boomer data has some particularities that make it difficult to be processed. Some of these include: low signal to noise ratio, variations in the acoustic signature, hemispherical spreading which results in lack of focusing, and the way in which the signal becomes attenuated in sediments (Dix et al, n.d.).

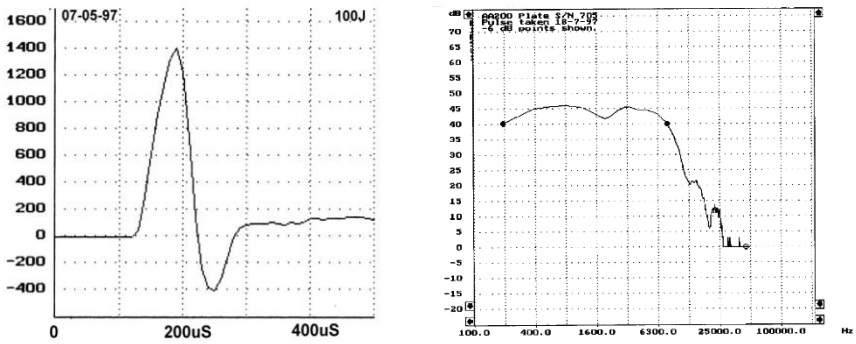

Figure 2.15 Typical pulse signature (left) and spectrum (right) of an AA200 boomer plate system (from Applied Acoustics, 2013).

2.3.1 Tables

Table 2.3 Sounds produced by boomers

Source (*Model*)	h_w [m]	SL [dB re 1µPa@1m]	Signal Characteristics	Description	Reference
Boomer (General)	N/A	212-215 dB_{pk}	τ = 0.12 - 0.4 ms	N/A	Cluster Maritime Français, 2014
Boomer (*Huntec*)	>200	205 dB_{rms}	T = 0.5-1 s τ = 0.34 ms Frequency range 0.5-8 kHz Main energy at 4.5 kHz	z_s = 10 - 100 m Energy input 340 J	USGS, 2000
Boomer (*AA301*)	N/A	209 dB_{rms} 215 dB_{rms}[a]	τ = 150-400 µs	Measured BW = 0.5-300 kHz [a]Energy input 300 J	Genesis, 2011; Applied Acoustics, 2010
Boomer (*GeoPulse*)	N/A	227 dB_{rms}	τ = < 0.2 ms	5313B transducer Energy input 280 J	Ashtead, 2014

2.4 The Marine Vibrator

In a *marine vibrator*, a moving plate oscillates in a controlled manner, excited by a hydraulic or electrical system (Tasker & Weir, 1998; OGP, 2011). The usual signal is a *chirp*, a frequency sweep in the range of 5 – 100 Hz with a typical duration of 10 s.

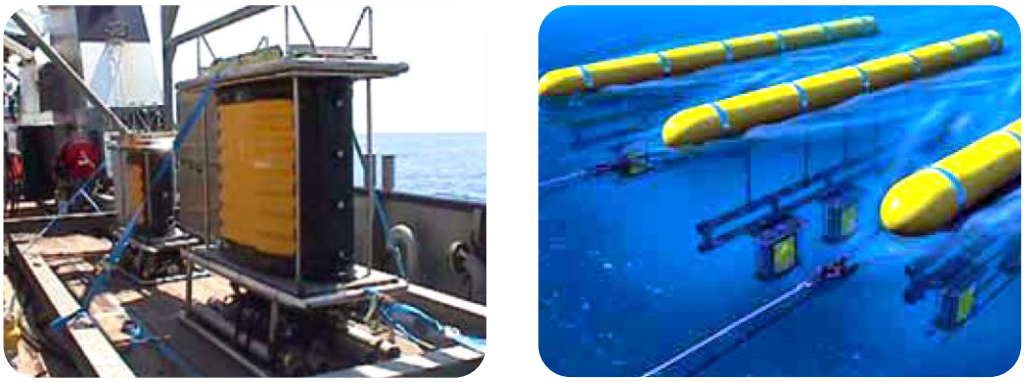

Figure 2.16 Marine vibrator unit (left) and illustration of the deployment of an array of marine vibrators (right). From OGP (2011).

The seismic image generated from a single marine vibrator after correlation is comparable to that from an air gun sub-array. However, its low frequency response has historically been poor, and has also suffered from frequent mechanical failure when compared to air guns (Tasker & Weir, 1998; OGP, 2011), although recent updates have further improved its acoustic behaviour. As complex mechanical systems, the dynamic response of marine vibrators experience non-linear effects and high-frequency harmonics (Sörnmo et al, 2016). These factors have resulted in a limited use of marine vibrators in the offshore industry.

However, the marine vibrator offers numerous environmental and operational advantages:

- The emitted acoustic energy is spread over time, for instance several seconds compared to the few hundred of milliseconds duration of an air gun signature, and that results in a lower instantaneous sound pressure level (Bird, 2003). A typical air gun array will generate 255 $dB_{0\text{-}p}$, whereas an array of four marine vibrators will generate approximately 223 $dB_{0\text{-}p}$ (Bird, 2003).
- Characteristics of the output signal such as frequency, amplitude and duration can be directly controlled. Having precise control on the acoustic output can reduce the environmental impact even further by attenuating the frequencies that are critical for marine life (Sönmo et al, 2016); but also means that the emitted signal is known, so that it can be used to extract the reflection information from the recorded data by correlation (Tasker & Weir, 1998).
- There is a deep understanding of the physics involved in the mechanical and acoustic behaviour of marine vibrators (OGP, 2011).
- The source depth affects the low frequency content of the emitted signal and its ability to penetrate the deeper layers of the seafloor. Marine vibrators can generate a full acoustic output at source depths as little as 1 m, which makes them better suited than air guns to shallow waters and transition zone environments. Moreover, the sound levels produced by these devices are considerably smaller than those from air guns, which contributes to reduce the acoustic impact in shallow waters, ecologically rich areas where the likelihood of affecting marine life is even higher (Bird, 2003; Tengham, 2006).
- Can be used as a standard towed acoustic source in shallow water, or as a stationary source in transition zone environments (Tengham, 2006).
- Requires only an electrical power supply and can be easily transported (Tengham, 2006).

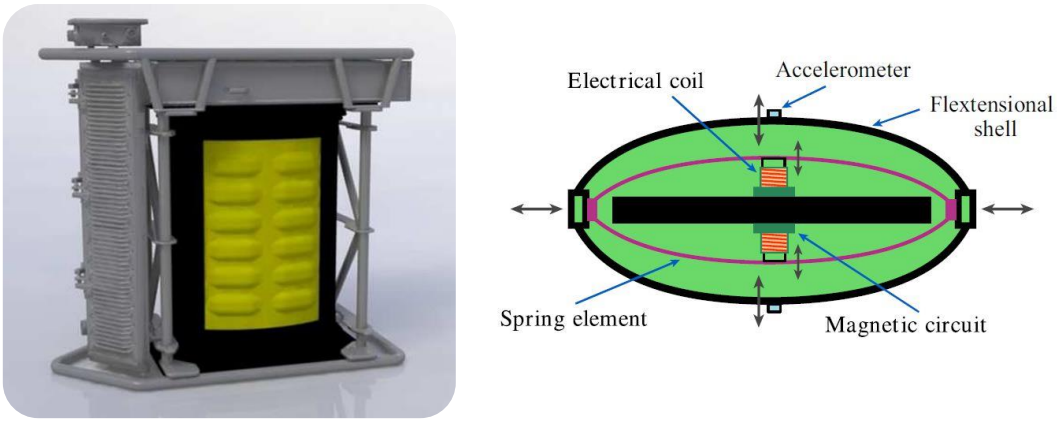

Figure 2.17 3D rendered image of a marine vibrator (left) and schematic of the principle of operation of the transducer (right) (from Sörnmo et al, 2016).

Constructing marine vibrators with high efficiency and linear dynamics is however difficult, and these systems suffer from friction, backlash and high-order harmonics (Sönmo et al, 2016; Tasker and Weir, 1998). Detailed descriptions of the mechanical design of marine vibrators can be found in Graydon & Delbert (1969), Tenghamn (2006), and Tenghamn (2009). Nevertheless, some advances have been achieved in the last few years and a Joint Industry Program is taking place to develop and test marine vibrators (Jenkerson et al., 2018; Feltham et al, 2016). In this project, three major oil and gas companies (Total, Shell and ExxonMobil) contribute with their own prototype. The systems have already been built and tested, and the results are currently being analysed to determine whether they fulfil the required technical specifications. Other companies are contributing with their own systems, each at a different stage of development. Among these companies are PGS, Applied Physical Sciences, Teledyne, CGG, Schlumberger, Geokinetics and GPUSA.

2.5 The Water Gun

Water guns appeared after the air gun as a new alternative to explosive charges. Today, the water gun is rarely used in seismic acquisition (Landrø & Amundsen, 2010), but it still can be found in certain research activities.

The operation of the water gun is similar to that from an air gun, with the difference that a volume of water is released instead of air. The same physical principle involved in the sound produced by a snapping shrimp is used by the water gun; strong local velocity variations will cause low pressure cavities, which will produce a high intensity pulse when collapsing by the effect of the hydrostatic pressure (Landrø & Amundsen, 2010). The activation process can be summarised in these four steps: 1) after release, the compressed air in the chamber propels the shuttle at high velocity, which in turn forces the water in the cylinder through the ports, forming a high velocity water jet outside each port (see Figure 2.18, image c); 2) the shuttle decelerates rapidly, and an internal cavity is formed in the nozzle as the displaced mass of water separates from the piston (see Figure 2.18, image d); 3) the cavity inside the air gun collapses, as external cavities are formed behind the water jets due to the high velocity contrast; 4) as the velocity of the water jet decreases, the pressure in the associated cavities increase, until they eventually collapse due to the hydrostatic pressure (Landrø et al., 1993).

The water gun signature comprises two signals: the precursor and the main pulse. The first peak of the precursor is caused by the water escaping through the ports, while the second peak is associated to the collapse of the internal cavity formed inside the port nozzles. The primary pulse results from a shock wave produced by the collapse of the external cavities attached to the water jets.

The cavities appear when the water jet reaches a minimum velocity. That critical velocity u_c can be approximated by $u_c = \sqrt{2P_w/\rho_w}$ in m/s, where P_w is the hydrostatic pressure in Pa and ρ_w the density of the surrounding water kg/m^3. This velocity limit increases with depth, making cavitation more difficult to induce. For a water gun, shuttle and water-jet velocity (~60 m/s) are well above the critical velocity for typical source depths (u_c = 17 m/s for water gun at 5 m depth). At depths of 180 m or more, cavitation in water guns is unlikely to occur. Similarly, the peak amplitude of a water gun is approximately proportional to the hydrostatic pressure, which means that the output sound level is lower at shallow source depths. Cavity noise is also expected to decrease as the depth of the water gun increases (Landrø & Amundsen, 2010).

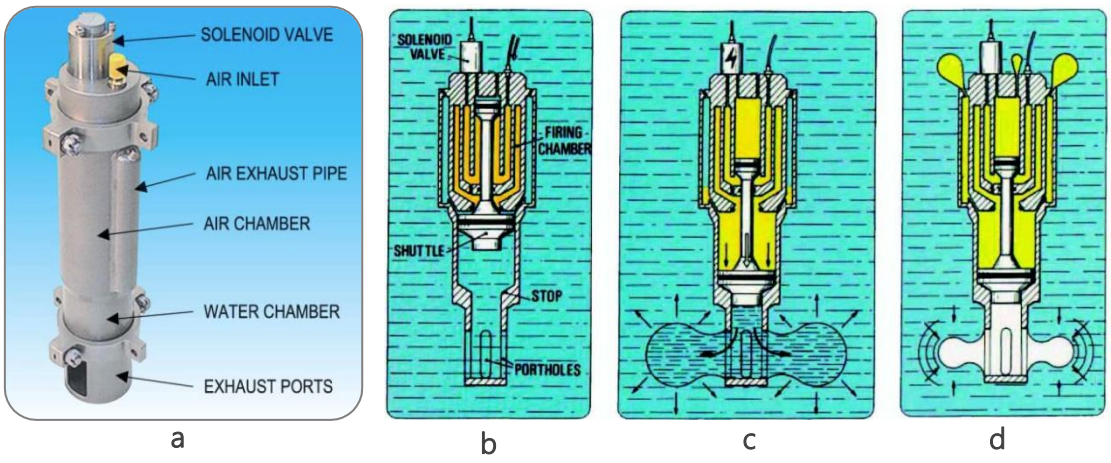

Figure 2.18 Photo (image a) and operation (images b-d) of a S15 water-gun. Compressed air pushes water through the ports, generating two water jets (image c); low pressure cavities appear inside the nozzle and behind the water jet (image d), which will eventually collapse producing high intensity pulses (from Sercel, 2006).

The duration of the water gun signature is much shorter than that of an air gun of comparable size, due to the absence of an oscillating air bubble. The water gun is richer in high frequency content, with most of its energy between 0.2 and 2.5 kHz, but it produces lower levels at low frequencies than air guns. Water guns are a good compromise between very high-resolution systems (3.5 kHz sub-bottom profilers and sparkers) and deep penetration, air gun arrays (Hutchinson & Detrick, 1984).

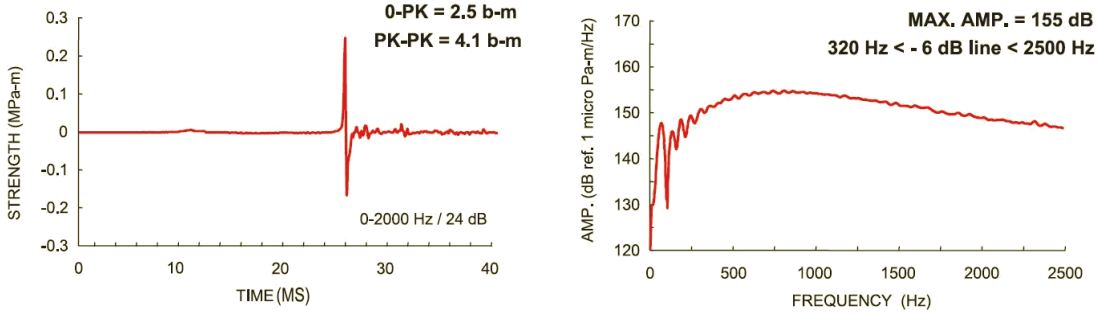

Figure 2.19 Far field signature (left) and spectrum (right) of a single S15 water gun, operated at 2000 psi and 0.22 m depth (from Sercel, 2006).

The advantage of a source that expels water instead of air is that there is no oscillation of an air bubble, and the need for an array of sources of different volumes disappears (Tasker & Weir, 1998).

2.5.1 Tables

Table 2.4 Sounds produced by water guns

Source (*Model*)	SL [dB re 1µPa@1m]	Signal Characteristics	Description	Reference
Water gun single (*Hydroshock*)	238 dB_{pk-pk}	T = 4 s	Broadband 0 Hz - 2 kHz	Bouyoucos, 1981
Water gun single	217 dB_{pk}	N/A	V_g = 55 in^3	Richardson et al, 1995
Water gun single (*S15*)	228 dB_{pk} 232.3 dB_{pk-pk}	$FR._{6dB}$ = 0.27-2 kHz τ = 10 ms	Op. pressure 2000 psi z_s = 0.22 m	Sercel, 2006
Water gun array	245 dB_{pk}	N/A	V_g = 1465 in^3	Richardson et al, 1995

2.6 The Sleeve Exploder

The *sleeve exploder* is a marine seismic source developed by Exxon Production Research Co. and put in service for oil exploration in 1967 (Bayhi et al, 1969). The system consists of twelve to twenty four rubber sleeves, each of them fitted to a gas mixing chamber. A mixture of oxygen and propane is fed into the chambers and ignited by a spark, producing an explosion which is contained within the rubber sleeve (see Figure 2.20). The expansion of the sleeve generates a shock wave. The gasses are evacuated through a tube to the surface as the initial explosion collapses and the sleeve retracts, thus eliminating the chance of a bubble pulse (Trabant, 1984).

The source is capable of continuous operations at high repetition activation rates, typically at 6 – 10 seconds intervals. The system can be mounted in a towed sled or suspended from davits on the side of the seismic vessel and is usually operated in shallow waters. The major drawbacks of this source are the size, weight and use of explosive gasses.

The development work on the sleeve exploder began with the objective of lowering marine seismic costs, and improving safety and data quality. At the time the research on this source started there were

only a few non-dynamite seismic sources, but when the system was made available at least twelve seismic sources suitable for deep water oil exploration were already on the market. A scaled down version of the original design, the *mini-sleeve exploder*, became popular in the following years for high resolution geophysical (HRG) surveys, in particular for sub-bottom hazard assessment previous to offshore drilling operations (Trabant, 1984). Nowadays, sub-bottom profiling systems based on small air guns or air gun arrays, boomers, sparkers and fixed-frequency or chirp sonar have replaced the rest of HRG systems, including the *mini-sleeve exploder*.

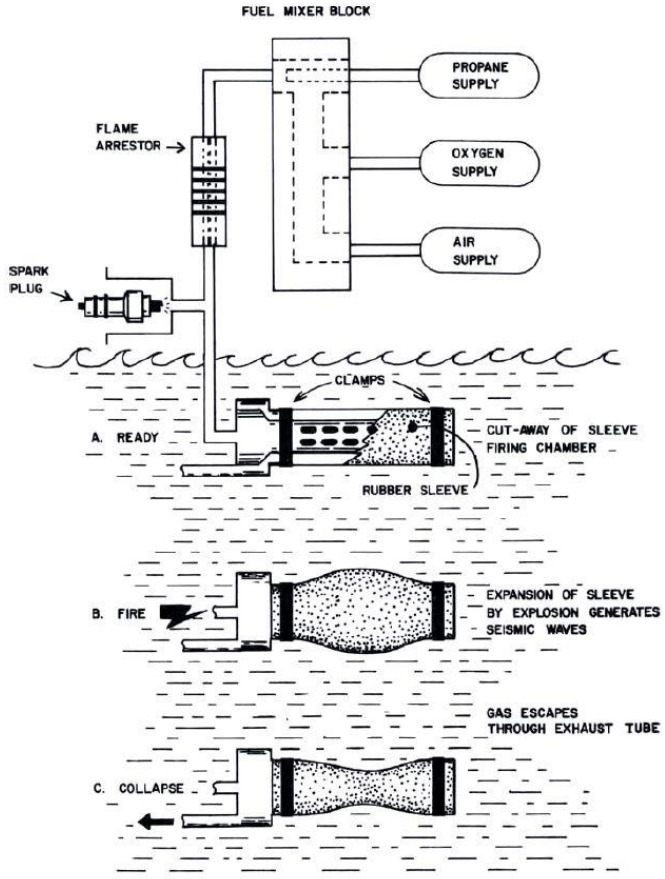

Figure 2.20 Schematic drawing of a mini-sleeve exploder system and operation (from Trabant, 1984).

2.6.1 Tables

Table 2.5 Sounds produced by sleeve exploders and open-bottom gas guns

Source (*Model*)	h_w [m]	Measurement [dB re 1µPa]	SL [dB re 1µPa@1m]	Signal Characteristics	Regression Equation	Description	Reference
Sleeve exploder 12 gun array	15-30	150.5 dB_{rms} @ 8 km 116 dB_{rms} @ 27 km	200.1 dB_{rms}	T = 6 s τ = 250 ms @ 8 km τ = 400 ms @ 29 km	RL = 200.1 -10$\log_{10}$r - 1.39·10^{-3}r	z_s = 6 m z_r = 9 m	Greene & Richardson, 1988
Sleeve exploder single	N/A	N/A	217 dB_{rms}	N/A	N/A	Ignition of gas mixture in rubber sleeve	Richardson et al, 1995
Open bottom gas gun array	9-11	177 dB_{rms} @ 0.9 km 123 dB_{rms} @ 14.8 km	199.2 dB_{rms}	Main energy at 72 Hz τ = 200 ms @ 0.9 km	RL = 199.2 -10$\log_{10}$r - 2.33·10^{-3}r	z_r = 8 m	Greene & Richardson, 1988

3 Engineering Sources

3.1 The Single-Beam Echo Sounder

Echo sounders are a type of sonar device used to measure the water depth remotely by emitting a series of acoustic pulses. Single-beam is the simplest type of echo sounder, and perhaps the most widely used man-made sonar (Ainslie, 2010).

Single-beam echo sounders project a single acoustic beam, oriented vertically downwards. The time the emitted pulse takes to travel down to the seafloor and return is used to estimate the water depth ($h_w = \bar{c}t/2$, where h_w is the water depth, t the total travel time and $\bar{c}$ the sound speed averaged in the vertical direction). SBES typically use a single transducer to emit and receive the acoustic pulse. The first pulse return provides information of the water depth immediately below the surveying vessel, whereas late returns tell about surrounding depths covered by the acoustic beam. The footprint of the acoustic beam on the seabed varies in size depending on water depth and is generally large, with typical beam widths of 10-30°. A narrow beam width is preferable to obtain the best resolution; this is especially important for deep water sounding. A single-beam provides depth information at a single point, usually just below the vessel, by measuring the shortest slant range to the seafloor within the main beam. The echo sounder emits acoustic pulses repeatedly as the vessel moves, producing a continuous depth profile along its track.

Echo sounders are not always calibrated, but often give a good estimate of the depth and type of seabed (Blondel, 2009). For precise applications, the speed of sound must be measured, typically by deploying a sound velocity or CTD probe. The sound speed is difficult to obtain accurately, and is the main source of error when estimating the water depth; knowing the exact position of the transducer is also important.

A typical source level value in SBES is 214 dB re 1µPa_{rms}. The SBES emits a short tonal pulse, with a duration ranging from a fraction of millisecond to several milliseconds (0.1 – 10 ms), and frequencies ranging from 12 to 200 kHz. The pulse may consist of a single frequency, multiple frequencies or a frequency sweep (*chirp*). Emitted sound levels depend on pulse duration and beam width: the highest levels are usually related to *narrow beams* (high directivity) and *short pulses* (same energy in a shorter signal results in higher RMS sound levels) (Ainslie, 2010). High frequencies (100 – 200 kHz) are suitable for in-shore measurements, but deeper waters require lower frequencies (12 – 40 kHz), which experience lower absorption in water.

Dual frequency echo sounders transmit two discrete frequencies simultaneously: low (~24 kHz) and high (~ 200 kHz). This system was originally designed to provide accurate navigation in shallow waters, while still giving reliable depths in deep waters. Other advantage of dual frequency echo-sounding is the ability distinguish layers of unconsolidated sediments on top of consolidated sediments and rocks.

The density of depth measurements depends on vessel speed and pulse repetition period, but is constrained by the beam width of the transducer. The higher number of pulses per second would result in higher survey efficiency, as the vessel can travel faster and cover a larger area in a shorter time, but more pulses will also create more noise, which will affect the quality of the received signal.

Single-beam echo sounders have long been the tool of choice to map the seabed topography (Blondel, 2009). SBES are installed in a wide range of marine vehicles, from pleasure boats to research

vessels and tankers, and are generally used for navigation and bottom avoidance, and for the generation of navigational charts. However, SBES can also be used to derive more information about the local habitat, bottom classification (sediment, rock, vegetation, etc.), fish finding and target localisation. Upward looking systems, such as Pressure Inverted Echo Sounders (PIES), can be used for average sound speed measurements, tide estimation and ice avoidance. Echo sounders used for fish finding are adapted by tilting the transducer away from the vertical direction; scanning at oblique angles increases the area of coverage (Ainslie, 2010).

Figure 3.1 Family of Simrad single-beam echo sounder transducers (www.km.kongsberg.com).

3.1.1 Tables

Table 3.1 Sounds produced by single-beam echo sounders

Source (*Model*)	SL [dB re 1µPa@1m]	Signal Characteristics	Reference
SBES (General)	223 - 231 dB_{rms}	f = 12 - 200 kHz τ = 0.06 - 16 ms	Cluster Maritime Français, 2014
SBES	235 dB_{rms}	f = 12 kHz DC = 0.4 % τ = 20 ms	André et al, 2009
SBES (Simrad *38/200*)	208 dB_{rms}	f = 38 kHz BW_{-6dB} = 0.38, 3.8 kHz τ = 0.3, 1, 3 ms	Ainslie, 2010; www.simrad.com
		f = 200 kHz BW_{-6dB} = 2, 20 kHz τ = 0.06, 0.2, 0.6 ms	
SBES (Simrad *HTL 430D*)	200 dB_{rms}	f = 42 kHz	Ainslie, 2010
SBES (Simrad *EK 500*)	214 dB_{rms}	f = 57 kHz	Ainslie, 2010
SBES (Simrad *SD 570*)	220 dB_{rms}	f = 57 kHz	Ainslie, 2010
SBES (Biosonics *DT 4000*)	221 dB_{rms}	f = 208 kHz	Ainslie, 2010

3.2 The Multi-Beam Echo Sounder

Multi-beam echo sounders measure water depth remotely, as single-beam echo sounders do, but instead of a single vertical beam, they use multiple beams aimed at the seafloor in different directions. MBES apply beamforming to distinguish between pulse seabed reflections arriving from multiple vertical angles. This approach provides a depth measurement along a broad corridor in the cross-track direction, rather than a single depth value below the vessel. As a result, a moving vessel will produce a swath of water depth information. Multi-beam bathymetric mapping became more accessible in the late 1980s, recent compared to the use of single-beam echo sounding, which started in the early 20th century.

MBES are equipped with an array of identical, equally spaced transducers, which allow for the transmission of several acoustic beams. The width of the swath, which extends along both sides of the

vessel, covers a distance that is about 4 times the water depth, and up to 20 times in some cases (Blondel, 2009). The beams are designed to be narrower than in an SBES, and accuracy of the depth measurement can be better than one metre.

The main parameters describing a multi-beam echo sounder are the operating frequency and bandwidth, pulse length, beam width and number of beams. Systems with 0.5° along-track beam widths are now quite common; cross-track beam widths are extremely broad in comparison, with values around 120 to 140°. Modern systems produce up to 400 *soundings* or depth measurements per pulse for a single head or transducer array, compared to the 100 soundings of older generations. Pulse lengths and operating frequencies are similar to those in single-beam echo sounders, although some systems can use frequencies up to 700 kHz. Many of the current systems allow for frequency selection.

Higher resolution is achieved with narrower beam widths, higher frequencies and reduced pulse lengths. To overcome the range limitations at high frequencies produced by the sound absorption in sea water, *chirp* (frequency sweep) pulses are introduced as an alternative to pings (continuous tone) to increase the energy in the pulse. As the MBES technology has progressed, smaller beam widths have come with an increase in the number of beams, to maintain the cross-track coverage or *swath width*. Some systems also include dual-swath transmission to provide simultaneous pulses from two transducer arrays, which doubles the density of collected soundings and allows for greater survey speeds.

Advances in beam forming offer greater control over the distribution of the acoustic beams. The possibilities of beam forming include: reducing or extending the swath coverage while maintaining the number of beams; steering the swath to one side; or compensating for vessel motion, to ensure good quality mapping regardless of sea state. Much of the advances achieved in MBES are related to signal processing and bottom detection algorithms. The processing and calibration methods for bathymetry mapping are well standardised (Blondel, 2009).

MBES are principally aimed at acquiring bathymetry measurements, but backscatter strengths (Blondel, 2009) and water column data can also be derived. Backscatter information can be used for the classification of seabed sediments and habitats. Overall, multi-beam echo sounders have better horizontal and vertical resolution than SBES, but lose efficiency at depths below 30 m.

Figure 3.2 Multi-beam echo sounder EM 2040C (left) and bow mounting detail (right). From www.km.kongsberg.com

3.2.1 Tables

Table 3.2 Sounds produced by multi-beam echo sounders

Source (*Model*)	SL [dB re 1µPa@1m]	Signal Characteristics	Description	Reference
MBES (*Hydrosweep*)	237 dB_{rms}	τ = 20 ms (typ.) T = 15 s f = 15.5 kHz BW = 40 Hz (τ=25 ms) to 1 kHz (τ=1 ms)	Application: depth sounder	ICES, 2005; Kremser et al, 2005
MBES (*Parasound*)	245 dB_{rms}	τ = 3.8 ms (typ.) T = 5 s f = 18 kHz BW = 40 Hz (τ=25 ms) to 5.5 kHz (τ=180 µs)	Application: depth sounder	ICES, 2005; Kremser et al, 2005
MBES (*EM710*)	232 dB_{rms} [a]	τ = 2 ms f = 70 - 100 kHz Beam width 0.5° x 140°	Application: shallow water bathymetry mapping [a]Far field measurement extrapolated to 1 m using TL = $20\log_{10}r$. Actual measured level at 0.3 m is 213 dB_{rms}.	Hildebrand, 2009; Hammerstad, 2005; Genesis, 2011
MBES (*EM122*)	245 dB_{rms} [a]	τ = 10 ms f = 10.5-13 kHz Beam width 0.5° x 120°	Application: deep water bathymetry mapping [a]Far field measurement extrapolated to 1 m using TL = $20\log_{10}r$. Actual measured level at 2.8 m is 208 dB_{rms}.	Hildebrand, 2009; Hammerstad, 2005; Genesis, 2011
MBES (*EM1002*)	225 dB_{rms} [a]	τ = 0.2, 0.7, 2 ms f = 95 kHz	Application: bathymetry mapping [a]Far field measurement extrapolated to 1 m using TL = $20\log_{10}r$. Actual measured level at 3.2 m is 210 dB_{rms}.	Hammerstad, 2005; Genesis, 2011
MBES	220 - 240 dB_{rms}	f = 13 - 700 kHz τ = 0.2 - 20 ms	N/A	Cluster Maritime Français, 2014
MBES (Simrad *EM120*)	245 dB_{rms}	f = 12 kHz	N/A	Ainslie, 2010
MBES (Simrad *EM121A*)	238 dB_{rms}	f = 12 kHz	N/A	Ainslie, 2010
MBES (ELAC Sea Beam 2000)	234 dB_{rms}	f = 12 kHz	N/A	Ainslie, 2010
MBES (ELAC Sea Beam 3012)	239 dB_{rms}	f = 12 kHz	N/A	Ainslie, 2010
MBES (Thomson Marconi *TSM 5265*)	235 dB_{rms}	f = 12 kHz	N/A	Ainslie, 2010
MBES (Simrad *EM12*)	238 dB_{rms}	f = 13 kHz	N/A	Ainslie, 2010
MBES (ELAC Sea Beam 2120)	247 dB_{rms}	f = 20 kHz	N/A	Ainslie, 2010
MBES (Simrad *EM300*)	241 dB_{rms}	f = 30 kHz	N/A	Ainslie, 2010
MBES (ELAC *Sea Beam 1050*)	234 dB_{rms}	f = 50 kHz	N/A	Ainslie, 2010
MBES (Simrad *EM710*)	232 dB_{rms}	f = 85 kHz	N/A	Ainslie, 2010
MBES (Simrad *EM1000*)	225 dB_{rms}	f = 95 kHz	N/A	Ainslie, 2010
MBES (Simrad *EM1002*)	226 dB_{rms}	f = 95 kHz	N/A	Ainslie, 2010
MBES (Simrad *EM950*)	225 dB_{rms}	f = 95 kHz	N/A	Ainslie, 2010
MBES (Simrad *EM952*)	226 dB_{rms}	f = 95 kHz	N/A	Ainslie, 2010
MBES (Atlas *Fansweep 20*)	227 dB_{rms}	f = 100, 200 kHz	N/A	Ainslie, 2010

Table 3.2 Sounds produced by multi-beam echo sounders (cont.)

Source (*Model*)	SL [dB re 1µPa@1m]	Signal Characteristics	Description	Reference
MBES (Thomson Marconi *TSM 5260*)	210 dB_{rms}	f = 100 kHz	N/A	Ainslie, 2010
MBES (Triton *ISIS100*)	219 dB_{rms}	f = 117, 234 kHz	N/A	Ainslie, 2010
MBES (ELAC *Sea Beam 1185*)	217 dB_{rms}	f = 180 kHz	N/A	Ainslie, 2010
MBES (ELAC *Sea Beam 1180*)	220 dB_{rms}	f = 180 kHz	N/A	Ainslie, 2010
MBES (Atlas *Fansweep 15*)	227 dB_{rms}	f = 200 kHz	N/A	Ainslie, 2010
MBES (Reson *Seabat 7125*)	220 dB_{rms}	f = 200 kHz	N/A	Ainslie, 2010
MBES (Reson *Seabat 8124*)	210 dB_{rms}	f = 200 kHz	N/A	Ainslie, 2010
MBES (Simrad *EM2000*)	218 dB_{rms}	f = 200 kHz	N/A	Ainslie, 2010
MBES (ECHOSCAN)	225 dB_{rms}	f = 200 kHz	N/A	Ainslie, 2010
MBES (Reson *Seabat 8101*)	217 dB_{rms}	f = 240 kHz	N/A	Ainslie, 2010
MBES (Simrad *EM3000*)	215 dB_{rms}	f = 300 kHz	N/A	Ainslie, 2010
MBES (Reson *Seabat 9001*)	210 dB_{rms}	f = 455 kHz	N/A	Ainslie, 2010

3.3 The Side-Scan Sonar

The *side-scan sonar* (SSS) is a device that uses sonar technology to generate a high-resolution image of the seafloor. This instrument projects an acoustic beam towards the seabed and on each side. The beam is narrow in the along-track direction and broad in the vertical plane. The SSS emits a tone burst or *ping* that travels to the seafloor, where the energy is scattered. Some of this energy returns to the transducer, and is then amplified and processed to image the seafloor along a narrow slice perpendicular to the travel direction. The slices from successive pings are combined to create a long, detailed continuous image of the seafloor.

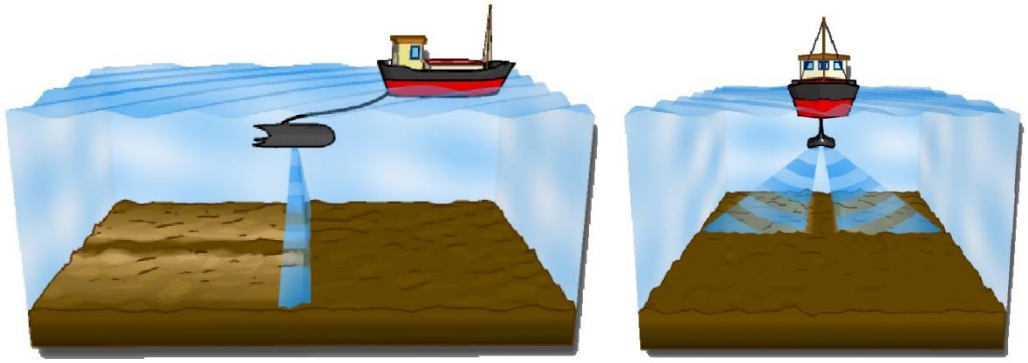

Figure 3.3 Operation of a towed side-scan sonar (from www.tritech.co.uk)

The image is the result of the scattering properties of the seabed, and these depend on the material, dimensions and roughness (shape) of the mapped sediment and protruding objects. Like an imperfect surface that is illuminated with a torch from an oblique angle, large objects in the seabed will appear as light areas (strong reflections), with relatively long shadows behind them. Materials with a very different density than water will reflect more sound: metal, rock, gravel and air are strong acoustic reflectors,

compared to fine sediments, which do not reflect sound so well. The incident angle has an important effect on the resulting image, potentially hiding strong reflectors, and depends on the proximity of the device to the seabed and its cross-track beam width.

Side-scan sonars are often towed from a surface vessel (*towfish*), but can be hull-mounted for shallow water operations or also be installed in AUVs. The SSS consists of three components: transducer (*towfish*), transmission cable and on-board processing and display unit. Most side-scan sonars cannot provide depth information, so are typically used in conjunction with a single or a multi-beam echo sounder.

Modern side-scan sonar systems may use *pings* (tone burst) or *chirps* (frequency sweep), with frequencies from 6.5 kHz to 1 MHz, and resolutions in the range of 0.01-60 m (Blondel, 2009). The cross-track coverage or *swath width* is given by the maximum range of the system, which depends on the frequency and energy of the pulse. The cross-track resolution is given by the pulse length, and the along-track resolution by the beam width (Hansen, 2011).

The altitude of the towfish is governed by the range of the system and the bathymetry, and is typically 10-20 % of the maximum range. The acoustic beams are projected towards the seafloor in an oblique angle, creating a shadow under the towfish. The altitude affects the width of this shadow, but also plays an important role on the formation of shades, which are key for interpreting the sonar image and identifying targets of interest.

The side-scan sonar is commonly used to locate and assess pipelines and cables, find objects such as shipwrecks or mines, detect obstructions that may be problematic for shipping or engineering work, or determine seabed characteristics from scattering data.

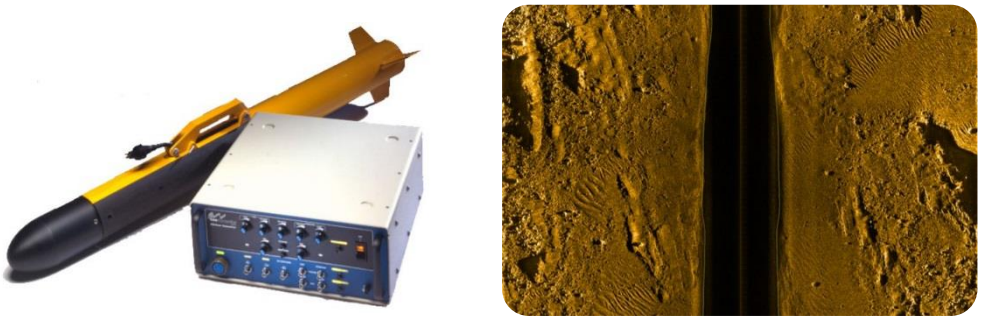

Figure 3.4 Dual frequency side-scan sonar system (left, from www.km.kongsberg.com) and high-resolution image from a Klein System 5900 SSS (from kleinmarinesystems.com).

3.3.1 Tables

Table 3.3 Sounds produced by side-scan sonars

Source (*Model*)	SL [dB re 1µPa@1m]	Signal Characteristics	Description	Reference
SSS (*Fugro SYS09*)	230 dB_{rms}	T = 0.5 - 20 s f = 9, 10 kHz	Application: bathymetry mapping	ICES, 2005; Fugro, 2008
SSS (Konsberg *196D*)	220 - 226 dB_{rms} [a]	f = 114, 410 kHz BW = 15 kHz T ≥ 20 ms τ = 88, 167 µs Beam width 50° x 1° @ 114 kHz Beam width 40° x 0.3° @ 410 kHz	Application: seabed mapping Dual Frequency [a] RL_{rms} = 167.2 - 15.8·log_{10}R	Konsberg, 2014b
SSS	220 dB_{rms}	f = 100 - 900 kHz τ = 0.1 - 1 s	N/A	Cluster Maritime Français, 2014
SSS (Racal *SeaMARC SB12*)	233 dB_{rms}	f = 12 kHz	N/A	Ainslie, 2010

Table 3.3 Sounds produced by side-scan sonars (cont.)

Source (*Model*)	SL [dB re 1µPa@1m]	Signal Characteristics	Description	Reference
SSS (Simrad *AMS 36/120SI*)	228 dB_{rms}	f = 33.3, 36 kHz	N/A	Ainslie, 2010
	224 dB_{rms}	f = 120 kHz		
SSS (Simrad *AMS 120SP*)	224 dB_{rms}	f = 120 kHz	N/A	Ainslie, 2010
SSS (Racal *SeaMARC SB50*)	200 dB_{rms}	f = 50 kHz	N/A	Ainslie, 2010
SSS (Simrad *AMS 60SI*)	227 dB_{rms}	f = 57.6 kHz	N/A	Ainslie, 2010
SSS (Neptune *990 Tow Fish*)	227 dB_{rms}	f = 59 kHz	N/A	Ainslie, 2010
SSS (Ultra *Deepscan 60*)	231 dB_{rms}	f = 60 kHz	N/A	Ainslie, 2010
SSS (Massa *TR-1101*)	223 dB_{rms}	f = 97 kHz	N/A	Ainslie, 2010
SSS (Innomar SES2000)	220 dB_{rms}	f = 100 kHz	N/A	Ainslie, 2010
SSS (Neptune 422 *Tow Fish*)	228 dB_{rms}	f = 100 kHz	N/A	Ainslie, 2010
	220 dB_{rms}	f = 500 kHz		
SSS (GEC Marconi *Bathyscan*)	220 dB_{rms}	f = 100, 300 kHz	N/A	Ainslie, 2010
SSS (Neptune *272 Tow Fish*)	234 dB_{rms} [a] 229 dB_{rms} [b]	f = 105 kHz	Dual beam model [a] main beam, [b] secondary beam	Ainslie, 2010
	229 dB_{rms}	f = 105 kHz	Dual frequency model	
	223 dB_{rms}	f = 500 kHz		
SSS (Geoacoustics *DSSS*)	223 dB_{rms}	f = 114, 410 kHz	N/A	Ainslie, 2010
SSS (Benthos *C3D*)	224 dB_{rms}	f = 200 kHz	N/A	Ainslie, 2010
SSS (Tritech *Seaking*)	208 dB_{rms}	f = 325, 675 kHz	N/A	Ainslie, 2010

3.4 The Sub-Bottom Profiler

A sub-bottom profiler (SBP) is a single-channel system used for shallow reflection seismic profiling. These geophysical exploration systems are based on the principles of vertical seismic reflection, and emit a low-frequency, regularly pulsed signal capable to penetrate the seafloor down to several tens of metres. The partial reflections produced at sub-surface layers of different acoustic impedance return to the surface, where they are captured by the receiver, amplified and processed to generate a stratigraphic image or *seismic reflection profile* (Ramsay, 2017; Saucier, 1970)

The first device designed specifically for sub-bottom profiling was the *Sonoprobe*, built by Magnolia Petroleum Co. The Sonoprobe was made operational in 1954, but almost a decade before, modified echo sounders were used to image the top layers of the seafloor in shallow coastal waters. In the 1970s hundreds of sub-bottom profiling systems were available and used throughout the world, and replaced seismic reflection operations that were so popular until the mid-1960s (Saucier, 1970).

Sub-bottom profilers consist of an acoustic source, one or more receivers and a signal processing system. Acoustic profiling systems are commonly classified according to the mechanism of sound generation: piezoelectric and magnetoestrictive (pinger, chirp, parametric SBP), electromechanical (boomer), electrical (sparker), pressurised chamber (air gun, water gun) and combustion (gas gun, sleeve gun). Ceramic sources, such as pingers and chirps, use the same transducer or transducer array for emission and reception; in boomers and sparkers, a separate hydrophone array is used to receive the reflected signal.

The selection of the source and processing system depends on the required seabed penetration, resolution and acquisition geometry. The resolution determines the ability of a system to discriminate between closely separated layers of sediment; layers with a lower thickness than the system resolution are perceived as one layer. The degree of resolution and penetration largely depends on the frequency content and energy of the generated acoustic signal. Higher resolution can be achieved with narrower beams, shorter distance to the seafloor and signal processing. Regardless of the sound source, both high resolution and penetration cannot be achieved, and a compromise must be found. Increased output power allows greater sub-bottom penetration, but it will result in multiple reflections and noisier data in a hard seabed. Higher frequencies allow for higher resolution, because of their short wavelengths, but are easily attenuated and result in lower seabed penetration. Longer pulse lengths yield increased energy, which favours penetration, but affect resolution. The relation between frequency and penetration is not linear, and below 800 Hz penetration increases dramatically (www.ozcoasts.gov.au; www.comm-tec.com).

Most commercial SBPs are small, low-powered, high-resolution and shallow-penetrating systems, used for detailed studies of stratigraphy; mid-size systems are generally installed in research vessels operated by oceanographic institutions, are characterised by moderate penetration and resolution, and are widely used for geological and geophysical studies in the continental shelf (Saucier, 1970). The available sub-bottom profiling systems are more than a commercial response from manufacturers: although these systems share some characteristics, each has its own features which make it more suitable for a particular application. SBPs are used in offshore, coastal and port engineering, geotechnical site surveys, dredging studies, mineral exploration, detection of buried structures and habitat mapping (Ramsay, 2017). Thickness and characteristics of sedimentary layers can be derived from these studies.

The following sub-sections describe the operation, signal characteristics and application of the main high and mid resolution seismic profiling systems: pinger, chirp, parametric SBP, boomer and sparker. The last two are included for comparison; for a detailed description and tabulated information of sparkers and boomers refer to Sections 2.2 and 2.3. Air guns are sub-bottom profilers, but as deep-penetration, non-compact multichannel systems, will not be included in this section (see Section 2.1 for details on air guns).

3.4.1 High Resolution SBP

High resolution acoustic profilers, also referred to as *tuned-frequency* profilers, produce a highly consistent, repeatable tonal signal. The frequencies used are between 1 and 30 kHz. These profilers have an improved resolution compared to lower frequency systems, but can only penetrate down to 30-50 m into the seabed. The same transducer is typically used for both transmitting and receiving the acoustic signal. There are three main types of high resolution profilers: the *pinger*, the *chirper* and the *parametric sub-bottom profiler*. These devices are hull mounted or towed underwater. The use of ceramic transducers allow for high resolutions with low output power.

A *pinger* (not to be confused with the single frequency, acoustic deterrent device) is similar to a single-beam echo sounder, but uses a lower frequency. This device emits a tone burst, with an operating frequency between 3.5 and 7 kHz and typical pulse durations between 0.1 and 16 ms. It offers a vertical resolution of 0.2 m, with penetrations of 10-50 m. The generated source levels are between 180 and 210 dB_{rms}. Today, many systems have the option to select the frequency and pulse duration. A pinger consists of a transceiver and a transducer. The transceiver (or separated transmitter and receiver/processing units) contains the power supply, storage capacitors, discharge circuitry, and amplification/processing for the received signal. The transducer in most pingers consists of an array of ADP crystals immersed in oil (Saucier, 1970). The use of magnetostrictive transducers, like the ones in the Sonoprobe, is very infrequent.

Figure 3.5 Pinger sub-bottom profiling system (from knudseneng.com)

The *chirp* sub-bottom profiler emits a short frequency sweep, which covers a range of frequencies somewhere between 2 and 30 kHz. *Chirps* are designed to replace pingers and boomers, since they can achieve higher vertical resolutions (~0.1 m) while maintaining penetration (5 - 50 m). Compared to pingers, the pulse duration is around ten times higher, with typical values between 1 to 100 ms. Ringing noise is reduced and resolution improved due to the lower peak input power fed into the transducer. These systems provide relatively artefact-free seismic reflection profiles. As with pingers, the chirp system is made up of two main components: the transceiver and the transducer; the first one contains the signal generator, power circuitry, and the recording/control/processing unit.

Figure 3.6 Chirp sub-bottom profiling system 3100, with towfish SB-216S and SB-424 (left) and deployment detail (right). From www.edgetech.com.

A *parametric* sub-bottom profiler transmits two high frequencies that interact with each other during propagation, producing a lower frequency with higher penetration capability. *Parametric* profilers are non-linear systems (Ramsay, 2017). The emitted frequencies are typically in the range of 2-20 kHz. These systems achieve resolutions similar to chirps (0.1 m), with a slightly lower penetration (5 – 30 m).

3.4.2 Low/Mid Resolution SBP

Low/mid resolution profilers produce a broadband signal with most of its energy below 1 kHz, for relatively deep sub-bottom penetration. None of these devices use ceramic transducers, so they all require a separate towed hydrophone array to receive the signal. Low/mid resolution acoustic profilers include sparkers, boomers, bubble pulsers, air guns, water guns and sleeve exploders. The most common single channel low/mid systems (sparkers and boomers) are described below (see Sections 2.2 and 2.3 for a more detailed description and tabulated data).

The *boomer* is an electro-mechanical source, which generates a short, broadband signal by transmitting an electrical impulse into a coil that is physically attached to a moving diaphragm and magnetically coupled to a metallic plate. The acoustic pulse extends from 0.3 to 6 kHz, and can penetrate down to 150 m into a clayey seabed (20 m for coarse grain sediments), with resolutions between 0.2 and

0.5 m. Source levels are in the range of 205-225 dB_{rms}, and the pulse duration is of the order of a fraction of millisecond (0.1-0.2 ms). The pulse is not as repeatable as the one generated by ceramic transducers. A boomer sub-bottom profiling system consists of a transducer (boomer plate), an energy source, a detection/processing unit and a hydrophone array. The boomer is generally installed in a small catamaran and can be operated from a small vessel. Other popular terms used to refer to an electro-mechanical source like the boomer are pulser, snapper and thumper. A *bubble pulser* shares the same principle of operation as the boomer, but has a lower dominant frequency and considerable longer pulse length, leading to deeper penetration but lower resolution (Saucier, 1970).

The *sparker* transmits a broadband, high-intensity, low-frequency signal by the generation of an electrical arc between its two electrodes. The acoustic signal is rather long (0.5-5 ms) and contains two major pulses: one associated to the formation of a steam bubble caused by the electrical discharge; and the other, an order of magnitude greater than the first one, resulting from the collapse of the bubble (Saucier, 1970). Sparkers cover a range of frequencies of 0.2-3 kHz, and yield better penetration (30-750 m) but poorer resolution (0.3-1 m) than boomers. Changing the voltage or the amount of stored energy will result in different acoustic signatures and relative amplitudes between the two main pulses, providing different results in terms of penetration and resolution. Like boomers, a sparker system consists of a transducer (electrode), an energy source, a detection/processing unit and a hydrophone array. Sparkers are normally used in regions of semi-consolidated sediments and compacted sands. Some sparkers incorporate a parabolic panel to create a downward-focused plane wave, which would experience little attenuation with distance.

3.4.3 Tables

Table 3.4 Sounds produced by single-frequency sub-bottom profilers or pingers

Source (*Model*)	SL [dB re 1µPa@1m]	Regression Equation	Signal Characteristics	Description	Reference
Pinger SBP (*Strata Box*)	167.2 dB_{rms}	RL_{rms} = 167.2 - 15.8·$\log_{10}$r, 90th percentile regression equation, range of validity 100 m to 1.5 km.	T = 200 ms f = 3.5 kHz	Area: Camden Bay, Beaufort Sea z_s = 1.5 m z_r = 1 m above seafloor Application: sub-bottom profiling	Ireland et al, 2009
Pinger SBP (*ORE140*)	186.4 dB_{rms}	RL_{rms} = 186.4 - 21.1·$\log_{10}$r, 90th percentile regression equation, range of validity 200 m to 1 km.	T = 300 ms f = 3.5 kHz	Area: Chukchi Sea, z_s = 1.5 m, towed from side h_w ~ 45 m Application: sub-bottom profiling	Ireland et al., 2009
Pinger SBP (*Geopulse, Towfish 136A*)	193.8 dB_{rms}	RL_{rms} = 193.8 - 29.7·$\log_{10}$r, 90th percentile regression equation, range of validity 200 m to 1.5 km.	T = 125 ms f = 3.5 kHz	Area: Camden Bay, Beaufort Sea, h_w ~ 35 m z_s = 3 m Application: sub-bottom profiling	Ireland et al., 2009
	175.2 dB_{rms}	RL_{rms} = 175.2 - 19.8·$\log_{10}$r, 90th percentile regression equation, range of validity 200 m to 1.5 km.		Area: Chukchi Sea h_w ~ 45 m z_s = 3 m z_r = 1 m above seafloor Application: sub-bottom profiling	Ireland et al., 2009
	214 dB_{rms}	N/A	f = 2-12 kHz (selectable) τ = 1,2,4,8,16 or 32 cycles	T135 transducer	Konsberg, 2014a; Ainslie, 2010
Pinger SBP (Ultra *Deepscan 60*)	212 dB_{rms}	N/A	f = 7.5-12.5 kHz (selectable)	N/A	Ainslie, 2010
Pinger SBP (Massa *TR-1061A*)	199 dB_{rms}	N/A	f = 5 kHz	N/A	Ainslie, 2010
Pinger SBP (Massa *TR-1061A*)	201 dB_{rms}	N/A	f = 4 kHz	N/A	Ainslie, 2010

Table 3.5 Sounds produced by frequency-modulated sub-bottom profilers or chirpers

Source (*Model*)	SL [dB re 1µPa@1m]	Regression Equation	Signal Characteristics	Description	Reference
Chirp SBP (General)	203 - 214 dB_{rms}	N/A	τ = 50 ms f = 1.8 - 6 kHz	Application: sub-bottom profiling	Cluster Maritime Français, 2014
Chirp SBP (-)	184.6 dB_{rms} 189.2 dB_{pk} 171 dB_E	RL_{rms} = 184.6 - 24.3·$\log_{10}$r RL_{pk} = 189.2 - 19.5·$\log_{10}$r RL_E = 171 - 24.1·$\log_{10}$r 50th percentile regression equation, range of validity 55 - 450 m.	T = 0.25 - 5 s τ = 5 - 120 ms f = 2-7 kHz, 8-23 kHz	Area: Beaufort Sea, h_w ~ 50 m z_s = 1 m z_r = 3 m above seafloor Endfire (bow+stern) Application: sub-bottom profiling (shallow penetration)	Patterson et al., 2007
Chirp SBP (*CAP6000 Chirp II*)	161.1 dB_{rms}	RL_{rms} = 161.1 - 16.7·$\log_{10}$R -3.24·10^{-3}r, 90th percentile regression equation, endfire direction (bow+stern), range of validity 40 m to 5 km.	f = 2 - 7 kHz	Area: Prudhoe Bay, Beaufort Sea. h_w = 22 m z_s ~ 1.5 m Application: sub-bottom profiling (shallow penetration)	Funk et al., 2008
Chirp SBP (*SBP120*)	230 dB_{rms}	N/A	T ≥ 0.25 s τ = 0.4 - 100 ms FR = 2.5 - 7 kHz (sweep) Beam width 3° x 35°	Application: sub-bottom profiling (medium penetration)	Hildebrand, 2009; Konsberg, 2005
Chirp SBP (Geoacoustics *Geochirp*)	205 dB_{rms}	N/A	f = 3-7 kHz (selectable)	N/A	Ainslie, 2010

Table 3.6 Sounds produced by bubble pulser sub-bottom profilers

Source (*Model*)	SL [dB re 1µPa@1m]	Regression Equation	Signal Characteristics	Description	Reference
Bubble Pulser SBP (-)	165.7 dB_{rms} 178.7 dB_{pk} 142 dB_E	RL_{rms} = 165.7 - 14.7·$\log_{10}$r RL_{pk} = 178.7 - 14.7·$\log_{10}$r RL_E = 142 - 11.2·$\log_{10}$r 50th percentile regression equation, range of validity 35 m to 2.5 km.	T = 0.5 - 5 s τ = 5 - 120 ms f = 400 Hz	Area: Beaufort Sea h_w ~ 50 m z_r = 3 m above seafloor Endfire (bow+stern) Application: sub-bottom profiling (medium penetration)	Patterson et al., 2007
Bubble Pulser SBP (*SPR1200 Bubble Pulser*)	174.3 dB_{rms}	RL_{rms} = 174.3 - 16.8·$\log_{10}$r -1.8·10^{-3}r, 90th percentile regression equation, endfire direction (bow+stern), range of validity 50 m to 11 km.	f = 400 Hz	z_s ~ 1.5 m Application: sub-bottom profiling (medium penetration)	Funk et al., 2008
Bubble Pulser SBP (*SPR1200 Bubble Pulser*)	176.8 dB_{rms}	RL_{rms} = 176.8 - 17.6·$\log_{10}$r, 90th percentile regression equation, range of validity 100 m to 1.5 km.	T = 1 s f = 400 Hz	Area: Camden Bay, Beaufort Sea h_w ~ 35 m z_s = 0.5 m z_r = 1 m above seafloor Application: sub-bottom profiling (medium penetration)	Ireland et al, 2009
Bubble Pulser SBP (*BP530 Bubble Pulser*)	164.9 dB_{rms}	RL_{rms} = 164.9 - 12.2·$\log_{10}$r, 90th percentile regression equation, range of validity 100 m to 1.5 km.	T = 500 ms f = 400 Hz	Area: Chukchi Sea h_w ~ 45 m z_s = 1.5 m, towed from side z_r = 1 m above seafloor Application: sub-bottom profiling (medium penetration)	Ireland et al., 2009

3.5 Acoustic Deterrents

Underwater acoustic devices have been used since the early 1980s in an attempt to resolve interactions between marine mammals and fishery. There are two main interactions causing conflict: marine mammal entanglement in nets and marine mammal predation in longline fishing and aquaculture areas (Petras, 2003). The most commonly used acoustic deterrents are the *Acoustic Deterrent Devices* (ADD) and *Acoustic Harassment Devices* (AHD). Less common solutions include pipe banging, seal bombs, firecrackers and predator sounds. During offshore industrial activities, for example pile driving during wind farm construction, ADDs may be recommended as an additional mitigation measure (www.dosits.com). In some fisheries, the use of ADDs has become mandatory to reduce bycatch of small cetaceans (Petras, 2003).

In general, ADDs target cetaceans, in particular harbour porpoises, whose foraging habits make them more likely to be entangled in gill nets; AHDs target pinnipeds, a common predator in aquaculture farms (Petras, 2003; Morton & Symonds, 2002). An ADD is essentially a low-powered version of an AHD. Source levels produced by an ADD are in the range of 130 to 150 dB_{rms}; in an AHD these are between 180 and 200 dB_{rms}.

Figure 3.7 AHD Airmar dB Plus II (left, from airmartechnology.com) and ADD AQUAmark 100 (right, Aquatec Group Ltd.)

ADDs are also known as *pingers* (not to be confused with single frequency sub-bottom profilers) because original standard models used single frequency pulses, of typically 10 kHz. Some manufacturers offer models which cover a different frequency range to target a particular species, such as the *Whale*, *Porpoise* and *Dolphin Pinger* from Future Oceans, with operating frequencies of 3, 10 and 70 kHz, respectively (www.futureoceans.com). Most AHDs are designed to increase the intensity of the emitted signal over one minute, to condition the flee response and alert non-target species (Petras, 2003).

ADDs and AHDs work in a similar way, and share many characteristics. Pulse durations are generally in the order of tens of milliseconds to several hundreds of milliseconds (50 – 2000 ms, 300 ms being a typical value). There is a large variety of signals that different models can produce: some devices generate trains of short pulses, whilst others emit longer, separated pulses, or more continuous noise (Götz & Janik, 2013). The signal emitted by these devices can be considerably complex, and may include frequency modulated tones (downward/upward chirps), multiple continuous tones and broadband noise, which can be combined or switched in a randomised pattern (Petras, 2003; Lepper, 2014). Figure 3.8 shows the spectrogram of the signal generated by an acoustic deterrent manufactured by Terecos (Lepper et al., 2014). Today, many models of ADDs produce very complex, randomised signals, covering frequencies from 3 to 160 kHz. Sometimes, establishing a delimiting line between ADDs and AHDs is difficult.

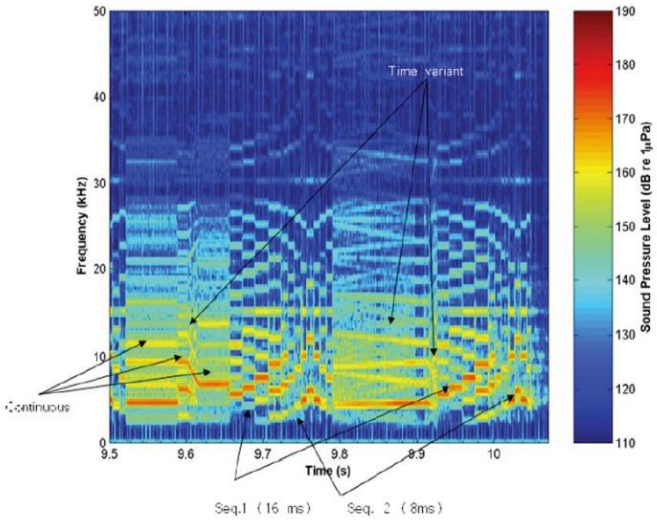

Figure 3.8 Spectrogram from Programme 4 of an AHD Terecos DSMS-4 (from Lepper et al., 2014).

Even though there are hundreds of acoustic deterrents in the market, very little is known about the way they work. More research is needed to understand the factors that trigger the aversive response and cause habituation of the marine mammal after prolonged exposure. There are two assumptions about how acoustic deterrents may work: 1) by producing a high enough sound level that exceeds the auditory pain threshold, or 2) by an acoustic stimulus that causes aversion but not pain (Götz & Janik, 2013).

Figure 3.9 Transducer (left) and control unit (right) of an of an AHD Terecos DSMS-4 (from Lepper et al., 2014).

The effectiveness of acoustic deterrents has been proved to vary considerably between studies, and to decrease over time. Reasons for differences in reported effectiveness include the deployment method, the presence of prey, reactions of different species, and sound propagation characteristics. Reasons for loss of effectiveness over time include habituation, "dinner bell" effect, adaptation (e.g. swimming with the head above the surface) and hearing damage due to sound exposure (Götz & Janik, 2013; Petras, 2003).

The variation in behavioural responses across studies and sites are the result of a series of poorly understood factors. Avoidance to sound in phocid seals is influenced by food motivation, learning processes, type of sound and auditory response. Seals habituate rapidly to sounds for received levels of 146 dB_{rms} and in presence of food; however, without food, deterrence occurs at received levels as low as 135 dB_{rms} (Götz & Janik, 2013; Götz & Janik, 2010). In general, ADDs have been proven ineffective in deterring seals and sea lions. AHDs seem to be only effective on unexposed animals (Petras, 2003).

The main problems associated with acoustic deterrents are the lack of long-term effectiveness and noise pollution, with a potential long-term effect on target and non-target species (Götz & Janik, 2013). AHDs produce sound levels high enough to cause hearing damage to marine mammals at close range (Hildebrand, 2005); hearing damage due to long cumulative exposure is also feasible (Götz & Janik, 2013).

In order to increase the efficiency of acoustic deterrents and minimise their impact on marine mammals, a series of design and operational tips are recommended: transmit a variety of waveforms and time intervals, account for the hearing ability of different species of marine mammals, use short signals and low duty cycles and reduce the energy above 5 kHz if odontocetes are present.

3.5.1 Tables

Table 3.7 Sounds produced by acoustic deterrent devices

Source (*Model*)	SL [dB re 1µPa@1m]	Signal Characteristics	Reference
ADD (General)	120 - 140 dB_{rms}	τ = 0.3 s Main energy at 12 - 17 kHz	Roussel, 2002
ADD (General)	150 dB_{rms}	τ = 0.2 - 0.3 s FR_{-10} = 5 - 160 kHz Beam width 90° x 360°	Hildebrand, 2009
ADD (General)	132 - 155 dB_{rms}	FR = 5 - 180 kHz	Cluster Maritime Français, 2014
ADD (Aquatec *AquaMark300*)	132 ± 4 dB_{rms}	Signal type: frequency modulated waveform, highly random T = 4 ±0.2 s (DC = 8 %) τ = 0.3 ±0.015 s f = 10 ±2 kHz Application: reduce bycatch on harbour porpoise	Aquatec, 2014; IACMST, 2006
ADD (Aquatec *AquaMark100*)	145 dB_{pk}	Signal type: frequency modulated waveform T = 4-30 s (DC = 0.5-8 %) τ = 0.2-0.3 s FR = 20-160 kHz Application: reduce bycatch on harbour porpoise	Aquatec, 2014

Table 3.7 Sounds produced by acoustic deterrent devices (cont.)

Source (*Model*)	SL [dB re 1µPa@1m]	Signal Characteristics	Reference
ADD (Aquatec *AquaMark210*)	150 dB_{pk}	Signal type: frequency modulated waveform, highly random T = 4-30 s (D = 0.2-8 %) τ = 0.05-0.3 s FR = 5-160 kHz Application: reduce bycatch (most porpoises and dolphins) and depredation	Aquatec, 2014
ADD (Airmar *Gillnet Pinger*)	132 dB_{rms}	Application: reduce bycatch on harbour porpoise f = 10 kHz T = 4 s τ = 0.3 s	Airmar, 2011
ADD (Fishtek *Banana Pinger*)	> 145 dB_{rms}	Application: reduce bycatch on porpoise and dolphin f = 50-120 kHz (outside the hearing frequency range of seals)	Fishtek (www.fishtekmarine.com)
	> 135 dB_{rms}	Application: reduce bycatch on porpoise and dolphin f = 10 kHz (+ harmonics)	
	> 135 dB_{rms}	Application: reduce bycatch on whales f = 3-4 kHz (+ harmonics)	
ADD (Marexi *Acoustic Pinger V2.2*)	132 ±4 dB_{rms}	Application: reduce bycatch f = 10 ±2 kHz (tonal) T = 4 ±0.2 s τ = 0.3 ±0.015 s	Marexi (www.marexi.com)
ADD (Future Oceans *Whale Pinger*)	135 ±4 dB_{rms}	Application: reduce humpback whale interactions with fishing gears f = 3 ±0.5 kHz	Future Oceans (futureoceans.com)
ADD (Future Oceans *Porpoise Pinger*)	132 dB_{rms}	Application: reduce bycatch on porpoises f = 10 kHz	Future Oceans (futureoceans.com)
ADD (Future Oceans *Dolphin Pinger*)	145 dB_{rms}	Application: reduce bycatch on dolphins f = 70 kHz τ = 0.3 ms T = 4 s (DC = 8 %)	Future Oceans (futureoceans.com)

Table 3.8 Sounds produced by acoustic harassment devices

Source (*Model*)	SL [dB re 1µPa@1m]	Signal Characteristics	Reference
AHD (General)	185 dB_{rms}	DC = 50 % τ = 0.5 - 2 s Main energy at 10 kHz BW = 600 Hz Omnidirectional	IACMST, 2006
AHD (General)	~190 dB_{rms}	Main energy at ~10 kHz	Roussel, 2002
AHD (General)	205 dB_{rms}	τ = 0.15 - 0.5 s FR = 8 - 30 kHz Beam Width 90° x 360°	Hildebrand, 2009
AHD (General)	178 - 193 dB_{rms}	Complex signal structure, varying with model	Cluster Maritime Français, 2014
AHD (Airmar, -)	195 dB_{rms}	f = 10 - 40 kHz Main energy at 27 kHz	Petras, 2003; Morton & Symonds, 2002
AHD (Airmar *dB Plus II*)	192 ±1 dB_{rms} [a] 198 dB_{pk-pk} [b]	Signal type: sequence of ~60 tone bursts every ~4 s τ_{seq} = 2.25 s, T_{seq} ~ 4 s Tone burst: f = 10 kHz, BW = 0.7 kHz τ = 1.4 ms, T = 40 ms (DC ~ 3 %) [a] 145 dB_{rms} harmonics <100 kHz [b] from per. comm. with Airmar	Lepper et al, 2014; Lepper et al, 2004
	183-198 dB_{rms} 206 dB_{pk}	Much lower levels reported, but measurements or device performance in doubt NOTE: data from various authors	Götz & Janik, 2013; Coram et al, 2014; MMO, 2018; Lepper et al, 2014

Table 3.8 Sounds produced by acoustic harassment devices

Source (*Model*)	SL [dB re 1µPa@1m]	Signal Characteristics	Reference
AHD (Terecos *DSMS-4*)	178 ±1 dB_{rms} @ 6.8 kHz[a]	Signal type: combination of 4 programmes (highly random) Programmes include: up/down frequency sweeps, randomly timed multi-tones [a] <146 dB_{rms} for f> 27 kHz, main energy 2-12 kHz	Lepper et al, 2014; Lepper et al, 2004; Götz & Janik, 2013; Coram, 2014; MMO, 2018
AHD (Ace Aquatec *Silent Scrammer*)	193 dB_{rms} @ 10 kHz[a]	Signal type: sequence of 28 multi-tone pulses, emitted every 5 s τ_{seq} = 3.3-14 ms T_{seq} = 5 s DC = 50% Multi-tones: varying length and frequency up-sweep (f = 5-20 kHz) τ = 3.3-14 ms [a] > 165 dB_{rms} @ 30 kHz	Lepper et al, 2014; Lepper et al, 2004; Götz & Janik, 2013
AHD (Ace Aquatec *US3*)	197 dB_{rms} @ 17 kHz[a]	BW_{-6dB} = 11 - 20 kHz [a] 195 ±2 dB_{rms} @ 13-18 kHz	Coram et al, 2014; MMO, 2018; Ace Aquatec (www.aceaquatec.com)
AHD (Ace Aquatec *US2*)	189 dB_{rms} @ 15.8 kHz[a]	BW_{-6dB} = 11 - 20 kHz [a] 188 ±2 dB_{rms} @ 12-19 kHz	Ace Aquatec (www.aceaquatec.com)
AHD (Ferranti-Thomson *MK2 Seal Scrammer*)	194 dB_{rms}	Signal type: pulses centred at 5 different frequencies, arranged in 5 randomly chosen preset sequences. Pulses repeated every 40 ms. f = 8 - 30 kHz DC ~3% (5.5 scrams/h) τ = 20 ms (pulse) Transmission duration = 20 s scram (double scram 40 s)	Lepper et al, 2014;
	194 dB_{pk} @ 27 kHz		Götz & Janik, 2013
AHD (Ferranti-Thomson *MK2 Seal Scrammer 4X*)	200 dB_{rms} @ 25.6 kHz	Identical signal characteristics to MK2 *Seal Scrammer*	Lepper et al, 2014; Götz & Janik, 2013; Coram et al, 2014; MMO, 2018
AHD (Ferranti-Thomson *MK3 Seal Scrammer*)	194 dB_{rms} @ 27 kHz	f = 10 - 40 kHz	Lepper et al, 2014
AHD (Simrad *Fishguard*)	191 dB_{rms}	f =15 kHz DC = 25-50% τ = 0.5 s (pulse) Transmission duration = 6 s	Lepper et al, 2014
AHD (Lofitech)	193 dB_{rms}[a]	f =15.6 kHz τ = 0.2 s (pulse) [a] 189 dB_{rms} from manufacturer, for model *Seal Scarer*	Lepper et al, 2014
AHD (Lofitech *Universal Scarer*)	182-193 dB_{rms}	Signal type: random number of pulses emitted in blocks. Pulse interval >0.5 s, block interval 20-60 s. f =14.9 kHz (tonal + harmonics) τ = 0.5 s typ. (pulse) DC = 10-25% NOTE: data from various authors	Götz & Janik, 2013; Coram et al, 2014; MMO, 2018;
AHD (Ocean Engineering Enterprise *DRS-8*)	202 dB_{rms}	f = 3 kHz	Lepper et al, 2014
AHD (Genuswave *SalmonSafe*)	180 dB_{rms}	f = 1 kHz (central band) τ = 0.2 s DT = 0.8-1%	MMO, 2018

3.6 Underwater Acoustic Communications

Underwater acoustic communications date back to the use of the first manned submarines. The "Gertrude" or underwater telephone allowed for audio communication using analog modulation with a carrier frequency of 2-15 kHz. Since then, the increase in the number of underwater operations has contributed to the development and improvement of data communication between underwater and surface nodes. The research has expanded from point-to-point links to underwater networks. Underwater acoustic communication is now a mature field, and many commercial devices are available, along with prototypes developed in research laboratories (Burrowes & Khan, 2011; Chitre et al, 2008; Stojanovic & Beaujean, 2016). Sound is the evident option for medium to long range underwater communications, due to the strong attenuation that affects radio and optical waves. Among the many different applications of underwater acoustic communications are environmental and oceanographic monitoring, assisted navigation, and offshore engineering (Sendra et al, 2016).

High bandwidth and long distance transmissions are difficult to achieve in the underwater environment. The advent of digital communication and signal processing techniques in the 1960s helped to overcome the difficulties of communications in imperfect channels (Chitre et al., 2008). In recent years, a significant effort has been put on developing technologies to mitigate the bandwidth, distance and latency limitations associated with the underwater environment (Sendra et al, 2016).

The *underwater acoustic modem* is the main device used for long distance underwater communications and consists of a power unit, a processing unit, electronic circuitry and a cylindrical or spherical piezoelectric transducer, generally used for both signal transmission and reception. The modem is usually cylindrical in shape, with diameters of 5-10 cm and lengths of 10-50 cm. The power consumption depends on the range and modulation, and is of the order of 0.1-1 W in receive mode, and 10-100 W in continuous transmission mode (Stojanovic & Beaujean, 2016).

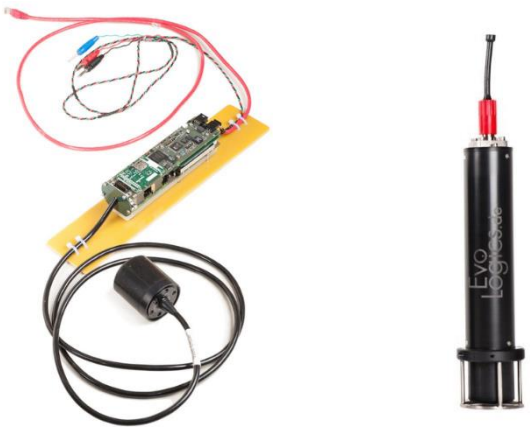

Figure 3.10 Acoustic mini modem Evologics S2C M, without case (left) and fully enclosed (right). From www.evologics.de

Commercial modems are available from several manufacturers, including Teledyne, LinkQuest, Evologics and Devologics. The performance of a modem changes dramatically depending on the application, and factors to take into account when selecting a model include data rate, maximum communication range, water depth, communication plane (vertical vs horizontal), power and networking capability. For transmissions below 10 km, data rates exceed 5 kbps, and transmission frequencies are between 10-40 kHz. There is an inverse relation between data rate and range, and for frequencies in the 100 kHz region transmission ranges do not exceed a few hundred meters, while frequencies below 1 kHz will allow for transmissions of several tens of kilometres. Modems designed for vertical transmission in deep waters use directional transducers and provide higher data rates; omni-directional, low data rate modems are preferable for shallow waters.

High data rate underwater communications are challenging due to the bandwidth limitation caused by strong high frequency absorption, multipath propagation, severe fading (shallow water), shadow zones (deep water), and relatively low propagation speed which results in large Doppler shifts.

Modulation methods originally developed for radio communications can be used in the underwater channel. Frequency-Shift Keying (FSK) was the first modulation method used in underwater acoustic modems. FSK relies on simple energy (non-coherent) detection, which makes it very sensitive to multi-path propagation, so FSK is better suited to vertical transmission. Motivated by these limitations, other modulation methods such as Phase-Shift Keying (PSK) and Quadrature-Amplitude Modulation (QAM) were studied to provide higher data rates. PSK and QAM are coherent modulations, and need to apply sound propagation algorithms to compensate for the effect of multipath reflections. Incoherent modulation methods are still in use in certain applications, since they require simple algorithms and processors, and thus lower power consumption. (Stojanovic & Beaujean, 2016; Chitre et al., 2008).

Table 3.9 Basic specifications of some commercial acoustic modems (from Stojanovic & Beaujean, 2016)

Modem	Max. Bit Rate [bps]	r [m]	FR [kHz]
Teledyne Benthos *ATM-916-MF1*	15360	6000	16-21
WHOI Micromodem	5400	3000	22.5-27.5
Linkquest *UWM 1000*	7000	1200	27-45
Evologics S2C R 48/78	31200	2000	48-78
Sercel MATS 3G 34 kHz	24600	5000	30-39
L3 Oceania *GPM-300*	1000	45000	N/A
Tritech Micron Data Modem	40	500	20-28
FAU Hermes	87768	180	262-375

3.6.1 Tables

Table 3.10 Sounds produced by acoustic modems

Source (*Model*)	SL [dB re 1µPa@1m]	Signal Characteristics	Description	Reference
Acoustic Modem (*Aquatec AQUAmodem*)	185 dB_{rms}	f = 8-12 kHz (20-27 and 55-65 kHz alternatives) Beam width: hemispherical	r_{max} = 10 km Application: acoustic communication in difficult environment (reverberant shallow waters and under-ice communications)	Hydro International, 2007
Acoustic Modem (*Evologics S2C M 7/17H*)	191 dB_{rms}	f = 48-78 kHz Beam width: hemispherical	r_{max} = 8 km Application: acoustic communication in deep sea, AUV, tsunami warning, etc.	Hydro International, 2007
Acoustic Modem (*Evologics S2C M 18/34*)	194 dB_{rms}	f = 18-34 kHz Beam width: horiz. omni	r_{max} = 3.5 km Application: AUV, hydrography, etc.	Hydro International, 2007
Acoustic Modem (*Evologics S2C M 48/78*)	194 dB_{rms}	f = 48-78 kHz Beam width: horiz. Omni	r_{max} = 2 km Application: high speed data and video transmission, AUV, hydrography, etc.	Hydro International, 2007
Acoustic Modem (*ELAC Nautik UM30*)	185 dB_{rms}	f = 10-14, 25-35 kHz Beam width: omni	r_{max} = N/A (depending on transducer) Application: data exchange between 2 computers using 2 x UM30	Hydro International, 2007
Acoustic Modem (*Sonardyne uCOMM Omni MF*)	188 dB_{rms}	f = 19-36 kHz Beam width: 240°	r_{max} = 3 km Application: real-time recovery data from sensors (pressure, temperature, current, etc)	Hydro International, 2007
Acoustic Modem (*Sonardyne uCOMM Dir MF*)	193 dB_{rms}	f = 19-36 kHz Beam width: ±50°	r_{max} = 5 km Application: N/A	Hydro International, 2007
Acoustic Modem (*Sonardyne uCOMM Dir LMF*)	196 dB_{rms}	f = 14-22 kHz Beam width: ±25°	r_{max} = 7 km Application: N/A	Hydro International, 2007

3.7 Underwater Acoustic Positioning

Underwater acoustic positioning is a method used to determine the location of a submerged object by means of the relative time delay of one or more acoustic impulses, as they travel between the tracked object and one or more transceivers or transponders. Underwater acoustic positioning systems were developed in the 1950s and 60s, and have greatly evolved since then, motivated by the demand for deep water exploration from the offshore industry. Depending on the positioning technology, these systems can locate an object with an accuracy that varies between centimetres and tens of metres, within a radius of metres to kilometres. These positioning methods are accurate and repeatable, but generally require time consuming calibration, determination of coordinates for the transponders and measurements of sound velocity profiles (Tomczak, 2011).

Underwater acoustic positioning is essential in almost all phases of offshore operations in the oil and gas industry. Applications include tracking of vehicles and towed sensors, locating underwater structures, and monitoring drilling and dredging operations. There are three main types of methodologies for underwater acoustic positioning: long baseline (LBL), short baseline (SBL) and ultra-short baseline (USBL). These methodologies are described below.

Long baseline (LBL) systems use a network of baseline transponders placed on the seafloor, around the perimeter of a work site within which the target (e.g. vehicle, diver) operates. The LBL technique yields high positioning accuracy, which is depth independent and is typically between 2-50 cm, depending on the frequency of the transmitted pulse. LBL provides better accuracy than SBL or USBL systems, and is primarily used in precision survey work. A typical LBL system consists of one transceiver and three or more transponders. The transceiver is mounted on the target and the transponders are installed on the seafloor at accurately determined positions. The transceiver in the target emits an acoustic pulse; the baseline transponders ping back as they detect the pulse from the transceiver. The two-way travel time of the pulse from the transceiver to each of the transponders and the sound speed measurement are used to calculate the distance transceiver-transponders. The target position is then obtained by a method called *trilateration*, which determines the unique point where all transceiver-transponder paths intersect. The information is transmitted to the surface via an umbilical connected to the target. LBL systems provide the maximum position accuracy independent of water depth, which is preserved over a wide area, but the calibration and configuration process can be relatively time consuming (Hillier, 2010).

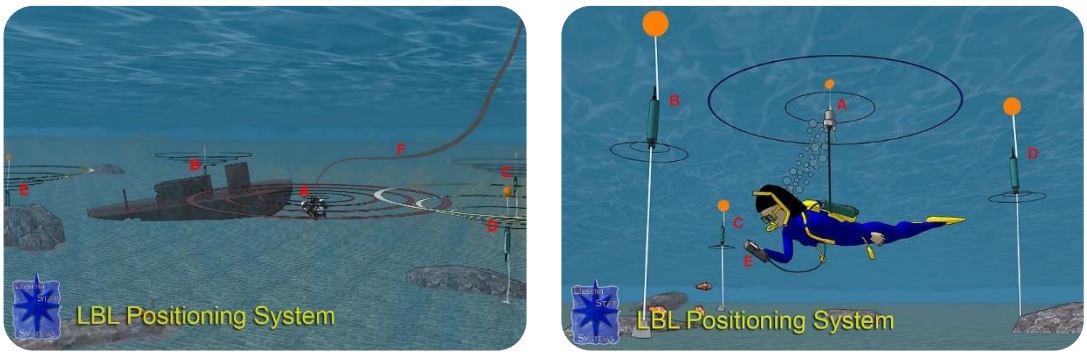

Figure 3.11 Long Baseline positioning system applied to an ROV and a diver. In the left image, A is the interrogator, B-E the baseline transponders and F the ROV umbilical; in the image on the right, A is the interrogator, B-D the baseline transponders and E the diver's positioning terminal (from www.deserstar.com)

Ultra-short baseline (USBL) systems use a compact transducer array, typically installed on the hull of a surface vessel, to determine the distance and angle to the target. The USBL technique is only applicable for shallow water or low-accuracy, deep water positioning because positioning accuracy rapidly decreases with depth. The typical positioning accuracy for USBL is 0.2-1 % of slant range (Tomczak, 2011). The USBL

system consists of a ship-mounted transceiver, made up of several transducers with a separation of half a wavelength (~10 cm), and a transponder, installed in the target (e.g. diver, towfish, ROV). The transceiver emits an acoustic pulse that is detected by the transponder in the target, which responds with a return pulse. The two-way time delay and the relative phase difference of the pulse received at each transducer in the transceiver are used to calculate the *range* and *angle* to the target, respectively. Attitude and heading sensors are included to maintain position accuracy. In inverted configurations (iUSBL) the transceiver is mounted in an AUV and the transponder on the target, and are useful for automatic docking and target tracking. USBL systems provide limited accuracy, but are easy to install and set up, only one transceiver is required to track all targets, and can be used in small boats or buoys (Hillier, 2010).

Short baseline (SBL) systems use three or more transceivers installed on the hull of a surface vessel, and as LBL systems, determine the position of the transponder in the target by *trilateration*. The position accuracy improves with transceiver spacing, and when operated from larger vessels or a dock the SBL system can achieve position accuracy similar to that of LBL systems. Transceiver spacings range from 10 to 50 m. One of the transceivers sends out an acoustic signal; the transponder responds with its own acoustic pulse, which is received by the baseline transceivers, so the time delay from each of them to the transponder can be used to calculate the target position. An SBL system needs inertial motion sensors to compensate for the roll, pitch and yaw movements.

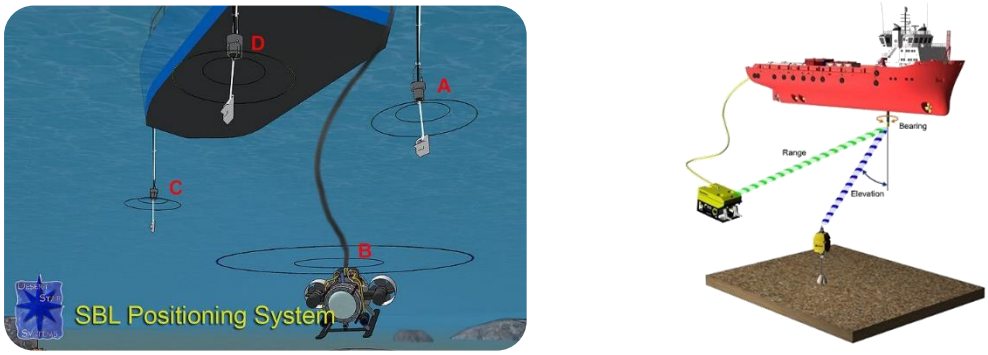

Figure 3.12 Configuration of hull-mounted Short Baseline (left, from www.desertstar.com) and Ultra-Short Baseline (right) positioning systems. In the left image, A,C,D are the surface transceivers and B the transponder mounted on the tracked object.

3.7.1 Tables

Table 3.11 Sounds produced by underwater positioning devices

Source (*Model*)	SL [dB re 1μPa@1m]	Signal Characteristics	Description	Reference
USBL/LBL Transponder and Modem (*Sonardyne Compatt 6 8300-3111*)	187-196 dB_{rms} (4 levels)	f = 19-34kHz Beam width: omni	z_{max} = 3 km Application: navigation reference transponder, autonomous data logger, and multi-purpose modem	Sonardyne, 2016
USBL/LBL Transponder and Modem (*Sonardyne Compatt 6 8300-3113*)	190-202 dB_{rms} (4 levels)	f = 19-34kHz Beam width: directional	z_{max} = 3 km Application: navigation reference transponder, autonomous data logger, and multi-purpose modem	Sonardyne, 2016
USBL/LBL Transponder and Modem (*Sonardyne Compatt 6 8300-5213*)	190-202 dB_{rms} (4 levels)	f = 19-34kHz Beam width: directional	z_{max} = 5 km Application: navigation reference transponder, autonomous data logger, and multi-purpose modem	Sonardyne, 2016
Transponder (*Sonardyne Coastal Transponder*)	184-187 dB_{rms}	f = 35-50 kHz	z_{max} = 500 m Application: tracking through external interrogation, installed in small targets	Sonardyne, 2013

Table 3.11 Sounds produced by underwater positioning devices (cont.)

Source (*Model*)	SL [dB re 1µPa@1m]	Signal Characteristics	Description	Reference
LBL Transponder (*Konsberg MPT163*)	186 dB_{rms} [a] 198 dB_{rms} [b]	f = 10-12.5 kHz (Rx), 13-15.75 kHz (Tx) Beam width: ±30°,±60°	z_{max} = 6 km Application: dynamic position reference for surface vessels, AUV, underwater structure works, riser angle, LBL transponder, etc [a] for ±60° beam width [b] for ±30° beam width	Konsberg, 2003
Multifunction Positioning Transponder (*Konsberg MPT31x Series*)	188 dB_{rms} [a] 195 dB_{rms} [b] 192 dB_{rms} [c]	f = 21-24.5 kHz (Rx), 27-31.5 kHz (Tx) Beam width: ±30°,±45°,±90°	z_{max} = 1 km Application: SSBL and LBL [a] for ±90° beam width [b] for ±45° beam width [c] for ±30° beam width	Konsberg, 2003
Multifunction Positioning Transponder (*Konsberg SPT31x Series*)			z_{max} = 1 km Application: SSBL [a] for ±90° beam width [b] for ±45° beam width [c] for ±30° beam width	
Multifunction Positioning Transponder (*Konsberg MPT33x Series*)	195 dB_{rms} [a] 206 dB_{rms} [b]	f = 21-24.5 kHz (Rx), 27-31.5 kHz (Tx) Beam width: ±15°,±90°	z_{max} = 1 km Application: SSBL and LBL [a] for ±90° beam width [b] for ±15° beam width	Konsberg, 2003
Multifunction Positioning Transponder (*Konsberg SPT33x Series*)			z_{max} = 1 km Application: SSBL [a] for ±90° beam width [b] for ±15° beam width	

3.8 The Acoustic Release

An *acoustic release* is an oceanographic device used for sea bottom deployment and recovery of underwater instrumentation. The device comprises a hydrophone, housing for battery, mechanic elements and electronics, and a release hook. In the deployment, the acoustic release and payload are attached to an anchor weight that remains on the seafloor and a float that keeps the deployed unit upright. The assembly remains underwater until an acoustic command is used to trigger the recovery. Acoustic releases have low power consumption and are typically designed for long-term operation (1-2 years). These support large payloads (up to 20 tonnes) and are especially useful in deep waters, where the instrumentation could not be easily recovered.

Figure 3.13 Acoustic release transponder P-DORT (from www.sonardyne.com).

The deployed package (release, payload, anchor and float) can remain underwater from minutes to several years, while the attached subsea device operates. Upon reception and verification of the specific trigger signal emitted from the control station (e.g. vessel) the acoustic release detaches from the anchor weight, and the package is raised to the surface by the floating unit. The release mechanism can be of three types: *high-torque motor*, for heavy payloads; *fusible link*, fast but only for small payloads; and *electrolytic erosion*, similar payloads to fusible links but slower release.

Acoustic releases are generally passive devices, but many models currently include both reception and transmission capabilities and incorporate features of positioning transponders and acoustic modems. The transmission function allows for accurate positioning and confirmation of release actuation.

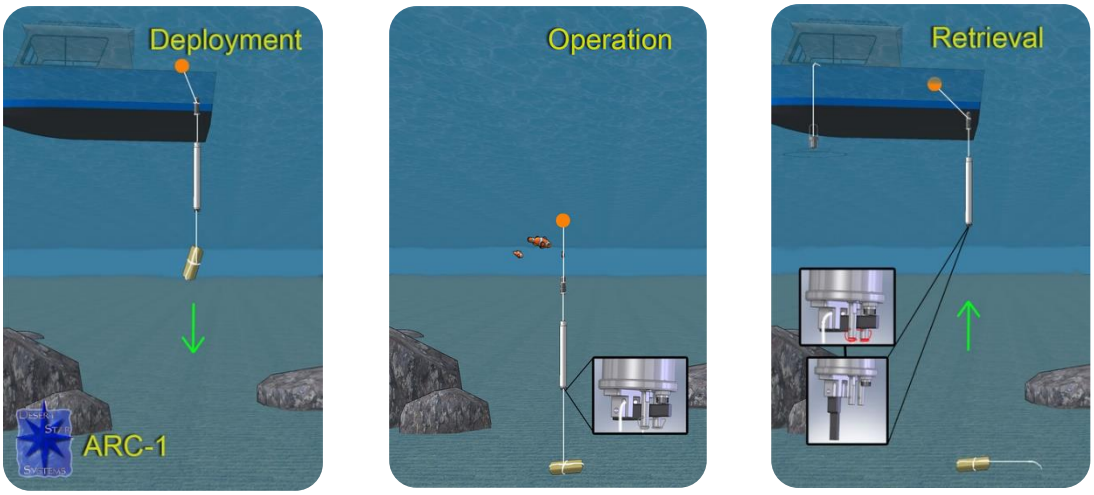

Figure 3.14 Deployment, operation and retrieval phases of an acoustic release package (from www.desertstar.com).

3.8.1 Tables

Table 3.12 Sounds produced by acoustic releases

Source (*Model*)	SL [dB re 1µPa@1m]	Signal Characteristics	Description	Reference
Acoustic Release (Sonardyne *7986 LRT*)	185 dB_{rms}	f = 35-50 kHz	z_{max} = 500 m Shallow water lightweight release transponder Release type: screw-off	Sonardyne, 2003
Acoustic Release (Sonardyne *7409 ORT*)	186 dB_{rms}	f = 19-36 kHz	z_{max} = 2 km Deep water release transponder. Release type: spring assisted hook	Sonardyne, 2003
Acoustic Release (Sonardyne *7710 DORT*)	190 dB_{rms}	f = 7.5-15 kHz	z_{max} = 6 km Very deep water release transponder Release type: spring assisted hook	Sonardyne, 2003
Acoustic Release (Sonardyne *8048 Heavy Load DORT*)	190 dB_{rms}[a]	f = 7.5-15 kHz	z_{max} = 7 km Very deep water release transponder Release type: spring assisted hook [a]with alkaline battery, 184 dB_{rms} with lithium	Sonardyne, 2007
Acoustic Release (Sub Sea Sonics *AR60 E*)	171.5 dB_{rms}	T = 1 s τ = 20 ms f = 33-39 kHz (Rx), 38.4 kHz (Tx)	z_{max} = 300 m Acoustic release Release type: electrolytic erosion	Sub Sea Sonics, 2012
Acoustic Release (Sub Sea Sonics *ARI60*)	181.5 dB_{rms}	T = 1 s τ = 2.5 (wake up signal), 20 ms (action pulses) f = 35.7-42 kHz (Rx), 33-35.7 kHz (Tx)	Acoustic release interrogator used with the AR60 E	Sub Sea Sonics, 2012
Acoustic Release (Teledyne *Benthos 875-TD*)	167 dB_{rms}	f = 9-14 kHz	z_{max} = 500 m r_{max} < 3 km (slant range) Release type: high torque motor	Teledyne, 2016
Acoustic Release (Teledyne *Benthos R2K*)	185 dB_{rms}	f = 9-14 kHz	z_{max} = 2 km r_{max} < 10 km (slant range) Release type: high torque motor	Teledyne, 2016
Acoustic Release (Teledyne *Benthos R12K*)	185 dB_{rms}	f = 9-14 kHz	z_{max} = 12 km r_{max} < 12 km (slant range) Release type: high torque motor	Teledyne, 2016
Acoustic Release (General)	185-190 dB_{rms}	τ = order of ms f = 7.5-50 kHz Omnidirectional beam	N/A	Boebel et al., 2005
Acoustic Release (General)	≤ 192 dB_{pk}	f = 7-15 kHz Omnidirectional beam	N/A	Boebel et al., 2005

3.9 The Acoustic Doppler Current Profiler

The *Acoustic Doppler Current Profiler* (ADCP) measures the speed, direction and depth in the water column of currents in the ocean using the principle of Doppler shift. The Doppler effect explains the change in frequency of the sound due to the relative speed between the source and the receiver.

The ADCP works by transmitting a tone burst or *ping* into the water. The small particles carried by the moving water (e.g. zooplankton, bubbles and suspended sediments) partially reflect the energy of the pulse as it travels through the water. Particles moving away from the acoustic beam return a signal of lower frequency; a higher frequency signal is received when the particles move towards the beam. This change in pitch or *Doppler shift* can be used to remotely measure the absolute speed and direction of currents at constant distance intervals, which is called a *current profile*; the intensity of the received signal gives an indication of the abundance of suspended particles. ADCPs can capture four types of measurements simultaneously: current profile, spatial distribution of suspended particles, ADCP speed over ground, and distance to seabed or surface.

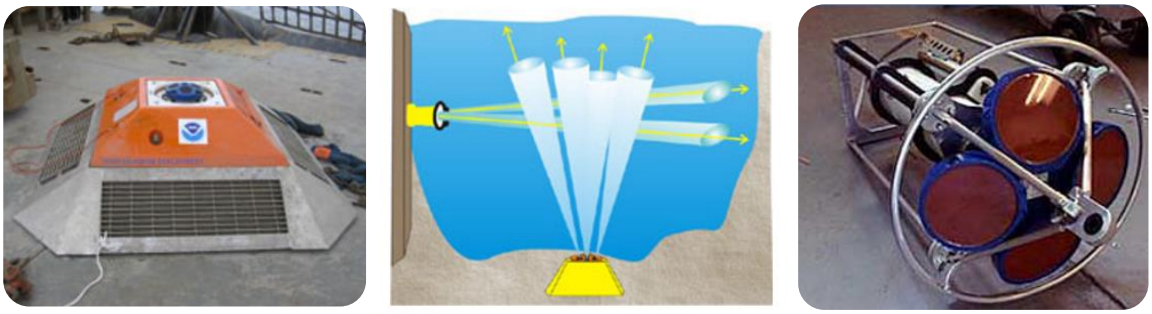

Figure 3.15 NOAA (left, from oceanservice.noaa.gov) and WHOI (right, from www.coml.org) Acoustic Doppler Current Profilers. Combination of vertically and horizontally oriented ADCPs for accurate measurements of currents through a waterway (centre, from oceanservice.noaa.gov).

These devices can be placed on the seafloor, or installed in the hull of a vessel or in a buoy. ADCPs can be oriented horizontally, upwards or downwards. Moored ADCPs contain a power supply, a processing unit, internal memory (data logger), and the transducer array; vessel-mounted ADCPs typically use an external on-board computer and GPS, to subtract the vessel movement from the water current data. ADCPs are usually equipped with three or four transducers pointing at different angles, to measure a three-dimensional current velocity profile.

The pulse frequency limits the maximum range of the current profile: higher frequencies yield more precise data, but lower frequencies travel further. The frequency of the acoustic pulse ranges from 100 kHz to 2 MHz, with covered ranges between 25-2000 m. If the water is relatively particle-free (e.g. clear waters in the tropics), the pulse may not produce reliable data.

3.9.1 Tables

Table 3.13 Sounds produced by acoustic doppler current profilers.

Source (*Model*)	Measurement [dB re 1µPa]	SL [dB re 1µPa@1m]	Signal Characteristics	Description	Reference
Ocean Observer & Ocean Surveyor	180 dB_{rms} @ 182 m 180 dB_{rms} @ 22 m	227 dB_{rms}	f = 38.4 kHz τ = 37 ms T > 2.5 s (typ. 3 s) FR_{-3dB} = 37.2-39.6 kHz	4 beams, 30° beam angle, phased array [a]beam axial direction [b]beam 20° off-axis	Teledyne, 2016; www.teledynemarine.com
	180 dB_{rms} @ 139 m[a] 180 dB_{rms} @ 12 m[b]	227 dB_{rms}	f = 76.8 kHz τ = 24 ms T > 1.4 s (typ. 2 s) FR_{-3dB} = 74.4-79.2 kHz		
	180 dB_{rms} @ 109 m[a] 180 dB_{rms} @ 11 m[b]	226 dB_{rms}	f = 153.6 kHz τ = 12 ms T > 0.7 s (typ. 1 s) FR_{-3dB} = 148.8-158.4 kHz		

Table 3.13 Sounds produced by acoustic doppler current profilers (cont.)

Source (*Model*)	Measurement [dB re 1µPa]	SL [dB re 1µPa@1m]	Signal Characteristics	Description	Reference
WorkHorse Long Ranger	180 dB_{rms} @ 107 m[a] 180 dB_{rms} @ 8 m[b]	223 dB_{rms}	f = 76.8 kHz τ = 23 ms T > 1 s (typ. 2 s) FR_{-3dB} = 67.2-86.4 kHz	4 beams, 20°/4° beam angle/width, convex [a]beam axial direction [b]beam 20° off-axis	Teledyne, 2016; www.teledynemarine.com
WorkHorse QuarterMaster	180 dB_{rms} @ 36 m[a] 180 dB_{rms} @ 1.4 m[b]	213 dB_{rms}	f = 153.6 kHz τ = 11 ms T > 1 s (typ. 1 s) FR_{-3dB} = 134.4-172.8 kHz	4 beams, 20°/4° beam angle/width, convex [a]beam axial direction [b]beam 20° off-axis	Teledyne, 2016; www.teledynemarine.com
WorkHorse Sentinel	180 dB_{rms} @ 40 m[a] 180 dB_{rms} @ 1.8 m[b]	215 dB_{rms}	f = 307.2 kHz τ = 5.7 ms T > 0.1 s (typ. 0.75 s) FR_{-3dB} = 268.8-345.6 kHz	4 beams, 20° beam angle, convex [a]beam axial direction [b]beam 20° off-axis	Teledyne, 2016; www.teledynemarine.com
	180 dB_{rms} @ 31 m[a] 180 dB_{rms} @ <1 m[b]	217 dB_{rms}	f = 614.4 kHz τ = 2.8 ms T > 0.1 s (typ. 0.5 s) FR_{-3dB} = 537.6-691.2 kHz		
	180 dB_{rms} @ 18 m[a] 180 dB_{rms} @ <1 m[b]	214 dB_{rms}	f = 1,229 kHz τ = 1.4 ms T > 0.1 s (typ. 0.5 s) FR_{-3dB} = 1,075-1,382 kHz		

3.10 Overview of Sound Levels and Spectral Coverage

This section presents a summary of some basic acoustic properties for the engineering sources addressed in this chapter.

Table 3.14 Main acoustic characteristics of different types of underwater engineering source (from Tab. 3.1-3.8 and 3.10-3.12)

Source	SL_{rms} [dB re. 1µPa]	FR [kHz]	τ [ms]	T [s]	Penetration [m]	Resolution [m]
SBP (Pinger)	170-210	3.5-12.5	0.1-16	0.125-0.3	10-50	0.2
SBP (Chirp)	170-230	2-23	1-100	> 0.25	5-50	0.1
SBP (Sparker)	190-220	0.2-3	0.2-5	4-6	30-750	0.3-1
SBP (Boomer)	205-225	0.3-6	0.1-0.4	0.5-1	20-150	0.2-0.5
SBP (Bubble Pulser)	165-180	0.4	5-120	0.5-5		
Transponder	185-205	13-50	20	1		
Acoustic Release (Tx)	170-190	7-50	20	1		
Acoustic Modem	185-195	8-80				
AHD	180-205	3-40	1-2000	0.04-5		
ADD	120-155	3-180	5-300	4-30		
SBES	200-235	12-200	0.1-20			
MBES	210-245	12-700	0.2-20	5-15		
SSS	200-235	50-900	0.09-0.2	0.5-20		
ADCP	214-227	35-1200	1-40	0.1-3		

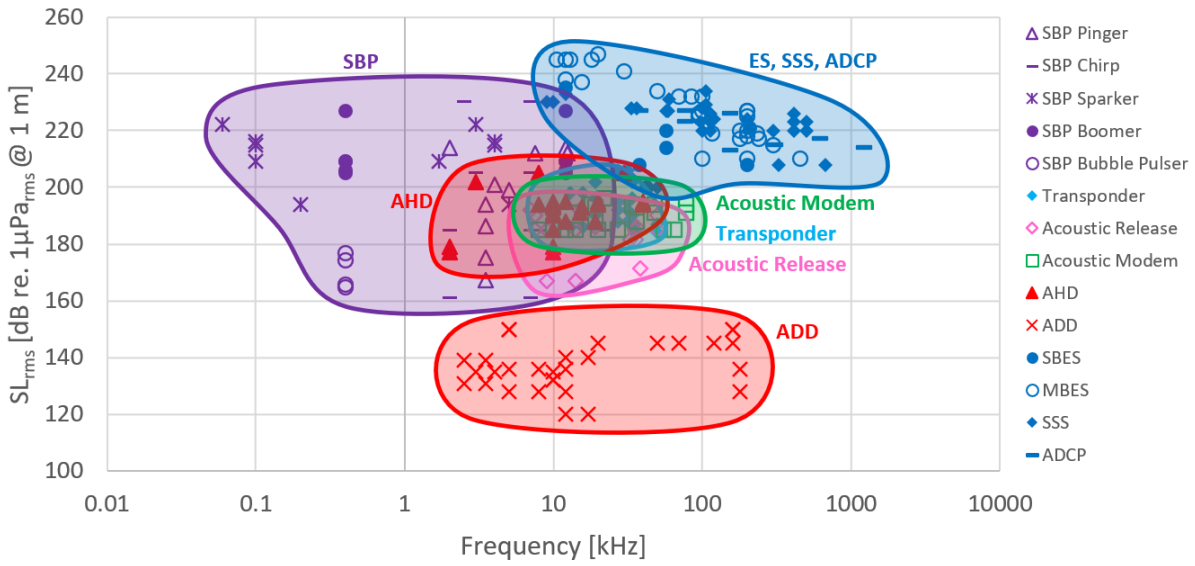

Figure 3.16 Sound level and spectral range of various categories of underwater engineering sources. The markers represent source levels at the operating frequency of the device (e.g. pinger, bubble pulser) or at the lower and upper frequencies of its operating band (e.g. chirp, air gun, acoustic modem). Values extracted from Tables Table 3.1-Table 3.8 and Table 3.10-Table 3.13.

4 Vessels

From among the several types of underwater acoustic sources associated with human activities, vessels are the main contributor to noise in the oceans, given their large number, wide distribution and mobility (Richardson et al., 1995). All vessels, from boats to supertankers, produce underwater sound. They share the same principal mechanisms of sound generation, but differences may exist between vessel types due to discrepancies in size, design and operation.

The main sources of sound generation in vessels are described in Section 4.1; details about the acoustic characteristics of different types of vessel are addressed in Sections 4.2-4.5; and a summary of the characteristics of sound produced by small, medium and large vessels is included in Section 4.6.

4.1 Sound Generation Mechanisms in Vessels

The sound produced by a vessel is a combination of tonal components and broadband energy. The spectral characteristics and sound levels are related to ship size and speed, but still significant variation may be found among vessels within the same group. The primary sources of sound in a vessel are the propeller, the machinery and the water flow. Above 25 knots, sound from propeller cavitation is dominant and tends to increase with speed, but below 25 knots flow noise prevails (Widjiati et al, 2012). The individual acoustic sources in a vessel are located in different places. From a certain distance the radiated noise will be perceived as a combination of these multiple sources, each of them with its own characteristics and dependence on operational conditions.

Understanding the mechanisms of sound generation is key for the definition of noise control measures in vessels, but also for the interpretation of noise measurements. In the following subsections, the acoustic radiation mechanisms of the propeller, machinery and water flow are described.

4.1.1 Propeller

A propeller is a fan-type device that converts rotational motion into thrust by an accelerated water flow, which results in a force that pushes the ship forward. Propellers typically consist of 3 to 5 blades, with diameters that range from less than 1 metre for small boats to 10 m for the largest vessels. The diameter is determinant for the efficiency of a propeller; a larger number of blades result in less efficiency, but provide more total blade area for the same diameter, also reducing the vibration associated with larger blades.

Propeller noise can be grouped into *cavitating* and *non-cavitating*. Non-cavitating noise includes *singing* effect associated to the resonance of the blades at their natural frequencies, and pressure pulses due to inhomogeneities in the fluid pressure.

Cavitating propellers are an important source of acoustic emissions, and the study of propeller cavitation has become a priority in the general effort made to reduce shipping noise (Firenze & Valdenazzi, 2015). Cavitation occurs when the pressure in the liquid suddenly drops, making the gas in solution evolve into bubbles. As the propeller rotates, the positive and negative pressures in the face and back of the blade generate the required thrust. At sufficiently high rotation speeds, cavitation appears in the region of negative pressure (see Figure 4.1, left). The cavity formed rapidly collapses when the pressure increases as the blade turns downward. The pressure is lower in the upper section of the propeller, and cavitation

consequently stronger, due to the nonuniform wake field created by the hull and to the lower hydrostatic pressure. The collapse of the bubbles produces a shock wave that over time will damage the surface of the propeller blades (see Figure 4.1, right).

The sound radiated from propeller cavitation is made of tonal and broadband components. Tonal components are associated with the fundamental blade passing frequency and its harmonics, since every time a blade passes the bottom high-pressure region the cavitating bubbles implode. The broadband sound is caused by the chaotic collapse of bubbles of different sizes. The blade rate is the dominant source of low frequency tones at high speed, when propeller cavitation dominates. For the diesel-powered vessel Overseas Harriette (Arveson & Vendittis, 2000) cavitation inception occurred at 86 rpm (10 kts), but for an older ship with a damaged propeller lower inception speeds may be expected. The wideband cavitation spectrum is characterised by a maximum energy region followed by a constant decay in sound level (for the Overseas Harriette, the peak is centred at 55 Hz, decreasing afterwards by 3 dB per octave). As the vessel speed exceeds the cavitation inception speed the overall level increases, but the shape of the spectrum remains practically the same.

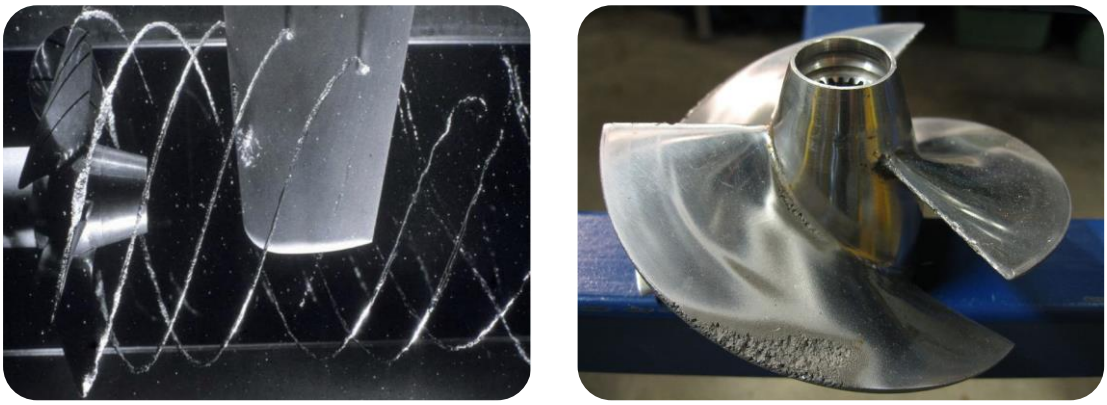

Figure 4.1 Propeller cavitation (left, from Abrahamsen, 2012) and damage produced by cavitation on the propeller blades (right, from www.wikipedia.org).

There are various types of cavitation according to the position on the propeller where they occur, and include (see Figure 4.2): tip vortex, hub or Boss vortex, sheet, face, root, propeller-hull vortex, cloud and bubble cavitation. Except the hub and root cavitation, the rest are generated in the blades. The particularities of these different types of cavitation are described below.

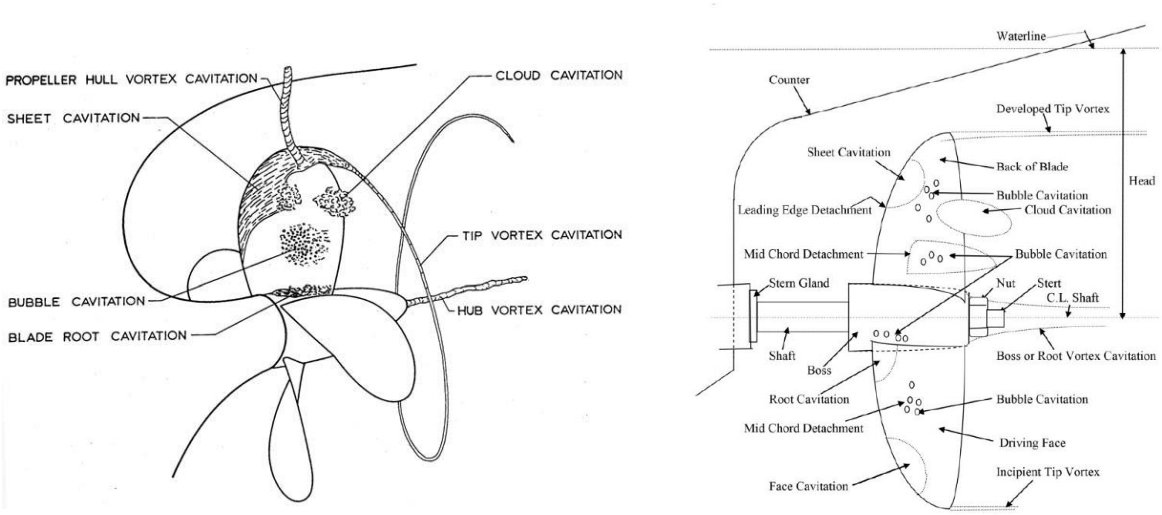

Figure 4.2 Main types of propeller cavitation (left, from Abrahamsen, 2012) and detailed schematic representation of the parts of a propeller and associated cavitation (right, from Casciani-Wood, 2015).

The *tip vortex cavitation* is caused by the low pressure vortices that appear at the tips of the propeller blade, as a result of a pressure difference between the suction and pressure sides of the blade (Abrahamsen, 2012). The vortices are cylindrical and describe a spiral as the blades move forward (see Figure 4.1-4.2, left). The strength of these vortices depend on the wake field, and the geometry and loading on the blade. The collapse of the bubbles occurs at a certain distance from the propeller and produces broadband sound, with a spectral peak that shifts to lower frequencies as the thrust loading increases.

Blade sheet cavitation occurs when large suction pressures appear near the leading edge, creating a sheet of bubbles on the back of the blade, where pressures are lowest (see Figure 4.3, left). The chance of sheet cavitation increases at high tip speeds and is a function of the angle of attack of the blade to the varying wake field. A propeller is considered *fully cavitating* when the entire back of the blade is covered in sheet bubbles (Cascianni-Wood, 2015). The generated sound is broadband in nature and similar to that from cavitating tip vortices. In propellers with a high or moderate degree of *skew* (i.e. lateral curvature) in their blades, vortices will appear along the leading edge, which can interact aggressively with the tip vortex.

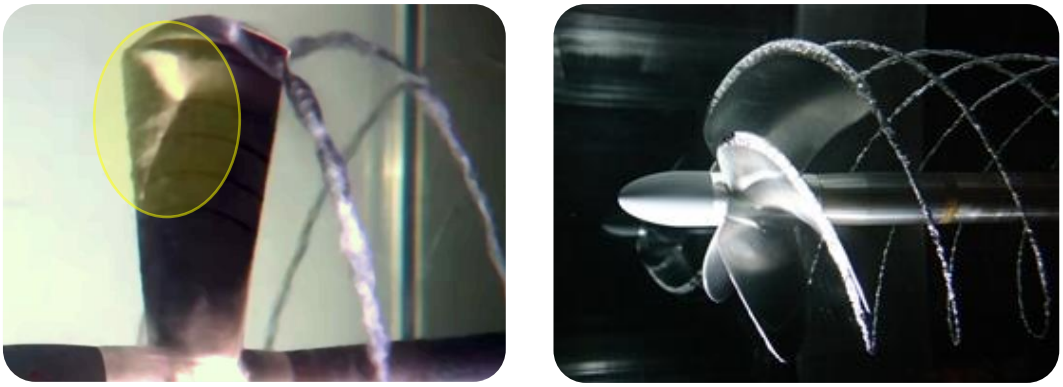

Figure 4.3 Sheet bubble cavitation behind the leading edge of the blade, in yellow circle (left, from www.axiompropellers.com). Leading edge cavitation in a propeller with a moderate degree of skew (right, from www.heliciel.com).

The existence and strength of *hub* or *Boss vortex cavitation* depends on the blade's pitch, and appears when the angle of incidence of the leading edge of the blade is high compared to the direction of water flow.

Root cavitation bubbles form on the hub and between blades and appear if the flow down the root is strong enough. If the root vortices reach the hub vortex they may end up forming a stranded rope, with as many strands as blades, similar to the tip vortex spirals.

Cloud cavitation occurs close to the collapse area of sheet cavitation, and can be extremely aggressive (Cascianni-Wood, 2015).

Bubble cavitation forms in the middle region of the blade. This type of cavitation is associated with a high curvature of the blade and can be eliminated at the design stage (Cascianni-Wood, 2015).

Face cavitation occurs in the driving or exposed face of the blade and is associated with an incorrect pitch distribution along the blade (Cascianni-Wood, 2015).

The *propeller-hull cavitation* creates a vortex between the tip of the blade and the vessel's hull and tends to occur at slow speed and high load conditions (e.g. vessel accelerating at rest).

The propeller *singing* is a non-cavitating effect that arises when the trailing edge vortices excite the natural frequencies of the blades. The result is a distinct tonal sound with frequencies between 100 to 1,000 Hz. The amplitude of these tones varies with the strength of the vortices, affected by the wake field. The singing effect is generally more intense in damaged propellers. Singing normally ceases when cavitation is strong, as cavitating bubbles absorb the vibrational energy from the blades (Richardson et al., 1995).

In summary, sheet and tip vortex cavitation evolve with the blade passing rate, and both contribute to the tonal part of the radiated sound. As clouds of bubbles associated with the various cavitation processes collapse, including those from sheet and tip vortex cavitation, broadband sound is produced. The sound reflected from the hull contributes to make the radiated acoustic pattern even more complex as it interferes with the direct sound; this interference phenomenon is only significant in the tonal region of the spectrum (Abrahamsen, 2012).

4.1.2 Machinery

Unlike the sound generated in the propeller, the sound associated to the machinery originates inside the vessel and is transmitted in the form of vibrations through the hull. The hull is partially submerged in the water and the machinery extends throughout its length. The acoustic radiation will strongly depend on the coupling of the machinery with the hull, and on the mechanical characteristics of the supporting structure and submerged shell plates. Low frequency sound is associated with the vibration of large hull areas (Abrahamsen, 2012).

The majority of the sound from machinery is produced by two systems: the *Ship's Service Diesel Generator* (SSDG) and the main propulsion engine. Arveson & Vendittis (2000) studied the acoustic signature of a cargo ship representative of many direct-drive, diesel-powered vessels, the *M/V Overseas Harriette*. The SSDG radiated a series of 6 Hz harmonics, stable in amplitude and frequency, which contributed to almost all the radiated sound at low ship speeds; some harmonics (24 and 30 Hz) were still important contributors at high speeds (see Figure 4.4). At higher speeds, the tones associated to the "piston slap" in the propulsion engine dominate; these firing rate tones are not as stable as those produced by the SSDG due to variations in propeller loading.

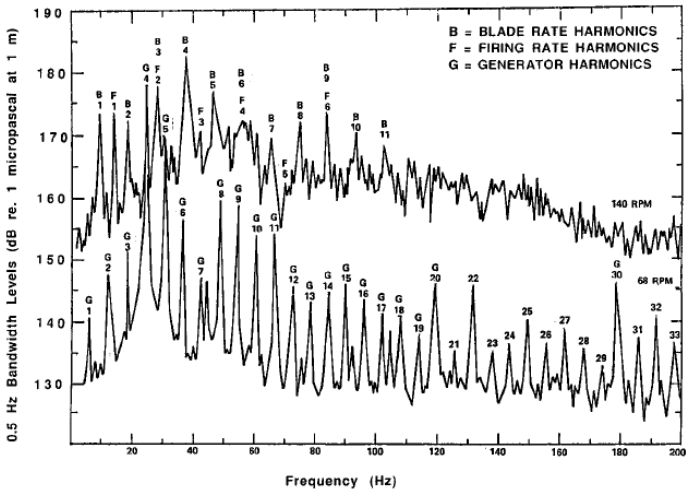

Figure 4.4 Narrowband spectra of *M/V Overseas Harriette* at low speed (68 rpm) and maximum speed (140 rpm). The harmonics from blade rate, firing rate and diesel generator are identified by letters B, F and G respectively (from Arveson & Vendittis, 2000)

4.1.3 Water Flow

The hull and any appendices and openings in it will generate turbulence and vortices by its interaction with the water. Flow noise is caused by these vortices, which extend throughout the hull and may excite some of its structural natural frequencies (Abrahamsen, 2012).

4.2 Commercial Vessels and Supertankers

The globalised economy has been accompanied by an increase in the number, size, power and complexity of commercial ships. The expansion of shipping since the 1960s has contributed to an important increase in ambient sound levels in the ocean. In the following subsections the types of commercial vessels and their acoustic characteristics are described.

4.2.1 Types of Vessel

The designs of different ship types are greatly influenced by the cargo they carry. Commercial vessels are classified into eight main categories according to the type of product they can transport: general cargo, container, RO-RO, bulk carrier, crude carrier, product carrier, liquified gas carrier and chemical carrier. The first four types are designed to transport dry cargo, and the last four to transport liquid products.

Figure 4.5 Types of dry cargo vessels, from left to right and top to bottom: general cargo vessel, container vessel, RO-RO vessel and bulk carrier (from www.tuscorlloyds.com)

General cargo vessels carry cargo in the form of pallets or bags, known as *breakbulk*, and loose and irregular cargo. The loading and unloading is usually carried out with cranes installed in the vessel. General cargoes comprise 4.4 % of the world fleet (UNCTAD, 2015).

Container vessels carry standard rectangular shipping containers, arranged in tiers and stacked on the deck of the vessel. Standard containers are measured in *Twenty-foot Equivalent Units* (TEU), are typically 8 feet wide, 8.5 feet high and 1 to 2 TEU long, and can accommodate from food, liquids and electric equipment to automobiles. Gantry cranes are used as an efficient way of loading and unloading containers, directly between the vessel and the truck. Container vessels are some of the biggest vessels (e.g. Emma Maersk, with a capacity of 15,000 TEU) and are mainly used on liner routes; the largest are unable to transit certain areas and ports due to size and draft. Container vessels did not exist until the 1960s, and currently they make up 13% of the world fleet (UNCTAD, 2015) and have become the main way of transporting manufactured products, comprising 52% of the global ocean trade.

Roll-On/Roll-Off vessels (RO-RO) are a type of container ship with a high box shape specialised in the transport of wheel cargo. The vehicles are loaded and unloaded using ramps. The largest RO-RO vessel is the Mark V Class, which is 265 m long and provides 138,000 m^3 of cargo space.

Bulk carriers are used to efficiently transport loose dry cargo with high weight to cost ratio (e.g. coal). These large vessels are divided into separate holds covered by hatches, and loaded by spouts, conveyors or grab cranes; this last method is the norm for unloading bulk cargo. Bulk carriers comprise 43.5% of the world fleet (UNCTAD, 2015).

Figure 4.6 Types of liquid cargo vessels, from left to right and top to bottom: crude oil tanker, product carrier, liquified gas carrier and chemical carrier (from www.tuscorlloyds.com)

Oil tankers are designed to transport crude oil to refineries. The Very Large and Ultra Large Crude Carriers (VLCC, ULCC), also known as supertankers, can carry 318,000 tons of oil and the largest of them, the Knock Nevis, was 460 m long. The largest oil tankers are too large to dock at ports and cargo is unloaded at offshore pumping stations. These vessels make up 28% of the world fleet (UNCTAD, 2015).

Product carriers are a smaller version of crude carriers and are used to transport refined petrochemicals such as petroleum, diesel, or tar from offshore stations to ports. The smaller carriers are also used to transport non-petroleum products (e.g. palm oil and molasses).

Liquified gas carriers are specialised vessels designed to transport *Liquified Natural* or *Petroleoum Gas* (LNG, LPG) within large spherical tanks under high pressures. LNG carriers are often larger than LPG carriers; he largest LNG carriers are the 'Q-Flex', 345 m long with a capacity of 266,000 m^3. Gas carriers comprise 2.8% of the world fleet (UNCTAD, 2015).

Chemical carriers are similar in size to product tankers but are designed to transport a range of chemicals. The material used for the cargo tanks, which includes stainless steel and phenolic epoxy coating, determines the type of cargo. These vessels make up 2.4% of the world fleet (UNCTAD, 2015).

Figure 4.7 Cruise ships *Universe Explorer* (from www.ssmaritime.com) and *Holland America Statendam* (from Kipple, 2000).

Cruise ships are the largest category of passenger vessel, and can be up to 360 m long, 60 m wide and carry more than 6,000 passengers. These large vessels are fitted with a wide range of facilities including restaurants, shops, pools, casinos and cinemas.

4.2.2 Acoustic Signature and Spectral Characteristics

Large commercial vessels and supertankers are equipped with powerful engines and low-speed propellers (80-110 rpm) which result in intense, low-frequency acoustic radiation (Richardson et al., 1995). McKenna et al. (2012) presented a series of opportunistic measurements on seven types of modern commercial vessels during normal operation, as they transited the Santa Barbara Channel, off the coast of southern California. The measurements included container ships, vehicle and bulk carriers, open hatch cargo ships, and crude oil, chemical and product tankers. The sound levels and spectral response from these different types of vessel are included in the article and the key conclusions can be summarised in the following points:

- For *container ships* the received levels are highest below 100 Hz, and mainly below 40 Hz, but higher frequency sound is produced at shorter distances from the vessel. A 54,000 GT container ship generated the highest broadband source level, of 188 dB re 1µPa@1m.
- The received levels from *bulk carriers* are highest near 100 Hz.
- Broadband received levels (20-1000 Hz) are highest for *container ships and bulk carriers*.
- For *crude oil*, *product* and *chemical tankers* most of the energy is below 100 Hz, and mainly below 40 Hz, but unlike *container ships* and *bulk carriers,* the energy above 300 Hz is lower.
- Tankers, open hatch cargoes and vehicle carriers have similar broadband received levels.

Measurements presented by Richardson et al. (1995) from two supertankers underway in deep water, the Mostoles and World Dignity, showed highest sound levels below 10 Hz, particularly near 2 Hz. The broadband components caused by propeller cavitation were centred at 40-50 Hz for *Mostoles* and near 100 Hz for *World Dignity*, which had propellers of diameter 6.3 and 9 m, respectively. If components down to 2 Hz are included, source levels can exceed 205 dB re 1µPa@1m.

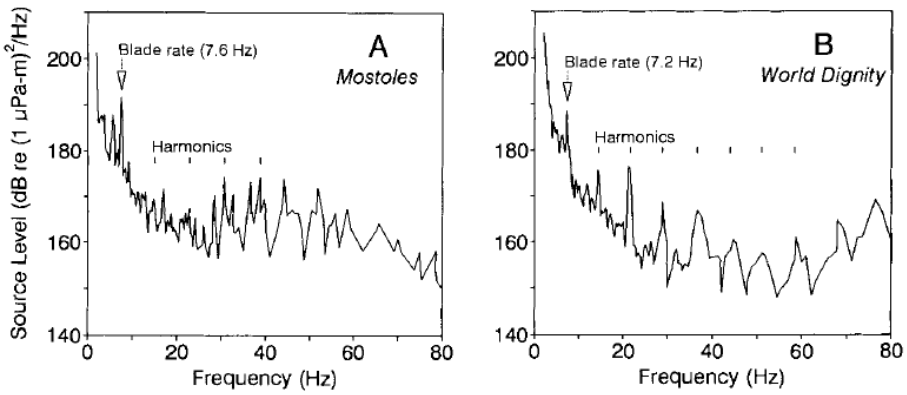

Figure 4.8 Low-frequency source level spectra for two supertankers: A) Mostoles, 103 kT, 266 m long, 12.6 kts; B) World Dignity, 271 kT, 337 m long, 17.7 kts (from Richardson et al, 1995)

The differences in the acoustic signature of the various types of vessel addressed in McKenna et al. (2012) may be related to ship load, propeller type, hull design and operation. Except for the chemical tanker with identifier 355799000, for which the high source level could be attributed to a damaged propeller, the state of the propeller is unlikely to be a factor of major differences between vessel types. Similar source levels for bulk carrier and container ships may be explained by the source depth, since a smaller draft (i.e. shorter distance between the real and image source of the dipole formed at the sea surface) will result in a lower

radiated sound level (i.e. lower strength of the dipole). In bulk carriers all cargo is stored below deck, increasing the source depth compared to container ships, where 60% of the cargo is stored on deck (McKenna et al., 2012). The vehicle carriers were larger and travelled faster than open hatch cargo vessels and chemical tankers, but produced the lowest source levels among all vessel types; this may be explained by the shallower draft of vehicle carriers that results from their boxlike shape.

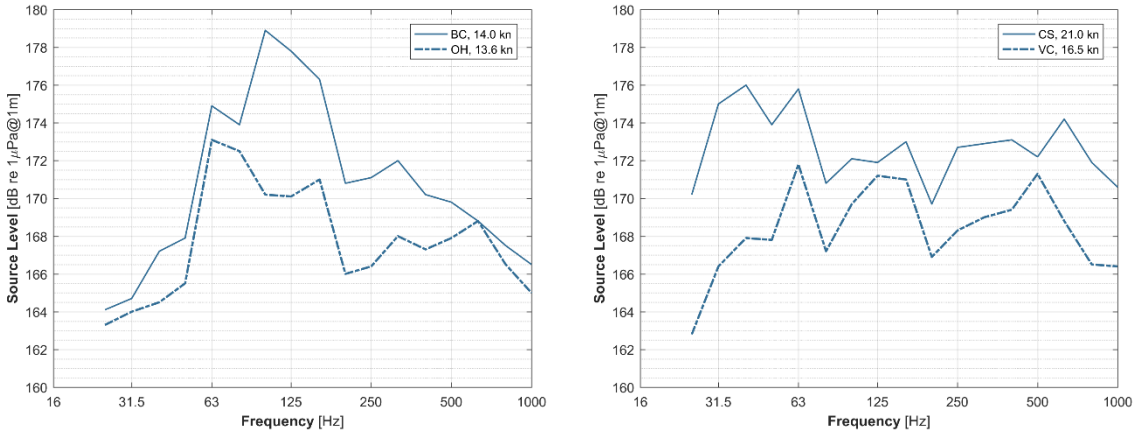

Figure 4.9 Source level spectra in third-octave bands for four types of commercial vessels: bulk carrier and open hatch cargo ship (left); container ship and vehicle carrier (right). From McKenna et al, 2012.

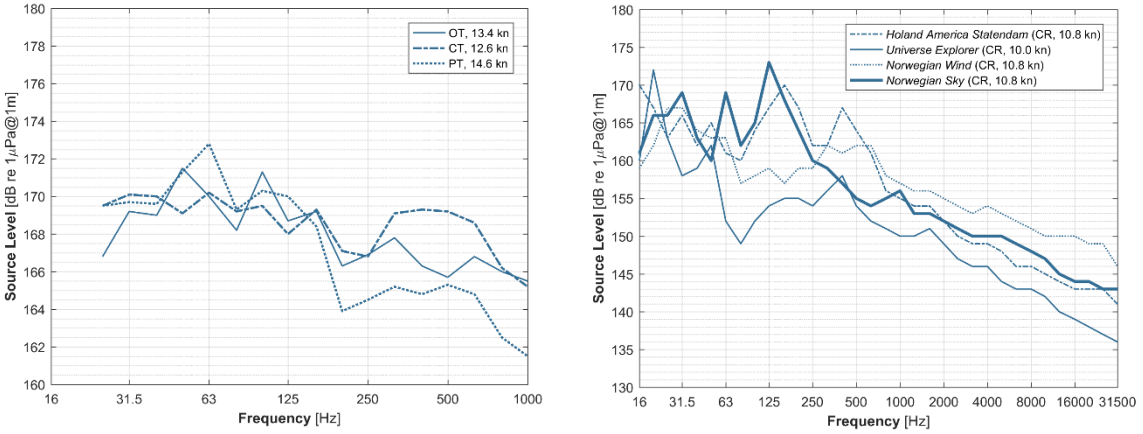

Figure 4.10 Source level spectra in third-octave bands for four cruise ships (right, from Kipple, 2002) and three types of tankers: oil, chemical and product (left, from McKenna et al, 2012).

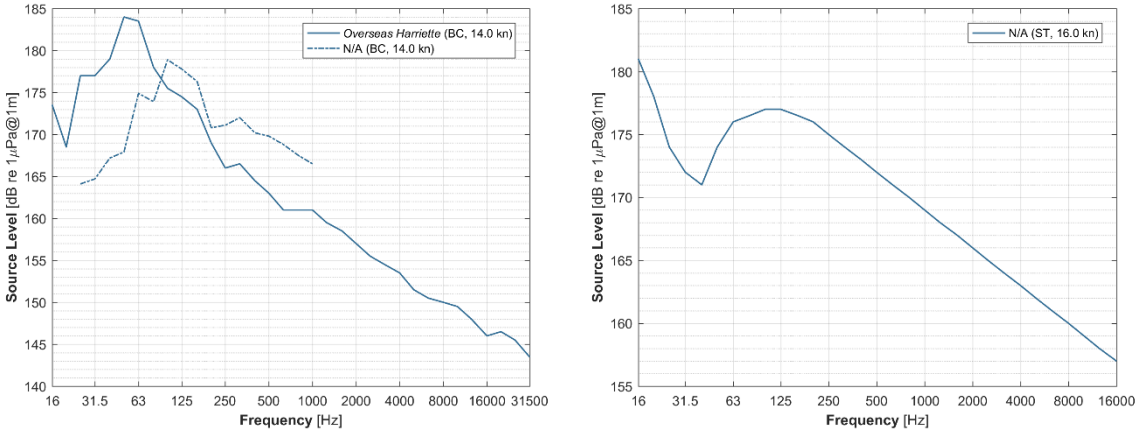

Figure 4.11 On the left, source level spectra in third-octave bands of bulk carrier *Overseas Harriette* (from Arveson & Vendittis, 2000) and the combined spectral response from five bulk carriers (from McKenna et al., 2012). On the right, a composite third-octave band source level spectrum of a supertanker (from Malme et al., 1989; Richardson et al., 1995).

In general, sound radiated from commercial vessels is mostly produced by propeller cavitation, which peaks at 50-150 Hz but can extend up to 10 kHz (McKenna et al., 2012).

An interesting effect that occurs in deep waters and at short distances from the vessel, mainly at high frequencies and under low sea state conditions, is the Lloyd's mirror effect. This phenomenon results in a spatial interference pattern and a spectral comb-filtering effect, caused by the coherent sum of the direct and surface reflected sound. The position of the nulls in the spatial interference pattern depend on the frequency, source and receiver depth, and distance between source and receiver. As the receiver approaches the vessel, it crosses a series of minima and maxima which are frequency dependent; the result is a spectrogram with a characteristic U-shape pattern (see Figure 4.12).

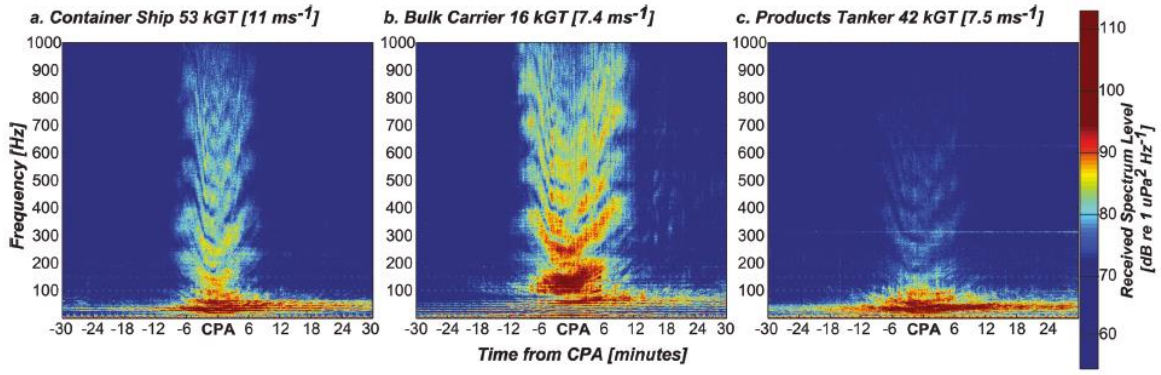

Figure 4.12 Received sound levels during 1 h passages for three types of commercial vessel: a) container ship (MMSI 1548719000), b) bulk carrier (MMSI 440223000), c) product tanker (MMSI 319768000). CPA is the closest point of approach. The negative time represents bow aspect (from McKenna et al., 2012).

4.2.3 Directivity

The horizontal radiation pattern is close to omnidirectional below 300 Hz, where blade rate, SSDG and engine firing rate predominate. Departures from azimuthal uniformity may be caused by hull natural resonances (Arveson & Vendittis, 2000). Above 300 Hz propeller cavitation dominates, which results in a relative sound level reduction of 3-5 dB in the fore and aft directions; this widely observed pattern is caused by the partial absorption of the stern aspect radiation by the bubble wake and the reduction of the bow aspect radiation by the presence of the hull (Arveson & Vendittis, 2000). Generally, there is also an asymmetry in the directivity pattern at low frequencies between bow and stern, with sound levels 5-10 dB higher in stern than in bow for container ships and tankers (McKenna et al., 2012).

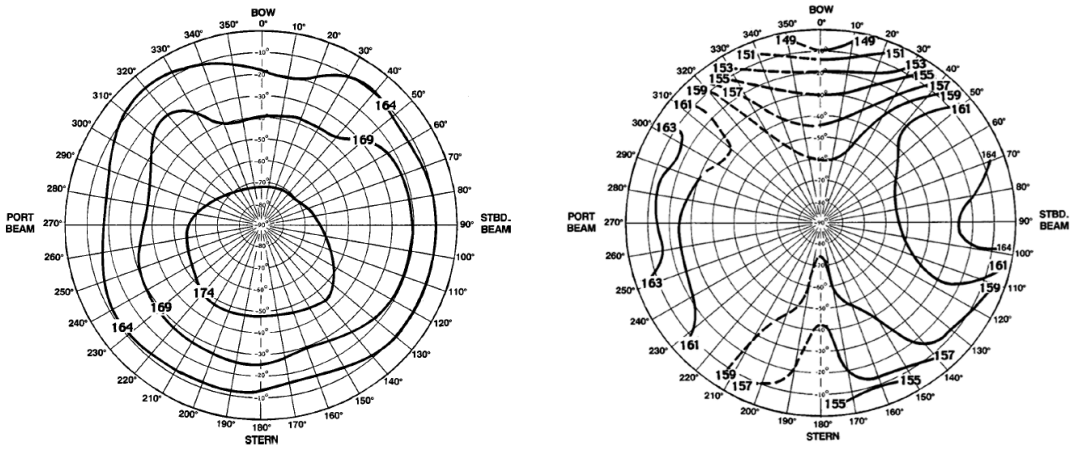

Figure 4.13 Directivity pattern from the *M/V Overseas Harriette* for the blade rate 9.3 Hz tone (left) and 340-360 Hz propeller cavitation band (from Arveson & Vendittis, 2000)

4.2.4 Effect of Vessel Speed and Size

McKenna et al. (2012) did not find a clear relationship between ship speed and source level for large commercial vessels and supertankers. For container ships there is some evidence of increasing radiated sound with increasing speed (see Figure 4.14). In a previous study from Ross (1976), the proposed formula to estimate the source level above 100 Hz shows a positive relationship with the size and speed of the vessel, but this formula may not be accurate for vessels over 30,000 GT. In the comprehensive statistical analysis done by Simard et al. (2016) on 255 merchant ships measured opportunistically while adhering closely to the ANSI S12.64-2009 standard, ships speed explained a small percentage of the observed source level variability. Ships longer than 250 m were the exception, as source levels showed a higher correlation with speed in that category. The relation with speed was stronger at frequencies below 100 Hz for all ship categories, and more prominent at all frequencies for larger vessels (> 250 m). In the study, length, breadth and draught worked as better descriptors, but no ship's physical parameters could explain a large percentage of the observed sound level variability. The analytical expressions provided by Simard accounted for a variability of 30 dB at all frequency bands (1st-99th percentile), which shows how complex vessels are as acoustic emitters and highlights the difficulty of arriving to an expression to model sound emissions with only a few simple parameters.

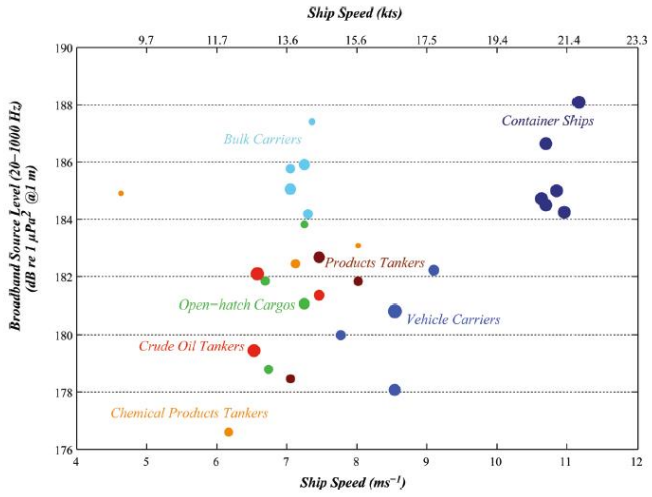

Figure 4.14 Broadband source level for seven types of commercial vessel as a function of speed. Point size represents the relative size of the ship, measured in GT (from McKenna et al, 2012).

In contrast to the results from McKenna et al. (2012) and Simard et al. (2016), measurements made by Arveson & Vendittis (2000) on the bulk cargo ship *Overseas Harriette* showed a clear increase in overall sound levels with vessel speed (see Figure 4.15).

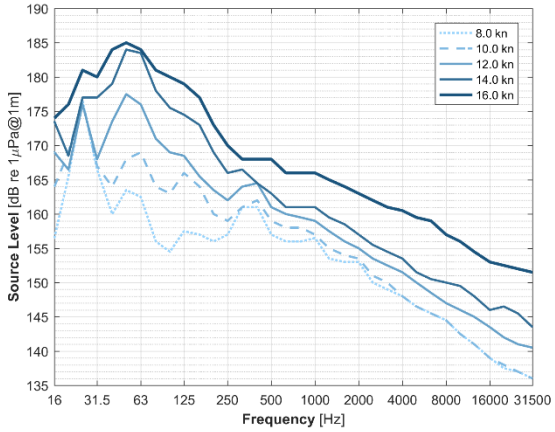

Figure 4.15 Third-octave band spectra measured from bulk cargo ship *Overseas Harriette* at five speeds: 8, 10, 12, 14 and 16 knots. The broadband source levels from the lowest to the highest speeds are respectively 178.2 180.1 183.7 189.4 and 192.1 dB_{rms}. (after Arveson & Vendittis, 2000).

Table 4.1 Sounds produced by commercial vessels: cruise ships

Vessel (*Name/ID*)	Length [m]	Displacement [Tonne]	h_w [m]	Speed [kn]	Measurement [dB re 1µPa$_x$]	SL [dB re 1µPa@1m]	Signal Characteristics	Regression Equation	Description	Reference
Cruise Ship (*Dawn Princess*)	261	77,000 (GT)	366	9.9	115.8 dB_{rms} @ 457 m [a]	178.1 dB_{rms} [a] 172 dB_{rms} @ 10 Hz 1/3 oct [b] 164 dB_{rms} @ 31.5 Hz 1/3 oct [c] 175 dB_{rms} @ 10 Hz 1/3 oct [d] 152 dB_{rms} @ 400 Hz 1/3 oct [e]	Spectrum dominated by synchroconverters and propulsion engine. Low cavitation noise.	TL = 20log$_{10}$r, for f > f_0 TL = 20log$_{10}$(r · f_0/f)*, for f < f_0 f_0 = 200 Hz Transmission loss used by Kipple for source level calculation. Includes the low-frequency energy cut-off effect for shallow water propagation. * Formula not explicitly given (derived from measurements *by reviewer*)	Propulsion type: diesel-electric z_r = 60, 90, 120 m combined [a] Broadband (10 Hz - 5 kHz 1/3 oct.) [b] from diesel generator [c] from machinery and diesel generator [d] propulsion and synchroconverter [e] electrical propulsion	Kipple, 2002
				5.6	114.7 dB_{rms} @ 457 m [a]	177.9 dB_{rms} [a]				
Cruise Ship (*Norwegian Sky*)	260	77,000 (GT)	366	10.8	118.7 dB_{rms} @ 457 m [a]	178.5 dB_{rms} [a] 169 dB_{rms} @ 31.5 Hz 1/3 oct [b] 169 dB_{rms} @ 63 Hz 1/3 oct [c] 173 dB_{rms} @ 125 Hz 1/3 oct [d] 156 dB_{rms} @ 1000 Hz 1/3 oct [e]	< 200 Hz propulsion system and synchroconverters dominate > 200 Hz cavitation dominates	TL = 20log$_{10}$r, for f > f_0 TL = 20log$_{10}$(r · f_0/f)*, for f < f_0 f_0 = 200 Hz Transmission loss used by Kipple for source level calculation. Includes the low-frequency energy cut-off effect for shallow water propagation. * Formula not explicitly given (derived from measurements *by reviewer*)	Propulsion type: diesel-electric z_r = 60, 90, 120 m combined [a] Broadband (10 Hz - 40 kHz 1/3 oct.) [b] from diesel generator [c] from propulsion and synchroconverter [d] from propulsion and synchroconverter [e] generator housing resonance	Kipple, 2002
				14.2	117.8 dB_{rms} @ 457 m [a]	178.7 dB_{rms} [a]				
Cruise Ship (*Crystal Harmony*)	241	49,000 (GT)	366	10.5	115.2 dB_{rms} @ 457 m [a]	185.6 dB_{rms} [a] 182.5 dB_{rms} @ 16 Hz 1/3 oct [b] 163 dB_{rms} @ 125 Hz 1/3 oct [c] 160 dBrms @ 400 Hz 1/3 oct [d]	< 500 Hz electric propulsion and cycloconverter dominate > 500 Hz cavitation dominates	TL = 20log$_{10}$r, for f > f_0 TL = 20log$_{10}$(r · f_0/f)*, for f < f_0 f_0 = 200 Hz Transmission loss used by Kipple for source level calculation. Includes the low-frequency energy cut-off effect for shallow water propagation. * Formula not explicitly given (derived from measurements *by reviewer*)	Propulsion type: diesel-electric z_r = 60, 90, 120 m combined [a] broadband (10 Hz - 40 kHz 1/3 oct.) [b] from electrical propulsion system [c] from machinery [d] from cycloconverter	Kipple, 2002
				15.3	121.7 dB_{rms} @ 457 m [a]	184.5 dB_{rms} [a]				
Cruise Ship (*Norwegian Wind*)	230	50,000 (GT)	366	10	117.1 dB_{rms} @ 457 m [a]	176 dB_{rms} [a] 167 dB_{rms} @ 12.5 Hz 1/3 oct [b] 167 dB_{rms} @ 31.5 Hz 1/3 oct [c] 163 dB_{rms} @ 63 Hz 1/3 oct [d] 162 dB_{rms} @ 315 Hz 1/3 oct [e]	Propulsion system dominates > 200 Hz cavitation important 315-630 Hz reduction gear	TL = 20log$_{10}$r, for f > f_0 TL = 20log$_{10}$(r · f_0/f)*, for f < f_0 f_0 = 200 Hz Transmission loss used by Kipple for source level calculation. Includes the low-frequency energy cut-off effect for shallow water propagation. * Formula not explicitly given (derived from measurements *by reviewer*)	Propulsion type: direct diesel z_r = 60, 90, 120 m combined [a] Broadband (10 Hz - 40 kHz 1/3 oct.) [b] from diesel generator and propulsion [c] from diesel propulsion [d] from air conditioning compressor [e] from reduction gear	Kipple, 2002
				19.2	131.1 dB_{rms} @ 457 m [a]	195.1 dB_{rms} [a]				
Cruise Ship (*Holland America Statendam*)	219	55,000 (GT)	366	10.8	120.5 dB_{rms} @ 457 m [a]	180.6 dB_{rms} [a] 177 dB_{rms} @ 10 Hz 1/3 oct [b] 176 dB_{rms} @ 31.5 Hz 1/3 oct [c] 175 dB_{rms} @ 50 Hz 1/3 oct [d] 177 dB_{rms} @ 400 Hz 1/3 oct [e]	< 100 Hz electric propulsion and diesel generator dominate > 800 Hz cavitation dominates	TL = 20log$_{10}$r, for f > f_0 TL = 20log$_{10}$(r · f_0/f)*, for f < f_0 f_0 = 200 Hz Transmission loss used by Kipple for source level calculation. Includes the low-frequency energy cut-off effect for shallow water propagation. * Formula not explicitly given (derived from measurements *by reviewer*)	Propulsion type: diesel-electric z_r = 60, 90, 120 m combined [a] Broadband (10 Hz - 40 kHz 1/3 oct.) [b] from diesel generator [c] from motor generator [d] propulsion related [e] shaftrate bark	Kipple, 2002
				18	122.9 dB_{rms} @ 457 m [a]	183.5 dB_{rms} [a]				
Cruise Ship (*Universe Explorer*)	188	23,000 (GT)	366	10	111.5 dB_{rms} @ 457 m [a]	174.6 dB_{rms} [a] 172 dB_{rms} @ 20 Hz 1/3 oct [b] 162 dB_{rms} @ 50 Hz 1/3 oct [c] 158 dB_{rms} @ 400 Hz 1/3 oct [d]	< 800 Hz turbine generators > 800 Hz cavitation dominates	TL = 20log$_{10}$r, for f > f_0 TL = 20log$_{10}$(r · f_0/f)*, for f < f_0 f_0 = 200 Hz Transmission loss used by Kipple for source level calculation. Includes the low-frequency energy cut-off effect for shallow water propagation. * Formula not explicitly given (derived from measurements *by reviewer*)	Propulsion type: steam turbine z_r = 60, 90, 120 m combined [a] broadband (10 Hz - 40 kHz 1/3 oct.) [b] from turbine generator [c] from main turbine rotation [d] from main reduction gears	Kipple, 2002
				15.5	120.7 dB_{rms} @ 457 m [a]	182.8 dB_{rms} [a]				

Table 4.1 Sounds produced by commercial vessels (cont., part 2): container ships and bulkers

Vessel *(Name/ID)*	Length [m]	Displacement [Tonne]	h_w [m]	Speed [kn]	Measurement [dB re 1µPa$_{rms}$]	SL [dB re 1µPa@1m]	Signal Characteristics	Regression Equation	Description	Reference
Container Ship (MMSI 211207740)	298	53,800 (GT)	580	21.8	118.9 dB_{rms} @ 2.9 km	188.1 dB_{rms}	N/A	TL = $20\log_{10}r$	Built in 1993, 49,600 hp Broadband 20 Hz - 1 kHz	McKenna et al, 2012
Container Ship (MMSI 636090869)	294	54,600 (GT)	580	20.6	114.9 dB_{rms} @ 3.1 km	184.7 dB_{rms}	N/A	TL = $20\log_{10}r$	Built in 2005, 62,200 hp Broadband 20 Hz - 1 kHz	McKenna et al, 2012
Container Ship (MMSI 353287000)	294	53,800 (GT)	580	21.2	114.9 dB_{rms} @ 3.2 km	185 dB_{rms}	N/A	TL = $20\log_{10}r$	Built in 2003, 67,200 hp Broadband 20 Hz - 1 kHz	McKenna et al, 2012
Container Ship (MMSI 235007500)	294	53,500 (GT)	580	20.8	117 dB_{rms} @ 3 km	186.6 dB_{rms}	N/A	TL = $20\log_{10}r$	Built in 2004, 55,900 hp Broadband 20 Hz - 1 kHz	McKenna et al, 2012
Container Ship (MMSI 548719000)	294	53,400 (GT)	580	21.4	114.6 dB_{rms} @ 3 km	184.2 dB_{rms}	N/A	TL = $20\log_{10}r$	Built in 1993, 42,100 hp Broadband 20 Hz - 1 kHz	McKenna et al, 2012
Container Ship (MMSI 352919000)	294	53,100 (GT)	580	20.8	116.1 dB_{rms} @ 2.6 km	184.5 dB_{rms}	N/A	TL = $20\log_{10}r$	Built in 1994, 42,100 hp Broadband 20 Hz - 1 kHz	McKenna et al, 2012
Bulk Carrier (MMSI 371978000)	229	42,900 (GT)	580	13.8	114.9 dB_{rms} @ 3.2 km	185.1 dB_{rms}	N/A	TL = $20\log_{10}r$	Built in 2006, 13,300 hp Broadband 20 Hz - 1 kHz	McKenna et al, 2012
Bulk Carrier (*Yu Lin Hai*, MMSI 412086000)	225	75,380 (GT)	22.5	12.1	N/A	149.9 dB_{rms} @ 8 kHz 1/3 oct[a] 147.8 dB_{rms} @ 50 kHz 1/3 oct[b]	N/A	[a]RL=149.9-14.2$\log_{10}$r-2.3·10^{-4}r [b]RL=147.8-14.9$\log_{10}$r-7.9·10^{-3}r	China, built 2012, width 32 m, CPA 262 m. Beaufort sea state 1, sandy/muddy seabed	Liu et al., 2017
Bulk Carrier (*Guo Yuan 16*, MMSI 414072000)	225	41,830 (GT)	33.2	11.9	N/A	143.8 dB_{rms} @ 8 kHz 1/3 oct[a] 135.9 dB_{rms} @ 50 kHz 1/3 oct[b]	N/A	[a]RL_{rms}=143.8-14.2$\log_{10}$r-2.7·10^{-4}r [b]RL_{rms}=135.9-14.7$\log_{10}$r-8.1·10^{-3}r	China, built 2012, width 32 m, CPA 720 m. Beaufort sea state 3, sandy/muddy seabed	Liu et al., 2017
Bulk Carrier (MMSI 240537000)	225	40,000 (GT)	580	14.2	116 dB_{rms} @ 3.1 km	185.9 dB_{rms}	N/A	TL = $20\log_{10}r$	Built in 2005, 12,700 hp Broadband 20 Hz - 1 kHz	McKenna et al, 2012
Bulk Cargo Ship (*Peter R. Cresswell*)	219.2	19,853 (GT)	10	0 (moored)	117.6 dB_{rms} @ 134 m	156.6 dB_{rms}	N/A	Measurements at 134 m, backprojected to 1 m using MONM, parabolic equation based model.	Self-propelled gravel carrier, 9464 bhp, 8.7 m draft, 23.1 m breadth Max. speed 15 kn Broadband (31.5 Hz - 2 kHz 1/3 oct)	Carr et al., 2006
Bulk Carrier (*Queen Jhansi*, MMSI 538006170)	190	32,415 (GT)	22.6	11.1	N/A	148.2 dB_{rms} @ 8 kHz 1/3 oct[a] 146.4 dB_{rms} @ 50 kHz 1/3 oct[b]	N/A	[a]RL=148.2-14.2$\log_{10}$r-2.2·10^{-4}r [b]RL=146.4-14.3$\log_{10}$r-8.5·10^{-3}r	Marshall Islands, built 2006, width 32 m, CPA 259 m, Beaufort sea 0, sandy/muddy	Liu et al., 2017
Bulk Carrier (MMSI 371940000)	190	30,700 (GT)	580	14.2	115.6 dB_{rms} @ 2.7 km	184.2 dB_{rms}	N/A	TL = $20\log_{10}r$	Built in 2007, 11,700 hp Broadband 20 Hz - 1 kHz	McKenna et al, 2012
Bulk Carrier (MMSI 576915000)	189	29,700 (GT)	580	13.8	115.2 dB_{rms} @ 3.4 km	185.8 dB_{rms}	N/A	TL = $20\log_{10}r$	Built in 2004, 9,300 hp Broadband 20 Hz - 1 kHz	McKenna et al, 2012

Table 4.1 Sounds produced by commercial vessels (cont., part 3): bulkers and open-hatch cargo ships

Vessel (*Name/ID*)	Length [m]	Displacement [Tonne]	h_w [m]	Speed [kn]	Measurement [dB re 1µPa$_{rms}$]	SL [dB re 1µPa@1m]	Signal Characteristics	Regression Equation	Description	Reference
Bulk Carrier (*Wan Hai 282*, MMSI 565647000)	182	17,609 (GT)	24.2	9.6	N/A	146.6 dB_{rms} @ 8 kHz 1/3 oct[a] 141.3 dB_{rms} @ 50 kHz 1/3 oct[b]	N/A	[a]RL_{rms}=146.6-14.1$\log_{10}$r-2.8·10^{-4}r [b]RL_{rms}=141.3-14.5$\log_{10}$r-9.8·10^{-3}r	Singapore, built 1998, width 28 m, CPA 410 m. Beaufort sea state 1, sandy/muddy seabed	Liu et al., 2017
Bulk Cargo Ship (*M/V Overseas Harriette*)	173	25,515 t (DWT)	1830	8	N/A	178.2 dB_{rms}	Major noise sources: service diesel generator (low speed, <200 Hz), propulsion diesel firing rate (high speed, <100 Hz), blade rate (high speed, <100 Hz), propeller cavitation (medium to high speeds, broadband)	Measurements at 600 m, backprojected to 1 m using TL = 20$\log_{10}$r (free field, radial distance)	Direct-drive, low-speed diesel engine Five hydrophones at depths 60-460 m Broadband (10 Hz - 40 kHz 1/3 oct)	Arveson & Vendittis, 2000
				10	N/A	180.1 dB_{rms}				
				12	N/A	183.7 dB_{rms}				
				14	N/A	189.4 dB_{rms}				
				16	N/A	192.1 dB_{rms}				
Bulk Carrier (MMSI 440223000)	167	16,300 (GT)	580	14.4	117.9 dB_{rms} @ 3 km	187.4 dB_{rms}	N/A	TL = 20$\log_{10}$r	Built in 1997, 9,100 hp Broadband 20 Hz - 1 kHz	McKenna et al, 2012
Bulk Carrier (*An Sheng 17*, MMSI 412458810)	118	N/A	22.5	9.1	N/A	146.2 dB_{rms} @ 8 kHz 1/3 oct[a] 140.6 dB_{rms} @ 50 kHz 1/3 oct[b]	N/A	[a]RL=146.2-15.1$\log_{10}$r-2.4·10^{-4}r [b]RL=140.6-15.4$\log_{10}$r-7.9·10^{-3}r	China, width 16 m, CPA 210 m Beaufort sea state 1, sandy/muddy seabed	Liu et al., 2017
Bulk Carrier (*Jin Hang 689*, MMSI 412501530)	100	2,984 (GT)	29.9	8.5	N/A	144.5 dB_{rms} @ 8 kHz 1/3 oct[a] 136.1 dB_{rms} @ 50 kHz 1/3 oct[b]	N/A	[a]RL_{rms}=144.5-15.3$\log_{10}$r-2.0·10^{-4}r [b]RL_{rms}=136.1-15.6$\log_{10}$r-7.9·10^{-3}r	China, width 16 m, CPA 176 m Beaufort sea state 2, sandy/muddy seabed	Liu et al., 2017
Bulk Cargo Ship (*Emerald Bulker*)	N/A	N/A	7	Full speed	134 dB_{rms}@ 540 m	188.8 dB_{rms}	N/A	RL_{rms} = 188.8 - 21$\log_{10}$r	Broadband 10 Hz - 20 kHz. Ship held at dock by two tugs, previous to departure	Blackwell & Greene, 2002
Open Hatch Cargo Ship (MMSI 563496000)	213	37,200 (GT)	580	14.2	111.5 dB_{rms} @ 3 km	181.1 dB_{rms}	N/A	TL = 20$\log_{10}$r	Built in 1995, 14,100 hp Broadband 20 Hz - 1 kHz	McKenna et al, 2012
Open Hatch Cargo Ship (MMSI 477657600)	199	29,800 (GT)	580	13	111.2 dB_{rms} @ 3.4 km	181.8 dB_{rms}	N/A	TL = 20$\log_{10}$r	Built in 2007, 12,900 hp Broadband 20 Hz - 1 kHz	McKenna et al, 2012
Open Hatch Cargo Ship (MMSI 257313000)	197	27,200 (GT)	580	13	109 dB_{rms} @ 3.1 km	178.8 dB_{rms}	N/A	TL = 20$\log_{10}$r	Built in 1986, 10,100 hp Broadband 20 Hz - 1 kHz	McKenna et al, 2012
Open Hatch Cargo Ship (MMSI 477653500)	190	20,200 (GT)	580	14.2	114.8 dB_{rms} @ 2.8 km	183.8 dB_{rms}	N/A	TL = 20$\log_{10}$r	Built in 2007, 9,000 hp Broadband 20 Hz - 1 kHz	McKenna et al, 2012

Table 4.1 Sounds produced by commercial vessels (cont., part 4): vehicle carriers and general cargo ships

Vessel (*Name/ID*)	Length [m]	Displacement [Tonne]	h_w [m]	Speed [kn]	Measurement [dB re 1µPa_{rms}]	SL [dB re 1µPa@1m]	Signal Characteristics	Regression Equation	Description	Reference
Vehicle Carrier (MMSI 232872000)	199	61,300 (GT)	580	16.5	111.3 dB_{rms} @ 3 km	180.8 dB_{rms}	N/A	TL = $20\log_{10}r$	Built in 2006, 16,500 hp Broadband 20 Hz - 1 kHz	McKenna et al, 2012
Vehicle Carrier (MMSI 353788000)	180	47,600 (GT)	580	16.5	108.6 dB_{rms} @ 3 km	178.1 dB_{rms}	N/A	TL = $20\log_{10}r$	Built in 1989, 14,700 hp Broadband 20 Hz - 1 kHz	McKenna et al, 2012
Vehicle Carrier (MMSI 636011280)	175	37,900 (GT)	580	17.7	111.8 dB_{rms} @ 3.3 km	182.2 dB_{rms}	N/A	TL = $20\log_{10}r$	Built in 2000, 12,200 hp Broadband 20 Hz - 1 kHz	McKenna et al, 2012
Vehicle Carrier (MMSI 413075000)	173	33,100 (GT)	580	15.2	110.6 dB_{rms} @ 2.9 km	180 dB_{rms}	N/A	TL = $20\log_{10}r$	Built in 1984, 10,700 hp Broadband 20 Hz - 1 kHz	McKenna et al, 2012
Cargo Ship (*An He 8*, MMSI 412457480)	112	N/A	29.8	8.6	N/A	140.6 dB_{rms} @ 8 kHz 1/3 oct[a] 130.9 dB_{rms} @ 50 kHz 1/3 oct[b]	N/A	[a] $RL_{rms}=140.6-14.1\log_{10}r-1.1\cdot10^{-4}r$ [b] $RL_{rms}=130.9-15.5\log_{10}r-7.3\cdot10^{-3}r$	China, width 16 m, CPA 241 m Beaufort sea state 3, sandy/muddy seabed	Liu et al., 2017
General Cargo Ship (*Vien Dong 3*, MMSI 574256000)	103	6,523 (GT)	22.5	10.5	N/A	150.4 dB_{rms} @ 8 kHz 1/3 oct[a] 142.5 dB_{rms} @ 50 kHz 1/3 oct[b]	N/A	[a] $RL_{rms}=150.4-15.2\log_{10}r-2.1\cdot10^{-4}r$ [b] $RL_{rms}=142.5-15.5\log_{10}r-9.1\cdot10^{-3}r$	Vietnam, built 2004, width 17 m, CPA 334 m. Beaufort sea state 1, sandy/muddy seabed	Liu et al., 2017
Cargo Ship (*Jiang Su San Hang*, MMSI 413813000)	98	N/A	29.8	10.0	N/A	140.3 dB_{rms} @ 8 kHz 1/3 oct[a] 138.8 dB_{rms} @ 50 kHz 1/3 oct[b]	N/A	[a] $RL_{rms}=140.3-14.4\log_{10}r-1.4\cdot10^{-4}r$ [b] $RL_{rms}=138.8-15.8\log_{10}r-6.4\cdot10^{-3}r$	China, width 16 m, CPA 296 m Beaufort sea state 3, sandy/muddy seabed	Liu et al., 2017
Cargo Ship (*Chang Hai 9*, MMSI 412503490)	96	N/A	20.5	8.7	N/A	141.2 dB_{rms} @ 8 kHz 1/3 oct[a] 136.3 dB_{rms} @ 50 kHz 1/3 oct[b]	N/A	[a] $RL_{rms}=141.2-14.3\log_{10}r-2.1\cdot10^{-4}r$ [b] $RL_{rms}=136.3-14.4\log_{10}r-7.1\cdot10^{-3}r$	China, width 16 m, CPA 518 m Beaufort sea state 1, sandy/muddy seabed	Liu et al., 2017
Cargo Ship (*Xin Heng Hua*, MMSI 412454220)	83	2,414 (GT)	20.5	9.8	N/A	142.3 dB_{rms} @ 8 kHz 1/3 oct[a] 133.3 dB_{rms} @ 50 kHz 1/3 oct[b]	N/A	[a] $RL_{rms}=142.3-13.5\log_{10}r-1.6\cdot10^{-4}r$ [b] $RL_{rms}=133.3-13.9\log_{10}r-6.3\cdot10^{-3}r$	China, width 13 m, CPA 260 m Beaufort sea state 0, sandy/muddy seabed	Liu et al., 2017
Cargo Ship (*Xin Chen Guang 20*, MMSI 413551040)	74	N/A	22.8	9.1	N/A	146.6 dB_{rms} @ 8 kHz 1/3 oct[a] 139.6 dB_{rms} @ 50 kHz 1/3 oct[b]	N/A	[a] $RL_{rms}=146.6-14.1\log_{10}r-1.7\cdot10^{-4}r$ [b] $RL_{rms}=139.6-14.4\log_{10}r-8.2\cdot10^{-3}r$	China, width 16 m, CPA 151 m Beaufort sea state 0, sandy/muddy seabed	Liu et al., 2017
Cargo Ship (*Xin Chen Guang 20*, MMSI 413551040)	74	N/A	22.8	9.1	N/A	146.6 dB_{rms} @ 8 kHz 1/3 oct[a] 139.6 dB_{rms} @ 50 kHz 1/3 oct[b]	N/A	[a] $RL_{rms}=146.6-14.1\log_{10}r-1.7\cdot10^{-4}r$ [b] $RL_{rms}=139.6-14.4\log_{10}r-8.2\cdot10^{-3}r$	China, width 16 m, CPA 151 m Beaufort sea state 0, sandy/muddy seabed	Liu et al., 2017
Cargo Ship (*Zhong Wei*, MMSI 412469380)	71	N/A	22.5	8.5	N/A	140.4 dB_{rms} @ 8 kHz 1/3 oct[a] 134.8 dB_{rms} @ 50 kHz 1/3 oct[b]	N/A	[a] $RL_{rms}=140.4-14.0\log_{10}r-1.8\cdot10^{-4}r$ [b] $RL_{rms}=134.8-14.2\log_{10}r-8.3\cdot10^{-3}r$	China, width 13 m, CPA 500 m Beaufort sea state 1, sandy/muddy seabed	Liu et al., 2017
Cargo Ship (*Hui Jin Qiao 218*, MMSI 413470850)	69	N/A	24.2	9.1	N/A	147.9 dB_{rms} @ 8 kHz 1/3 oct[a] 137.7 dB_{rms} @ 50 kHz 1/3 oct[b]	N/A	[a] $RL_{rms}=147.9-15.1\log_{10}r-1.7\cdot10^{-4}r$ [b] $RL_{rms}=137.7-15.4\log_{10}r-8.8\cdot10^{-3}r$	China, width 16 m, CPA 320 m Beaufort sea state 2, sandy/muddy seabed	Liu et al., 2017

Table 4.1 Sounds produced by commercial vessels (cont., part 5): oil, product and chemical tankers

Vessel (*Name/ID*)	Length [m]	Displacement [Tonne]	h_w [m]	Speed [kn]	Measurement [dB re 1µPa$_{rms}$]	SL [dB re 1µPa@1m]	Signal Characteristics	Regression Equation	Description	Reference
Oil Tanker (*Olympic Leader* , MMSI 241264000)	333	160,046 (GT)	22.8	11.2	N/A	145.1 dB_{rms} @ 8 kHz 1/3 oct[a] 143.6 dB_{rms} @ 50 kHz 1/3 oct[b]	N/A	[a]$RL_{rms}=145.1-14.4\log_{10}r-2.6\cdot10^{-4}r$ [b]$RL_{rms}=143.6-14.9\log_{10}r-8.4\cdot10^{-3}r$	Greece, built 2005, width 58 m, CPA 250 m. Beaufort sea state 0, sandy/muddy seabed	Liu et al., 2017
Crude Oil Tanker (MMSI 636012853)	243	57,200 (GT)	580	12.8	112.1 dB_{rms} @ 3.1 km	182.1 dB_{rms}	N/A	$TL = 20\log_{10}r$	Built in 2006, 18,400 hp Broadband 20 Hz - 1 kHz	McKenna et al, 2012
Crude Oil Tanker (MMSI 564924000)	241	10,800 (GT)	580	12.6	108.7 dB_{rms} @ 3.5 km	179.4 dB_{rms}	N/A	$TL = 20\log_{10}r$	Built in 2003, 16,000 hp Broadband 20 Hz - 1 kHz	McKenna et al, 2012
Crude Oil Tanker (MMSI 636090885)	229	37,000 (GT)	580	14.6	112.1 dB_{rms} @ 2.9 km	181.3 dB_{rms}	N/A	$TL = 20\log_{10}r$	Built in 2000, 13,000 hp Broadband 20 Hz - 1 kHz	McKenna et al, 2012
Oil Tanker (*Lian Xing Hu* , MMSI 413247000)	228	43,153 (GT)	22.6	11.2	N/A	149.6 dB_{rms} @ 8 kHz 1/3 oct[a] 148.9 dB_{rms} @ 50 kHz 1/3 oct[b]	N/A	[a]$RL_{rms}=149.6-14.7\log_{10}r-1.7\cdot10^{-4}r$ [b]$RL_{rms}=148.9-15.0\log_{10}r-9.2\cdot10^{-3}r$	China, built 2006, width 32 m, CPA 308 m. Beaufort sea state 0, sandy/muddy seabed	Liu et al., 2017
Oil Tanker (*Hai Guan Shan 266* , MMSI 413591380)	53	N/A	29.9	8.5	N/A	135.5 dB_{rms} @ 8 kHz 1/3 oct[a] 127.6 dB_{rms} @ 50 kHz 1/3 oct[b]	N/A	[a]$RL_{rms}=135.5-14.2\log_{10}r-2.6\cdot10^{-4}r$ [b]$RL_{rms}=127.6-14.5\log_{10}r-6.6\cdot10^{-3}r$	China, width 9 m, CPA 111 m Beaufort sea state 3, sandy/muddy seabed	Liu et al., 2017
Oil Tanker (*Yu Shun 106*, MMSI 413431330)	53	N/A	24.2	11.2	N/A	136.8 dB_{rms} @ 8 kHz 1/3 oct[a] 127.7 dB_{rms} @ 50 kHz 1/3 oct[b]	N/A	[a]$RL_{rms}=136.8-14.4\log_{10}r-2.2\cdot10^{-4}r$ [b]$RL_{rms}=127.7-14.6\log_{10}r-8.9\cdot10^{-3}r$	China, width 9 m, CPA 345 m Beaufort sea state 1, sandy/muddy seabed	Liu et al., 2017
Oil Tanker (*Hai Guan Shan 129* , MMSI 413591820)	53	N/A	24.2	11.5	N/A	139.8 dB_{rms} @ 8 kHz 1/3 oct[a] 131.4 dB_{rms} @ 50 kHz 1/3 oct[b]	N/A	[a]$RL_{rms}=139.8-14.5\log_{10}r-1.9\cdot10^{-4}r$ [b]$RL_{rms}=131.4-14.9\log_{10}r-9.5\cdot10^{-3}r$	China, width 9 m, CPA 257 m, Beaufort sea state 1, sandy/muddy seabed	Liu et al., 2017
Product Tanker (MMSI 319768000)	228	42,400 (GT)	580	14.6	112.7 dB_{rms} @ 3.1 km	182.7 dB_{rms}	N/A	$TL = 20\log_{10}r$	Built in 2007, 18,400 hp Broadband 20 Hz - 1 kHz	McKenna et al, 2012
Product Tanker (MMSI 371924000)	180	28,800 (GT)	580	15.6	111.2 dB_{rms} @ 3.4 km	181.8 dB_{rms}	N/A	$TL = 20\log_{10}r$	Built in 2006, 12,900 hp Broadband 20 Hz - 1 kHz	McKenna et al, 2012
Product Tanker (MMSI 371604000)	182	28,100 (GT)	580	13.8	109.3 dB_{rms} @ 2.9 km	178.5 dB_{rms}	N/A	$TL = 20\log_{10}r$	Built in 2005, 12,600 hp Broadband 20 Hz - 1 kHz	McKenna et al, 2012
Chemical Product Tanker (MMSI 636010515)	181	26,200 (GT)	580	12	106 dB_{rms} @ 3.3 km	176.6 dB_{rms}	N/A	$TL = 20\log_{10}r$	Built in 1996, 11,300 hp Broadband 20 Hz - 1 kHz	McKenna et al, 2012
Chemical Product Tanker (MMSI 352329000)	149	10,800 (GT)	580	13.8	112.5 dB_{rms} @ 3.2 km	183.1 dB_{rms}	N/A	$TL = 20\log_{10}r$	Built in 1993, 8,200 hp Broadband 20 Hz - 1 kHz	McKenna et al, 2012
Chemical Product Tanker (MMSI 355799000)	148	10,800 (GT)	580	9	114.9 dB_{rms} @ 3.4 km	184.9 dB_{rms}	N/A	$TL = 20\log_{10}r$	Built in 1985, 6,900 hp Broadband 20 Hz - 1 kHz. High level attributed to damaged propeller	McKenna et al, 2012
Tanker (*Hui Hang 126*, MMSI 413432850)	190	N/A	22.8	10	N/A	140.3 dB_{rms} @ 8 kHz 1/3 oct[a] 132.3 dB_{rms} @ 50 kHz 1/3 oct[b]	N/A	[a]$RL=140.3-14.2\log_{10}r-2.3\cdot10^{-4}r$ [b]$RL=132.3-15.4\log_{10}r-9.3\cdot10^{-3}r$	China, width 9 m, CPA 316 m Beaufort sea state 1, sandy/muddy seabed	Liu et al., 2017
Supertanker (-)	83	N/A	N/A	16	N/A	190 dB_{rms}[a] 205 dB_{rms} @ 2 Hz	N/A	Fast-field program (FFP) used by Cybulski to estimate source levels	Large oil tanker [a] Broadband 12.5 Hz - 16 kHz 1/3 oct bands (from Fig. 3.14 in Malme et al., 1989)	Malme et al., 1989; Richardson et al, 1995; Cybulski, 1977

Table 4.1 Sounds produced by commercial vessels (cont., part 6): statistical analysis from 255 vessels (Simard et al.,2016)

Vessel (*Name/ID*)	Length [m]	Displacement [Tonne]	h_w [m]	Speed [kn]	Measurement [dB re 1µPa_{rms}]	SL [dB re 1µPa@1m]	Signal Characteristics	Regression Equation	Description	Reference
Cargo and Container Ships	192 ± 51	N/A	350	13.4 ± 2.9	N/A	197.6 dB_{rms} [a]	Main energy at 40 Hz 1/3 oct (188.2 dB_{rms}@ 1 m) Maximum source level variability ~ 30 dB (1-99 percentile envelopes)	Empirical transmission loss for r > 300 m, calibrated Wavenumber Integration (WI) model for r < 300 m	*Context*: opportunistic measurement of 255 spectral source levels from merchant ships *Area*: St. Lawrence Seaway (Canada) *Total tested fleet*: 191 ships, 15.4 ± 12.5 years old, 26.5 ± 7.1 draft, 485 ± 262 m CPA. z_r = 62, 161, 288 m [a]from 177 SL spectra from cargo and container ships. Broadband 20-500 Hz	Simard et al, 2016
Tankers	192 ± 51	N/A	350	13.4 ± 2.9	N/A	196.8 dB_{rms}	Main energy at 50 Hz 1/3 oct (189.4 dB_{rms}@ 1 m) Maximum source level variability ~30 dB (1-99 percentile envelopes)	Empirical transmission loss for r > 300 m, calibrated Wavenumber Integration (WI) model for r < 300 m	*Context*: opportunistic measurement of 255 spectral source levels from merchant ships *Area*: St. Lawrence Seaway (Canada) *Total tested fleet*: 191 ships, 15.4 ± 12.5 years old, 26.5 ± 7.1 draft, 485 ± 262 m CPA z_r = 62, 161, 288 m Broadband 20-500 Hz, from 66 SL spectra of tankers.	Simard et al, 2016
Merchant Ships (by length)	100-150	N/A	350	13.4 ± 2.9	N/A	195.8 dB_{rms} [a]	Main energy at 63 Hz 1/3 oct (187.2 dB_{rms}@ 1 m)	Empirical transmission loss for r > 300 m, calibrated Wavenumber Integration (WI) model for r < 300 m	*Context*: opportunistic measurement of 255 spectral source levels from merchant ships *Area*: St. Lawrence Seaway (Canada) *Total tested fleet*: 191 ships, 15.4 ± 12.5 years old, 26.5 ± 7.1 draft, 485 ± 262 m CPA z_r = 62, 161, 288 m Broadband 20-500 Hz [a-d]from 56, 66, 102 and 23 SL spectra, respectively. Maximum source level variability ~30 dB (1-99 percentile envelopes)	Simard et al, 2016
	150-200			13.4 ± 2.9		197.6 dB_{rms} [b]	Main energy at 50 Hz 1/3 oct (189.3 dB_{rms}@ 1 m)			
	200-250			13.4 ± 2.9		197.2 dB_{rms} [c]	Main energy at 50 Hz 1/3 oct (188.7 dB_{rms}@ 1 m)			
	>250			13.4 ± 2.9		200.9 dB_{rms} [d]	Main energy at 40 Hz 1/3 oct (193.8 dB_{rms}@ 1 m)			

4.3 Icebreakers

The icebreaker is a special class of vessel designed to navigate through ice covered waters and make paths accessible to other ships. The icebreaker accelerates to break the ice, then it often stops and reverses to prepare for another ram. Strong cavitation sound is generated when the icebreaker accelerates forward and when it is suddenly stopped by the ice; cavitation normally ceases during reverse. The result is a fluctuating sound level and spectrum (see Figure 4.16). The sound levels emitted by an icebreaker are normally higher than those produced by a vessel of the same size and power (Richardson et al., 1995).

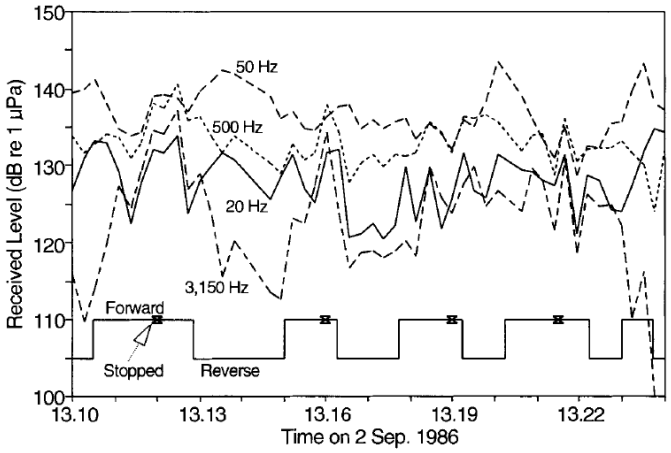

Figure 4.16 Received levels from icebreaker *Robert Lemeur* for four different third octave bands, recorded during several forward-reverse periods in a 14 minutes sequence (from Richardson et al., 1995).

The highest sound levels emitted by an icebreaker are caused by propeller cavitation during the little forward motion that occurs after the ice block is hit. This phase generally lasts about one minute and is followed by a few minutes of reverse and fast forward motion. The intermittent propeller cavitation that occurs while reversing direction may produce higher sound levels during the astern phase (5-10 dB) compared to the forward phase (Richardson et al., 1995). Roth et al. (2013) reported an increase in noise level of 10–15 dB in the 50 Hz and 100 Hz octave bands during heavy ice conditions (80-90% ice cover) while propellers were operating astern (*full reverse*) or in opposing directions (*side movement*) as compared to forward propulsion. The sound from ice breaking has little contribution to the overall radiated sound level (Malme et al., 1989). Continuous forward navigation is possible when the ice is thin, but more noise is produced under these conditions than when the icebreaker is underway in open water.

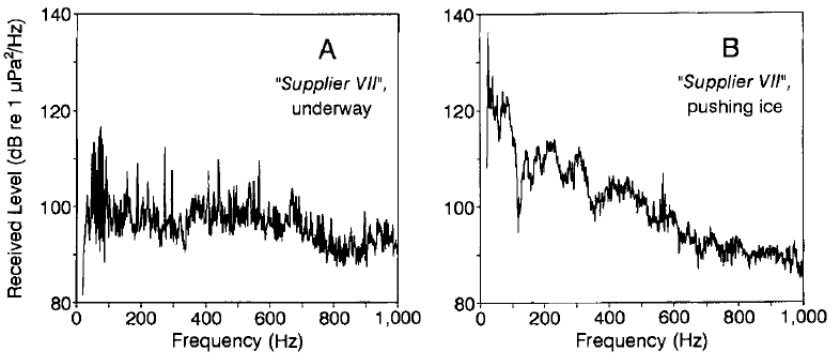

Figure 4.17 Received level spectra for the icebreaker *Canmar Supplier VII*: a) underway in open water, 130 dB broadband; b) icebreaking, 144 dB broadband (from Richardson et al., 1995).

Icebreakers pushing ice emit sound levels 10-15 dB higher than when the vessel is underway in open water. For example, for the icebreaker *Robert Lemeur* the received sound levels in the band of 20-1000 Hz increased by 12 dB during icebreaking compared to underway (Richardson et al., 1995). Roth et al. (2013)

reported an increase of 5-15 dB between 50 Hz, and 1 kHz and ~10 dB in broadband sound level, during ice-breaking in heavy ice conditions (80% ice cover) compared to open water transit (30% ice cover). Nozzles can significantly reduce the acoustic output of the propellers during icebreaking.

The icebreaker sound spectrum is highly variable over time and is dominated by blade rate tones below 200 Hz. The strong cavitation generated while pushing ice mainly contributes to frequencies below 1 kHz (see Figure 4.17 and Figure 4.18).

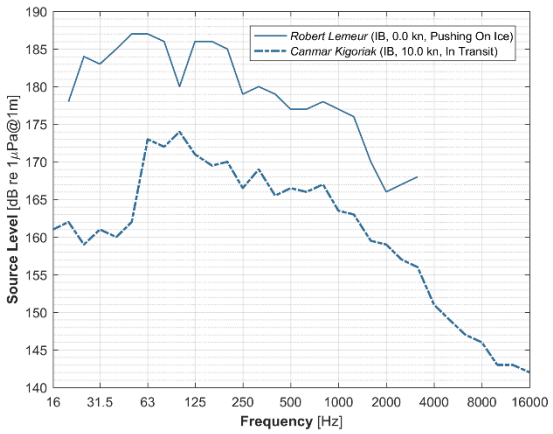

Figure 4.18 Third-octave spectra of icebreaker *Robert Lemeur* while pushing on hard ice and icebreaker *Canmar Kigoriak* while in transit (after Malme et al., 1989).

Table 4.2 Sounds produced by icebreakers

Vessel (*Name/ID*)	Length [m]	Displacement [Tonne]	h_w [m]	Speed [kn]	Measurement [dB re 1µPa$_x$]	SL [dB re 1µPa@1m]	Signal Characteristics	Regression Equation	Description	Reference
Ice-Breaker (US Coast Guard Cutter *Healey*)	128	16,660	3k-4k	2-8 (*transit*, variable ice cover)	N/A	192 (192) dB_{rms} @ 14 Hz oct[a] 188 (182) dB_{rms} @ 56 Hz oct[a] 190 (178) dB_{rms} @ 113 Hz oct[a] 183 (168) dB_{rms} @ 0.9 kHz oct[a] 172 (168) dB_{rms} @ 7.2 kHz oct[a]	High amplitude variability (177-198 dB_{rms} while transiting waters with 20-90% ice cover)	TL = $20\log_{10}r$	Context: opportunistic acoustic monitoring of *USCGC Healey* during reseach expedit. Area: Chukchi and Beaufort seas. *USCGC Healey*: modern, largest non-nuclear icebreaker. 128 m long, 25 beam, 8.9 m draft (full load). 11.2 MW diesel-electric propulsion. Two rudders and two 4-blade propellers for control (30,000 hp). Bow thrusters (2,500 hp). Max speed 17 kn. z_r = 122 m Highest levels during backing and ramming due to propeller cavitation, primarily during shaft operating astern or in opposing directions. [a]One-octave levels for 80%(30%) ice coverage.	Roth et al., 2013
				< 8 (*backing and ramming*, 80% ice cover)	N/A	175-196 dB_{rms} @ 14 Hz oct 174-197 dB_{rms} @ 56 Hz oct 172-194 dB_{rms} @ 113 Hz oct 167-185 dB_{rms} @ 0.9 kHz oct 160-175 dB_{rms} @ 7.2 kHz oct	High amplitude variability with time. Higher levels correlated with rapid ship deceleration and negative rpm of propeller (side-movement or reverse)			
				< 8 (*backing and ramming*, 90% ice cover)	N/A	173-200 dB_{rms} @ 56 Hz oct 172-200 dB_{rms} @ 113 Hz oct 166-194 dB_{rms} @ 0.9 kHz oct	High amplitude variability with time. Higher levels correlated with rapid ship deceleration during forward strike and during reverse after ramming.			
				< 1 (*dynamic position*., 90% ice cover)	N/A	188 dB_{rms} @ 14 Hz oct 193 dB_{rms} @ 56 Hz oct 185 dB_{rms} @ 113 Hz oct 173 dB_{rms} @ 0.9 kHz oct 171 dB_{rms} @ 7.2 kHz oct	Primary tones at 30 and 55 Hz produced by bow thrusters while in DP			
Icebreaker (*Canmar Kigoriak*)	90	7000	N/A	10	N/A	181.4 dB_{rms}	N/A	N/A	Icebreaking anchor boat, 19 m beam, 8.5 m draught, 16,400 shaft hp, 17 kn max. speed. In transit, no ice. Broadband 12.5 Hz - 16 kHz 1/3 oct (203 dB_{rms} @ 4 Hz)	Malme et al., 1989
Icebreaker (*Robert Lemeur*)	83	5,850 (3,285 GT)	N/A	0	N/A	196 dB_{rms}	N/A	N/A	Icebreaking supply vessel, 2x MaK 12M453AK engines, 9,600 bhp total horsepower, 19 m beam, 5.5 draught, 13.5 kn max. speed Area: Beaufort Sea (Alaska) Broadband 20-3150 Hz 1/3 oct, 14 min, vessel pushing on hard ice at full power (7.2 MW)	Malme et al., 1989; Richardson et al, 1995
Icebreaker Cargo Ship (*Polar Prince*)	67.1	N/A	55	5	123-125 dB_{rms} @ 400 m	163.3 dB_{rms}[a]	N/A	RL_{rms} = 163.3 - 14.4$\log_{10}r$ - 4.9·10^{-4}r, range of validity 0.4 - 12 km, 90th percentile regression equation. General	Motor icebreaker cargo, beam 15 m, draft 6 m Area: Beaufort Sea z_r = 3 m above seafloor [a]Broadband (f_s = 96 kHz). Also reported broadband level of 176.9 dB_{rms} from 10 Hz - 25 kHz 1/3 oct, applying TL = $20\log_{10}r$ to closest measurement.	Beland et al, 2013
Ice-Breaker (*Jim Kilabuk*)	62.5	1261 (GT)	~50	10	144 dB_{rms}@ 320 m	185.3 dB_{rms}	N/A	RL_{rms} = 185.3 -18.7$\log_{10}r$, range of validity 0.4 - 3 km, 50th percentile regression equation (mean). Bow	Icebreaking support vessel, 2xdiesel engines Area: Chuckchi Sea z_r ~ 3 m above seafloor Broadband 10 Hz - 20 kHz	Patterson et al, 2007
					130 dB_{rms}@ 310 m	156.8 dB_{rms}		RL_{rms} = 156.8 -10.6$\log_{10}r$, range of validity 0.1 - 2 km, 50th percentile regression equation (mean). Stern		
					137 dB_{rms}@ 280 m	170.1 dB_{rms}		RL_{rms} = 170.1 -14.2$\log_{10}r$, range of validity 0.1 - 2 km, 50th percentile regression equation (mean). Broadside		
			30	4.5	122-129 dB_{rms}@ 400 m	170.7 dB_{rms}	N/A	RL_{rms} = 170.7 -16$\log_{10}r$, range of validity 0.2 - 2 km, 50th percentile regression equation (mean). Endfire (bow+stern)	Icebreaking support vessel, 2xdiesel engines Area: Prudhoe Bay, Beaufort Sea Broadband (f_s = 48 kHz)	Funk et al., 2008

4.4 Small and Medium Size Vessels

Fishing, research and offshore support vessels, ferries and tugs are some of the most common medium size vessels. *Tugs* are highly manoeuvrable and powerful vessels used to assist (tow or push) large ships or barges around ports, or even tow drilling rigs and oil production platforms. *Research vessels* include the equipment necessary to collect geophysical, oceanographic, environmental or fisheries data. *Ferries* are ships used for the transport of passengers or vehicles on a regular basis between close locations. *Fishing vessels* are classified in different groups according to the fishing technique and include seiners, longliners, gillnetters, crabbers, drifters and trawlers, the last one being one of the most common. *Offshore support vessels* provide support services during offshore oil exploration, development, production and decommissioning and include Anchor Handling Tugs and Tug Supplies (AHT/AHTS), Platform Supply Vessels (PSV) and barges; these vessels are not very standardised and their specifications can vary considerably.

Figure 4.19 Tug assisting a cargo ship (left, from www.tuscorlloyds.com) and fishing trawler (right, from www.marineinsight.com)

Medium size, support vessels (50-90 m long) generally use a pair of diesel-powered propellers. These propellers are typically four-bladed and 3 m in diameter, with lower rotation speeds (~160 rpm) than those in boats, producing a fundamental tone of 10-11 Hz (Richardson et al., 1995). Supply vessels commonly have *bow thrusters* to help manoeuvre, which rotate at high speed and generate a series of harmonics with a high fundamental tone (~120 Hz). From the analysis on two supply vessels made by Richardson et al. (1995), it was observed that the first nine harmonics (up to ~1000 Hz) contributed to the broadband level, and the sound level increased in 11 dB after the thrusters started operating.

The *nozzle* installed around a propeller assists in restricting the water flow to the propeller tips, generating more thrust, especially at low speeds. Apart from increasing thrust, improving manoeuvrability and protecting the propellers, nozzles tend to reduce radiated noise. In an example presented by Richardson et al. (1995) a supply vessel without nozzles produced higher sound levels than a more powerful vessel with nozzles.

Medium and small sized vessels produce broadband source levels in the range of 160 to 185 dB; larger vessels tend to produce higher sound levels. Fishing vessels are generally small, and their acoustic impact is generally much lower than that of large vessels, however when seasons open for the capture of a specific species of fish, the large number of fishing vessels in the area will cause an important increase in the ambient noise levels (Malme et al., 1989).

Table 4.3 Sounds produced by small and medium vessels – length < 100 m

Vessel (*Name/ID*)	Length [m]	Displacement [Tonne]	h_w [m]	Speed [kn]	Measurement [dB re 1µPa$_{rms}$]	SL [dB re 1µPa@1m]	Signal Characteristics	Regression Equation	Description	Reference
Research Vessel (*Gilavar*)	84.9	3779 (GT)	~50	12	140 dB_{rms}@ 200 m	172.6 dB_{rms}	N/A	RL_{rms} = 172.6 -16.5log_{10}r, range of validity 0.7 - 10 km, 50th percentile regression equation (mean). Bow	Seismic vessel, 5 x diesel electric engines Area: Chuckchi Sea z_r ~ 3 m above seafloor Broadband 10 Hz - 20 kHz	Patterson et al, 2007
					128 dB_{rms}@ 200 m	156.9 dB_{rms}		RL_{rms} = 156.9 -11.6log_{10}r, range of validity 0.1 - 10 km, 50th percentile regression equation (mean). Stern		
					136 dB_{rms}@ 200 m	162.9 dB_{rms}		RL_{rms} = 162.9 -11.7log_{10}r, range of validity 0.1 - 10 km, 50th percentile regression equation (mean). Broadside		
			~30	4.5	135-140 dB_{rms}@ 400 m	173.1 dB_{rms}	N/A	RL_{rms} = 173.1 -13.3log_{10}r - 3.7·10^{-4}r, range of validity 0.4 - 6 km, 50th percentile regression equation (mean). Endfire (bow + stern)	Seismic vessel, 5 x diesel electric engines Area: Camden Bay, Beaufort Sea z_r = 3 m above seafloor Broadband (f_s = 48 kHz)	Funk et al., 2008
			~40	3.8	134.5-137 dB_{rms}@ 500 m	170.3 dB_{rms}	N/A	RL_{rms} = 170.3 -12.4log_{10}r, range of validity 0.4 - 10 km, 90th percentile regression equation. General	Seismic vessel, 5 x diesel-elec engines *Area*: Point Lay, Chukchi Sea z_r = 1 m above seafloor Broadband 1 Hz - 24 kHz (f_s = 48 kHz)	Ireland et al., 2009
Survey Vessel (*Geo Arctic*)	81.8	N/A	55	4	127-131 dB_{rms}@ 400 m	181 dB_{rms}	Max. level 175.5 dB_{rms} @ 25 Hz 1/3 oct band	TL = 20log_{10}r from loudest (closest) measurement.	Motor seismic vessel, beam 14.8 m, draft 5.4m Area: Beaufort Sea z_r = 3 m above seafloor Broadband 10 Hz - 25 kHz 1/3 oct (f_s = 96 kHz). Contamination from air gun pulse reverberation	Beland et al, 2013
Survey Vessel (*Mt Mitchell*)	70.4	1453	~45	3.8	130 dB_{rms} @ 400 m	180.3 dB_{rms}	N/A	RL_{rms} = 180.3 - 18.4log_{10}r - 10^{-3}r, range of validity 0.2 - 5 km, 90th percentile regression equation. General	Research vessel *Area*: Honeyguide, Chukchi Sea z_r = 1 m above seafloor Broadband (f_s = 48 kHz)	Reiser et al., 2010
			~45	3.5	132.5 dB_{rms} @ 400 m 137 dB_{rms} @ 400 m	175.1 dB_{rms} 174.8 dB_{rms}	N/A	RL_{rms} = 175.1 - 15.9log_{10}r, range of validity 0.2 - 5 km. Fwd endfire (bow) RL_{rms} = 174.8 - 14.1log_{10}r, range of validity 0.2 - 5 km. Bwd endfire (stern) 90th percentile regression equations	Research vesel Area: Burguer area, Chukchi Sea z_r = 1 m above seafloor Broadband (f_s = 48 kHz)	
Survey Vessel (*Gulf Provider*)	58	926 (GT)	~30	4.6	118-122 dB_{rms} @ 400 m	168.6 dB_{rms}	N/A	RL_{rms} = 168.6 -18.6log_{10}r+1·10^{-4}r, range of validity 0.5 - 5 km, 50th percentile regression equation (mean). General	Support vessel, 1x 1100 hp engine *Area*: Camden Bay, Beaufort Sea z_r ~ 3 m above seafloor Broadband (f_s = 48 kHz)	Funk et al., 2008
			~40	12.6	133 dB_{rms} @ 400 m 128 dB_{rms} @ 400 m	158.6 dB_{rms} 158.3 dB_{rms}	N/A	RL_{rms} = 158.6 -9.4log_{10}r, range of validity 0.3 - 2 km, 90th percentile regression equation. Bwd endfire (stern) RL_{rms} = 158.3 -11.3log_{10}r, range of validity 0.3 - 5 km, 90th percentile regression equation. Fwd endfire (bow)	Support vessel, 1x 1100 hp engine *Area*: Point Lay, Chukchi Sea z_r = 1 m above seafloor Broadband 1 Hz - 24 kHz (f_s = 48 kHz)	Ireland et al., 2009
Survey Vessel (*Cape Flattery*)	56.7	496 (GRT)	~40	4	115-120 dB_{rms} @ 400 m	151.6 dB_{rms}	N/A	RL_{rms} = 151.6 - 12.4log_{10}r, range of validity 0.2 - 3 km, 90th percentile regression equation. General	Research vessel, 1x 1250 hp engine *Area*: Chukchi Sea z_r = 1 m above seafloor Broadband 1 Hz - 24 kHz (f_s = 48 kHz)	Ireland et al., 2009

Table 4.3 Sounds produced by small and medium vessels – length < 100 m (cont., part 2)

Vessel (*Name/ID*)	Length [m]	Displacement [Tonne]	h_w [m]	Speed [kn]	Measurement [dB re 1µPa$_{rms}$]	SL [dB re 1µPa@1m]	Signal Characteristics	Regression Equation	Description	Reference
Survey Vessel (*Alpha Helix*)	40.5	289 (GRT)	~45	4.5	114-121 dB_{rms} @ 400 m	151.5 dB_{rms}	N/A	RL_{rms} = 151.5 - 11.8$\log_{10}$R, range of validity 0.2 - 3 km, 90th percentile regression equation. General	Research vessel, 1x 820 hp engine Area: Chukchi Sea z_r = 1 m above seafloor Broadband 1 Hz - 24 kHz (f_s = 48 kHz)	Ireland et al., 2009
			~35		120-124 dB_{rms} @ 400 m	150.5 dB_{rms}	N/A	RL_{rms} = 150.5 - 10$\log_{10}$r, range of validity 0.2 - 2 km, 90th percentile regression equation. General	Research vessel, 1x 820 hp engine Area: Camden Bay, Beaufort Sea z_r = 1 m above seafloor Broadband 1 Hz - 24 kHz (f_s = 48 kHz)	
Survey Vessel (*Peregrine*)	27.4	N/A	<8	3.3 (±1)	101 dB_{rms} @ 400 m	172.5 dB_{rms} 173.8 dB_{rms}	N/A	RL_{rms} = 172.5 -28.4$\log_{10}$r, range of validity 25 - 500 m, 50th percentile regression equation (mean). Fwd endfire (bow) RL_{rms} = 173.8 -27.1$\log_{10}$r, range of validity 25 - 500 m, 50th percentile regression equation (mean). Bwd endfire (stern)	Motor seismic vessel, 3x 405 hp engines, 7.3 m beam, 0.9 m draft, all alluminium Area: Foggy Island Bay, Beaufort Sea z_r ~ 0.3 m above seafloor	Aerts et al, 2008
				8.1	104 dB_{rms} @ 400 m	181.3 dB_{rms}		RL_{rms} = 181.3 -31.8$\log_{10}$r, range of validity 40 - 300 m, 90th percentile regression equation. General		
Rig Tender Ship (*Pacific Ariki*)	64	2600 t (DT)	~110	11	126.5 dB_{rms} @ 400 m	165.5 dB_{rms}	N/A	TL = 15$\log_{10}$r	Anchor handling vessel, 5 m draft, 4 x 2000 hp engines Area: 160 km N Melville Island Broadband (20 Hz - 10 kHz 1/3 oct.)	McCauley, 1998
Tug/Supply Vessel (*Maersk Rover*)	67	1894 t	N/A	N/A	N/A	187.8 dB_{rms}[a] 182.3 dB_{rms}[b] 173.9 dB_{rms}[c] 181.8 dB_{rms}[d]	N/A	N/A	16 m wide, 5.2 m draft, 4 x main engines (total 10.6 MW), max. speed 16.5 kn. Thrusters 2x 600 hp (ø 1.5 m), 1 x 800 hp (ø 1.8 m) Broadband 1 Hz - 10 kHz [a]Engines on (100% power), thrusters off [b]Engines on (50% power), thrusters off [c]Engines on (0% power), thrusters on (0% power) [d]Engines on (0% power), thrusters on (100% power)	Austin et al., 2005
Pusher Tug (*Henry Christoffersen*)	56.4	783 (GT)	~45	10 - 12	122 dB_{rms}@ 480 m	157.8 dB_{rms}	N/A	RL_{rms} = 157.8 -11.7$\log_{10}$r, range of validity 0.1 - 1 km, 50th percentile regression equation (mean). Broadside	Shallow hazard, 4x diesel engines Area: Beaufort Sea z_r ~ 3 m above seafloor Broadband 10 Hz - 20 kHz	Patterson et al, 2007
			~40	3.6	125-128 dB_{rms} @ 400 m	155 dB_{rms}	N/A	RL_{rms} = 155 -10.4$\log_{10}$r+1.4·10^{-3}r, range of validity 0.2 - 2 km, 90th percentile regression equation. General	Shallow hazard, 4x diesel engines Area: Camden Bay, Beaufort Sea z_r ~ 3 m above seafloor Broadband (f_s = 48 kHz)	Funk et al., 2008
			22	4	124-127 dB_{rms} @ 400 m	173.7 dB_{rms}	N/A	RL_{rms} = 173.7 -17.6$\log_{10}$r+9.3·10^{-4}r, range of validity 50 - 500 m, 90th percentile regression equation. General	Shallow hazard, 4x diesel engines Area: Beechey Point, Beaufort Sea z_r ~ 3 m above seafloor Broadband (f_s = 48 kHz)	
				14	125-136 dB_{rms} @ 400 m	183.7 dB_{rms}	N/A	RL_{rms} = 183.7 -18.8$\log_{10}$r+1.1·10^{-4}r, range of validity 50 - 500 m, 90th percentile regression equation. General		
			~35	3.5	126-128 dB_{rms} @ 400 m	151.2 dB_{rms}	N/A	RL_{rms} = 151.2 -8.9$\log_{10}$r, range of validity 0.1 - 1 km, 90th percentile regression equation. General	Shallow hazard, 4x diesel engines Area: Camden Bay, Beaufort Sea z_r = 1 m above seafloor Broadband 1 Hz - 24 kHz (f_s = 48 kHz)	Ireland et al., 2009
				10	126-133 dB_{rms} @ 400 m	161.9 dB_{rms}	N/A	RL_{rms} = 161.9 -11.6$\log_{10}$r + 6·10^{-5}r, range of validity 0.1 - 3 km, 90th percentile regression equation. General		

Table 4.3 Sounds produced by small and medium vessels – length < 100 m (cont. part 3)

Vessel (*Name/ID*)	Length [m]	Displacement [Tonne]	h_w [m]	Speed [kn]	Measurement [dB re 1µPa$_x$]	SL [dB re 1µPa@1m]	Signal Characteristics	Regression Equation	Description	Reference
Landing Craft (Arctic Wolf)	41.2	N/A	<8	7.3	103-107 dB_{rms} @ 400 m	203.6 dB_{rms}	N/A	RL_{rms} = 203.6 -35.7log_{10}r, range of validity 47 - 1000 m, 90th percentile regression equation. General	Multipurpose motor vessel, 3x 425 engines, beam 11.6 m, draft 1.4 m Area: Foggy island Bay, Beaufort Sea z_r ~ 0.3 m above seafloor Broadband (f_s = 48 kHz)	Aerts et al, 2008
Support Vessel (*Torsvik*)	39.2	370 (GT)	~40	12	126.5 dB_{rms} @ 1000 m 119-122 dB_{rms} @ 1000 m	163.9 dB_{rms} 153.9 dB_{rms}	N/A	RL_{rms} = 163.9 - 12.6log_{10}r, range of validity 0.5 - 5 km, 90th percentile regression equation. Bwd endfire (stern) RL_{rms} = 153.9 - 10.4log_{10}r, range of validity 0.6 - 5 km, 90th percentile regression equation. Fwd endfire (bow)	Support vessel, 1x 880 hp engine Area: Point Lay, Chukchi Sea z_r = 1 m above seafloor Broadband 1 Hz - 24 kHz (f_s = 48 kHz)	Ireland et al., 2009
Support Vessel (*Norseman II*)	35	199 (GT)	~30	10	117-121 dB_{rms} @ 400 m	160 dB_{rms}	N/A	RL_{rms} = 160 -14.4log_{10}r, range of validity 0.1 - 2 km, 50th percentile regression equation (mean). Endfire (bow+stern)	Support vessel, 1x 850 hp engine Area: Prudhoe Bay, Beaufort Sea z_r ~ 3 m above seafloor Broadband (f_s = 48 kHz)	Funk et al., 2008
			~40	10.4	123-126 dB_{rms} @ 400 m	162.7 dB_{rms}	N/A	RL_{rms} = 162.7 -12.9log_{10}r, range of validity 40 m to 3 km, 90th percentile regression equation. General	Support vessel, 1x 850 hp engine Area: Point Lay, Chukchi Sea z_r = 1 m above seafloor Broadband 1 Hz - 24 kHz (f_s = 48 kHz)	Ireland et al., 2009
			~20	9.5	123-126 dB_{rms} @ 400 m	188.8 dB_{rms}	N/A	RL_{rms} = 188.8 - 23.2log_{10}r, range of validity 0.1 - 15 km, 90th percentile regression equation. General	Support vessel, 1x 850 hp engine Area: Prudhoe Bay, Beaufort Sea z_r = 1 m above seafloor Broadband 1 Hz - 24 kHz (f_s = 48 kHz)	
Support Vessel (*Theresa Marie*)	28	190 (GT)	~40	10.5	126-133 dB_{rms} @ 400 m	151.7 dB_{rms}	N/A	RL_{rms} = 151.7 - 8.4log_{10}r, range of validity 0.1 - 8 km, 90th percentile regression equation. General	Support vessel, 1x 940 hp engine Area: Point Lay, Chukchi Sea z_r = 1 m above seafloor Broadband 1 Hz - 24 kHz (f_s = 48 kHz)	Ireland et al., 2009
Bathymetric Survey Boat (*American Islander*)	30	N/A	~30	7.5	115-125 dB_{rms} @ 400 m	158.9 dB_{rms}	N/A	RL_{rms} = 158.9 -13.6log_{10}r+1.1·10^{-3}r, range of validity 0.5 - 5 km, 50th percentile regression equation (mean). General	Tug support vessel for the *Gilavar* Area: Camden Bay, Beaufort Sea z_r ~ 3 m above seafloor Broadband (f_s = 48 kHz)	Funk et al., 2008
Fishing Trawler (-)	30-50	N/A	N/A	5	N/A	157 dB_{rms}	N/A	N/A	Fishing trawler, trawling Broadband 20-16k Hz 1/3 oct bands	Malme et al., 1989

4.5 Boats and Hovercrafts

A boat is a small vessel with a wide variety of shapes, sizes and applications, which can be classified as human-powered, wind-powered (sailboats) and engine-powered (motorboats). Small boats with outboard engines are common in coastal waters; these engines produce strong, high frequency tones. The tonal frequencies produced by the outboard engines of somewhat larger boats are lower and their source levels are of the order of 175 dB re 1µPa@1m (Richardson et al, 1995). Kipple & Gabriele (2003) make an exhaustive analysis of 14 watercrafts 4-20 m long used by the Glacier Bay National Park, in Alaska. The results are summarised in Table 4.4.

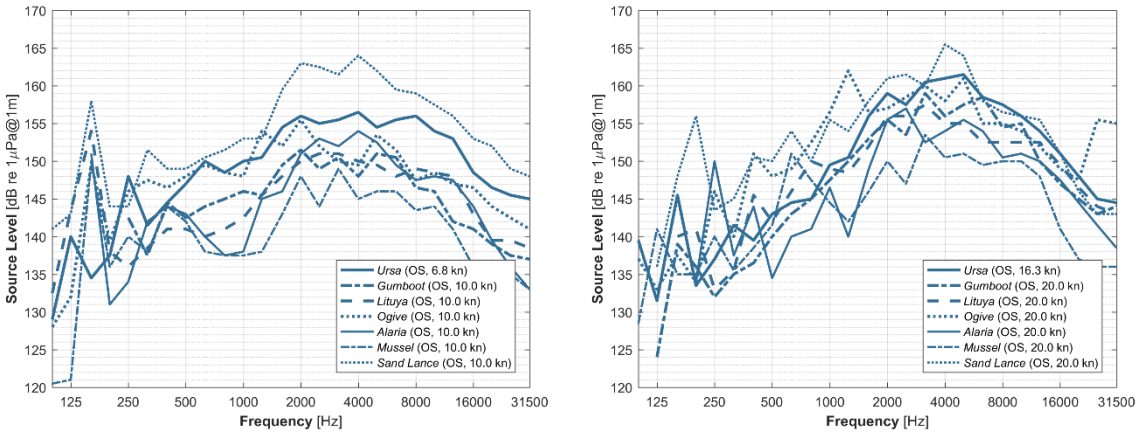

Figure 4.20 Third-octave spectra of seven open skiffs at low-medium speeds (left) and high speeds (right). After Kipple, 2002.

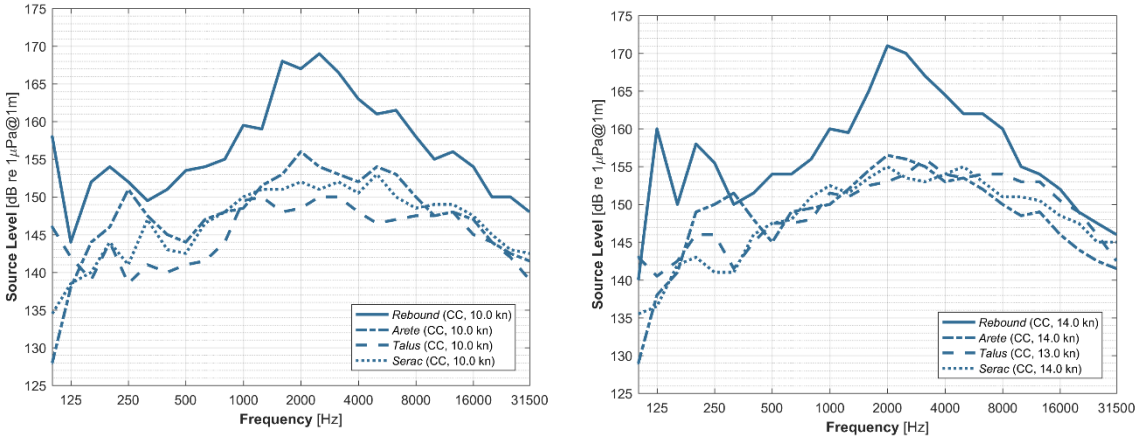

Figure 4.21 *Third-octave spectra of four cabin cruisers at medium (left) and medium-high speeds (right). After Kipple, 2002.*

Hovercrafts create an air cushion under the hull above atmospheric pressure that lifts the craft over the operating surface. These hybrid vessels can travel over land, water and ice. The most detailed study on the sounds produced by a hovercraft in water was published by Blackwell & Greene (2005). In this study, underwater and in-air measurements were made in Prudhoe Bay (Alaska) while a Griffon 2000TD hovercraft operated at near full power. The Griffon 2000TD is a small hovercraft, 11.9 m long and 4.8 m wide, with a 35 kts top speed at full load. The model consists of a 12-bladed lift fan running at a maximum rotation speed of 2100 rpm, and a 4-bladed thrust propeller with maximum speed of 1380 rpm (fan-thruster pulley ratio of 1.52). The lift fan and thrust propeller are both driven by a single Deutz 265 kW diesel engine.

The sources of tonal sound in the hovercraft include the engine, the lift fan and the thrust propeller. The 2000TD was tested at near full power in four passes; engine, fan and propeller were all above the water. The sound radiated by the hovercraft covered a broad range of frequencies: the blade rate of the thrust propeller produced the largest peak at 87 Hz, with four lower level harmonics; the blade rate tone

of 397 Hz of the lift fan was barely detectable, despite its proximity to water. The broadband sound levels recorded with the hydrophone at 1 m depth were higher than at 7 m (133 and 131 dB re 1µPa at CPA). The sound sources in the hovercraft remain in air, reducing the horizontal propagation of sound in water. The hovercraft was considerably quieter than vessels of similar size.

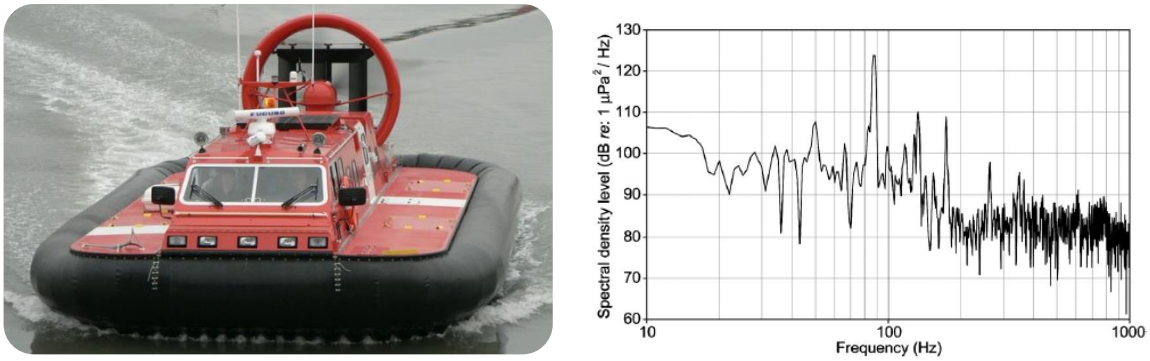

Figure 4.22 Hovercraft Griffon 2000TD (left) and spectral density of a 1.5 s sample recorded at 7 m depth (right, from Blackwell & Greene, 2005)

Table 4.4 Sounds produced by small vessels (length <25 m), boats and hovercrafts

Vessel (*Name/ID*)	Length [m]	Displacement [Tonne]	h_w [m]	Speed [kn]	Measurement [dB re 1µPa$_{rms}$]	SL [dB re 1µPa@1m]	Signal Characteristics	Regression Equation	Description	Reference
Fishing Ship (*Reef Venture*)	20	30	~110	12.5	137 dB_{rms} @ 30 m	159.1 dB_{rms}	N/A	TL = 15$\log_{10}$r	Fishing vessel, 2 m draft, 6.1 m beam, 1 x 450 hp engine Area: 160 km N Melville Island Broadband (20 Hz - 10 kHz 1/3 oct.)	McCauley, 1998
Military Boat (*Nunatak*)	19.8	N/A	55	6.7	N/A	163.8 dB_{rms}	N/A	Measurements at 462 m, backprojected to 1 m using TL = 20$\log_{10}$r	Military boat, 1.2 m draft, steel hull Diesel engine, 375 hp z_r = 30 m Broadband 25 Hz - 31.5 kHz 1/3 oct	Kipple & Gabriele, 2003
				8.5	N/A	169.6 dB_{rms}				
Tug (*Leo*)	N/A	N/A	7	Low	149 dB_{rms}@ 102 m[a] 124 dB_{rms}@ 180 m[b]	178.9 dB_{rms}[a] 163.8 dB_{rms}[b]	Most energy 100 Hz to 2 kHz Harmonics at f = n·25 Hz Low energy < 200 Hz due to very shallow water depth	RL_{rms} = 178.9 - 17.8$\log_{10}$r RL_{rms} = 163.8 - 17.4$\log_{10}$r	Broadband 10 Hz - 20 kHz [a] Pushing *Katie II* (gravel barge) into dock, [b] Holding *Katie II* against dock	Blackwell & Greene, 2002
Tug Vessel (*Alaganik*)	24	N/A	< 8	3.6	103-110 dB_{rms}@ 400 m	167.6 dB_{rms}	N/A	RL_{rms} = 167.6 - 23.2$\log_{10}$r, range of validity 77 - 400 m, 90[th] percentile regression equation. General. Combined noise from *Alganik* and *Hook Point* vessels	Survey fishing vessel, no engines, 7 m beam, 0.9 m draft Area: Foggy Island Bay, Beaufort Sea z_r ~ 0.3 m above seafloor Broadband (f_s = 48 kHz)	Aerts et al, 2008
Survey Vessel (*Hook Point*)	10	N/A	< 8						Tug fishing vessel, 2x 315 engines, 5 m beam, 0.6 m draft Area: Foggy Island Bay, Beaufort Sea z_r ~0.3 m above seafloor Broadband (f_s = 48 kHz)	
Survey Vessel (*Wiley Gunner*)	14.6	N/A	9	7.7	105-125 dB_{rms} @ 400 m	171.3 dB_{rms}	N/A	RL_{rms} = 171.3 - 17.5$\log_{10}$r, range of validity 10 m to 2 km, 90[th] percentile regression equation. General	Seismic source vessel, 3x engines, 800 hp, beam 3.6 m, draft 0.7 m Area: Colvile River Delta, Beaufort Sea z_r = 1.5 m above seafloor	Hauser et al., 2008
Crew Vessel (*American Discovery*)	12.2	N/A	9	16.1	117-122 dB_{rms} @ 400 m	183.2 dB_{rms}	N/A	RL_{rms} = 183.2 - 21.2$\log_{10}$r, range of validity 30 m to 5 km, 90[th] percentile regression equation. General	Crew and supply vessel, 2x 336 hp engines, beam 5.5 m, draft 0.5 m Area: Colvile River Delta, Beaufort Sea z_r = 1.5 m above seafloor	Hauser et al., 2008
Landing Craft (*Miss Diane*)	16.8	N/A	< 8	2.4 (±0.7)	100 dB_{rms} @ 400 m[a] 109 dB_{rms} @ 400 m[b]	158.1 dB_{rms}[a] 155.1 dB_{rms}[b]	N/A	[a] RL_{rms} = 158.1 - 22.9$\log_{10}$r, range of validity 38 - 500 m, 50[th] percentile regression equation (mean). Fwd endfire (bow) [b] RL_{rms} = 155.1 - 16.8$\log_{10}$r, range of validity 40 - 500 m, 50[th] percentile regression equation (mean). Bwd endfire (stern)	Motor seismic vessel, 1x 300 hp engine, 5.5 m beam, 0.6 m draft, all alluminium Area: Foggy Island Bay, Beaufort Sea z_r ~0.3 m above seafloor Broadband (f_s = 48 kHz)	Aerts et al, 2008
				6.1 (±0.9)	106 dB_{rms} @ 200 m[a] 105 dB_{rms} @ 200 m[b]	165.7 dB_{rms}[a] 163.1 dB_{rms}[b]		[a] RL_{rms} = 165.7 -25.6$\log_{10}$r, range of validity 23 - 300 m, 50[th] percentile regression equation (mean). Fwd endfire (bow) [b] RL_{rms} = 163.1 -25$\log_{10}$r, range of validity 40 - 280 m, 50[th] percentile regression equation (mean). Bwd endfire (stern)		

Table 4.4 Sounds produced by small vessels (length <25 m), boats and hovercrafts (cont., part 2)

Vessel (*Name/ID*)	Length [m]	Displacement [Tonne]	h_w [m]	Speed [kn]	Measurement [dB re 1µPa$_{rms}$]	SL [dB re 1µPa@1m]	Signal Characteristics	Regression Equation	Description	Reference
Landing Craft (*Maxime*)	12	N/A	7.6	5.4	113-140 dB_{rms} @ 400 m	149 dB_{rms}	N/A	RL_{rms} = 149 -13log_{10}r+2·10^{-4}r, range of validity 70 - 700 m, 50th percentile regression equation (mean). Endfire (bow+stern)	Crew vessel, water-jet propelled landing craft. Area: Prudhoe Bay, Beaufort Sea Broadband (f_s = 48 kHz)	Funk et al., 2008
				6.5	115-135 dB_{rms} @ 300 m	151 dB_{rms}	N/A	RL_{rms} = 151 -15log_{10}r+2·10^{-4}r, range of validity 20 - 400 m, 50th percentile regression equation (mean). Endfire (bow+stern)		
			~25	8	112-116 dB_{rms} @ 400 m	156.5 dB_{rms}	N/A	RL_{rms} = 156.5 -16.1log_{10}r, range of validity 20 m - 4 km, 90th percentile regression equation. General	Crew vessel, water-jet propelled landing craft. Area: Point Barrow, Beaufort Sea z_r = 1 m above seafloor Broadband 1 Hz - 24 kHz (f_s = 48 kHz)	Ireland et al., 2009
Crew Vessel (*Qayaq Spirit*)	12.2	N/A	<8	7.3 (±0.7)	111 dB_{rms} @ 400 m[a] 106 dB_{rms} @ 400 m[b]	151 dB_{rms} [a] 148.8 dB_{rms} [b]	N/A	[a] RL_{rms} = 151 -16.1log_{10}r, range of validity 18 - 500 m, 50th percentile regression equation (mean). Fwd endfire (bow) [b] RL_{rms} = 148.8 -17.1log_{10}r, range of validity 30 - 500 m, 50th percentile regression equation (mean). Bwd endfire (stern)	Crew motor vessel, 3x engines, 1280 hp, 4.3 m beam, 0.6 m draft, aluminium hull Area: Foggy Island Bay, Beaufort Sea z_r ~ 0.3 m above seafloor Broadband (f_s = 48 kHz)	Aerts et al, 2008
				20.7 (±4.3)	120 dB_{rms} @ 400 m[a] 108-109 dB_{rms} @ 400 m [b]	184.7 dB_{rms} [a] 184.3 dB_{rms} [b]		[a] RL_{rms} = 184.7 -25.1log_{10}r, range of validity 50 - 500 m, 50th percentile regression equation (mean). Fwd endfire (bow) [b] RL_{rms} = 184.3 -29.3log_{10}r, range of validity 60 - 500 m, 50th percentile regression equation (mean). Bwd endfire (stern)		
Crew Vessel (*Gwydyr Bay*)	N/A	N/A	<8	7.1	102 dB_{rms} [a] 97 dB_{rms} [b]	172.5 dB_{rms} [a] 168.1 dB_{rms} [b]	N/A	[a] RL_{rms} = 172.5 -26.1log_{10}r, range of validity 13 - 900 m, 90th percentile regression equation. Fwd endfire (bow) [b] RL_{rms} = 168.1 -26.4log_{10}r, range of validity 13 - 600 m, 90th percentile regression equation. Bwd endfire (stern)	Crew vessel (*reserved vessel information*) Area: Foggy Island Bay, Beaufort Sea z_r ~0.3 m above seafloor Broadband (f_s = 48 kHz)	Aerts et al, 2008
				20.5	123 dB_{rms} [a] 103 dB_{rms} [b]	184.1 dB_{rms} [a] 194.8 dB_{rms} [b]		[a] RL_{rms} = 184.1 -22.7log_{10}r, range of validity 10 - 900 m, 90th percentile regression equation. Fwd endfire (bow) [b] RL_{rms} = 194.8 -33.5log_{10}r, range of validity 10 - 900 m, 90th percentile regression equation. Bwd endfire (stern)		
Support Vessel (*Mariah B*)	10.4	N/A	<8	8	93-100 dB_{rms}	166.4 dB_{rms}	N/A	RL_{rms} = 166.4 -25.7log_{10}r, range of validity 35 - 600 m, 90th percentile regression equation. General	HSE support fishing vessel, 2x 440 hp engines Area: Foggy Island Bay, Beaufort Sea z_r ~0.3 m above seafloor Broadband (f_s = 48 kHz)	Aerts et al, 2008
				22.5	95-102 dB_{rms}	179 dB_{rms}		RL_{rms} = 179 -29.4log_{10}r, range of validity 36 - 1000 m, 90th percentile regression equation. General		

Table 4.4 Sounds produced by small vessels (length <25 m), boats and hovercrafts (cont., part 3)

Vessel (*Name/ID*)	Length [m]	Displacement [Tonne]	h_w [m]	Speed [kn]	Measurement [dB re 1µPa$_x$]	SL [dB re 1µPa@1m]	Signal Characteristics	Regression Equation	Description	Reference
Bowpicker (*Rumple Minze*)	9.8	N/A	<8	2.2 (±0.7)	102 dB_{rms} @ 400 m[a] 102 dB_{rms} @ 400 m[b]	141.4 dB_{rms}[a] 136.3 dB_{rms}[b]	N/A	[a] RL_{rms} = 141.4 -15.9log_{10}r, range of validity 15 - 500 m, 50[th] percentile regression equation (mean). Fwd endfire (bow) [b] RL_{rms} = 136.3 -14.4log_{10}r, range of validity 20 - 500 m, 50[th] percentile regression equation (mean). Bwd endfire (stern)	Bowpicker fishing vessel, 2x 505 hp engines, 4.3 m beam, 0.6 m draft Area: Foggy Island Bay, Beaufort Sea z_r ~ 0.3 m above seafloor Broadband (f_s = 48 kHz)	Aerts et al, 2008
				5.8 (±1)	105 dB_{rms} @ 400 m[a] 102-105 dB_{rms} @ 400 m[b]	142.4 dB_{rms}[a] 142.3 dB_{rms}[b]		[a] RL_{rms} = 142.4 -14.4log_{10}r, range of validity 8.5 - 500 m, 50[th] percentile regression equation (mean). Fwd endfire (bow) [b] RL_{rms} = 142.3 -15.2log_{10}r, range of validity 11 - 500 m, 50[th] percentile regression equation (mean). Bwd endfire (stern)		
				3.2	92-94 dB_{rms} @ 200 m[a] 93-95 dB_{rms} @ 200 m[b]	142.8 dB_{rms}[a] 162.3 dB_{rms}[b]		[a] RL_{rms} = 142.8 -21.2log_{10}r, range of validity 38 - 200 m, 90[th] percentile regression equation. Fwd endfire (bow) [b] RL_{rms} = 162.3 -28.2log_{10}r, range of validity 38 - 200 m, 90[th] percentile regression equation. Bwd endfire (stern)		
Bowpicker (*Canvasback*)	9.8	N/A	<8	1.9 (±0.4)	102-104 dB_{rms} @ 100 m[a] 103 dB_{rms} @ 100 m[b]	129.2 dB_{rms}[a] 131.8 dB_{rms}[b]	N/A	[a] RL_{rms} = 129.2 -13.2log_{10}r, range of validity 5 - 100 m, 50[th] percentile regression equation (mean). Fwd endfire (bow) [b] RL_{rms} = 131.8 -13.3log_{10}r, range of validity 10 - 100 m, 50[th] percentile regression equation (mean). Bwd endfire (stern)	Bowpicker fishing vessel, 2x 315 hp engines, 4.3 m beam, 0.6 m draft Area: Foggy Island Bay, Beaufort Sea z_r ~ 3 m above seafloor Broadband (f_s = 48 kHz)	Aerts et al, 2008
				6 (±1.4)	113 dB_{rms} @ 50 m[a] 108 dB_{rms} @ 50 m[b]	145.3 dB_{rms}[a] 143.2 dB_{rms}[b]		[a] RL_{rms} = 145.3 -17.7log_{10}r, range of validity 13 - 75 m, 50[th] percentile regression equation (mean). Fwd endfire (bow) [b] RL_{rms} = 143.2 -21log_{10}r, range of validity 11 - 100 m, 50[th] percentile regression equation (mean). Bwd endfire (stern)		
Bowpicker (*Cape Fear*)	9.8	N/A	<8	1.6 (±0.5)	104 dB_{rms} @ 90 m[a] 106 dB_{rms} @ 90 m[b]	131.1 dB_{rms}[a] 138.2 dB_{rms}[b]	N/A	[a] RL = 131.1 -13.2log_{10}r, range of validity 15 - 120 m, 50th percentile regression equation (mean). Fwd endfire (bow) [b] RL = 138.2 -15.3log_{10}r, range of validity 18 - 120 m, 50[th] percentile regression equation (mean). Bwd endfire (stern)	Bowpicker fishing vessel, 2x 315 hp engines, 3.8 m beam, 0.6 m draft Area: Foggy Island Bay, Beaufort Sea z_r ~ 3 m above seafloor Broadband (f_s = 48 kHz)	Aerts et al, 2008
				4.1	100-103 dB_{rms} @ 200 m	160.4 dB_{rms}		RL_{rms} = 160.4 - 24.1log_{10}r, range of validity 58 - 300 m, 90[th] percentile regression equation. General		
				7.2	92-103 dB_{rms} @ 400 m	164.5 dB_{rms}		RL_{rms} = 164.5 - 23.6log_{10}r, range of validity 40 - 1000 m, 90[th] percentile regression equation. General		
Bowpicker (*Sleep Robber*)	9.8	N/A	<8	3.2	N/A	152.1 dB_{rms}	N/A	N/A	Bowpicker fishing vessel, 2x 318 hp engines, 4.3 m beam, 0.6 m draft, aluminium hull Area: Foggy Island Bay, Beaufort Sea z_r ~0.3 m above seafloor Broadband (f_s = 48 kHz)	Aerts et al, 2008
				7.5	92-103 dB_{rms} @ 400 m	174.3 dB_{rms}		RL_{rms} = 174.3 - 29.7log_{10}R, range of validity 44 - 550 m, 90th percentile regression equation. General		

Table 4.4 Sounds produced by small vessels (length <25 m), boats and hovercrafts (cont., part 4)

Vessel (*Name/ID*)	Length [m]	Displacement [Tonne]	h_w [m]	Speed [kn]	Measurement [dB re 1µPa$_x$]	SL [dB re 1µPa@1m]	Signal Characteristics	Regression Equation	Description	Reference
Inflatable Boat (*DIB 1*)	12.5	N/A	9	4	115-120 dB_{rms} @ 400 m	180.5 dB_{rms}	N/A	RL_{rms} = 180.5 - 22.2$\log_{10}$r, range of validity 0.2 - 2 km, 90th percentile regression equation. General	Inflatable boat, 2x 200 hp engines, beam 4.2 m, draft 0.8 m Area: Colvile River Delta, Beaufort Sea z_r = 1.5 m above seafloor Broadband 10 Hz - 24 kHz (f_s = 48 kHz)	Hauser et al., 2008
Inflatable Boat (*DIB 2*)	12.5	N/A	9	9.1	115-121 dB_{rms} @ 400 m	168.2 dB_{rms}	N/A	RL = 168.2 - 18.7$\log_{10}$r, range of validity 10 m to 2 km, 90th percentile regression equation. General	Inflatable boat, 2x 200 hp engines, beam 4.2 m, draft 0.8 m Area: Colvile River Delta, Beaufort Sea z_r = 1.5 m above seafloor Broadband 10 Hz - 24 kHz (f_s = 48 kHz)	Hauser et al., 2008
Inflatable Boat (*DIB 3*)	12.5	N/A	9	7.2	112-118 dB_{rms} @ 400 m	173.2 dB_{rms}	N/A	RL_{rms} = 173.2 - 21.7$\log_{10}$r, range of validity 10 m to 2 km, 90th percentile regression equation. General	Inflatable boat, 2x 200 hp engines, beam 4.2 m, draft 0.8 m Area: Colvile River Delta, Beaufort Sea z_r = 1.5 m above seafloor Broadband 10 Hz - 24 kHz (f_s = 48 kHz) Note that DIB 1, 2 and 3 are the same model (*Demaree Inflatable Boat*) but different boat	Hauser et al., 2008
Alluminium Hull Boat (*Reliance 1*)	12.5	N/A	9	8	122-130 dB_{rms} @ 400 m	189.3 dB_{rms}	N/A	RL_{rms} = 189.3 - 23.2$\log_{10}$r, range of validity 10 m to 4 km, 90th percentile regression equation. General	Alluminium hull boat, 2x 330, beam 4.9 m, draft 0.8 m Area: Colvile River Delta, Beaufort Sea z_r = 1.5 m above seafloor Broadband 10 Hz - 24 kHz (f_s = 48 kHz)	Hauser et al., 2008
Alluminium Hull Boat (*Reliance 2*)	12.5	N/A	9	6.3	127-135 dB_{rms} @ 400 m	216.7 dB_{rms}	N/A	RL_{rms} = 216.7 - 31.3$\log_{10}$r, range of validity 10 m to 4 km, 90th percentile regression equation. General	Alluminium hull boat, 2x 330, beam 4.9 m, draft 0.8 m Area: Colvile River Delta, Beaufort Sea z_r = 1.5 m above seafloor Broadband 10 Hz - 24 kHz (f_s = 48 kHz) Note that Reliance 1 and 2 are the same model but different boat	Hauser et al., 2008
Jet Boat (*Storm Warning*)	N/A	N/A	~2	6.3	111-113 dB_{rms} @ 400 m	134.6 dB_{rms}	N/A	RL_{rms} = 134.6 -5.7$\log_{10}$R - 1.8·10^{-2}r, range of validity 10 m - 1 km, 90th percentile regression equation. Endfire (bow+stern)	Jet boat Area: Simpson Lagoon, Beaufort Sea z_r = 1 m above seafloor Broadband <10 kHz (f_s = 96 kHz)	McPherson & Warner, 2012
Jet Boat (*Resolution*)	N/A	N/A	~13	5.5	106-111 dB_{rms} @ 400 m	154.8 dB_{rms}	N/A	RL_{rms} = 154.8 - 17.2$\log_{10}$r, range of validity 14 - 300 m RL_{rms} = 140.5 -11.5$\log_{10}$r, range of validity 0.3 - 3 km 90th percentile regression equations. Endfire (bow+stern)	Jet boat Area: Simpson Lagoon, Beaufort Sea z_r = 1 m above seafloor Broadband <10 kHz (f_s = 96 kHz)	McPherson & Warner, 2012
Propeller Boat (*Margarita*)	N/A	N/A	~13	7.6	122-127 dB_{rms} @ 400 m	178.3 dB_{rms}	N/A	RL_{rms} = 178.3 - 20.6$\log_{10}$r, range of validity 14 - 300 m RL_{rms} = 151.3 -9$\log_{10}$r - 3.2·10^{-3}r, range of validity 0.3 - 3 km 90th percentile regression equations. Endfire (bow+stern)	Propeller boat Area: Simpson Lagoon, Beaufort Sea z_r = 1 m above seafloor Broadband <10 kHz (f_s = 96 kHz)	McPherson & Warner, 2012

Table 4.4 Sounds produced by small vessels (length <25 m), boats and hovercrafts (cont., part 5)

Vessel (*Name/ID*)	Length [m]	Displacement [Tonne]	h_w [m]	Speed [kn]	Measurement [dB re 1µPa$_{rms}$]	SL [dB re 1µPa@1m]	Signal Characteristics	Regression Equation	Description	Reference
Cabin Cruiser (*Serac*)	10.4	N/A	61	10	N/A	161.8 dB_{rms} [a]	N/A	Measurements at 383 m (419 yd), backprojected by Kipple & Gabriele to 0.91 m (1 yd) using TL = $20\log_{10}r$. Source levels calculated from spectrum plot, and corrected to 1 m.	Cabin cruiser, 0.67 m draft, aluminium hull. 2x Diesel jet drive, 310 hp z_r = 50 m Broadband from [a]25 Hz, [b]31.5 Hz to 31.5 kHz 1/3 oct bands	Kipple & Gabriele, 2003
				14	N/A	163.9 dB_{rms} [b]				
				20	N/A	165.8 dB_{rms} [b]				
Cabin Cruiser (*Talus*)	9.1	N/A	55	10	N/A	160.6 dB_{rms}	N/A	Measurements at 462 m (505 yd), backprojected by Kipple & Gabriele to 0.91 m (1 yd) using TL = $20\log_{10}r$. Source levels calculated from spectrum plot and corrected to 1 m.	Cabin cruiser, 0.6 m draft, aluminium hull. Diesel jet drive, 420 hp z_r = 30 m Broadband 25 Hz - 31.5 kHz 1/3 oct	Kipple & Gabriele, 2003
				13	N/A	165.2 dB_{rms}				
Landing Craft (*Capelin*)	7.9	N/A	55	10	N/A	175.7 dB_{rms}	N/A	Measurements at 462 m (505 yd), backprojected by Kipple & Gabriele to 0.91 m (1 yd) using TL = $20\log_{10}r$. Source levels calculated from spectrum plot and corrected to 1 m.	Landing craft, 0.76 m draft, aluminium hull out/inboard engine, 350 hp z_r = 30 m Broadband 31.5 Hz - 31.5 kHz 1/3 oct	Kipple & Gabriele, 2003
				13	N/A	178.4 dB_{rms}				
				20	N/A	181.3 dB_{rms}				
Cabin Workboat (*Sigma T*)	7.9	N/A	55	10	N/A	172.3 dB_{rms} [a]	N/A	Measurements at 462 m (505 yd), backprojected by Kipple & Gabriele to 0.91 m (1 yd) using TL = $20\log_{10}r$. Source levels calculated from spectrum plot and corrected to 1 m.	Cabin workboat 0.76 m draft, alum. 4-stroke inboard engine, 250 hp z_r = 30 m Broadband from [a]40 Hz, [b]50 Hz to 31.5 kHz 1/3 oct bands	Kipple & Gabriele, 2003
				13	N/A	173.6 dB_{rms} [b]				
				20	N/A	176.2 dB_{rms} [b]				
Cabin Cruiser (*Arete*)	7.6	N/A	61	10	N/A	164.2 dB_{rms} [a]	N/A	Measurements at 383 m (419 yd), backprojected by Kipple & Gabriele to 0.91 m (1 yd) using TL = $20\log_{10}r$. Source levels calculated from spectrum plot, and corrected to 1 m.	Cabin cruiser, 0.58 m draft, fiberglass hull out/inboard engine, 380 hp z_r = 50 m Broadband from [a]31.5 Hz, [b]25 Hz to 31.5 kHz 1/3 oct bands	Kipple & Gabriele, 2003
				14	N/A	165.1 dB_{rms} [b]				
				20	N/A	169.1 dB_{rms} [b]				
Cabin Cruiser (*Rebound*)	6.7	N/A	55	10	N/A	175.3 dB_{rms} [a]	N/A	Measurements at 462 m (505 yd), backprojected by Kipple & Gabriele to 0.91 m (1 yd) using TL = $20\log_{10}r$. Source levels calculated from spectrum plot and corrected to 1 m.	Cabin cruiser, 1.2 m draft, fiberglass hull out/inboard engine, 350 hp z_r = 30 m Broadband from [a]31.5 Hz, [b]40 Hz to 31.5 kHz 1/3 oct bands	Kipple & Gabriele, 2003
				14	N/A	176.4 dB_{rms} [a]				
				20	N/A	176.8 dB_{rms} [b]				
Small Craft (*Boston Whaler*)	6.4	N/A	30	27-31	138 dB_{rms}@ 13 m	147.2 dB_{rms}	N/A	RL_{rms} = 147.2 - $7.8\log_{10}r$	2-stroke engine, 250 hp Broadband 10 Hz - 20 kHz	Blackwell & Greene, 2002
Small Craft (*Avon Rubber*)	5.4	N/A	30	27-31	142 dB_{rms}@ 8.5 m	155.9 dB_{rms}	N/A	RL_{rms} = 155.9 - $14\log_{10}r$	4-stroke engine, 80 hp Broadband 10 Hz - 20 kHz	Blackwell & Greene, 2002
Open Skiff (*Sand Lance*)	5.8	N/A	55	10	N/A	171.8 dB_{rms} [a]	N/A	Measurements at 462 m (505 yd), backprojected by Kipple & Gabriele to 0.91 m (1 yd) using TL = $20\log_{10}r$. Source levels calculated from spectrum plot and corrected to 1 m.	Open skiff, 0.6 m draft, aluminium hull 4-stroke outboard engine, 115 hp z_r = 30 m Broadband from [a]31.5 Hz, [b]125 Hz to 31.5 kHz 1/3 oct bands	Kipple & Gabriele, 2003
				13	N/A	173.6 dB_{rms} [a]				
				20	N/A	171.5 dB_{rms} [b]				
Open Skiff (*Mussel*)	5.5	N/A	61	10	N/A	157.5 dB_{rms} [a]	N/A	Measurements at 383 m (419 yd), backprojected by Kipple & Gabriele to 0.91 m (1 yd) using TL = $20\log_{10}r$. Source levels calculated from spectrum plot, and corrected to 1 m.	Open skiff, 0.3 m draft, aluminium hull 4-stroke outboard engine, 40 hp z_r = 50 m Broadband from [a]25 Hz, [b]31.5 Hz to 31.5 kHz 1/3 oct bands	Kipple & Gabriele, 2003
				14	N/A	161.1 dB_{rms} [a]				
				20	N/A	161.2 dB_{rms} [b]				
Open Skiff (*Ogive*)	5.2	N/A	61	10	N/A	163.6 dB_{rms} [a]	N/A	Measurements at 383 m (419 yd), backprojected by Kipple & Gabriele to 0.91 m (1 yd) using TL = $20\log_{10}r$. Source levels calculated from spectrum plot, and corrected to 1 m.	Open skiff, 0.45 m draft, fiberglass hull 2-stroke outboard engine, 60 hp z_r = 50 m Broadband from [a]50 Hz, [b]25 Hz to 31.5 kHz 1/3 oct bands	Kipple & Gabriele, 2003
				14	N/A	166.2 dB_{rms} [b]				
				20	N/A	169.5 dB_{rms} [b]				

Table 4.4 Sounds produced by small vessels (length <25 m), boats and hovercrafts (cont., part 5)

Vessel (*Name/ID*)	Length [m]	Displacement [Tonne]	h_w [m]	Speed [kn]	Measurement [dB re 1µPa$_{rms}$]	SL [dB re 1µPa@1m]	Signal Characteristics	Regression Equation	Description	Reference
Open Skiff (*Alaria*)	4.9	N/A	55	10	N/A	161.8 dB_{rms} [a]	N/A	Measurements at 462 m (505 yd), backprojected by Kipple & Gabriele to 0.91 m (1 yd) using TL = $20\log_{10}r$. Source levels calculated from spectrum plot and corrected to 1 m.	Open skiff, 0.3 m draft, aluminium hull 4-stroke outboard engine, 40 hp z_r = 30 m Broadband from [a]160 Hz, [b]200 Hz, [c]125 Hz to 31.5 kHz 1/3 oct bands	Kipple & Gabriele, 2003
				13	N/A	161 dB_{rms} [b]				
				20	N/A	164.2 dB_{rms} [c]				
Open Skiff (*Gumboot*)	4.9	N/A	61	10	N/A	160.3 dB_{rms}	N/A	Measurements at 383 m (419 yd), backprojected by Kipple & Gabriele to 0.91 m (1 yd) using TL = $20\log_{10}r$. Source levels calculated from spectrum plot, and corrected to 1 m.	Open skiff, 0.3 m draft, aluminium hull 2-stroke outboard engine, 30 hp z_r = 50 m Broadband 40 Hz - 31.5 kHz 1/3 oct	Kipple & Gabriele, 2003
				14	N/A	162.1 dB_{rms}				
				20	N/A	166.3 dB_{rms}				
Open Skiff (*Lituya*)	4.9	N/A	55	10	N/A	161.2 dB_{rms} [a]	N/A	Measurements at 462 m (505 yd), backprojected by Kipple & Gabriele to 0.91 m (1 yd) using TL = $20\log_{10}r$. Source levels calculated from spectrum plot and corrected to 1 m.	Open skiff, 0.6 m draft, aluminium hull 2-stroke outboard engine, 60 hp z_r = 30 m Broadband from [a]100 Hz, [b]160 Hz to 31.5 kHz 1/3 oct bands	Kipple & Gabriele, 2003
				13	N/A	161.9 dB_{rms} [a]				
				20	N/A	165.3 dB_{rms} [b]				
Open Skiff (*Ursa*)	4.3	N/A	55	6.8	N/A	166.1 dB_{rms} [a]	N/A	Measurements at 462 m (505 yd), backprojected by Kipple & Gabriele to 0.91 m (1 yd) using TL = $20\log_{10}r$. Source levels calculated from spectrum plot and corrected to 1 m.	Open skiff, 0.6 m draft, aluminium hull 2-stroke outboard engine, 25 hp z_r = 30 m Broadband from [a]40 Hz, [b]100 Hz, [c]50 Hz to 31.5 kHz 1/3 oct bands	Kipple & Gabriele, 2003
				13	N/A	167 dB_{rms} [b]				
				16.3	N/A	169.1 dB_{rms} [c]				
Hovercraft (*Griffon 2000TD*)	11.9	3.2 t (DT)	7.3	10-12	133 dB_{rms}@ 6.5 m [a] 131 dB_{rms} @ 6.5 m [b]	145.2 dB_{rms} [a] 143.2 dB_{rms} [b]	Harmonics at f = n·87 Hz from thrust propeller	TL = $15\log_{10}r$ measured for the area. Broadband sound levels at 6.5 m calculated from plotted values at frequencies between 20 Hz and 6.3 kHz. Source levels obtained from sound levels at 6.5 m and TL = $15\log_{10}r$	Diesel engine, 355 hp Area: Prudhoe Bay, Beaufort Sea Broadband 10 Hz - 10 kHz z_r = [a]1 m, [b]7 m	Blackwell & Greene, 2005
Hovercraft	N/A	N/A	3	6.5	133.4±6.9 dB_{rms}@ 48-117 m	N/A	Main energy < 400 Hz	N/A	z_r = 1.5 m [a]16 measurements (avg. & stdev. over sound levels)	Roof & Fleming, 2001
Snowmobile	N/A	N/A	3	N/A	130.4±6.2 dB_{rms}@ 9-78 m [a]	151.2 dB_{rms}	N/A	RL_{rms} = 151.2 -15.1$\log_{10}r$, obtained *by reviewer* with linear least square fitting to measurements	z_r = 1.5 m [a]29 measurements (avg. & stdev. over sound levels)	Roof & Fleming, 2001

4.6 Summary of Sound Radiated from Vessels

The design, speed and size affect the acoustic signature of a vessel. Some of the conclusions about acoustic characteristics of large, medium and small vessels are extracted from Richardson et al. (1995) and Malme et al. (1989) and summarised in Table 4.5.

Table 4.5 General acoustic characteristics of small, medium and large size vessels

Large Vessels	Medium Vessels	Small Vessels
- Main energy content below 100 Hz, due to slow-turning engines and propellers, great power, large hulls and drafts. - Low-frequency spectrum dominated by blade rate - Propeller cavitation contributes to frequencies up to 10 kHz. - Slow speed diesel engines (<250 rpm) are relatively quiet compared to those used in smaller vessels. - Large oil tankers and cargo carriers are the loudest, with source levels typ. in the range 175-185 dB.	- The low-frequency spectrum is dominated by tones related to blade rate, and in second place by the engine firing rate. - Broadband components are associated to propeller cavitation and flow noise, which peak at 50-150 Hz and may extend up to 100 kHz. - Pumps and compressors can also contribute with high frequency tones. - Source levels from medium-small vessels are typ. in the range of 165-175 dB. - Icebreakers produce higher frequency content and broadband sound levels than vessels of comparable size, due to their greater power and increased propeller cavitation.	- The spectra in small vessels is dominated by high frequencies. - These vessels are equipped with small propellers that operate at high speeds. - Blade rate tones are produced at relatively high frequencies, and propeller cavitation dominates in the 0.5-10 kHz region. - The medium and high speed diesel engines typically installed in small vessels are very noisy. The radiated levels can mask propeller cavitation. - Source levels in small vessels are generally < 165 dB.

The mechanisms of sound radiation are common to most vessels. The effects of vessel design and operation on the radiated sound are summarised in the following points (Richardson et al., 1995):

- Propeller cavitation produces dominant tones at the propeller blade rate and most of the broadband sound
- Propulsion engines and auxiliary machinery contribute to the overall sound levels
- Radiated noise is related to ship size and operation, and increases with ship speed
- Propellers generate more noise if damaged, operate asynchronously or without nozzles
- Large vessels tend to be noisier than smaller ones
- Fully laden vessels underway are noisier than unladen vessels

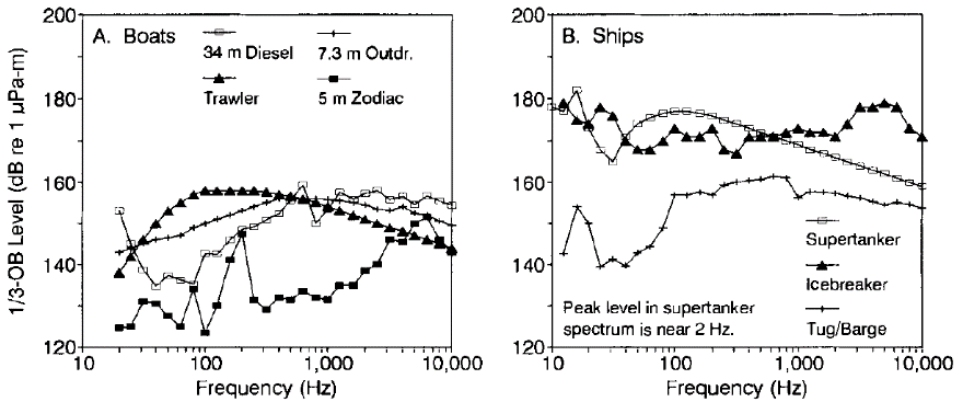

Figure 4.23 Third-octave source level spectra of various types of boats (left) and large vessels (right). From Richardson et al., 1995.

5 Exploration, Development, Production & Decommissioning

5.1 Dredging

Dredging is a process common in coastal waters that consists of removing sediment from a sea, estuary, river of lake and transporting it to a new location to be deposited. Dredging can be classified in three main categories: 1) navigation dredging, which includes capital or maintenance dredging; 2) remedial dredging to handle contaminated sediments; 3) mining and marine aggregate extraction for commercial purposes and construction (Reine et al., 2014). *Capital dredging* takes place in undredged areas to create new channels, basins, harbours, berths, or to deepen or widen existing facilities; *maintenance dredging* aims at maintaining navigable existing waterways, harbours and channels that have become too shallow due to sedimentation. Navigation, remedial and mining dredging are possibly the most common applications, but dredging is actually undertaken for a wider variety of reasons, which include (CEDA, 2011; Thomsen et al., 2009; Todd et al., 2015; Richardson et al., 1995):

- Alter areas of the seabed to make them optimal for the construction of ports, waterways and other marine infrastructure (capital dredging)
- Maintain the navigability of shipping lanes
- Reclamation of new land, constructed with marine aggregate extracted from another location
- Flood prevention by increasing the channel depth
- Beach nourishment, which consists of the extraction of sand offshore to replace the sand in a beach that has been eroded by natural processes or human action, with the purpose of maintaining the recreational and protective function of the beach
- Extraction of sand and gravel that will be used as raw material for construction, mainly in concrete.
- Seabed mining, for recovery of valuable metals
- Environmental remediation of contaminated sediments, affected by chemical spills, sewage sludge or other causes
- Removing of debris and human litter from rivers, canals and harbours
- Remediation of hypertrophication by removing sediment that contains elevated phosphorus levels; this measure is common to control eutrophication in rivers, but is expensive and controversial in terms of its effectiveness.

5.1.1 Dredging Sound

Five of the most common types of dredge used in the majority of projects are: Cutter Suction Dredge (CSD), Trailing Suction Hopper Dredge (TSHD), Grab Dredge (GD), Bucket Ladder Dredge (BLD) and Backhoe Dredge (BHD). The CSD and TSHD are *hydraulic dredges*, and use suction to transfer material from the seabed to a barge or hopper. The GD, BLD and BHD are *mechanical dredges* and use bucket-type tools operated in different ways to dig the seabed. The selection of the dredging method depends on the seabed type, purpose, scale of operation and environmental impact (Thomsen et al., 2009).

The sound generated by the dredging activity is the result of the combination of various of the following processes: collection of seabed material, pump operation, sediment transport through the pipe (CSD, TSHD) or by the mechanical system (GD, BLD, BHD), deposition of material in the barge or hopper, and vessel machinery and propulsion (Thomsen et al, 2009; Robinson et al., 1995; CEDA, 2011; Genesis, 2011). The sound from dredging is continuous in character, but certain types of operation can generate impulsive sounds, such as the impact of the bucket onto the seafloor in GD or BHD. The acoustic signature of the dredging operation results from the combination of various simultaneous processes, which depend on the dredging system and operational conditions. While in most dredging operations the individual processes cannot be separated, in Grab Dredges a sequence of individual processes occur within each operational cycle.

The propeller generates noise, but not all dredging vessels are self-propelled. The propulsion engine and power plant used to drive the dredges produce relatively strong continuous sound that is transferred into the water through the hull. Lack of maintenance and lubrication of the mechanical parts of the dredge system and engines can contribute to increase sound levels (CEDA, 2011). The radiated sound levels and acoustic signature of different dredges, even within the same category, are significantly affected by differences in the number, size and installation of the drag head or bucket, size of the vessel or engine power (Thomsen, 2009).

The aggregate type can affect the high frequency radiated levels (> 1 kHz) and excavating hard, consolidated sediments may generate more intense sounds than porous, unconsolidated sediments. Before dredging, the use of explosives or hammering is sometimes necessary (CEDA, 2011; Robinson et al., 2015).

Dredging generates sound in the low frequency range (< 1 kHz), with source levels typically in the range of 165-185 dB re 1µ@1m. Dredging systems predominate in coastal regions, where low frequencies do not propagate well, and acoustic pressure attenuates rapidly due to multiple sea bottom interactions; dredging sounds are normally undetectable beyond 25 km. The sound is continuous and broadband in nature and can include tonal components up to a few kHz. Sound levels are lower than those from larger vessels, but dredging systems operate in an area for days or weeks, which may result in a higher sound exposure for species that inhabit coastal regions (Richardson et al., 1995).

5.1.2 Cutter Suction Dredge (CSD)

In a *Cutter Suction Dredge* a cutter-head installed at the end of a suction pipe is lowered from the dredge and moved in an arc to loosen the material from the seabed. The removed material is pumped and brought to the surface where it is discharged into a barge or transported through a pipeline. The CSD is most often used to remove hard substrates without the need of explosives. A TSHD is sometimes used to pump the material cut by the CSD. The CSD is commonly used in capital dredging (Reine & Clarke, 2014; Genesis, 2011; Thomsen, 2009).

A CSD is not self-propelled and has to be towed by tugs to the dredging site. Once in site, the CSD is moored in place with the aid of two spud poles, heavy pipes installed at the rear of the dredge hull. The spud poles are sequentially raised and dropped into the seafloor to keep the vessel in position while allowing forward movement. The ladder or cutter head describes an arc around the *walking spud*, which is mounted in a movable carriage that allows the advance or *stepping* of the dredge to the next digging position. The *auxiliary spud* is used to keep the vessel in place while the walking spud is raised (Reine & Clarke, 2014; IADC, 2014; CEDA, 2011).

The sources of noise in a CSD include the continuous sound from dredge pumps above and under water, the excavating sound from the cutter head, the seabed impact of the spuds and carriage operation for the walking spud, the machinery in the dredge, the tug, and if used, the pipeline for the transport of

the excavated material (see Figure 5.1). The removed material will produce a rumbling sound with irregular pulses in the pipe when pumped, especially if it consists of large fragments of consolidated sediment and rock (CEDA, 2011).

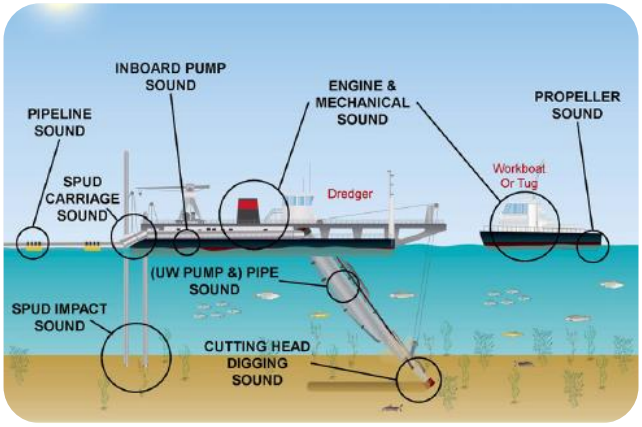

Figure 5.1 Potential sound sources in a cutter suction dredge (from Reine & Clarke, 2014)

Hydraulic dredges (CSD and TSHD) are generally louder than mechanical dredges (CEDA, 2011). Figure 5.2 and Figure 5.3 is show the third-octave band spectrum and spectral density of various CSD dredges.

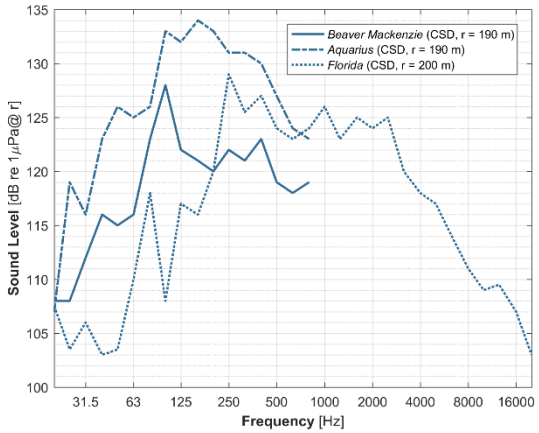

Figure 5.2 Third-octave spectra of cutter suction dredges *Florida* (after Reine & Clarke, 2014), *Beaver Mackenzie* and *Aquarius* (after Greene, 1987).

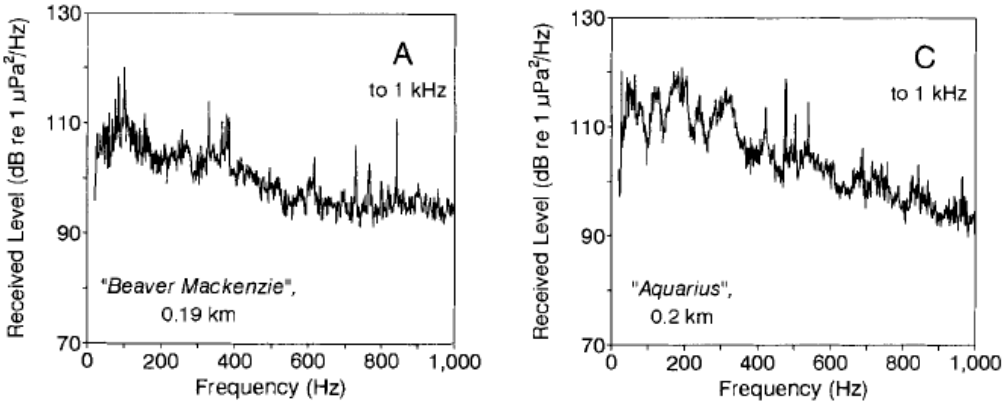

Figure 5.3 Power spectral density of cutter suction dredges *Beaver Mackenzie* (left) and *Aquarius* (centre), dredging at 0.19 and 0.2 km from the receiver (from Richardson et al., 1995).

5.1.3 Trailing Suction Hopper Dredge (TSHD)

A *Trailing Suction Hopper Dredge* is a self-propelled vessel that trails a drag-head across the seafloor while in transit. The suction pipe or drag-head pumps the excavated material, which is deposited into one or more hoppers in the vessel. When the hoppers are full, the TSHD travels to a discharge area to offload the material either by pumping it out or by releasing the load through gates located in the hull. A THSD is effective in removing loose material, but is less effective at removing harder substrates (Richardson et al., 1995; Reine et al, 2014; Thomsen et al., 2009; Todd et al., 2015; Genesis, 2011).

The main sources of noise in a TSHD include the inboard and underwater pump, drag-head excavation, pumped substrate hitting the pipe interior, vessel sounds related to propeller, thruster and machinery, hopper loading and offloading and support vessels (see Figure 5.5). Pump sounds occur intermittently during dredging and discharge. Much of the radiated sound is originated in the propeller and vessel engine, along with pumps and generators. The intensity of the digging sound produced by the drag-head is relatively low in fine sediments typically found during maintenance dredging (Reine & Clarke, 2014). The aggregate extraction process increases the sound levels above 1 kHz; the transport of the material through the pipe is possibly the major contributing source in this range of frequencies (CEDA, 2011). The sound levels are also dependent on the substrate type; coarser sediments produce the highest sound levels (CEDA, 2011). Propeller cavitation is also an important sound source at high frequencies.

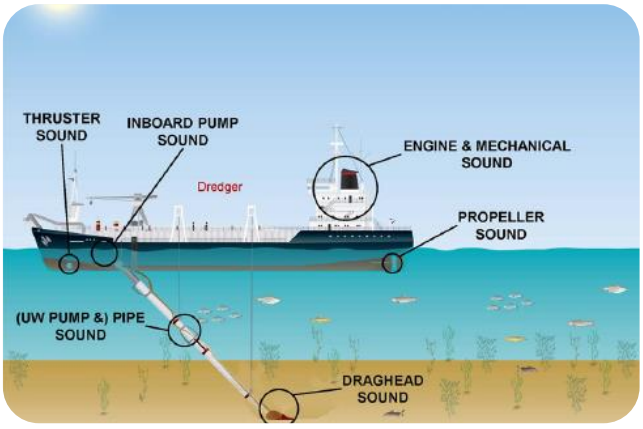

Figure 5.4 Potential sound sources in a trailing suction hopper dredge (from Reine & Clarke, 2014).

The effects of pumping, drag-head excavation and sediment type on the received sound level spectrum are shown in Figure 5.5 and Figure 5.6 (left). The sound produced by a TSHD is mainly continuous and most of the energy is below 1.2 kHz (Reine et al., 2014; see Figure 5.7, left). Some dredging operations may be characterised by a higher dominant frequency (see Figure 5.7, right).

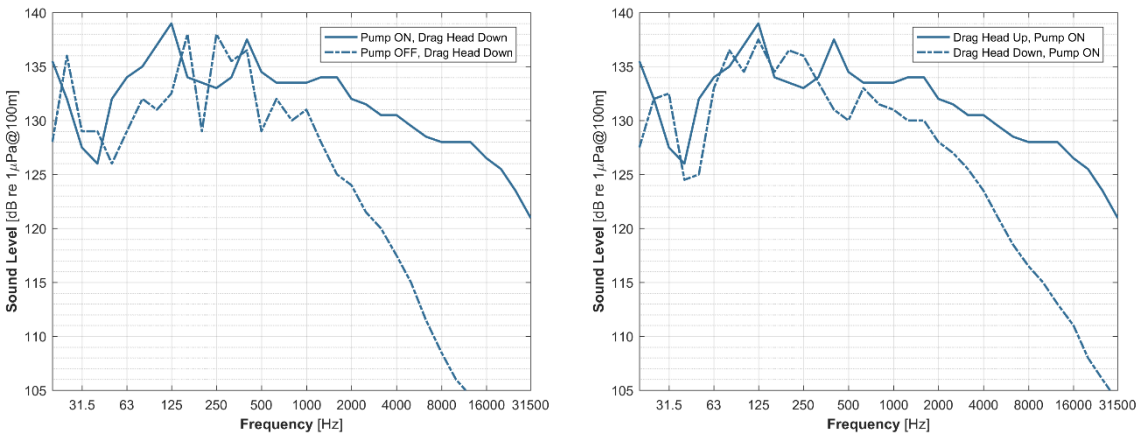

Figure 5.5 Effect of pump (left) and drag-head (right) on the received spectrum of TSHD Sand Falcon (after Theobald et al., 2011).

The acoustic signature results from the combination of various simultaneous sound radiating processes, however the dredging operation can be separated into *excavation* and *transit*. The spectra of the various processes involved in dredging operations are shown in Figure 5.6, right. The spectrogram of a full dredging activity is represented in Figure 5.8.

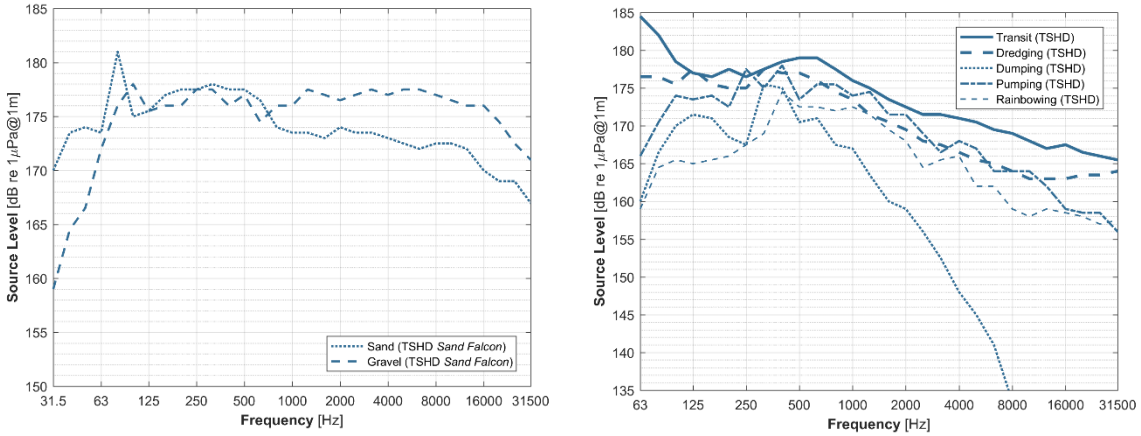

Figure 5.6 Effect of sediment type on the received dredging spectrum (left, after Lepper et al., 2012; Theobald et al., 2011; Robinson et al., 2011) and third-octave band spectra of different activities occurring during dredging operations (right, Jong et al., 2010).

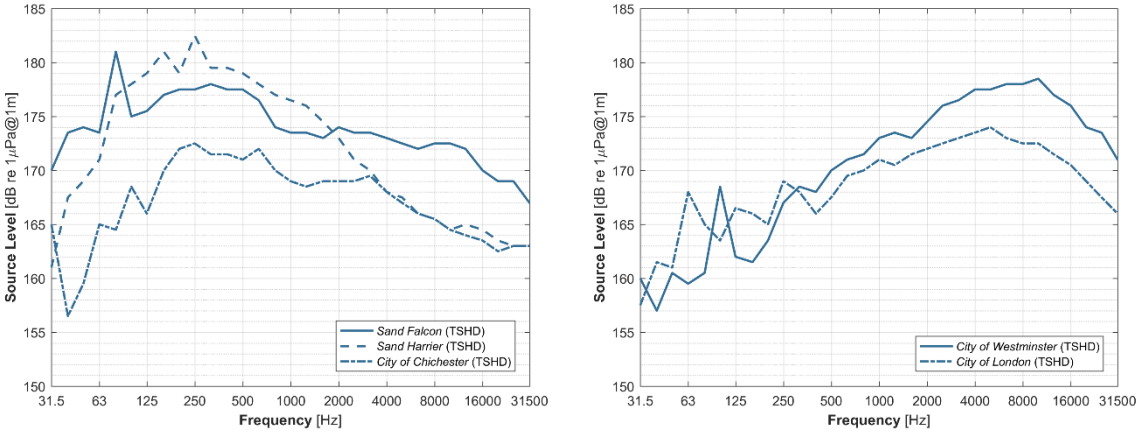

Figure 5.7 Third-octave band spectra for five TSHDs, with predominant low frequency (left) and high frequency (right) content. After Lepper et al., 2012; Theobald et al., 2011; and Robinson et al., 2011.

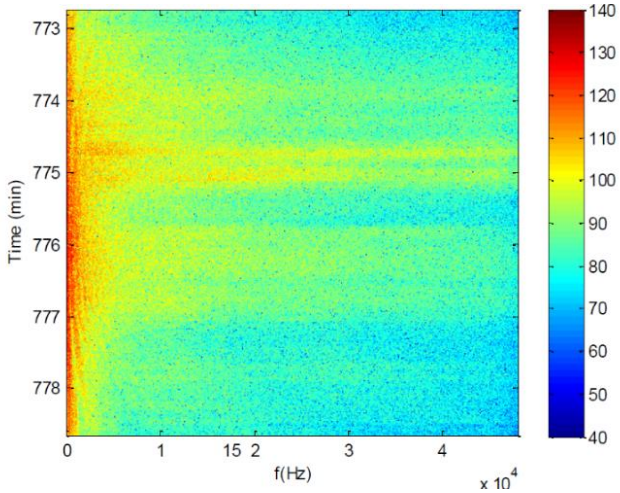

Figure 5.8 Spectrogram of a full dredging activity from TSHD *Sand Falcon* at the closest point of approach (from Robinson, 2015).

5.1.4 Grab Dredge (GD)

A *Grab Dredge* is a mechanical dredging system that uses a crane-operated clamshell bucket to dig into the seabed. The clamshell consists of two buckets that clamp together and close as they reach the seafloor. The grab full of sediment is then raised and the material is deposited into a barge or hopper. Grab dredges come in different forms and most of them use spud poles to move the pontoon and keep position, which allow easy operation over large areas (see Section 5.1.2 "*Cutter Suction Dredge*"). This dredging system is economical, is often used in excavation of bay mud and unconsolidated sediments, and is a good option to reach areas of difficult access. Grab dredges are often called *bucket dredges*, and should not be confused with *Bucket Ladder Dredges* (BLD), which operate in a completely different way (Dickerson et al., 2001; Thomsen et al., 2009; Richardson et al., 1995).

Figure 5.9 Grab dredge *Viking* operating in Cook Inlet, Alaska (from Dickerson et al., 2001).

A grab dredge produces a repetitive sequence of sounds associated to seven separate dredging events: winch lowering, bucket striking the bottom, digging, bucket closing, winch rise, discharge of material into barge and discharge of barge material (Dickerson et al., 2001; see Figure 5.10). The monitoring of sound produced by two grab dredges, the GD *Viking* for capital dredging (see Figure 5.9) and the smaller GD *Crystal Gayle* for maintenance dredging, was conducted in Cook Inlet (Alaska) by Dickerson et al. (2001). Most of the energy content of sounds registered in this study was in the range of 20-1,000 Hz. The acoustic measurements on the grab dredge *Viking* showed that the clamshell striking the seabed produced the most intense sounds within the dredging cycle. The splash caused by the clamshell hitting the water surface could be detected at relatively short distances. The intensity of the sound produced by the sediment discharge varied with the amount of material existing in the barge; the sediment in the barge dampens the sound from additional dumped material, thus an empty barge tends to produce higher sound levels. The clamshell closing resulted in the least intense sounds. The barge emptying occurred less frequently, at intervals of several hours. The characteristics of the excavating sounds also appeared to be greatly influenced by the type of seabed material, and fine unconsolidated sediments resulted in lower radiated sound levels compared to more compacted coarse sediments.

Miles et al. (1987) showed that source levels during the operating cycle of a grab dredge at the 250 Hz 1/3 octave band varied between 150 to 162 dB re 1µPa@1m. The sound associated with the closing of the clamshell contained little energy, but in contrast with the study from Dickerson et al. (2001), the winch rise with the loaded clamshell produced the highest source level within the cycle, with a broadband value of 167 dB re 1µPa@1m. This disagreement between the measurements from Miles et al. (1987) and Dickerson et al. (2001) for the winch phase suggests that poorly maintained gears can generate very intense sounds. Miles et al. (1987) indicated that the sound radiated by the tug and barge used to transfer the material was stronger than the dredging operation itself.

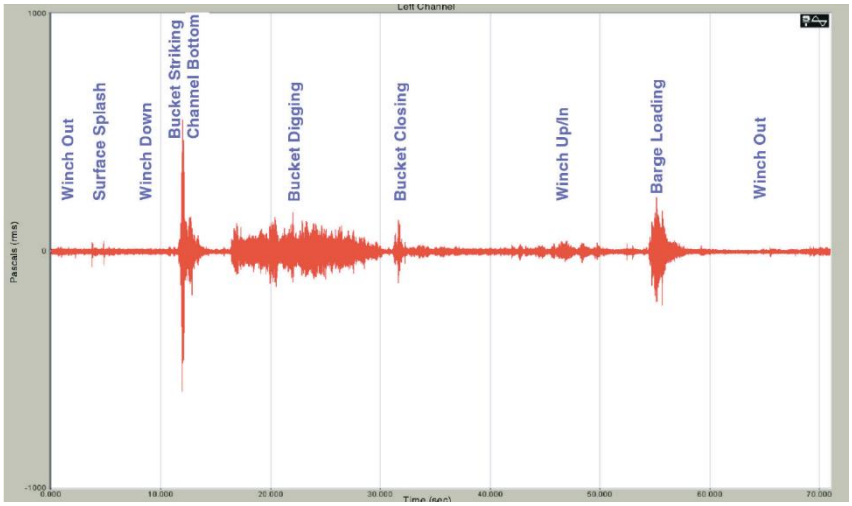

Figure 5.10 Waveform of a typical operating cycle of the grab dredge *Viking*. The noise events within the cycle are described in blue (from Dickerson et al., 2001).

Some additional factors that may have an impact on the radiated sounds include the size of the bucket, the state of the various types of equipment and the skill of the plant operator Dickerson et al. (2001). The characteristics of the dredging sound can vary considerably with the actions of the operator, as these will affect the speed, position and orientation of the bucket as it impacts the seafloor.

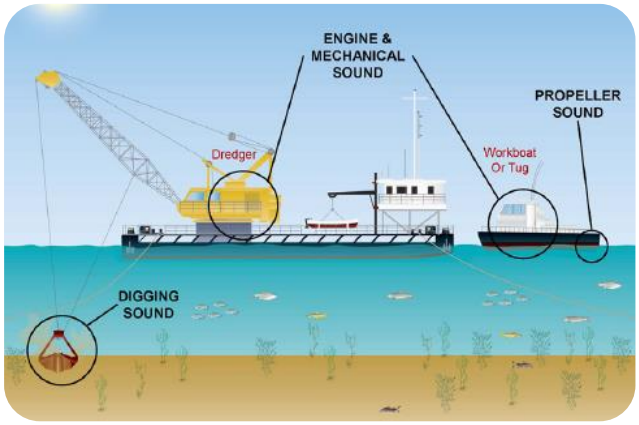

Figure 5.11 Potential sound sources in a grab dredge (from Reine & Clarke, 2014).

5.1.5 Bucket Ladder Dredge (BLD)

A *Bucket Ladder Dredge*, sometimes called a bucket dredge, is a mechanical dredging system that uses a set of buckets on a circulating chain to scrape the seafloor. The removed material is carried to the surface and deposited inside the dredge. The BLD is moored in place with anchors and is suitable for most substrates with the exception of rock. The BLD is one of the older forms of dredger (Thomsen et al., 2009; Genesis, 2011). No studies about the acoustic output of this type of dredge have been found.

Figure 5.12 Bucket ladder dredge during operation (from static.wixstatic.com).

5.1.6 Backhoe Dredge (BHD)

A *Backhoe Dredge* is a mechanical dredging system similar to a *Grab Dredge*, but instead of a crane-operated clamshell it uses a *backhoe* or hydraulic articulated arm ended in an open bucket, which is operated from the rear of the vessel. The excavated material is normally deposited in barges. The vessel is normally equipped with spud poles for anchoring and movement.

In a study published by Reine & Clarke (2014), the sounds produced by a CSD and a BHD in the shallow waters (< 15 m) of New York Harbour for the Harbour Deepening Project were presented. The hydraulic dredge, *Florida*, was used for rock fracturing, whereas the mechanical dredge *New York* was used to remove the fractured rock left by *Florida*. The source levels produced by the BHD *New York* for six distinct acoustic sources were presented: the onboard engine/generator, bucket bottom impact and excavation, hydraulic ram operation, barge loading, anchoring and walking spuds, and an unidentified popping noise clearly related to the dredging operation. The excavation and bucket impact produced the most intense sounds, followed by the operation of the spud poles. The loading of the barge may or may not produce detectable sounds, depending on the amount of sediment accumulated in the barge, which provides a damping mechanism to the dumped material. The source levels are summarised in Tab. 5.1.

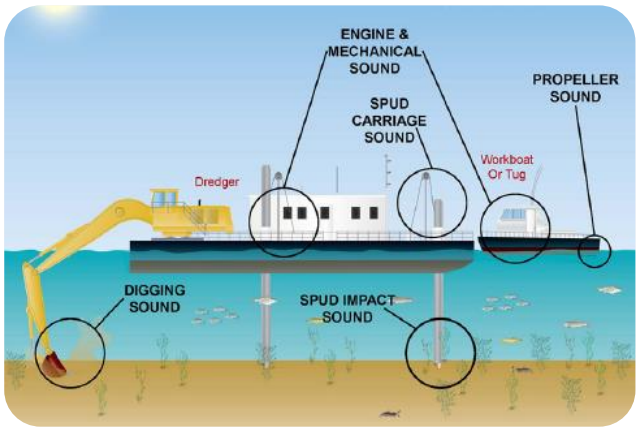

Figure 5.13 Potential sound sources in a backhoe dredge (from Reine & Clarke, 2014).

Table 5.1 Sounds produced by dredging activities: Cutter Suction Dredges

Dredge (*Name/ID*)	h_w [m]	Sediment	Dredge Activity	Measurement [dB re 1µPa$_{rms}$]	SL [dB re 1µPa@1m]	Signal Characteristics	Regression Equation	Description	Reference
Dredges (General)	N/A	Sand to gravel	Dredging	N/A	168-186 dB_{rms}	FR = 30 - 20k Hz	N/A	N/A	Götz et al., 2009
CSD (General)	N/A	N/A	Dredging	N/A	172-185 dB_{rms}	FR = 30 - 20k Hz Main energy 100 - 500 Hz	N/A	N/A	Cluster Maritime Français, 2014
CSD (*Beaver Mackenzie*)	13	N/A	Dredging	133 dB_{rms} @ 190 m [a]	157.1 dB_{rms} [b]	Tones at 1604 and 1678 Hz	RL_{rms} = 157.1 -10log_{10}r - 1.2·10^{-3}r	Aggregate extraction in Alaskan waters Transfer dredger, 86.5 m long Transfer capability 60-10^5 m^3/day Area: Beaufort Sea, N Tuktoyaktuk Broadband level 20-1000 Hz [a] z_r = 9 and 13 m [b] z_r = 9 m	Greene, 1987
CSD (*Aquarius*)	46	N/A	Dredging	140 dB_{rms} @ 200 m [a]	167.6 dB_{rms} [b] 165.3 dB_{rms} [c]	Tones at 171 and 423 Hz	RL_{rms} = 167.6 -12log_{10}r - 6.25·10^{-4}r RL_{rms} = 165.3 -10.2log_{10}r -3.51·10^{-4}r	Aggregate extraction in Alaskan waters Transfer dredger Transfer capability 10^5 m^3/day Area: Beaufort Sea, N Tuktoyaktuk Broadband level 20-1000 Hz [a] z_r = 3 and 18 m [b] z_r = 3 m [c] z_r = 9 and 18 m	Greene, 1987
CSD (*JFJ de Nul*)	9	N/A	Dredging	N/A	182.9 dB_{rms}	N/A	N/A	Large TSHD, hopper size 18000 m^3 Broadband level 31.5-10k Hz 1/3 oct	Hannay et al, 2004; Ainslie et al, 2009
CSD (*Florida*)	<15	Mixture of cobbles, pebbles, silt and clay	Rock fracturing (limestone)	151 dB_{rms} @ 152 m, 300 Hz [a] 151 dB_{rms} @ 100 m, 300 Hz [b]	175 dB_{rms}	N/A	RL_{rms} = 175 -15log_{10}r	Dredging for navigation channel maintenance and deepening project Dredge CSD *Florida*: 450 t, 159 m long, 18 m beam, 4.3 m draft Area: New York Harbour, USA z_r = [a]3 m, [b]9 m [a,b] maximum 1/3 oct band level within 20-20k Hz	Reine & Clarke, 2014

Table 5.1 Sounds produced by dredging activities (cont., part 2): Trailing Suction Hopper Dredges

Dredge (*Name/ID*)	h_w [m]	Sediment	Dredge Activity	Measurement [dB re 1µPa$_x$]	SL [dB re 1µPa@1m]	Signal Characteristics	Regression Equation	Description	Reference
TSHD (General)	N/A	N/A	Dredging	N/A	186-188 dB_{rms}	FR = 30 - 20k Hz Main energy 100 - 500 Hz	N/A	N/A	Cluster Maritime Français, 2014
TSHD (*Cornelis Zanen*)	20	N/A	Loading	142 dB_{rms} @ 930 m [a]	N/A	No distinctive tones	N/A	Aggregate extraction in Alaskan waters Hopper dredger, capacity 8000 m^3. Area: Beaufort Sea, N Tuktoyaktuk z_r = [a]18 m, [b]13 m [a,b] broadband level 20-1000 Hz 1/3 oct. Atenuation of 20 dB/oct above 1 kHz	Greene, 1987
	20	N/A	Underway	127 dB_{rms} @ 2.4 km [a]	N/A	Tone at 55, 278 and 1030 Hz	N/A		
	13	N/A	Pumping	117 dB_{rms} @ 13.3 km [b]	N/A	No distinctive tones	N/A		
TSHD (*Geopotes X*)	21	N/A	Loading	139 dB_{rms} @ 430 m[a]	N/A	Tone at 480, and 1028 Hz	N/A	Aggregate extraction in Alaskan waters Hopper dredger, capacity 8000 m^3. Area: Beaufort Sea, N Tuktoyaktuk Broadband level 20-1000 Hz 1/3 oct z_r = [a]18 m, [b] 13 m [b] high levels caused by damgaged propeller	Greene, 1987
	25	N/A	Underway	150 dB_{rms} @ 460 m[b]	204.6 dB_{rms}	Tones at 480, 811 and 1006 Hz	RL_{rms} = 204.6 - 20.9$\log_{10}$r - 8·10^{-4}r		
TSHD (*Gateway*)	12	N/A	Dumping load	131 dB_{rms} @ 1.5 km	N/A	No distinctive tones, LF dip below 200 Hz due to water depth	N/A	Aggregate extraction in Alaskan waters Hopper dredger, capacity 6000 m^3. Area: Beaufort Sea, N Tuktoyaktuk Broadband level 20-1000 Hz 1/3 oct z_r = 9 m	Greene, 1987
TSHD (*Taccola*)	N/A	N/A	Dredging	N/A	180.4 dB_{rms}	N/A	N/A	TSHD, small version of *Gerardus Mercator*, capacity 4,400 m^3 Broadband level 10-2k Hz 1/3 oct	Hannay et al, 2004
TSHD (*Gerardus Mercator*)	33	N/A	Dredging	N/A	188.3 dB_{rms}	N/A	N/A	Large TSHD, hopper size 18000 m^3 Broadband level 10-10k Hz 1/3 oct	Hannay et al, 2004; Ainslie et al, 2009
TSHD (from 7 dredges)	20	Medium sand	Transit	N/A	192.7 dB_{rms}	N/A	N/A	Broadband source level calculated from 31.5 - 40k Hz 1/3 oct spectrum. NOTE: Band spectrum estimated by de Jong et al from measurements of each dredge and activity using Urick's source image model (Urick, 1983). Spectrum for each activity is the upper envelope of all 7 dredges.	de Jong et al, 2010
			Dredging	N/A	190.6 dB_{rms}	N/A	N/A		
			Dumping	N/A	182.1 dB_{rms}	N/A	N/A		
			Pumping	N/A	186.7 dB_{rms}	N/A	N/A		
			Rainbowing	N/A	182.5 dB_{rms}	N/A	N/A		
TSHD (*Sand Falcon*)	25-45	Sand to gravel	Full dredging (draghead dragging, pumping water, sand and gravel)	148.2 dB_{rms} @ 100 m	N/A	N/A	N/A	Dredging for aggregate extraction Area: UK waters, East coast region and East English channel. Broadband level from 20-40k Hz 1/3 oct spectrum z_r = 6.5 - 10 m from sea surface	Theobald et al., 2011
	25-45	Sand to gravel	Pumping water (draghead lifted, all pumps running)	146 dB_{rms} @ 100 m	N/A				
	25-45	Sand to gravel	Pump off (draghead dragging, no pumps running)	145.8 dB_{rms} @ 100 m	N/A				

Table 5.1 Sounds produced by dredging activities (cont., part 3): Trailing Suction Hopper Dredges

Dredge (*Name/ID*)	h_w [m]	Sediment	Dredge Activity	Measurement [dB re 1µPa$_{rms}$]	SL [dB re 1µPa@1m]	Signal Characteristics	Regression Equation	Description	Reference
TSHD (*Arco Axe*)	<45	Sand to gravel	Dredging	N/A	176.8 dB_{rms} [a]	173.9 dB_{rms} @ 1 m, 31.5-1k Hz [b] 173.6 dB_{rms} @ 1 m, 1.25-40 kHz [c]	SL spectrum calculated with image source model and dipole approximation.	*Arco Axe:* 98.3 m, 2890 m3, 2940 kW Aggregate extraction in UK waters Vessel f < 1 kHz, dredge > 1kHz [a]Broadband level 31.5-40k Hz 1/3 oct. (L_{bb}) [b,c]LF/HF band levels (L_{lf}, L_{hf}) NOTE: $L_{bb} = 10\log_{10}(10^{Llf/10} + 10^{Lhf/10})$	Lepper et al., 2012; Theobald et al., 2011; Robinson et al., 2011
TSHD (*Sand Falcon*)	25-45	Sand	Dredging	N/A	189.8 dB_{rms} [a]	188.5 dB_{rms} @ 1 m, 31.5-1k Hz [b] 184 dB_{rms} @ 1 m, 1.25-40 kHz [c]	SL spectrum calculated with image source model and dipole approximation.	*Sand Falcon: 120 m, 4832 m3, 2x2460 kW* Aggregate extraction in UK waters Vessel f < 1 kHz, dredge > 1kHz [a]Broadband level 31.5-40k Hz 1/3 oct. (L_{bb}) [b,c]LF/HF band levels (L_{lf}, L_{hf}) NOTE: $L_{bb} = 10\log_{10}(10^{Llf}/10 + 10^{Lhf}/10)$	
	25-45	Gravel	Dredging	N/A	190.9 dB_{rms} [a]	187.4 dB_{rms} @ 1 m, 31.5-1k Hz [b] 188.3 dB_{rms} @ 1 m, 1.25-40 kHz [c]			
TSHD (*Sand Harrier*)	<45	Sand to gravel	Dredging	N/A	190.7 dB_{rms} [a]	190.1 dB_{rms} @ 1 m, 31.5-1k Hz [b] 181.7 dB_{rms} @ 1 m, 1.25-40 kHz [c]	SL spectrum calculated with image source model and dipole approximation.	*Sand Harrier:* 99 m, 2700 m3, 3824 kW Aggregate extraction in UK waters Vessel f < 1 kHz, dredge > 1kHz [a]Broadband level 31.5-40k Hz 1/3 oct. (L_{bb}) [b,c]LF/HF band levels (L_{lf}, L_{hf}) NOTE: $L_{bb} = 10\log_{10}(10^{Llf/10} + 10^{Lhf/10})$	
TSHD (*City of Chichester*)	<45	Sand to gravel	Dredging	N/A	183.3 dB_{rms} [a]	181.5 dB_{rms} @ 1 m, 31.5-1k Hz [b] 178.7 dB_{rms} @ 1 m, 1.25-40 kHz [c]	SL spectrum calculated with image source model and dipole approximation.	*City of Chichester: 72 m, 1418 m3, 2720 kW* Aggregate extraction in UK waters Vessel f < 1 kHz, dredge > 1kHz [a]Broadband level 31.5-40k Hz 1/3 oct. (L_{bb}) [b,c]LF/HF band levels (L_{lf}, L_{hf}) NOTE: $L_{bb} = 10\log_{10}(10^{Llf/10} + 10^{Lhf/10})$	
TSHD (*City of Westminster*)	<45	Sand to gravel	Dredging	N/A	188.6 dB_{rms} [a]	179.6 dB_{rms} @ 1 m, 31.5-1k Hz [b] 188 dB_{rms} @ 1 m, 1.25-40 kHz [c]	SL spectrum calculated with image source model and dipole approximation.	*City of Westminster: 99.7 m, 2999 m3, 4080 kW* Aggregate extraction in UK waters Vessel f < 1 kHz, dredge > 1kHz [a]Broadband level 31.5-40k Hz 1/3 oct. (L_{bb}) [b,c]LF/HF band levels (L_{lf}, L_{hf}) NOTE: $L_{bb} = 10\log_{10}(10^{Llf/10} + 10^{Lhf/10})$	
TSHD (*City of London*)	<45	Sand to gravel	Dredging	N/A	184.9 dB_{rms} [a]	179.1 dB_{rms} @ 1 m, 31.5-1k Hz [b] 183.6 dB_{rms} @ 1 m, 1.25-40 kHz [c]	SL spectrum calculated with image source model and dipole approximation.	*City of London: 99.9 m, 2652 m3, 4080 kW* Aggregate extraction in UK waters Vessel f < 1 kHz, dredge > 1kHz [a]Broadband level 31.5-40k Hz 1/3 oct. (L_{bb}) [b,c]LF/HF band levels (L_{lf}, L_{hf}) NOTE: $L_{bb} = 10\log_{10}(10^{Llf/10} + 10^{Lhf/10})$	

Table 5.1 Sounds produced by dredging activities (cont., part 4): Grab Dredges and Back Hoe Dredges

Dredge (*Name/ID*)	h_w [m]	Sediment	Dredge Activity	Measurement [dB re 1µPa$_{rms}$]	SL [dB re 1µPa@1m]	Signal Characteristics	Regression Equation	Description	Reference
GD (*Viking*)	<50	Coarse sand and/or gravel	Winch in/out	116.6 dB_{rms} @ 158 m, 35 Hz	N/A	N/A	N/A	Navigation channel deepening project Bucket (clamshell) dredger Area: The Cook Inlet, Alaska Measured values at each dredge activity represent the maximum RMS level in the calibrated spectra, at the given frequency (44.1 kHz sampling rate, 2^{15} FFT points). Note these are not broadband levels	Dickerson et al, 2001; Jones & Marten, 2016
			Bucket bottom contact	124 dB_{rms} @ 158 m, 163 Hz	N/A	N/A	N/A		
			Bucket digging	113.2 dB_{rms} @ 158 m, 40 Hz	N/A	N/A	N/A		
			Bucket closing	99.2 dB_{rms} @ 158 m, 316 Hz	N/A	N/A	N/A		
			Loading barge	108.6 dB_{rms} @ 158 m, 82 Hz	N/A	N/A	N/A		
			Empying barge	108.7 dB_{rms} @ 316 m, 46 Hz	N/A	N/A	N/A		
GD (*Crystal Gayle*)	<50	Unconsolidated sediment (mud)	Bucket bottom contact	107 dB_{rms} @ 555 m, 92 Hz	N/A	N/A	N/A	Maintenance at port docks Bucket (clamshell) dredge Area: The Cook Inlet, Alaska Measured values at each dredge activity represent the maximum RMS level in the calibrated spectra, at the given frequency (44.1 kHz sampling rate, 2^{15} FFT points). Note these are not broadband levels	Dickerson et al, 2001; Jones & Marten, 2016
BHD (*New York*)	<15	Mixture of cobbles, pebbles, silt and clay	Between dredging activities	133 dB_{rms} @ 75 m, 125 Hz [a] 134 dB_{rms} @ 135 m, 125 Hz [b]	167 dB_{rms}	Engine/generator noise	RL_{rms} = 167 -15log_{10}r	Dredging for navigation channel maintenance and deepening project Dredge backhoe *New York*: 61 m long, 17 m beam, 2.1 m draft Area: New York Harbour, USA z_r = [a]3 m, [b]9 m [a,b] maximum 1/3 oct band level within 20-20k Hz.	Reine & Clarke, 2014
			Bottom impact and excavating fractured rock and gravel left by CSD *Florida*	137 dB_{rms} @ 60 m, 315 Hz [*a] 148 dB_{rms} @ 60 m, 315 Hz [b]	179 dB_{rms}	Dredge bottom impact and excavation noise	RL_{rms} = 179 -15log_{10}r		
			Barge loading	139 dB_{rms} @ 60 m, 100 Hz [a] 139 dB_{rms} @ 60 m, 100 Hz [b]	166 dB_{rms}	Barge loading noise	RL_{rms} = 166 -15log_{10}r		
			Pre/after excavation	133 dB_{rms} @ 60 m, 2.5 kHz [a] 138 dB_{rms} @ 60 m, 2.5 kHz [b]	164 dB_{rms}	Hydraulic ram noise	RL_{rms} = 164 -15log_{10}r		
			During excavation	140 dB_{rms} @ 60 m, 250 Hz [a]	167 dB_{rms}	Unidentified popping noise	RL_{rms} = 167 -15log_{10}r		
			Anchoring spuds	136 dB_{rms} @ 75 m, 1.2 kHz [a] 138 dB_{rms} @ 220 m, 1.2 kHz[b]	173 dB_{rms}	Noise from anchoring spuds	RL_{rms} = 173 -15log_{10}r		
			Walking spuds	147 dB_{rms} @ 75 m, 200 Hz [a] 137 dB_{rms} @ 210 m, 200 Hz [b]	176 dB_{rms}	Noise from walking spuds	RL_{rms} = 176 -15log_{10}r		

5.2 Drilling

The facilities used for offshore drilling can be classified in three main groups: 1) *islands*, which can be natural or man-made (artificial and caisson); 2) *platform standing on legs*, including fixed platforms and jack-up rigs; and 3) *drilling vessel*, including semi-submersibles and drill ships (Richardson et al., 1995; Götz et al., 2009). The most common type of mobile drilling platform is the jack-up rig, with 363 vessels operating worldwide compared to the existing 169 semi-submersibles and 50 drill ships (Genesis, 2011). Drill rigs are very large structures, of the order of 100 m each side. The selection of the facility depends on water depth, oceanography, ice cover, required duration for the activities planned for the platform and other factors. The operation and acoustic characteristics of the main types of offshore drilling facilities are described in the following sections.

The main sources of sound in a drilling platform include: 1) *machinery and drilling equipment*, including pumps, compressor and generators; 2) *drilling on the seabed*, during drilling the turntable will operate and the machinery will work at higher power; 3) *dynamic positioning thrusters*, used for positioning, can generate high cavitating noise (see Chapter 4 "Vessels"); and 4) *aircraft and vessel support*, generally from powerful vessels equipped with dynamic positioning thrusters (Genesis, 2011). The sound produced by drilling is continuous and its level is typically quoted as RMS. During drilling, low-frequency tonal components are generated, including infrasonic tones in some cases.

5.2.1 Fixed Platforms

The platform deck in *fixed platforms* is installed on top of a jacketed platform built on concrete or steel legs anchored directly onto the seabed, or even on top of a spar, tension leg platform (TLP) or gravity structure. The platform deck contains the drilling rig, production facilities and crew quarters. The drilling rig is not a permanent part of the fixed structure, but it can be left on the platform for future drilling or for cost reasons. The size of a drilling platform depends on the oil field and machinery required for production.

Fixed platforms are immobile, unlike jack-up rigs, semi-submersibles or drill ships. As a result of their immobility, these platforms are designed for long term use to drill new development wells. In shallow water, jack-up rigs are a more economical solution (see Subsection 5.2.2, "Jack-up Rigs"); in deeper waters and for depths up to about 500 m fixed platforms are economically feasible.

Figure 5.14 Conventional jacket (left) and spar (right) fixed drilling platforms

Sound produced from fixed drilling platforms is relatively unstudied. A study from Gales (1982) on one drilling platform and three combined drilling/production platforms suggests that fixed drilling platforms may not be very noisy, and their sound levels are apparently somewhere in between those from drill vessels and islands (Richardson et al., 1995; Götz et al., 2009). The strongest tones in all platforms were found near 5 Hz, with sound levels of 119-127 dB_{rms} from near field measurements; the highest tone occurred at 1.2

kHz. One of the reasons that may explain why fixed platforms produce relatively low levels compared to drill vessels and semi-submersibles is that all the machinery is located above the water (Genesis, 2011).

5.2.2 Jack-Up Rigs

Jack-up rigs are moveable, non-self-propelled drilling facilities anchored using a set of three large open-truss legs or *spudcans*. The platform deck floats on the sea surface allowing it to be towed by tugs to the drill location. When the drill position is reached, the spudcans are lowered until they make firm contact with the seabed and the platform rises above the sea surface. The platform deck contains the drilling equipment, machinery and crew quarters. Jack-up rigs are used in shallower waters than fixed platforms, typically up to 100 m.

The only study available on sounds generated by jack-up rigs was produced by Erbe and McPherson (2017). In their paper, Erbe and McPherson report sound levels for drilling and standard penetration testing (SPT) carried out from jack-up rig *Sideson II* during geotechnical site investigations in two different locations in Western Australia. Maximum recorded broadband source levels for drilling and SPT were 145 and 160 dB re 1µPa @1m (RMS, 90% energy window), respectively. For details, see Table 5.2, part 4.

Figure 5.15 Plan view (left, from www.ogj.com) and lateral view (right, from www.pvdrilling.com) of two jack-up drilling rigs.

5.2.3 Artificial Islands

An *artificial island* is man-made rather than formed by natural means. Artificial islands have been used since the seventieth century for coastal defence against invading armies (Karam, 2015) but remain extremely rare for drilling. These islands are built with sand extracted from the seabed in a different location with dredging techniques. Artificial islands can be constructed in waters of maximum depths of 70 m; in deeper waters the large amount of required sediment, and the associated cost and environmental implications, make artificial islands impracticable.

The main advantages of artificial islands for exploratory drilling are summarised in the following points (Karam, 2015):

- Easy to combine gathering pipelines on the island with pipeline network on land
- In situ treatment of waste, including oil, drilling mud, chemicals, etc.
- Reducing turbidity and acoustic pollution
- Personnel lives and works in the island, reducing travelling time and costs
- Safer working environment
- Increased number of potential wells
- No need for decommissioning

In natural or man-made islands, sound from the drill rig is poorly transmitted into the water. The transmitted sound is low in frequency and source levels are rather low (~145 dB re 1µPa@1m), making the radiated sound inaudible at ranges beyond a few kilometres (Richardson et al., 1995; Götz et al., 2009). In a study from Blackwell et al. (2004) the maximum broadband sound level was 124 dB re 1µPa@1 km (see Table 5.2 for details). Drilling sound from icebound islands has low source level and is generally confined to low frequencies (Richardson et al., 1995); a study from Malme & Mlawski (1979) on sounds produced by two icebound gravel islands, natural and man-made, in Prudhoe Bay (Alaska) showed that most of the acoustic energy was below 200 Hz. Sound produced by drilling activities in islands varies considerably with ongoing operations (Richardson et al., 1995).

During winter in shallow arctic waters drilling may be done from ice pads resting on the bottom and artificially thickened by pumping water on their surface. In these type of installations sound does not propagate far; in a 6-7 m water column, drilling sound was attenuated rapidly from 125 dB@130 m to 85 dB@2,000 m (Richardson et al., 1995).

Figure 5.16 Artificial drilling and production island Northstar in open water (left, from www.wikipedia.org) and icebounded (right, from oilrig-photos.com)

5.2.4 Caissons

An alternative method to build an artificial island, different than the direct accumulation of sand or gravel, consists of using a watertight shaping structure know as *caisson*. There are three main types of caissons: *Caisson Retained Island* (CRI), *Concrete Island Drilling System* (CIDS) and *Single-Steel Drilling Caisson* (SSDC).

A *Caisson Retained Island* (CRI) is a platform for exploratory drilling consisting of four to eight steel caissons, which form the outer perimeter of the island. The CRI system is composed of three structural elements: the base or *berm*, the steel retaining structure or *caisson ring*, and the sand core. The ring of caissons is ballasted down onto the bottom foundation or berm and the interior of the ring is filled with dredged sand or gravel. Each steel caisson weighs several thousand tonnes when fully ballasted. The drill rig and support facilities are installed on the sand core as on a conventional island.

The development of the CRI took place as exploration activities moved into areas with scarce seabed material, where sacrificial-beach islands are impracticable. Oil exploration in the shallow waters of the Beaufort Sea made use of temporary artificial islands since 1973. Caisson islands are designed to resist the forces of ice and the effects of summer storm waves; these artificial islands operate throughout the year, in contrast to the seasonal limitation of drill ships and jack-up rigs. An additional advantage of CRI is the requirement of significantly less sand than conventional artificial islands. The caisson can also be detached to be used in another location (Mancini et al., 1983; Der, 1983; Comyn, 1984; Richardson et al., 1995).

Figure 5.17 Caisson-retained island *Tarsuit* at different stages. Ballasted ring caisson and beginning of dredged sand infill (left) and completed island with drill in operation under full ice cover (right). From www.bittner-shen.com)

A *Concrete Island Drilling System* (CIDS) is a self-contained, mobile island floated into place and ballasted down onto a subsea berm or *Steel Mud Base* (SMB). The Concrete Basic Brick (CBB) is the central module that sits on top of the SMB and is directly exposed to the extreme environmental conditions of the arctic. The top module is the Deck Storage Barge, which comprises the Integrated Drilling Unit (IDU), living quarters and storage. Examples of CIDS are the *Molikpaq* and *Glomar*, the last one depicted in Figure 5.18.

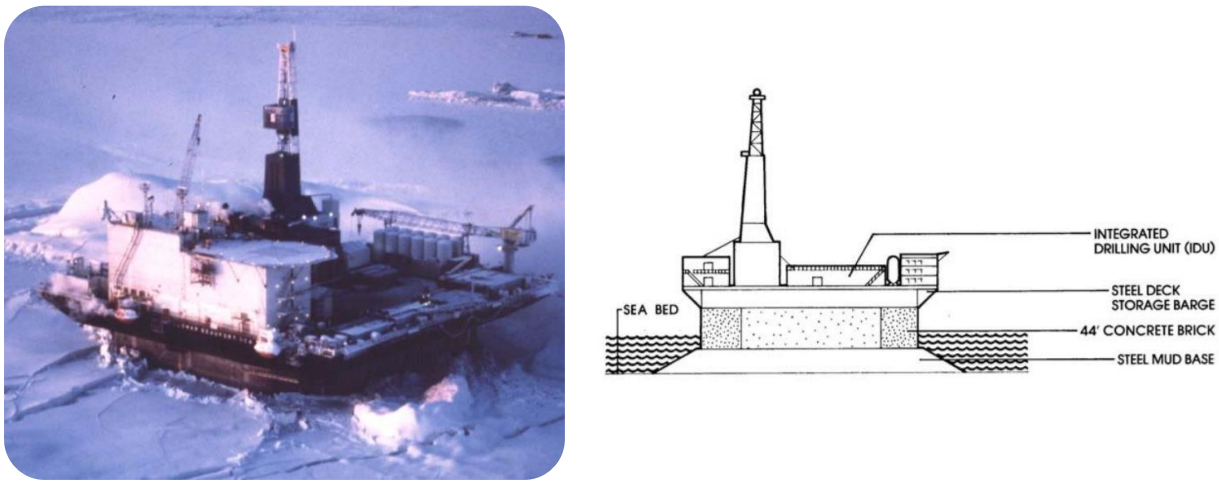

Figure 5.18 Concrete island drilling system *Glomar Beaufort 1* (aka *Orlan*) under severe ice pressure conditions (left) and diagram of its structural elements (right). From www.precastdesign.com

The *Single-Steel Drilling Caisson* (SSDC) is an ice-resistant, mobile offshore drill facility converted from an old oil tanker in the 1980s, the *World Saga*, purchased by Canadian Marine Drilling and renamed as *Canmar*. The hull of the SSDC consists of the forward two thirds of the original tanker and is used as a submersible barge, on top of which is installed the drill rig. The barge acts as an artificial steel berm when ballasted with water onto the seafloor. The system has six Caterpillar 1,000 hp diesel generators, and is not self-propelled so it has to be towed to location. The SSDC can drill a well to a maximum depth of 7,600 m. This type of drill barge was designed for exploratory drilling in the shallow, ice-covered waters of the Beaufort Sea, to overcome the limitations of the other offshore drilling solutions, such as the limited station keeping ability of drill ships of the expensive and time consuming relocation of CRI and CIDS.

Figure 5.19 Single steel drilling caisson *Canmar* (from www.yergens.net)

Little data exists on sounds produced by these three types of caisson drilling facilities, but are apparently intermediate between those from drill-ships and conventional artificial islands. Greene (1987) presented sound measurements from a caisson-retained island (CRI), and the broadband source levels (20-1,000 Hz) appeared to be much higher than those from artificial islands but lower than those from drill-ships. During open water conditions, sound is better transmitted into the water than at artificial islands, resulting in higher sound levels (Richardson et al., 1995, see also Table Main). Hall & Francine (1991) measured sounds from the self-contained concrete drilling caisson *Glomar*, which showed that the radiated energy above 30 Hz was relatively low, and after including infrasonic components sound levels increased in about 15 dB; a strong tone near 1.4 Hz was attributed to the rotation rate of the drilling turntable (Richardson et al., 1995). Gallagher et al. (1992) measured sounds produced by the single-steel drilling caisson *Canmar* during drilling operation in 15 m waters with 100% ice cover. Although the tonal component associated to the rotation rate of the drilling turntable (1.5 Hz) was detected with an accelerometer, it did not appear in the sound pressure measurements and the drilling sound was several decibels higher at sonic frequencies (Richardson et al., 1995).

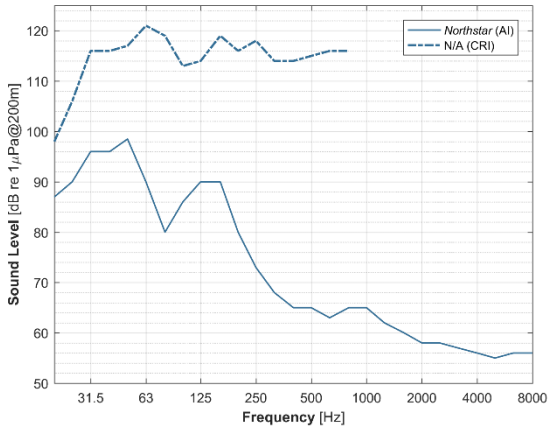

Figure 5.20 Third-octave band sound level spectra at 200 m from the artificial gravel island *Northstar* (from Blackwell et al., 2004) and a caisson retained island (from Greene, 1987).

5.2.5 Semi-Submersibles

A *semi-submersible* is a mobile floating platform supported on large pontoons submerged in water. The pontoons are filled with water until they reach the desired depth. They can be anchored by six to twelve anchors tethered by chains and wire cables or kept in place using dynamic positioning. The deck is elevated more than 30 m above the pontoons and supported on large steel columns. Semi-submersibles can operate in a wide range of depths, from 60 to 3,000 m, and are frequently used for drilling new wells. These systems are reliable in rough seas.

Figure 5.21 Self-propeller semi-submersible drilling rig MOSS CS-50 Mk II *Polyarnaya Zvezda* (left, from www.oaoosk.ru) and diagram of a deep-water semi-submersible (right, from www.glossary.oilfield.slb.com)

Unlike in a drill ship, in a semi-submersible there is no direct contact between the hull and the water. The deck remains several metres above the water surface, which means that the only transmission paths of sound and vibration produced by machinery and deck activity are the air or the steel risers (Richardson et al., 1995).

Greene (1986) measured sounds produced by the semi-submersible drill rig *SEDCO 708* during drilling operations near the Aleutian Islands, in the Bering Sea, in water depths of 114 m. The broadband source level in the range of 80-4k Hz with the hydrophone at 30 m depth was 155 dB re 1µPa@1 m. Several tonal components were present, which varied depending on the operating speed of the drill rig; the only stable tonal components were associated to the 60 Hz alternating electric current and potential harmonics at 181 and 301 Hz.

McCauley (1998) measured sounds produced by the exploratory drilling semi-submersible *Ocean General* in the Timor Sea during drilling and non-drilling periods. A broadband sound level of 117 dB re 1µPa@125m was reached during drilling, 4 dB higher than during the non-drilling period.

Nedwell & Edwards (2004) published sound measurements from the semi-submersible drilling rig *Jack Bates* in deep waters northwest the Shetland Islands for three different operational stages: plant operation, dynamic positioning and drilling. Dynamic positioning generated a source level of 188 dB@1m, 12 dB higher than drilling and 29 dB higher than plant operation. Drilling caused an increase of 10 to 20 dB in the band of 20-500 Hz and clear tonal components appeared at about 130, 200, 350 and 600 Hz, probably produced by cutting forces from the seabed or driving forces from the machinery. Thrusters contributed to increase the radiated acoustic energy in the band of 2-30 Hz.

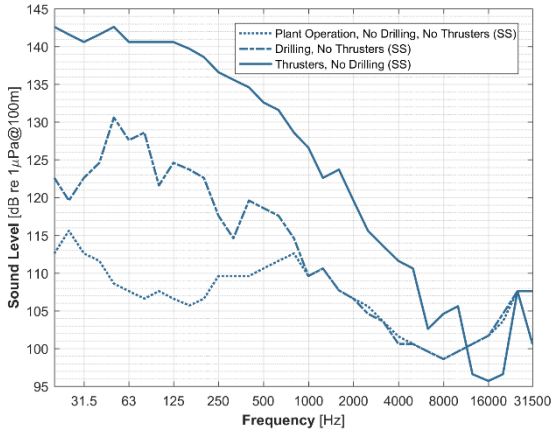

Figure 5.22 Third-octave band sound level spectra at 200 m from semi-submersible drill rig *Jack Bates* for three operating phases: plant operation, drilling and dynamic positioning (after Nedwell & Edwards, 2004).

5.2.6 Drill Ships

A *drill-ship* is a self-propelled vessel outfitted with a drilling unit and kept in position by anchors or dynamic positioning. Purpose-built designs are used today, but in the early years drill ships were built from modified tanker hulls. Drill ships are mostly used for exploratory drilling and can reach depths of up to 3,700 m.

Figure 5.23 Conical drilling unit *Kulluk* (left) and drill-ship *West Navion* (right)

The hull of the drill ship is large and remains in direct contact with the water, which provides good acoustic coupling and favours the transmission of machinery vibrations. Drill ship spectra contain tonal components up to 600 Hz attributable to diesel-electric generators, with varying frequency depending on electric load (Richardson et al., 1995). Drill ships are normally noisier than semi-submersibles under similar operating conditions, with source levels as high as 195 dB (Genesis, 2011; Götz et al., 2009; Richardson et al., 1995). Other types of offshore drilling facilities tend to generate lower sound levels and frequencies.

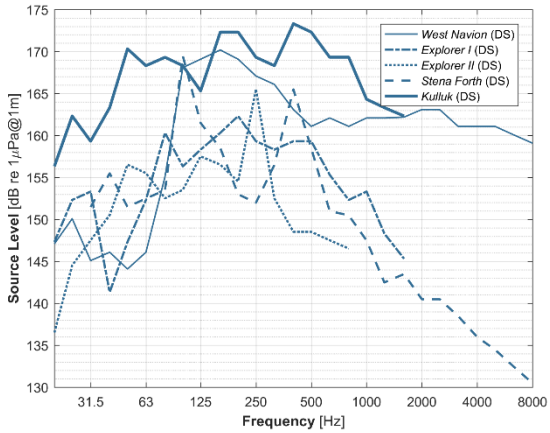

Figure 5.24 Third-octave band source level spectra from five drill ships: *West Navion* (from Nedwell & Edwards, 2004), *Explorer I*, *Explorer II*, circular drill barge *Kulluk* (from Greene, 1987), and *Stena Forth* (from Kyhn et al., 2011).

There exist a few more studies on sounds produced by drill-ships than for the other categories of offshore drilling facilities (Greene, 1987; Nedwell & Edwards, 2004; Kyhn et al, 2011). Sound levels in two converted freighters, the *Canmar Explorer I* and *II*, were significantly higher during drilling than during well-logging (Greene, 1987). Measurements of sounds generated by *Canmar Explorer II* in different years showed that sound levels change with time, probably due to changes in machinery operation (Miles et al., 1987). Greene (1987) also measured drilling sounds from the Conical Drilling Unit (CDU) *Kulluk*, a floating drilling platform specifically designed for arctic waters, which produced a broadband source level of 179.6 dB in the range of 20-1.6k Hz; Hall et al. (1994) reported a source level for *Kulluk* during drilling of 191 dB in the range of 10-10k Hz. The highest reported source levels during drilling operation are those from drill-ship *West Navion*, with a value of 195 dB re 1µPa@1m for the 100-400 Hz band (Nedwell & Edwards, 2004).

Table 5.2 Sounds produced by drilling activities: artificial islands and caissons

Drilling Platform (*Name/ID*)	h_w [m]	Activity	Measurement [dB re 1µPa]	SL [dB re 1µPa@1m]	Signal Characteristics	Regression Equation	Description	Reference
Oil Production Artificial Gravel Island (*Northstar Island*)	12	Drilling	105-115 dB_{rms} @ 200 m[a]	N/A	High energy < 100 Hz due to baseline island sounds (e.g. power generation). High peak at 1 kHz, likely machinery related to drilling operations (not always present)	$RL_{rms} = SL_{rms} - 21.5\log_{10}r$ [b], The high level variability (~30 dB) made it difficult to define a single source level value SL_{rms}	Nabors rig 33E: Drill rig installed E of the artificial gravel island *Northstar* Area: NW Prudhoe Bay, Beaufort Sea Surrounding land-fast ice 1.5 m thick z_r = close to bottom surface of ice layer [a] broadband level 20-8k Hz 1/3 oct [b] broadband level 10-10k Hz	Blackwell et al. 2004
CRI	26	Drilling	128.6 dB_{rms} @ 200 m	185.4 dB_{rms}	N/A	$RL_{rms} = 185.4 - 18.9\log_{10}r - 1.74{\cdot}10^{-4}r$	CRI: octagonal ring of caissons, ballasted down, filled with sand, drill rig on top Area: Beaufort Sea z_r = 18 m Broadband level 20-800 Hz 1/3 oct	Greene, 1987
CIDS (*Glomar*)	16	Drilling	89.7 dB_{rms} @ 1370 m[a] 111.9 dB_{rms} @ 1370 m[b]	N/A	Most energy < 20 Hz Strong tones at 1.4-1.5 Hz caused by rotation of drilling turntable	N/A	CIDS: offshore drilling platform consisting of a 9 m steel footing, 13 m steel and concrete structure and surface deck with the drill rig. Area: Camden Bay, Beaufort Sea [a]broadband level 20-1k Hz, z_r = 12 m [b]broadband level 0.2-1k Hz, z_r = 8 m	Hall & Francine, 1991
SSDC (*Canmar*)	15	Drilling	117 dB_{rms} @ 215 m[a] 119 dB_{rms} @ 115 m[b]	N/A	Dominant tone at 5 Hz. Other tones at 20, 60, 150 and 450 Hz	N/A	*Canmar*: converted 2/3 front section of oil tanker, 162 m long, 53 m wide, 80,000 t drill unit, 6x 1,000 hp diesel generators 100% ice cover [a] broadband level 20-1k Hz [b]at 5 Hz	Gallagher et al, 1992; Richardson et al, 1995

Table 5.2 Sounds produced by drilling activities (cont., part 2): semi-submersibles

Drilling Platform (*Name/ID*)	h_w [m]	Activity	Measurement [dB re 1µPa]	SL [dB re 1µPa@1m]	Signal Characteristics	Regression Equation	Description	Reference
Drilling (General)	N/A	Drilling	N/A	145-190 dB_{rms}	FR = 10 - 10k Hz Main energy < 100 Hz	N/A	N/A	Cluster Maritime Français, 2014; Götz et al., 2009
Semi-Submersible Drill Rig (*Jack Bates*)	N/A	Plant operating (no drilling, thrusters disabled)	124.1 dB_{rms} @ 40 m	159.3 dB_{rms}	For tones within 20-600 Hz	TL = 20·log$_{10}$r	Deep water drilling operations Area: NW Shetlands, z_r = 100 m (under the rig, 40 m from shaft) Broadband level 20-40k Hz 1/3 oct	Nedwell & Edwards, 2004
	N/A	Drilling (thrusters disabled)	136.5 dB_{rms} @ 40 m	176.3 dB_{rms}	Clear tones at 130, 200, 350 and 600 Hz, possibly resulting from resonances of the drill shaft.			
	N/A	Thrusters active (no drilling)	151.9 dB_{rms} @ 40 m	188.4 dB_{rms}	Significant increase in low frequency energy (2-30 Hz) compared to inactive thrusters. Clear tones from blade rate			
Semi-Submersible Drill rig (*Ocean General*)	110	Drilling	115 dB_{rms} @ 405 m 117 dB_{rms} @ 125 m	N/A	Measurements 4 dB higher during drilling period due to tones < 100 Hz. Dominant tones at 31 and 63 Hz 1/3 oct	N/A	*Ocean General*: exploratory dilling rig Area: 160 km NNW Melville Island, Timor Sea	McCauley, 1998
Semi-Submersible Drill rig (*SEDCO 708*)	114	Drilling	118 dB_{rms} @ 185 m[a] 110 dB_{rms} @ 926 m[a] 106 dB_{rms} @ 1852 m[a]	138.2 dB_{rms}[a] 131.7 dB_{rms}[b]	Multiple tones, varying frequency Consistent tones at 60, 181 and 301 Hz from alternate current	[a] RL_{rms} = 138.2 -9.3log$_{10}$r [b] RL_{rms} = 131.7 -10log$_{10}$r - 4·10^{-4}r	*SEDCO 708:* semi-submersible rig with 43 m drill tower, platform 81 m above water and 90 m^2 surface, drill turn rate 100-120 rpm No thrusters operating during drilling z_r = 30 m [a] broadband level 80-4k Hz 1/3 oct [b] 60 Hz tone	Greene, 1986
Semi-Submersible Drill Rig (Polar Pioneer)	46	Excavation of Mudline Cellar (MLC)	141.8 dB_{rms} @ 1 km[a]	193.3 dB_{rms}[a]	Dominant tones < 2 kHz. High-energy, tonal region <100 Hz caused by power generation, engines, pumps and motors. 30% of drilling operations were associated with MLC	Source levels calculated from measurements at 1 km using parabolic equation model for elastic seabed (<2 kHz) and ray tracing code (>2 kHz)	*Context*: offshore exploration drilling (2015) *Area:* Chukchi Sea *Polar Pioneer*: semi-submersible drill unit z_r = 0.3 m above seafloor Measurements include noise contribution from nearby vessels. Lower acoustic output due to main platform detached from water. Broadband levels from 10-32k Hz band MLC excavation[a] produces higher levels than drilling[b] due to the high power operation (8x wider drill bit, more pumping)	Austin et al, 2018
		Drilling	123.3 dB_{rms} @ 1 km[b]	170.1 dB_{rms}[b]	Dominant tones < 2 kHz. Harmonics > 10 kHz. High-energy, tonal region < 100 Hz caused by power generation, engines, pumps and motors. 70% of drilling operation were associated with pilot and conductor hole drilling	Source levels calculated from measurements at 1 km using parabolic equation model for elastic seabed (<2 kHz) and ray tracing code (>2 kHz)		
Semi-Submersible Drill Rig (*West Capricorn*)	2.5k-3k	Dynamic Positioning (DP), DP + Drilling	113-128 @ <1 km[a]	193.3 ± 7 dB_{rms}	Main energy (90%) < 250 Hz Tones at 0.5, 0.8 and 2.5 kHz No tonal components > 2 km Strong short-term sound level variability (< 20 dB in 1 h), medium long-term variability (< 5 dB in several hours)	No overall attenuation with range due to time varying MODU operational conditions, and possible contribution from nearby vessels and reverberation from distant LF seismic pulses. Source level calculation with numerical models for elastic seabed, RAMSGeo (LF) and Bellhop (HF)	*Context*: opportunity sound field mapping during normal operation of MODU. *Area:* north Atlantic *West Capricorn:* 6th gen. semi-submersible, 100 m x 100 m, 8 DP thrusters (2 per corner). Significant vessel activity (oil platform ~ 8 km NE, support vessels < 6 km, survey vessel 3-6 km W, two survey vessels ~10 km SE) *Ambient noise sources*: distant vessels and LF reverberation from remote seismic ops. Potential ~2.5 dB increase for a portion of 1 s segments. z_r = 30 m z_s = 20 m Broadband levels from 20-4k Hz 1/3 oct bands. [a]DP levels. Increase of 3-8 dB during drilling	Jiménez-Arranz et al., 2019

Table 5.2 Sounds produced by drilling activities (cont., part 3): drill ships

Drilling Platform (*Name/ID*)	h_w [m]	Activity	Measurement [dB re 1µPa]	SL [dB re 1µPa@1m]	Signal Characteristics	Regression Equation	Description	Reference
Drill Ship (*West Navion*)	N/A	Drilling	137.7 dB_{rms} @ 500 m	N/A	N/A	N/A	Drillship *West Navion*: 250 m long Deep water drilling operations Area: Hebrides, UK z_r = 100 m Measured broadband levels calculated from 20-40k Hz 1/3 oct spectrum, generated by *reviewer* from PSD spectrum (fig. 5.4a)	Nedwell & Edwards, 2004
	N/A	Drilling	132.3 dB_{rms} @ 1000 m		N/A			
	N/A	Drilling	121.1 dB_{rms} @ 2000 m		N/A			
Drill Ship (*Explorer I*)	17	Well Logging	125.6 dB_{rms} @ 900 m	145.4 dB_{rms}	N/A	RL_{rms} = 145.4 -10.3log_{10}r - 2.54·10^{-4}r Range of validity 0.1-10 km	*Explorer I*: conventional drill ship, converted Liberty freighter, 115 m long, 13137 t displacement, 7x 840 kW diesel engines Area: Beaufort Sea Standby vessels in the vicinity z_r = 9 m Broadband level 20-1.6k Hz 1/3 oct	Greene, 1987
Drill Ship (*Explorer II*)	27	Drilling	133.7 dB_{rms} @ 200 m	158.4 dB_{rms}	N/A	RL_{rms} = 158.4 -10log_{10}r - 9.85·10^{-4}r Range of validity 0.1-10 km Regression equation forced to fit cylindrical spreading	*Explorer II*: sister drill ship, same as *Explorer I* Area: Beaufort Sea Supply boat idling nearby z_r = 9 m Broadband level 20-800 Hz 1/3 oct	Greene, 1987
Drill Ship (*Stena Forth*)	484	Drilling	131.9 dB_{rms} @ 500 m	184 dB_{rms}	Drilling noise detectable for FR = 100 - 10k Hz Peaks at 100 and 400 Hz	RL_{rms} = 184 -20log_{10}r	*Stena Forth*: double hull drillship, 228 m long, 42 m wide, 6x 5.5 MW azimuth thrusters, 16x drill motors, 6x 7430 kW diesel generators Support vessels at drilling site. At least one always present (*Esvagt Connector*) Area: Baffin Bay, Greenland z_r = 90 m Broadband level 31.5-20k Hz	Kyhn et al., 2011
Drill Ship (*Noble Discoverer*)	46	Excavation of Mudline Cellar (MLC)	140.4 dB_{rms} @ 1 km[a]	191.8 dB_{rms}[a]	Dominant tones < 2 kHz. High-energy, tonal region <100 Hz caused by power generation, engines, pumps and motors.	Source levels calculated from measurements at 1 km using parabolic equation model for elastic seabed (<2 kHz) and ray tracing code (>2 kHz)	*Context*: offshore exploration drilling (2012) *Area:* Chukchi Sea *Noble Discoverer*: self-propelled drill ship z_r = 0.3 m above seafloor Broadband levels from 10-32k Hz band MLC excavation[a] produces higher levels than drilling[b] due to the high power operation (8x wider drill bit, more pumping)	Austin et al, 2018
		Drilling	122.7 dB_{rms} @ 1 km[b]	174.9 dB_{rms}[b]	Dominant tones < 2 kHz. Harmonics > 10 kHz. High-energy, tonal region < 100 Hz caused by power generation, engines, pumps and motors.	Source levels calculated from measurements at 1 km using parabolic equation model for elastic seabed (<2 kHz) and ray tracing code (>2 kHz)		
Circular Drill Barge (*Kulluk*)	31	Drilling	137.5 dB_{rms} @ 900 m	179.6 dB_{rms}	N/A	RL_{rms} = 179.6 -13.3log_{10}r - 8.36·10^{-4}r	*Kulluk*: conical drilling unit, 80 m Ø Area: Beaufort Sea Work boat dragging for lost anchors, other boats nearby (significant noise contribution) Ice floes present. z_r = 18 m Broadband level 20-1.6k Hz 1/3 oct	Greene, 1987
	33	Excavation of Mudline Cellar (MLC)	138.9 dB_{rms} @ 1 km[a]	193.0 dB_{rms}[a]	High-energy, tonal region <100 Hz caused by power generation, engines, pumps and motors.	Source levels calculated from measurements at 1 km using parabolic equation model for elastic seabed (<2 kHz) and ray tracing code (>2 kHz)	*Context*: offshore exploration drilling (2012) *Area:* Beaufort Sea *Kulluk*: underwent machinery-vibration isolation and ice-strenghtening of hull with 76mm reinforced steel prior to 2012 and after Greene (1987). Explanation for lower levels. z_r = 0.3 m above seafloor Broadband levels from 10-32k Hz band MLC excavation[a] produces higher levels than drilling[b] due to the high power operation (8x wider drill bit, more pumping)	Austin et al, 2018
		Drilling	117.3 dB_{rms} @ 1 km[b]	168.6 dB_{rms}[b]	Dominant tones < 2 kHz. Harmonics > 10 kHz. High-energy, tonal region < 100 Hz caused by power generation, engines, pumps and motors.	Source levels calculated from measurements at 1 km using parabolic equation model for elastic seabed (< 2 kHz) and ray tracing code (> 2 kHz)		

Table 5.2 Sounds produced by drilling activities (cont., part 4): jack-up drilling rigs

Drilling Platform (*Name/ID*)	h_w [m]	Activity	Measurement [dB re 1µPa]	SL [dB re 1µPa@1m]	Signal Characteristics	Regression Equation	Description	Reference
Jack-Up Drill Rig (*Sideson II*)	7-13	Standard Penetration Testing (SPT)	167 ± 1 dB_{pk} @ 10 m[a] 172 ± 1 $dB_{pk\text{-}pk}$ @ 10 m[a] 154 ± 1 dB_{rms} @ 10 m[a] 151 ± 4 dB_{t25ms} @ 10 m[a] 140 ± 1 dB_E @ 10 m[a]	160 dB_{rms}[a]	PSD levels from SPT exceeded ambient noise by up to 25 dB within 20 Hz-24 kHz τ_{90} = 35 ± 12 ms	Source levels calculated from measurement at shortest range using spherical spreading law ($20\log_{10}r$)	*Context:* geotechnical work prior to marine construction in west Australia. *Area:* Port of Geraldton (Australia) *Sideson II*: 17 m x 16.5 m, 160 hp engine, PQ3 drill bit (ø = 83 mm), rot. speed 1600 rpm. *Weather*: light breeze (5-10 kn), min. swell *Geology:* sand, mudstone and limestone Ambient activity: two large grain carriers operating 450 m away. Trains and construction in land by the water. Drilling: penetration depth 4-20 m. z_r = 1-2 m above seafloor [a] broadband level 20-24k Hz [b] broadband level 30-2k Hz.	Erbe & McPherson, 2017
		Drilling	N/A	145 dB_{rms}[b]	PSD levels from drilling exceeded ambient noise by up to 20 dB within 30 Hz-2 kHz	Source levels calculated from measurement at shortest range using spherical spreading law ($20\log_{10}r$)		
	12	Standard Penetration Testing (SPT)	158 ± 2 dB_{pk} @ 10 m[a] 164 ± 2 $dB_{pk\text{-}pk}$ @ 10 m[a] 144 ± 1 dB_{rms} @ 10 m[a] 147 ± 5 dB_{t25ms} @ 10 m[a] 131 ± 1 dB_E @ 10 m[a] 155 ± 2 dB_{pk} @ 20 m[b] 161 ± 2 $dB_{pk\text{-}pk}$ @ 20 m[b] 141 ± 2 dB_{rms} @ 20 m[b] 144 ± 6 dB_{t25ms} @ 20 m[b] 128 ± 1 dB_E @ 20 m[b]	151 dB_{rms}[c]	PSD levels from SPT exceeded ambient noise by up to 35 dB within 20 Hz-24 kHz [a]τ_{90} = 50 ± 7 ms [b]τ_{90} = 48 ± 5 ms	Source levels calculated from measurement at shortest range using spherical spreading law ($20\log_{10}r$)	*Context:* geotechnical work prior to marine construction in north-west Australia. *Area:* James Price Point (Australia) *Sideson II*: 17 m x 16.5 m, 160 hp engine, PQ3 drill bit (ø = 83 mm), rot. speed 1600 rpm. *Weather*: light breeze (5-10 kn), min. swell *Geology:* sand Ambient activity: none Drilling: penetration depth 16-17 m. z_r = 10 m [a-c] broadband level 20-24k Hz [d] broadband level 30-2k Hz.	
		Drilling	N/A	142 dB_{rms}[d]	PSD levels from drilling exceeded ambient noise by up to 35 dB within 30 Hz-2 kHz	Source levels calculated from measurement at shortest range using spherical spreading law ($20\log_{10}r$)		

5.3 Production

An oil offshore platform is a large structure that includes facilities for subsea drilling, extraction and processing of hydrocarbons or temporary storage of drilled product, and most of them also include crew quarters. After completion of drilling work the platform is adapted or replaced by a permanent oil and gas production platform. The types of platform used for production are essentially the same types that can be used for well drilling and can be grouped in three main categories: 1) *fixed platforms*, such as conventional rigs and compliant towers; 2) *artificial islands* and *caissons*; 3) *floating platforms*, such as semi-submersibles, drill-ships, FPSOs, tension leg platforms and spars (see Figure 5.25). A remote subsea well can be connected to a permanent production platform via flow lines (see Figure 5.25, platform 10).

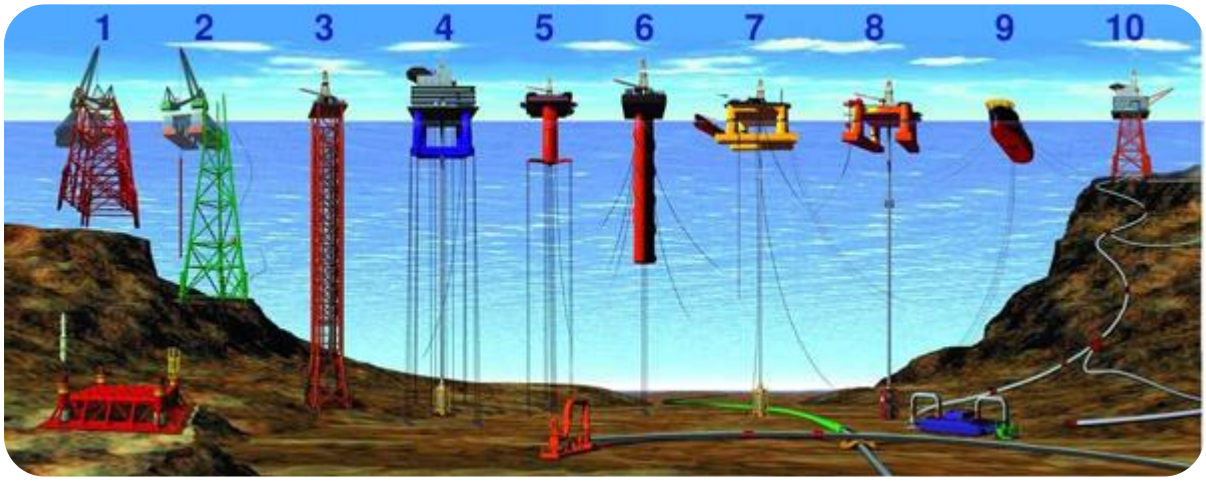

Figure 5.25 *Compilation of different types of offshore oil and gas platforms: 1, 2) conventional fixed platforms; 3) compliant tower; 4, 5) vertically moored tension leg and mini-tension leg platform; 6) spar; 7, 8) semi-submersibles; 9) floating production, storage, and offloading facility; 10) sub-sea completion and tie-back to host facility (from oceanexplorer.noaa.gov)*

Offshore production platforms produce underwater sound, but the aircraft and vessel support will also contribute to the sound field. Figure 5.26 shows the spectra of three types of production platform.

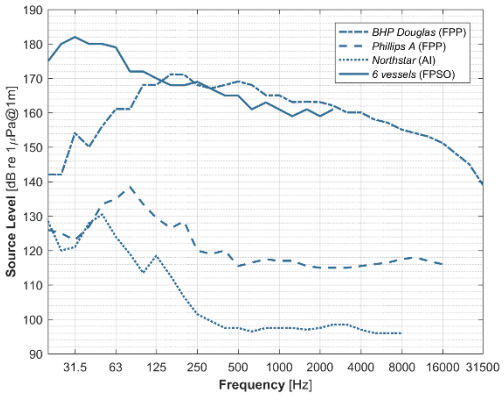

Figure 5.26 Third-octave source level spectra of fixed production platforms *BHP Douglas* (after Nedwell et al., 2003) and *Phillips A* (after Blackwell & Greene, 2003), artificial gravel island *Northstar* (after Blackwell et al., 2004), and 95th percentile spectra from 6 FPSO vessels (after Erbe et al., 2013).

5.3.1 Fixed Platforms

Conventional fixed platforms are supported by jacketed structures consisting of concrete or steel legs attached to the seafloor. The platform deck includes the drilling unit, production facilities and crew quarters. Fixed production platforms are designed for long term use in waters up to 500 m deep.

The sound produced by a platform depends on several factors, such as size and shape of the underwater structure surfaces, structural design and material, operation and degree of coupling of the machinery to the structure, energy supply from external generators, muffling of engine exhausts, etc (Gales, 1982). Figure 5.27 shows the typical pathways and sources of sound in a fixed platform. Underwater sounds produced by jacketed fixed platforms standing on metal legs are expected to be relatively weak, due to the placement of the deck well above the sea surface and the small contact area of the structure with the water (Richardson et al., 1995).

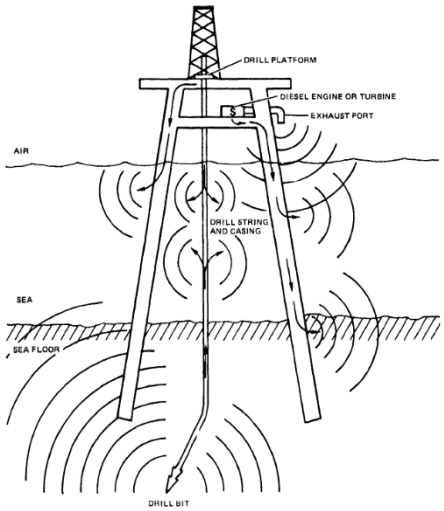

Figure 5.27 Diagram of possible sound pathways in a fixed platform during drilling and production (Gales, 1982)

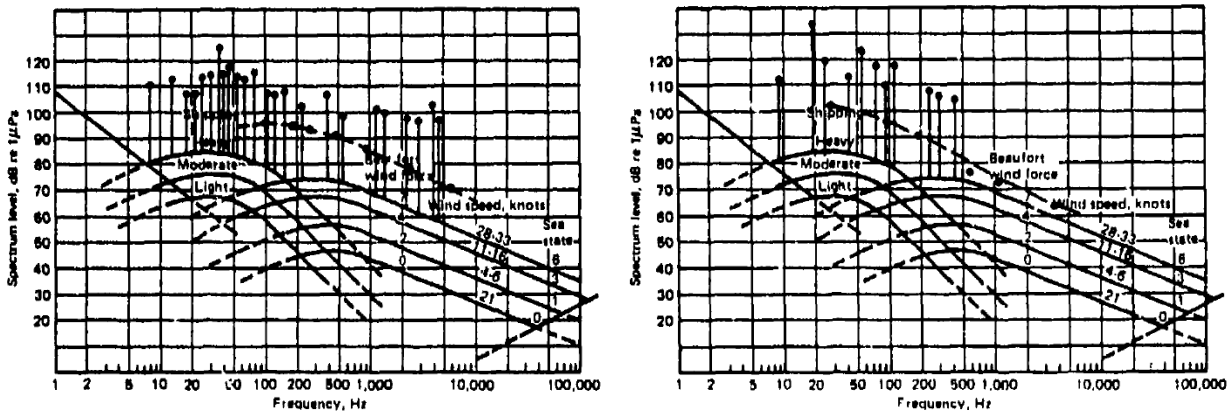

Figure 5.28 Spectra of the multi-leg fixed platform FP1 at 18 m water depth and 9 m hydrophone depth (left) and multi-leg fixed platform FP2 at 23 m water depth and 50 m hydrophone depth (right). Both spectra are obtained at a distance of 9 m from each platform. The dashed line shows the contour of the broadband spectrum and the vertical lines are the main tones. The spectra are represented on top of the standard deep sea ambient noise curves (Gales, 1982)

Gales (1982) presented data on sound generated by eighteen oil and gas platforms including semi-submersibles, fixed multi-legged platforms and an artificial island, during drilling and/or production in areas of Santa Barbara (CA), Upper Cook Inlet (AK), Baltimore Canyon (NJ) and Santa Barbara-Carpenteria (CA). Eleven bottom-standing fixed platforms with multiple steel legs were studied during production operations. The radiated sound was steady with a broadband spectrum combined with tonal components. The strongest tones were below 100 Hz, particularly at frequencies between 4 and 38 Hz, with sound levels of 110 to 130 dB re 1µPa@100m. Peak spectral levels appeared somewhere in between 50 and 500 Hz. The platforms produced less noise than the supply vessel activity, which resulted in an increase of 20 to 30 dB in the overall underwater sound level. Underwater sounds recorded during production activities did not appear to be much different than those from drilling operations. The noise generated by the 11 multi-leg

fixed platforms engaged in production activities were classified as *moderate*, except two of them that were classified as *quiet* and *noisy*.

Measurements presented by Nedwell et al. (2003) from the production platform *Douglas* situated northeast of the North Hoyle windfarm (Wales) showed a sound level of 135 dB re @500m while support vessels were operating nearby.

5.3.2 Artificial Islands and Caissons

The sounds produced by artificial islands and caissons during production activities are likely to be strongly attenuated, as it occurs during drilling (see Section 5.2, "Drilling").

Gales (1982) studied the sounds produced by various types of oil and gas facilities, including an artificial island. The sounds from the island were recorded during production activities in Santa Barbara (CA) in waters 14 m deep with a sandy and rocky seabed. The radiated sound levels were low and the island was rated as "very quiet", compared to the "moderate" levels of most fixed multi-leg platforms. The major sound source was a submerged pump, which was not operating continuously. At a distance of 34 m from the island, tones in the 30-120 Hz frequency range had sound levels of only 89-94 dB. The low noise of the artificial island was probably the result of a combination of factors, including remote electricity supply, poor sound transmission through the island and into the water, and high attenuation of low frequency sound in shallow water.

Measurement of sounds generated during production by the artificial gravel island *Northstar* were obtained during different periods and presented by Blackwell et al. (2004) and Blackwell & Greene (2006). Sound levels were around 97 dB_{rms} at a distance of 500 m.

5.3.3 Floating, Production, Storage and Offloading

A *Floating, Production, Storage and Offloading* or FPSO facility is a double-hull structure, generally ship-shaped, used for processing and storage of hydrocarbons at sea. This type of offshore platform is moored in place for long periods and equipped with processing and storage facilities; FPSOs do not drill for oil and gas. Some variants are used exclusively for storage (FSO, FSU) or production (FPS). FPSOs gather hydrocarbons from multiple wells through flow lines into the riser at its bow, and are mostly used for small fields. Their advantages are the easy deployment in deep water, quick mooring detachment in case of severe weather and use of shutter tankers in replacement of expensive oil pipelines.

Figure 5.29 Photo from *Cossack Pioneer* FPSO (from Erbe et al., 2013).

The processing equipment is located on deck and the storage area lies below it, reducing the amount of machinery vibrations transmitted into the water. The highest sound levels are produced during docking and undocking of shutter tankers used to transport the treated oil from the FPSOs. Such operations are dominated by the sound from dynamic positioning thrusters, propulsion system and machinery in the

FPSOs, shutter tankers and support tugs. The propulsion system from FPSOs and tankers operate at low and constant revolutions per minute, making propeller cavitation less likely. FPSOs, unless transiting or using dynamic positioning, are quieter than tankers, rig tenders and tugs (Erbe et al., 2013).

The most detailed study found on sounds generated by FPSOs is made by Erbe et al. (2013), in which acoustic recordings during production activities from six FPSOs moored off Western Australia are presented. The broadband source levels were of the order of 180 dB re 1µPa@1m.

5.3.4 Tension-Leg and Spar Platforms

A *tension-leg platform* (TLP) is a floating drilling and production facility moored to the seabed by vertical tendons. Standard tension-leg platforms are used in water depths up to 2,000 m; mini tension-leg platforms are more economical than the standard units and are used as satellite or early production facilities in waters up to 1,300 m deep.

A *spar platform* is a drilling and production platform with a hollow cylindrical hull secured to the seabed in a similar way to TLPs but with more conventional mooring systems. The spar is more stable than the TLP due to its large counterweight at the bottom

No studies on sounds produced by tension leg or spar platforms were found.

Figure 5.30 Illustration of a tension-leg platform (left) and a spar platform (right)

5.3.5 Semi-submersibles and Drill-Ships

Semi-submersible and drill-ships are mobile floating platforms used for offshore drilling and production of oil and gas (see Section 5.2, "Drilling"). No studies on sounds produced by these types of facilities during production activities were found.

Table 5.3 Sounds produced by production activities: fixed production platforms and artificial islands

Production Station (*Name/ID*)	h_w [m]	Sediment	Activity	Measurement [dB re 1µPa]	SL [dB re 1µPa@1m]	Signal Characteristics	Regression Equation	Description	Reference
Oil and Gas Production Platform (*BHP Douglas*)	7-11	Gravelly sand (14 m) over Sandstone	production	134.7 dB_{rms} @ 500 m[a]	195.6 dB_{rms} [b]	Most energy < 1 kHz Strong tonal components ("machinery-like noise")	RL = 195.6 - 17log_{10}R, range of validity 1-6.5 km	Area: N of North Wales Coast Measured levels include support vessels (supply vessel + guard ship Grampian Supporter) Broadband level 20-40k Hz [a] z_r = N/A, [b] z_r = 5 m	Nedwell et al., 2003
Oil Production Platform (*Phillips A*)	23-28	glacial (moraine)	production	107.3 dB_{rms} @ 340 m	129.1 dB_{rms}	Main energy at 80 Hz 1/3 oct Notch at ~30 Hz (shallow water) Tonal components < 200 Hz Primary tonal components at 60, 68, 75, 90 and 105 Hz	RL = 129.1 - 7.4log_{10}R, range of validity 300 m to 20 km	Area: NW Cook Inlet, Alaska z_r = 10 m Broadband level 10-20k Hz	Blackwell & Greene, 2003
Oil Production Artificial Gravel Island (*Northstar Island*)	14-37	N/A	drilling and/or production	97 dB_{rms} @ 500 m[a] 99 dBrms @ 500 m[b]	115.2 dB_{rms} [a]	Most energy < 100 Hz Numerous tones and peaks of unknown origin	RL = 115.2 - 6.3log_{10}R, range of validity 500 m to 4 km	*Northstar*: artificial oil production island, made of gravel and located in shallow waters Area: Prudhoe Bay, Beaufort Sea Measurements on 5-6th Sep 2002. Boats not present at the island (good recording conditions) z_r ~ 10 m Broadband level 10-10k Hz [a] production, [b] production and drilling	Blackwell & Greene, 2006; Richardson & Kim, 2015
Oil Production Artificial Gravel Island (*Northstar Island*)	12	N/A	drilling and/or production (pumping crude oil while gas is injected into the formations)	102 dB_{rms} @ 230 m[a] 105 dB_{rms} @ 230 m[b]	154.8 dB_{rms} [a] 155.5 dB_{rms} [b]	Most energy < 100 Hz Peak also at 125-160 Hz (oil production or gas turbines related)	RL = 154.8 - 22log_{10}R, range of validity 200 m to 2 km RL = 155.5 - 21.5log_{10}R, range of validity 200 m to 5 km	*Northstar*: artificial oil production island, made of gravel and located in shallow waters Area: Prudhoe Bay, Beaufort Sea Measurements on 28th Feb and 1st Mar 2002 z_r ~ 1 m above seafloor Broadband level 5-8k Hz [a] production, [b] production and drilling	Blackwell et al. 2004; Richardson & Kim, 2015

Table 5.3 Sounds produced by production activities (cont., part 2): FPSOs

Production Station (*Name/ID*)	h_w [m]	Sediment	Activity	Measurement [dB re 1µPa]	SL [dB re 1µPa@1m]	Signal Characteristics	Regression Equation	Description	Reference
FPSO (*Cossack Pioneer*)	75	Sand (3 m) over Calcarenite	production	N/A	181 ±4 dB_{rms}	Main energy< 70 Hz	Monopole source level estimated with WI model from spectra measured at 1012 m	*Cossack Pioneer*: 340 m long, 16 m draft, 24 MW Area: Western Australia continental shelf Recordings in calm sea z_r = on seafloor z_s = 10 m (in model, deeper than half draft) Broadband level 20-2.5k Hz	Erbe et al., 2013
FPSO (*Griffin Venture*)	130	Sand (3 m) over Calcarenite	production	N/A	179 ±3 dB_{rms}	Main energy< 70 Hz	Monopole source level estimated with WI model from spectra measured at ~2 km	*Griffin Venture*: 209 m long, 10.8 m draft Area: Western Australia continental shelf (21.5S,114E) Recordings in calm sea z_r = 55 m z_s = 10 m (in model, approx. full draft) Broadband level 20-2.5k Hz	Erbe et al., 2013
FPSO (*Pyrenees Venture*)	200	Sand (3 m) over Calcarenite	production	N/A	178 ±2 dB_{rms}	Main energy< 70 Hz	Monopole source level estimated with WI model from spectra measured at 1,840 m	*Pyrenees Venture*: 264 m long, 15 m draft, 17 MW Area: Western Australia continental shelf (21.5S,114E) Recordings in moderately rough sea z_r = on seafloor z_s = 10 m (in model, deeper than half draft) Broadband level 20-2.5k Hz	Erbe et al., 2013
FPSO (*Ningaloo Vision*)	350	Sand (3 m) over Calcarenite	production	N/A	183 ±2 dB_{rms}	Main energy< 70 Hz	Monopole source level estimated with WI model from spectra measured at 1970 m	*Ningaloo Vision*: 238 m long, 12 m draft, 16 MW Area: Western Australia continental shelf (21.5S,114E) Recordings in calm sea z_r = on seafloor z_s = 10 m (in model, approx. full draft) Broadband level 20-2.5k Hz	Erbe et al., 2013
FPSO (*Nganhurra*)	350	Sand (3 m) over Calcarenite	production	N/A	174 ±3 dB_{rms}	Main energy< 70 Hz	Monopole source level estimated with WI model from spectra measured at 500 m	*Nganhurra*: 259 m long, 15 m draft Area: Western Australia continental shelf (21.5S,114E) Recordings in calm to moderate sea z_r = 30 m z_s = 10 m (in model, deeper than half draft) Broadband level 20-2.5k Hz	Erbe et al., 2013
FPSO (*Ngujima-Yin*)	350	Sand (3 m) over Calcarenite	production	N/A	175 ±5 dB_{rms}	Main energy< 70 Hz	Monopole source level estimated with WI model from spectra measured at 500 m	*Ngujima-Yin*: 333 m long, 12 m draft, 27 MW Area: Western Australia continental shelf (21.5S,114E) Recordings in moderate to rough sea z_r = 30 m z_s = 10 m (in model, approx. full draft) Broadband level 20-2.5k Hz	Erbe et al., 2013

5.4 Pipe Laying

Pipe-laying is a marine construction process used to connect offshore production platforms with on-shore refineries by the installation of underwater pipelines. During pipe-laying, a pipe-lay vessel prepares the pipeline onboard and lowers it into the water as the vessel advances itself or with the assistance of anchor handling tugs (Zykov et al., 2013). Types of pipe-lay vessels include barges, reel lay vessels, modified bulk carriers and semi-submersible lay vessels (Genesis, 2011).

Pipelines can be either laid directly on the seabed or buried after trenching. During *trenching*, a large plough (~12 m long) is lowered onto the seabed above the pipeline and pulled by the vessel, at the time the pipe is lifted, creating a trench where the pipeline will lie. The backfilling with sediments normally occurs naturally by the effect of currents.

The buoyancy of the pipe affects the pipe-laying process, and a downward force is required to keep it in place. In shallow waters, concrete is normally poured over the pipe; in deep waters, the required thickness required for the pipe to resist the high hydrostatic pressures is usually enough to keep it on the seabed. The downward force can also be provided by the oil passing through the pipeline.

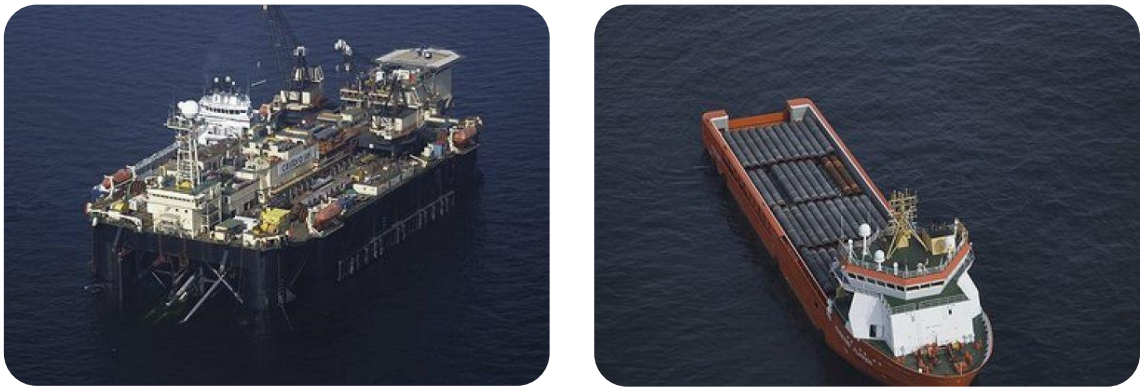

Figure 5.31 Photo of pipe-lay vessel *Castoro Sei* (left) and pipe-carrier *Normand Flipper* (right). From Johansson & Andersson (2012).

Figure 5.32 Photo of post-lay trenching vessel *Far Samson* (left) and sketch of post-lay trenching plough (right). From Johansson & Andersson (2012).

5.4.1 Pipe-Laying Methods

The three most common pipe-laying methods are lay barge, tow-in and reel barge.

In the *tow-in* method one or two tug boats tow a floating pipe, suspended in the water via buoyancy modules, which are generally removed or filled with water when the placement location is reached. The pipe is welded and tested on shore. There are four main techniques in tow-in pipe laying: 1) *surface tow*,

where the buoyancy modules keep the pipe on the surface; 2) *below-surface tow*, where modules of less buoyancy are used to keep the pipe at mid depth with the forward motion of the tug boat, so the pipe can settle when the vessel stops; 3) *off-bottom tow*, where a combination of buoyancy modules and weights are used to keep the pipe just above the seabed, so the pipe will settle when the floats are removed; and 4) *bottom tow*, where the pipe is dragged along a flat seabed, typically in shallow waters with soft sediments.

Lay-barge is the most common pipe-laying method. The barge includes facilities for pipeline assembly and a lifting crane. Pipe sections 12-24 m long are covered with a special anticorrosion coating, welded and lowered into the seabed, one at a time. There are two types of lay-barge techniques: 1) *S-lay*, where the pipe is eased off the stern of the vessel directly from its deck, making the pipeline acquire an S-shape as more sections are attached and lowered into the seabed (see Figure 5.33 and Figure 5.34, left); and 2) J-lay, where the pipeline is lowered from almost a vertical position by a crane, making the pipeline to curve only at the bottom, thus reducing the stress at the barge (see Figure 5.33 and Figure 5.34, right). *J-lay* operations are suitable for pipe installation in deep water and high energy environments.

Figure 5.33 S-lay barge SEMAC-1 (left, from www.drillingformulas.com) and J-lay barge (right, from www.rigzone.com)

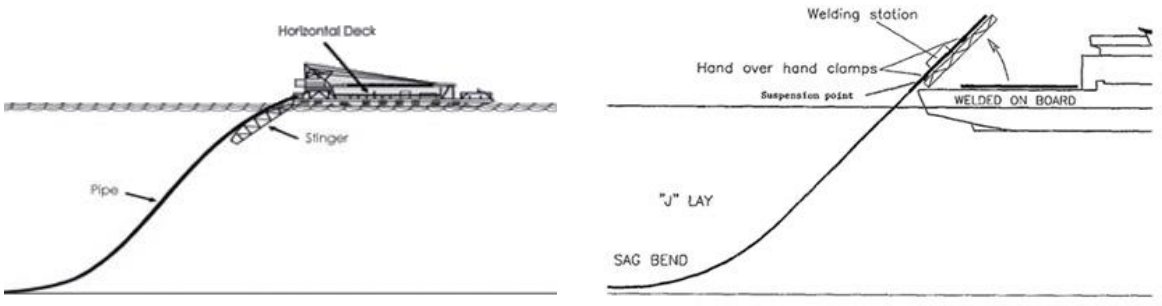

Figure 5.34 Diagram of S-lay (left) and J-lay (right) pipe-laying methods (from www.rigzone.com)

Figure 5.35 Vertical reel barge (from www.rigzone.com)

Reel barges carry a long, low diameter pipeline (<0.4 m) coiled in a reel drum (see Figure 5.35). The pipes are prepared and welded together on shore.

5.4.2 Pipe-Laying Sounds

The pipe-laying activity itself is unlikely to have a noticeable contribution to the sound field; the largest contribution comes instead from the pipe-laying vessel, supply ships and tugs, moving anchors, trenching and backfilling (Johanson & Andersson, 2012). The handling of the several heavy anchors used by the pipe-laying vessel for station keeping and forward movement is a noisy process, especially considering the use of dynamic positioning thrusters by the anchor handling tugs. During pipe-laying, up to 10 ships can operate in the same area, which will also contribute to the overall sound levels.

Measurements made by Hannay et al. (2004) showed that the sound radiated by pipe-laying vessels was in the range of 10-1k Hz, with peak levels below 500 Hz. Anchored pipe-laying vessels generated lower sound levels than the anchor handling tugs and support vessels. Rock placement may be necessary to achieve the required burial depth of the pipeline; when comparing the sound levels produced during rock placement and normal operations by pipe-lay vessel *Rollingstone* (Nedwell & Edwards, 2004) there was no noticeable level increase, which again suggests that sound levels are dominated by vessel noise.

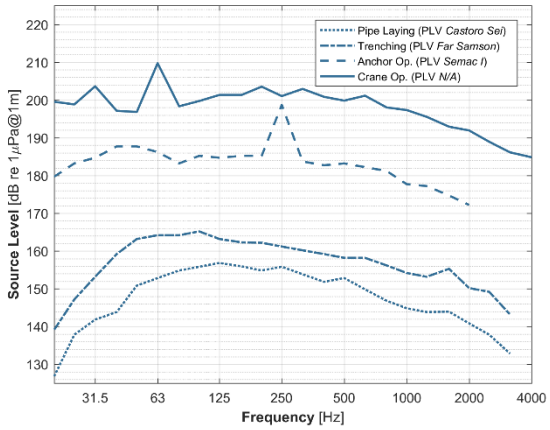

Figure 5.36 Third-octave band source spectra of four pipe laying vessels during four different operating phases: *Castoro Sei* and *Far Samson* during pipe laying and trenching (after Johansson & Andersson, 2012), *Semac I* during anchor operations (after Austin et al., 2004), and crane operations from an unidentified pipe-lay vessel (after MacGillivrai & Racca, 2006). Assumed a transmission loss factor of 15 for all bands to calculate the source level spectra.

Table 5.4 Sounds produced by pipe-laying activities

Source (*Name/ID*)	h_w [m]	Sediment	Activity	Measurement [dB re 1µPa]	SL [dB re 1µPa@1m]	Signal Characteristics	Regression Equation	Description	Reference
Pipe-Laying Vessel (*Solitaire*)	<200	N/A	Laying pipe	134.7 dB_{rms} @ 192 m [a]	N/A	Water surface noise < 20 Hz Vessel noise f = 20 - 50k Hz Main vessel energy 100-800 Hz, LF rumble caused by thrusters	N/A	*Solitaire*: largest pipelay vessel in the world Area: Schiehallion oilfield, W Shetland Islands z_r = 10 m [a] Broadband level 20-40k Hz 1/3 oct, generated *by reviewer* from PSD spectrum (fig. 6.4b)	Nedwell & Edwards, 2004
Pipe-Laying Vessel (*Castoro Sei*)	40	Sand	Laying pipe	120 (123.2) @ 24.2 km[a] 130.5 (134.0) @ 1.5 km[a]	182.6 dB_{rms}	N/A	N/A	Pipe laying operations near the natural protected area Norra Midsjöbanken Area: 50 km E south tip Öland, Sweedish EEZ z_r = 2 m above seafloor Broadband level 20-3.15k Hz 1/3 oct [a] Mean (95th percentile)	Johansson & Andersson, 2012
Pipe-Laying Barge (*Semac I*)	68	N/A	Anchor operations	N/A	179.3 dB_{rms}	N/A	N/A	*Semac I*: deep water semi-submersible pipelay barge, held in position by anchor spreads, support from 2 AHTS Broadband level 20-10k Hz 1/3 oct bands . Source level from 35 m measurement	Hannay et al, 2004; Austin et al., 2004; Carr et al., 2006
Pipe-Laying Barge (*Castoro II*)	10	N/A	Anchor operations	N/A	166.6 dB_{rms}	N/A	N/A	*Castoro II*: shallow water mono-hull pipelay barge, held in position by anchor spreads, support from 1 or 2 AHTS to maintain lay rate Broadband level 20-8k Hz 1/3 oct bands . Source level from 28 m measurement	Hannay et al., 2004
Pipe-Laying Barge (-)	65.5	N/A	Crane operation	N/A	180.9 dB_{rms}	N/A	$TL = 15\log_{10}r$	Self-propelled pipelay vessel with crane Broadband level 20-10k Hz 1/3 oct bands . Source level from 180 m measurement	MacGillivray & Racca, 2006
Trenching Vessel (*Far Samson*)	40	Sand	Laying pipe	117.4 (123) @ 24.2 km[a] 126 (129.8) @ 1.5 km[a]	183.5 dB_{rms}	N/A	$TL = 17\cdot\log_{10}r$	Pipe laying operations near the natural protected area Norra Midsjöbanken Area: 50 km E south tip of Öland z_r = 2 m above seafloor Broadband level 20-3.15k Hz 1/3 oct bands [a] Mean (95th percentile)	Johansson & Andersson, 2012
Trenching Vessel	7-11	Gravelly sand (14 m) over sandstone	Trenching	123 dB_{rms} @ 160 m	178 dB_{rms}	Trenching noise: combination of broadband noise, machinery tones and rock breakage sounds	$RL_{rms} = 178 - 22\log_{10}r$	Project: North Hoyle Offshore Windfarm Area: North Wales (7.5 km north) z_r = 2 m	Nedwell et al., 2003
Backhoe (*Hitachi EX-450*)	12	N/A	Trenching	124.8 dB_{rms} @ 100 m	177.7 dB_{rms}	Main energy at 10 Hz 1/3 oct	$RL_{rms} = 177.7 - 26.4\log_{10}r$	Construction of Northstar Island Area: NW Prudhoe Bay, Beaufot Sea Area covered by landfast ice 1.2-1.6 mm thick z_r = 1 m above seafloor Broadband level 10-10k Hz	Greene et al., 2008
Anchor Handling Vessel (*Katun*)	10	N/A	Anchor Pull	N/A	184.4 dB_{rms} [a]	N/A	N/A	*Katun*: anchor handling vessel (AHTS) Broadband level 10-10k Hz 1/3 oct bands [a] measured at 30 m, extrapolated to 1 m [b] measured at 115 m, extrapolated to 1 m	Hannay et al., 2004
	24	N/A	Transiting	N/A	190.3 dB_{rms} [b]	N/A	N/A		
Support Vessel (*Pompei*)	7	N/A	Discharging spoil	N/A	184 dB_{rms}	N/A	N/A	*Pompei*: support vessel to CSD. Nominal operations on DP. Broadband level 10-10k Hz 1/3 oct bands . Source level from 73 m measurement	Hannay et al., 2004
Support Vessel (Fujisan Maru)	7	N/A	Transiting	N/A	191.5dB_{rms}	N/A	N/A	*Fujisan Maru*: support vessel to CSD Broadband level 10-10k Hz 1/3 oct . Source level from 80 m measurement	Hannay et al., 2004

5.5 Decommissioning and Explosives

Decommissioning takes place at the end of the lifecycle of an oil and gas production platform. In this stage, the removal of structures attached to the seabed, such as wellheads and platform legs, comprises an important part of the work. There are three main activities associated with well decommissioning: explosions, shipping activity and drilling (Genesis, 2011). Explosives provide a fast and reliable way of detaching the structure of an oil rig, but alternative cutting techniques such as tungsten-carbide blade, diamond wire or hydraulic sheer cutters predominate today. However, explosives are still used and are included as a contingency measure in case of failure of the mechanical cutting system. No acoustic studies were found on cutting techniques; this section will focus on decommissioning with explosives, for which more information is available.

Until the 1960's 14-23 kg charge explosives were the main acoustic source used in marine seismic surveys for the detection of hydrocarbon deposits nearshore; in the 1970's these were largely replaced by air gun arrays. Small charge explosives have also been used in scientific studies to determine the transmission loss and characteristics of the sea bottom, for submarine detection and even to deter seals and dolphins from fishing gear (Richardson et al., 1995).

For the removal of oil and gas structures three main types of explosives can be used: bulk, configured bulk and cutting charges (Genesis, 2011). *Bulk charges*, such as Comp-B and C-4, are mouldable, powerful and have a high detonation velocity, and for these reasons are the most common method of explosive cutting. *Configure bulk charges* are designed to focus the explosive energy along the cutting line, reducing in this way the size of the charge. *Cutting charges* use the explosive energy to accelerate a band of cutting material (e.g. copper) through the structure, and includes linear shaped charges and cutting tape.

5.5.1 The Underwater Explosion. Unconfined and Confined Explosives

The detonation underwater of an unconfined explosive charge produces an initial shock wave followed by a sequence of damped periodic pulses, related to the oscillation of the bubble of hot gas created after the explosion. The bubble initially expands beyond its equilibrium radius until it reaches its maximum. Then, the collapse is initiated and the bubble is forced past equilibrium by the momentum of the surrounding water, until the minimum radius is reached. The bubble expands once again, starting a process of expansion and compression. The underlying physics of an oscillating gas bubble in water are the same for air guns and explosive charges.

The acoustic characteristics of the initial shock wave are often represented by empirical equations, derived from explosion shock theory and confirmed by experiments (Richardson et al., 1995). The sound pressure of an underwater explosion reaches its maximum in about one microsecond. For *unconfined charges*, detonated far from any boundary such as the sea surface or seafloor, the peak pressure of the shock wave is given by (Urick, 1983):

$$p_{pk\_unconf} = 5.24 \cdot 10^7 \left(\frac{{m_c}^{1/3}}{r} \right)^{1.13} \tag{5.1}$$

where p_{0p_unconf} is the maximum pressure of the shock wave in Pa, m_c the charge mass in kg and r the distance from the explosion in m.

A similar equation was derived by Barrett (1996) from systematic military experiments:

$$p_{pk\_unconf} = 5 \cdot 10^7 \frac{{m_c}^{0.27}}{r^{1.13}}. \tag{5.2}$$

Eq. 5.1 and 5.2 were obtained from deep water experiments, and are not necessarily applicable to shallow water explosions. Nedwell & Edwards (2004) affirms that Eq. 5.1 and 5.2 represents the worst-case scenario, in that sound levels from unconfined explosions are significantly lower in shallow than in deep waters.

The sound pressure experiences an exponential decay after it reaches its maximum. The instantaneous pressure at time t after the pressure maximum of the shock wave is given by (Richardson et al., 1995):

$$p_{unconf}(t) = p_{pk\_unconf} e^{-t/\tau_c} \quad (5.3a)$$

$$\tau_c = 92.5\, {m_c}^{1/3} \left(\frac{{m_c}^{1/3}}{r} \right)^{-0.22} \quad (5.3b)$$

where τ_c is the time constant in μs, which represents the time required for the pressure to drop to 37% of its initial value.

The *rise time* is the time between the detonation of the explosive and the initial pressure maximum of the shock wave. The rise time of an explosion is extremely short compared to that of an air gun array, and the shorter it is the higher is the potential biological injury (Richardson et al., 1995).

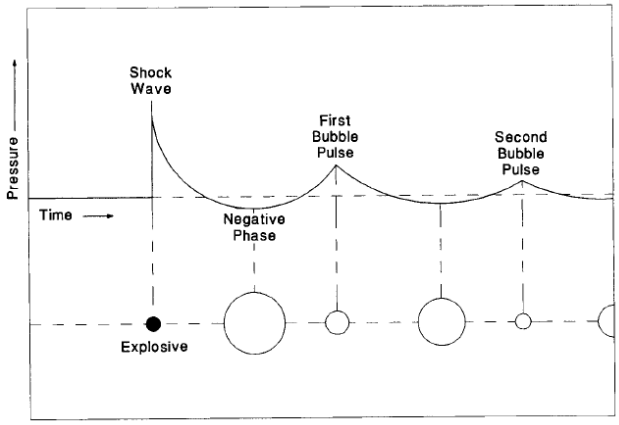

Figure 5.37 Evolution of the sound pressure and gas bubble from an unconfined underwater explosion (from Richardson et al., 1995)

Eq. 5.1-5.3 apply close to the unconfined explosion, but are not applicable to long ranges. The limiting range of applicability of the experimental equations is given by (Rogers, 1977):

$$r_0 = 4.76 {m_c}^{1/3} \quad (5.4)$$

where r_0 is the maximum range of applicability of Eq. 5.1-5.3 in m. The equations for the initial maximum peak pressure and time constant for long ranges are derived by Rogers (1977) from weak-shock theory.

The *bubble period* or time between the shock wave and the first bubble pulse is given by (Arons, 1948; Urick, 1983):

$$T_b = \frac{0.48 K {m_c}^{1/3}}{(z_c + 10)^{5/6}} \quad (5.5)$$

where T_b is the bubble period in s, z_c the charge depth in m and K a constant that depends slightly on the type of explosive and is 4.36 for TNT. The bubble frequency is the reciprocal of T_b and decreases as charge weight m_c increases and charge depth z_c decreases.

Explosive charges used for decommissioning are not freely suspended in the water, far from the surface and bottom; instead, explosives are either buried or attached to the structure. The embedment or confinement of an explosive charge in a borehole results in a significant reduction of the sound level, with the peak pressure limited to 5% of an equivalent unconfined charge, high frequency components are lost,

and the rise time is greatly increased to the order of a millisecond (Nedwell & Edwards, 2004). An empirical equation to estimate the initial maximum peak pressure of *confined explosive charges* is given by Nedwell & Edwards (2004):

$$p_{pk\_conf} = 0.25 \cdot 10^7 \frac{{m_c}^{0.27}}{r^{1.13}} \quad (5.6)$$

where p_{pk_conf} is the maximum pressure of the shock wave in Pa.

5.5.2 Sound Characteristics

The pressure wave produced by the detonation of explosives underwater is characterised by its short duration, short rise time, high peak pressure and wide frequency bandwidth. Explosions generate sound in the range of 2-1,000 Hz, with the main energy concentrated in the 6-21 Hz band, and durations lower than 10 ms (Genesis, 2011). The sound levels produced by explosives underwater are the largest of all anthropogenic sources in the sea, with values of 280 dB re 1µPa@1m or even higher (see Table 5.5). Pressure pulses from high explosives have the potential to cause physical injury or death to marine mammals (Richardson et al., 1995).

The sound pressure drops rapidly close to the charge due to large heat dissipation of the initial shock wave. For detonations close to the sea surface, a portion of the energy is lost by pressure release (Richardson et al., 1995). The initial wave front contributes to most of the high frequency content; the bubble oscillations have lower energy and contribute primarily to the low end of the spectrum. During decommissioning of a hydrocarbon platform in the Gulf of Mexico, the pressure amplitude of the bubble pulse from severance detonations was 2-10 times greater than that of the initial shock wave (Genesis, 2011). Explosive cutting techniques using shock wave focusing require a smaller charge and result in lower radiated sound levels (Thomsen & Schack, 2013). The peak pressure does not show a strong dependence on charge weight (see Eq. 5.1 and 5.2), and a low charge can generate a high acoustic output comparable to somewhat larger charges.

5.5.3 Tables

Table 5.5 Sounds produced by confined and unconfined explosives

Charge [kg]	z_c [m]	h_w [m]	Measurement [dB re 1µPa]	SL [dB re 1µPa@1m]	z_r [m]	Description	Reference
0.025	Not buried (deployed from boat at 5 m depth)	< 4	N/A	226.9 dB_{pk}	N/A	Perchlorate explosives	Nedwell & Edwards, 2004
0.2	3	< 4	169.3 dB_{pk} @ 470 m	302.9 dB_{pk}	2	*Context*: preliminary study with explosives pre seismic survey *Area*: Poole Bay Sediment: clayey silt Charges buried in land, close to water edge NOTE: SL calculated using $TL \sim 50\log_{10}r$, quoted by Nedwell. For comparison, *the reviewer* applied linear-square fitting to this data, obtaining a received level dependence with range of $RL = 269.6 - 37.2\log_{10}(R)$	Nedwell & Edwards, 2004
0.4	11	< 4	172.2 dB_{pk} @ 470 m	305.8 dB_{pk}			
0.6	2	< 4	163.1 dB_{pk} @ 470 m	296.7 dB_{pk}			
	3	< 4	171.1 dB_{pk} @ 470 m	304.7 dB_{pk}			
	6	< 4	146.2 dB_{pk} @ 470 m 168 dB_{pk} @ 470 m	279.8 dB_{pk} 301.6 dB_{pk}			
	N/A	< 4	172.6 dB_{pk} @ 470 m 150.9 dB_{pk} @ 1.9 km	306.2 dB_{pk} 314.8 dB_{pk}			
	N/A	< 4	173.9 dB_{pk} @ 470 m 145.4 dB_{pk} @ 1.9 km	307.5 dB_{pk} 309.3 dB_{pk}			
	N/A	< 4	192.1 dB_{pk} @ 470 m 146.6 dB_{pk} @ 1.9 km	325.7 dB_{pk} 310.5 dB_{pk}			
0.8	15	< 4	172.2 dB_{pk} @ 470 m	305.8 dB_{pk}			
1	N/A	< 4	171.6 dB_{pk} @ 470 m	305.2 dB_{pk}			
0.5	N/A	60	N/A	267 dB_{pk} [a]	N/A	TNT charge Broadband 50-6.3k Hz 1/3 oct. Peak frequencies [a]20, [b]12, [c]6 Hz	Thomsen & Schack, 2013; Richardson, 1995
2	N/A	60	N/A	271 dB_{pk} [b]			
14	N/A	N/A	N/A	278 dB_{pk}			
20	N/A	60	N/A	279 dB_{pk} [*c]			

Table 5.5 Sounds produced by confined and unconfined explosives (cont., part 2)

Charge [kg]	z_c [m]	h_w [m]	Measurement [dB re 1µPa]	SL [dB re 1µPa@1m]	z_r [m]	Description	Reference
1	Charges placed on the seabed, not buried	22	~190 dB_{pk} @ 1 km	N/A	6	*Context*: blasting work for land reclamation for industrial activities. *First set* of measurements (Dec 2000) *Area*: Jurong Island, Singapore	Nedwell & Edwards, 2004
			196.7 dB_{pk} @ 1 km 204.3 dB_{pk} @ 1 km 203.2 dB_{pk} @ 1 km 201.6 dB_{pk} @ 1 km 194 dB_{pk} @ 1 km	N/A	12		
2	Charges placed on the seabed, not buried	22	196.9 dB_{pk} @ 1 km 198.5 dB_{pk} @ 1 km 195.4 dB_{pk} @ 1 km 194.8 dB_{pk} @ 1 km	N/A	6		
			195.3 dB_{pk} @ 1 km 197.1 dB_{pk} @ 1 km 195.7 dB_{pk} @ 1 km 197.7 dB_{pk} @ 1 km	N/A	12		
4	Charges placed on the seabed, not buried	22	198.9 dB_{pk} @ 1 km 197.8 dB_{pk} @ 1 km 198.5 dB_{pk} @ 1 km	N/A	6		
			198.3 dB_{pk} @ 1 km 199.2 dB_{pk} @ 1 km 200.2 dB_{pk} @ 1 km	N/A	12		
1-4	Charges placed on the seabed, not buried	22	192.9 (209.5) dB_{pk} @ 1.25 km[a]	N/A	3	Context: blasting work for land reclamation for industrial activities. *Second set* of measurements (Mar-Jun 2001) Area: Jurong Island, Singapore Measurement direction: [a]50°, [b]250°, [c]140°, [d]290° [a-d]mean (maximum)	Nedwell & Edwards, 2004
			186.8 (206.3) dB_{pk} @ 1.8 km[b]	N/A	3, 6		
			198.2 (210.0) dB_{pk} @ 1 km[c]	N/A	6		
			172.0 (196.3) dB_{pk} @ 1 km[d]	N/A	6		
40	Few metres under the seabed	116	227.5 dB_{pk} @ 75 m	N/A	N/A	*Context*: wellhead removal using explosives. Piles 1-5 m high, buried 2-3 m. 45 kg charge of high explosive liquid *Area*: North Sea NOTE: Sound levels similar to predictions of unconfined explosives, which reveals that neither the sediment nor the surrounding pipe-work acted as effective confinement NOTE: linear least-square fitting *by reviewer* to this data resulted in a received level dependence with range of RL = 258.4 - 14.6log_{10}(R)	Nedwell & Edwards, 2004; Nedwell et al, 2001; Genesis, 2011
		87	226.1 dB_{pk} @ 125 m	N/A			
		110	224.6 dB_{pk} @ 200 m	N/A			
		84	229.9 dB_{pk} @ 300 m	N/A			
		91	231.9 dB_{pk} @ 300 m	N/A			
		108	223.3 dB_{pk} @ 400 m	N/A			
		25	211.1 dB_{pk} @ 575 m	N/A			
		30	211.4 dB_{pk} @ 575 m	N/A			
		25	214-215.1 dB_{pk} @ 600 m	N/A			
		30	214.3-220 dB_{pk} @ 600 m	N/A			
		35	214.1 dB_{pk} @ 600 m	N/A			
		40	213.4 dB_{pk} @ 600 m	N/A			
		25	213.8-225.9 dB_{pk} @ 650 m	N/A			
		30	212.7-221.4 dB_{pk} @ 650 m	N/A			
		35	216.7-222.3 dB_{pk} @ 650 m	N/A			
		40	214.6-221.2 dB_{pk} @ 650 m	N/A			
		30	221.4 dB_{pk} @ 800 m	N/A			

6 Aircrafts

The characteristics and propagation of aircraft sound in water depend on the air-water transmission process and the properties of the underwater environment. Airborne sound can propagate in water in four main ways (Urick, 1972): 1) direct refracted path, 2) multi-path underwater reflection of transmitted sound, 3) surface-travelling wave, 4) scattering from a rough sea surface (see Figure 6.1).

In the air-water interface there exists a *critical angle of incidence* above which the sound wave is totally reflected; its value is given by Snell's law and is close to 13°, relative to the normal. Rough sea states increase the area of sea surface with appropriate orientation for the transmission of airborne sound into the water. The sea surface roughness enhances the air-water transmission at grazing angles, increasing the sound levels between 3-7 dB in the direction of wave travel, but also reduces sound levels by 3-5 dB in the region below the source, where the strongest sounds are normally found under calm sea states. The effect of waves is noticeable at frequencies higher than 150 Hz; for lower frequencies the sea surface is effectively flat (Richardson et al., 1995).

Level and duration of the sound received underwater from a passing aircraft depend on several factors, including acoustic strength and aspect of the aircraft, range, surface conditions, receiver depth, water depth and bottom characteristics. The amount of acoustic energy being transmitted into the water depends on the altitude of the aircraft and sea state. For an aircraft that passes directly overhead, sound levels decrease with increasing source altitude and receiver depth; however, for an aircraft not directly overhead, sound levels can be higher at deeper receiver depths.

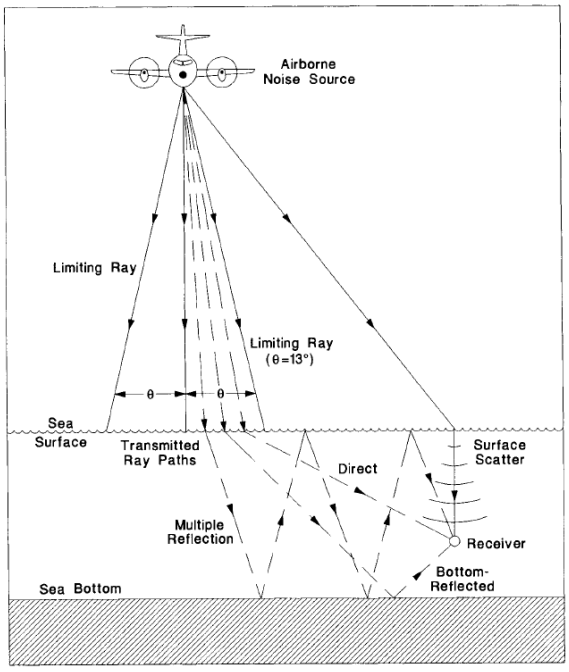

Figure 6.1 Air-water propagation paths for airborne noise from an aircraft (from Richardson et al., 1995).

Water depth and bottom properties also have a strong effect on level, frequency content and duration of the underwater sound produced by an aircraft. Horizontal sound propagation is better in shallow waters,

especially when the seabed is highly reflective. The multiple underwater reflections contribute to increase the generally short duration of a passing aircraft and also the distance at which the aircraft sound becomes undetectable. The duration of the noise event in water also tends to increase with the altitude of the aircraft.

Aircraft take-off and climb tend produce higher sound levels, generally between 5-15 dB, than those during cruise or approach.

The concept of *source level* or sound level at 1 m is not very meaningful in the case of airborne sound transmitted into water, since the propagation of sound takes place in two media. The source level in the tables of aircraft noise (see Table 6.1) is included for comparison purposes and is defined as the sound level in air at 1 m from the aircraft, calculated by Richardson et al. (1995) using the method of Young (1973).

6.1 Sound Characteristics

Aircrafts are powered by either *reciprocating* (piston) or *turbine* engines. Both types of engine can drive propellers or helicopter rotors, but turbine engines can additionally be used for jet propulsion (i.e. turbojet and turbofan).

Reciprocating engine sounds are dominated by a series of harmonics associated with the firing rate of the engine's cylinder, with the fundamental frequency f_e given by (Richardson et al., 1995):

$$f_e = \frac{\mathrm{rpm} \cdot N}{60 \cdot M} \tag{6.1}$$

where rpm is the turning rate of the engine in revolutions per minute, N the number of cylinders, and M the number of revolutions per cylinder and firing. For example, in a four-stroke engine, which results in two revolutions per firing and cylinder ($M = 2$), with six cylinders ($N = 6$) and 2000 rpm, the fundamental frequency would be 100 Hz.

In *propeller-driven aircrafts*, the propeller or main and tail rotors are the main source of noise. Their blades produce the dominant tones in the spectrum; the fundamental frequency of the turning propeller or rotor f_b can be calculated with the following simple formula (Richardson et al., 1995):

$$f_b = \frac{\mathrm{rpm} \cdot B}{60} \tag{6.2}$$

where rpm is the turning rate of the blade in revolutions per minute and B is the number of blades. For example, a three-bladed propeller turning at 3000 rpm produces a tone of 150 Hz; in a helicopter with two-bladed main and tail rotors turning at 300 and 1620 rpm, the respective fundamental tones are 10 and 54 Hz.

There may be additional tones associated with other sound generating mechanisms in the engine and rotating parts. The Doppler shift effect, caused by the relative speed between source and receiver, will also alter the frequency of these tones.

Dominant tones in *helicopters* and *fixed-wing, propeller-driven aircrafts* are associated with blade rate and are generally below 500 Hz. Helicopters produce sound that is dominated by frequencies below 50 Hz, tend to produce a higher number of tones and are noisier than similar fixed-wing aircraft (~10 dB higher). The sound radiated by helicopters is also more intense forward than backward. In propeller-driven aircrafts, the fundamental and second harmonic of the propeller-blade rate dominate. In general, large aircrafts tend to produce higher sound levels than smaller ones (Richardson et al., 1995).

Jet aircrafts lack rotors and propellers, which results in a sound spectrum that is not dominated by low frequency tones and is broadband in nature, with frequency content extending up to 5 kHz (Richardson et al., 1995; Blackwell & Greene, 2002). The high frequency content is dominated by the blade-rate tones

from the turbine engine, characterised by frequencies ranging from a few hundred Hz to above 1 kHz. The fundamental frequency of the blade-rate of a turbine engine f_b is obtained from Eq. 6.2. The jet mixing sound contributes to the lower end of the spectrum. High performance military jets are extremely noisy, with sound levels significantly higher than conventional jet aircrafts above 150 Hz (Blackwell & Greene, 2002). Additionally, older jet transport aircrafts are noisier than those with new generation engines (Richardson et al., 1995). Figure 6.2 shows the spectrum of four types of commercial and military jet aircrafts (see also Figure 6.4, right).

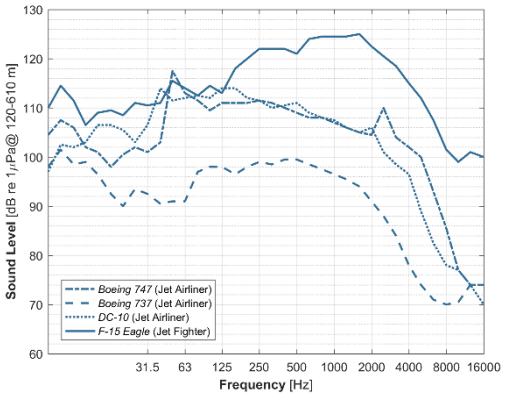

Figure 6.2 Third-octave band noise spectra from four types of commercial and military jet aircrafts at overflight distances between 120-610 m (after Blackwell & Greene, 2004).

Aircrafts flying at a higher speed than the speed of sound in air produce an instantaneous, low-frequency pressure pulse known as *sonic boom*. In a sonic boom, an initial shock wave is followed by a relaxation period and an abrupt return to ambient pressure. Most of the energy in a sonic boom is contained within the first 100 Hz (50-300 Hz), with durations of tens to several hundreds of milliseconds. The high acoustic pressure generated on the sea surface decreases rapidly with increasing depth (Richardson et al., 1995).

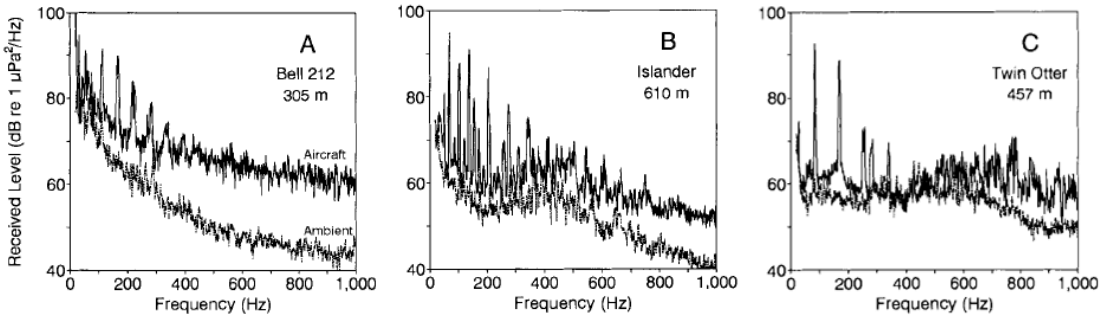

Figure 6.3 Power spectral density of aircraft noise during overflights by: A) helicopter Bell 212; B,C) two fixed-wing aircrafts. Tones in A and C are related to propeller rotor, and tones in B to piston firing rate (from Richardson et al., 1995).

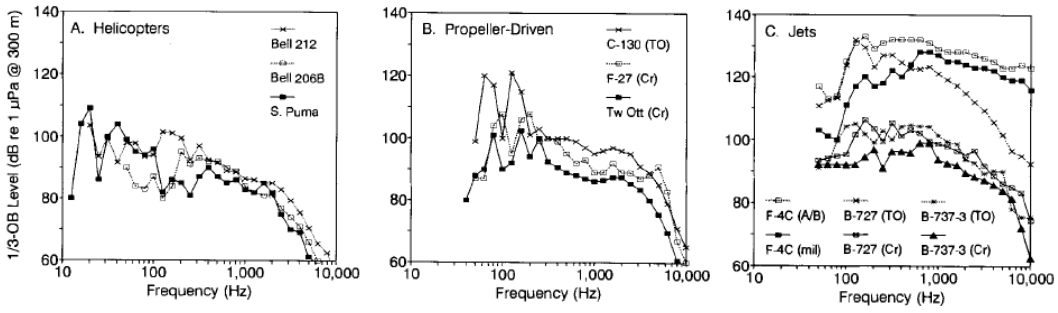

Figure 6.4 Third-octave band noise spectra from three categories of aircraft: helicopter (left), propeller-driven (centre) and jet (right). The sound levels are estimated at the water surface from aircraft overflight at 300 m altitude. TO = takeoff or climb, Cr = cruise, A/B afterburners and mil = maximum without afterburner (from Richardson et al., 1995).

6.2 Tables

Table 6.1 Sounds produced by aircrafts: military and commercial passenger jets

Aircraft (*Model*)	h_w [m]	Sediment	Flight Phase	Measurement [dB re 1µPa]	SL [dB re 1µPa@1m]	Signal Characteristics	Description	Reference
Jet Fighter Aircraft (*F-15 Eagle*)	24-30	Mixture of different grain size (glacial sediment, moraine)	Landing	134 dB_{rms} @ 120 m [a] 122 dB_{rms} @ 120 m [b]	N/A	Most energy < 5 kHz Notable higher levels than commercial aicrafts > 150 Hz	*F-15 Eagle*: single-seat jet fighter aircraft, 2x turbofan engines, power 79.2 kN/engine, 19.5 m long, 5.6 m high, 13.1 m wing span, 2500 km/h Area: nearshore, by Elmendorf Air Force Base (AFB), Cook Inlet, Alaska z_r = 10 m Broadband level 10-20k Hz Overflight at [a]90°(overhead) and [b]80° [a,b]120 m is the aircraft altitude	Blackwell & Greene, 2002
Military transport aircraft (*C-5 Galaxy*)	24-30	Mixture of different grain size (glacial sediment, moraine)	Takeoff	111 dB_{rms} @ 610 m[a]	N/A	N/A	*C-5*: military transport aircraft, 4x turbofan engines, power 191.3 kN/engine, 75.5 m long, 19.9 m high, 67.9 m wing span, 919 km/h speed Area: 1 km N Anchorage International Airport (ANC), Cook Inlet, Alaska z_r = 10 m Broadband level 10-20k Hz [a] 70° overflight, 610 m is the aircraft altitude	Blackwell & Greene, 2002
Widebody Jet Airliner (*Boeing 747*)	24-30	Mixture of different grain size (glacial sediment, moraine)	Takeoff	123 dB_{rms} @ 610 m [a] 120 dB_{rms} @ 610 m [b] 110 dB_{rms} @ 610 m [c]	N/A	Most energy < 5 kHz Lack of low frequency tones 2.5 kHz tone from jet turbines	*Boeing 747*: widebody commercial jet airliner, 4x turbofan engines, power 275.8 kN/engine, 70.6 m long, 19.4 m high, 64.4 m wing span, 982 km/h Area: 1 km N Anchorage International Airport (ANC), Cook Inlet, Alaska z_r = 10 m Broadband level 10-20k Hz [a] 60°, [b] 50° and [c] 45° overflight [a-c] 610 m is the aircraft altitude	Blackwell & Greene, 2002
Widebody Jet Airliner (*DC-10*)	24-30	Mixture of different grain size (glacial sediment, moraine)	Takeoff	124 dB_{rms} @ 610 m [a] 122 dB_{rms} @ 610 m [b]	N/A	Most energy < 3 kHz 2 and 4 kHz tones (turbine)	*D-10*: widebody jet airliner, 3x turbofan engines, power 226 kN/engine, 55.5 m long, 17.7 m high, 15.4 m wing span, 907 km/h Area: 1 km N Anchorage International Airport (ANC), Cook Inlet, Alaska z_r = 10 m Broadband level 10-20k Hz [a] 90°(overhead) and [b] 60° overflight [a,b] 610 m is the aircraft altitude	Blackwell & Greene, 2002

Table 6.1 Sounds produced by aircrafts (cont., part 2): commercial passenger jets

Aircraft (*Model*)	h_w [m]	Sediment	Flight Phase	Measurement [dB re 1µPa]	SL [dB re 1µPa@1m]	Signal Characteristics	Description	Reference
Commercial Passenger Airplanes	7	Soft mud	Takeoff	110 dB_{rms} @ 150 m [a]	N/A	τ = 10-15 s DC = 6-8% (peak time) Downward tone sweep around CPA (Doppler effect). Plane noise level exceeds ambient noise by up to 36 dB in PSD spectrum between 12 Hz and 10kHz.	*Context:* recording of underwater noise from commercial flights from Ngurah Rai International Airport (Denpasar, Bali) in the sea z_r ~ 0.3 m above seafloor [a]median broadband level from 12 Hz to 10 kHz 1/3 oct bands on 1-s samples from 170 overflights. 150 m refers to plane altitude	Erbe et al, 2018
	11	Soft mud	Takeoff	117 dB_{rms} @ 300 m [a]	N/A	τ = 10-15 s DC = 6-8% (peak time) Downward tone sweep around CPA (Doppler effect). Plane noise level exceeds ambient noise by up to 36 dB in PSD spectrum between 12 Hz and 10kHz.	*Context:* recording of underwater noise from commercial flights from Ngurah Rai International Airport (Denpasar, Bali) in the sea. Variable weather, winds 9.4 ± 5.9 km/h z_r ~ 0.3 m above seafloor [a] median broadband level from 12 Hz to 10 kHz 1/3 oct bands over 1-s samples from 192 overflights. 300 m refers to plane altitude	
	1	Silty mud	Cruise, Landing	91 dB_{rms} @ 400-800 m [a]	N/A	τ = 30-40 s Downward tone sweep around CPA (Doppler effect) Plane noise level exceeds ambient noise by up to 36 dB in PSD spectrum between 12 Hz and 2 kHz.	*Context:* recording of underwater noise from commercial flights from Perth International Airport (Western Australie) in Canning River. Warm weather, calm river with occasional ripples z_r ~ 0.3 m above seafloor [a] median broadband level from 12 Hz to 2 kHz 1/3 oct bands over 1-s samples from 33 overflights. 400-800 m refer to plane altitude	

Table 6.1 Sounds produced by aircrafts (cont., part 3): helicopters and fix-wing propeller aircrafts

Aircraft (*Model*)	h_w [m]	Sediment	Flight Phase	Measurement [dB re 1µPa]	SL [dB re 1µPa@1m]	Signal Characteristics	Description	Reference
Piston-powered Airliner (*DC-6*)	24-30	Mixture of different grain size (glacial sediment, moraine)	Takeoff	119 dB_{rms} @ 610 m[a]	N/A	N/A	*D-6*: widebody jet airliner, 4x radial engines (piston), power 1864 kW/engine, 32.2 m long, 8.7 m high, 35.8 m wing span, 507 km/h Area: 1 km N Anchorage International Airport (ANC), Cook Inlet, Alaska z_r = 10 m Broadband level 10-20k Hz [a] 25° overflight, 610 m is the aircraft altitude	Blackwell & Greene, 2002
Piston-Powered Utility Aircraft (*Britten-Norman Islander*)	N/A	N/A	N/A	101 dB_{rms} @ 152 m[a]	142 dB_{rms}	Propeller tone 70 Hz Engine tone 102 Hz	*B-N Islander*: light utility aircraft and regional airliner, 2x piston engines, power 194 kW/engine, 10.9 m long, 4.2 m high, 15 m wing, 272 km/h z_r = 3-18 m Broadband level 1-8 kHz oct bands [a] 152 m is the aircraft altitude	Richardson et al, 1995
Turboprop STOL Utility Aircraft (*Twin Otter*)	N/A	N/A	N/A	107 dB_{rms} @ 457 m [a] 100 dB_{rms} @ 610 m [b]	147 dB_{rms} [a] 150 dB_{rms} [b]	Propeller tone 82 Hz	*Twin Otter*: STOL utility aircraft, 2x turboprop engines, power 507 kW/engine, 15.8 m long, 5.9 m high, 19.8 wing span, 348 km/h z_r = 3-18 m Broadband level 1-8 kHz oct bands [a,b] 457 and 610 m refer to aircraft altitude	Richardson et al, 1995
Maritime Patrol Aircraft (*P-3 Orion*)	N/A	N/A	N/A	124 dB_{rms} @ 76 m [a] 121 dB_{rms} @ 152 m [a] 114 dB_{rms} @ 305 m [a] 112 dB_{rms} @ 76 m [b] 107 dB_{rms} @ 152 m [b]	162 dB_{rms} [a] 162 dB_{rms} [a] 160 dB_{rms} [a] 150 dB_{rms} [b] 148 dB_{rms} [b]	[a] Most energy from 68 Hz tone	*P-3 Orion*: maritime patrol and anti-submarine aircraft, 4x turboprop engines, power 3661 kW/engine, 35.6 m long, 10.3 m high, 34.4 wing span, 761 km/h z_r = 3-18 m Level from [a] 56-80 Hz band, and [b] 1 kHz 1/3 oct band [b] 76, 152 and 305 m refer to aircraft altitude	Richardson et al, 1995
Medium Utility Helicopter (*Bell 212*)	N/A	N/A	N/A	109 dB_{rms} @ 152 m [a] 107 dB_{rms} @ 305 m [a] 101 dB_{rms} @ 610 m [a]	149 dB_{rms} 151 dB_{rms} 151 dB_{rms}	[a] Tones 10.8 Hz and harmonics (dominant 22 Hz tone)	*Bell 212*: medium-size utility helicopter, 2x turboshaft engines, power 1342 kW/engine, 17.5 m long, 4.5 m high, rotor blades 2x main 2x tail, rotor diameter 14.7 m main 2.6 m tail, 230 km/h, main rotor speed 324 rpm z_r = 3-18 m Broadband level 1-8 kHz oct bands [a] 152, 305 and 610 m refer to helicopter altitude	Richardson et al, 1995

7 References

Abrahamsen, K. (2012). "The ship as an underwater noise source". *Proceedings of Meeting on Acoustics, 11th European Conference on Underwater Acoustics (EACUA 2012), 2-6 July*, 17, p. 10. doi: 10.1121/1.4772953

Aerts, L., Blees, M., Blackwell, S., Greene, C., Kim, K., Hannay, D. and Austin, M. (2008). *Marine mammal monitoring and mitigation during BP Liberty OBC seismic survey in Foggy Island Bay, Beaufort Sea, July-August 2008: 90-day report*. LGL Alaska Research Associates Inc., Greeneridge Sciences Inc. and JASCO Research Ltd., Rep. P1011-1, p. 199.

Ainslie, M.A., Jong, C.A.F. de, Dol, H.S., Blacquière, G., and Marasini, C. (2009). *Assessment of natural and anthropogenic sound sources and acoustic propagation in the North Sea*. TNO Rep. TNO-DV 2009 C085, p. 114

Ainslie, M. A. (2010). *Principles of Sonar Performance Modeling*. Heilderberg: Springer, p. 737. doi: 10.1007/978-3-540-87662-5

Airmar (2011). *Gillnet Pinger*. Airmar Technology Corporation, Technical Specifications, p. 1

D'Amico, A., Gisiner, R.C., Ketten, D.R., Hammock, J.A., Johnson, C., Tyack, P.L., and Mead, J. (2009). "Beaked whale strandings and naval exercises". *Aquatic Mammals*, 35(4), 452-472. doi: 10.1578/AM.35.4.2009.452

D'Amico, A., and Pittenger, R. (2009). "A brief history of active sonar". *Aquatic Mammals*, 35(4), 426-434. doi: 10.1578/AM.35.4.2009.426

André, M., Morell, M., Mas, A., Solé, M., van der Schaar, M., Houégnigan, S. Z., Castell, J. V., Baquerizo, C. A., and Roch, L.R. (2009). *Best Practices in Management, Assessment and Control of Underwater Pollution*. Laboratory of Applied Bioacoustics, p. 105

Applied Acoustics (2008). *Squid 500, Squid 2000 & Delta Sparker Seismic Sound Source,Sparker Assemblies*. Applied Acoustics Underwater Technology, Technical Specification.

Applied Acoustics (2010). *AA201 and AA301 Seismic Sound Source, Boomer Plates*. Applied Acoustics Underwater Technology, Technical Specification.

Applied Acoustics (2013). *AA2xx series seismic source, operation manual*. Applied Acoustics Underwater Technology, Doc. BPL-0200-8000/1, p. 17

Aquatec (2014). *AQUAmark® Selection Guide*. Aquatec Group, Technical Specifications, p. 1

Arons, A.B. (1948). "Secondary pressure pulses due to gas globe oscillation in underwater explosions. II. Selection of adiabatic parameters in the theory of oscillation". *J. Acoust. Soc. Am.*, 20(3), 277-282. doi: 10.1121/1.1906372

Arveson, P. T., and Vendittis, D. (2000). "Radiated noise characteristics of a modern cargo ship," *J. Acoust. Soc. Am.*, 107(1), 118-129. doi: 10.1121/1.428344

Ashtead (2000). *GeoAcoustics Boomer System*. Ashtead Technology, Technical Specification.

Austin (2004). *Sound level Measurements of SEMAC-1*. Australia, 2004 Sakhalin Energy Jasco Research Ltd, 7 pages.

Austin, M., MacGillivrai, A., and Hannay, D. (2005). *Sakhalin Energy/ Maersk Rover acoustic source level measurements*. JASCO Research Ltd., Doc. No. 0000-S-90-04-P-7058-00, Rev. 01

Austin, M.E., Hannay, D.E., and Bröker, K.C. (2018). "Acoustic characterization of exploration drilling in the Chukchi and Beaufort Seas". *J. Acoust. Soc. Am.*, 144(1), 115-123. doi: 10.1121/1.5044417

Barrett, R.W. (1996). *Guidelines for the safe use of explosives underwater*. Marine Technology Directorate.

Bayhi, J.F., Chalmers, F.E., Barry, A.F. and Pearson, J.B. (1969). "The sleeve exploder, a nondynamite marine source". *Offshore Technology Conference, 18-21 May, Houston, Texas*, p. 8

Beland, J., Ireland, D., Bisson, L., and Hannay, D., (2013). *Marine mammal monitoring and mitigation during a marine seismic survey by ION Geophysical in the Arctic Ocean, October-November 2012: 90-day report*. LGL Rep. P1236-5, p. 156 plus appendices.

Bird, J. (2003). "The marine vibrator". The Leading Edge, 22(4), 368-370. doi: 10.1190/1.1572092

Blackwell, S.B., and Greene, C.R. (2002). *Acoustic measurements in Cook Inlet, Alaska, during August 2001*. Greeneridge Sciences, Inc., Aptos, CA, Rep. 271-1, p. 42

Blackwell, S.B., and Greene, C.R. (2003). *Acoustic measurements in Cook inlet, Alaska, during August 2001*. Greeneridge Sciences, Inc., Rep. 271-2, p. 44

Blackwell, S.B., Greene, C. R. and Richardson, W. J. (2004). "Drilling and operational sounds from an oil production island in the ice-covered Beaufort Sea". *J. Acoust. Soc. Am.*, 116(5), 3199-3211. doi: 10.1121/1.1806147

Blackwell, S. B., and Greene, C. R. (2005). "Underwater and in-air sounds from a small hovercraft," J. Acoust. Soc. Am, 118(6), 3646-3652. doi: 10.1121/1.2118347

Blackwell, S.B. and Greene, C.R. (2006). "Sounds form an oil production island in the Beaufort Sea in summer: Characteristics and contribution of vessels". *J. Acoust. Soc. Am.*, 119(1), 182-196. doi: 10.1121/1.2140907

Blees, M., Hartin, K., Ireland, D. and Hannay, D. (2010). *Marine mammal monitoring and mitigation during open water seismic exploration by Statoil USA E&P Inc. in the Chukchi Sea, August–October 2010: 90-day report*. LGL Rep. P1119, p. 220

Blondel, P. (2009). *The Handbook of Sidescan Sonar*. Heilderberg: Springer, p. 344. doi: 10.1007/978-3-540-49886-5

Boebel, O., Clarkson, P., Coates, R., Larter, R., O'Brien, P.E., Ploetz, J., Summerhayes, C., Tyack, T., Walton, D.W.H., and Wartzok, D. (2005). "Risks posed to the Antarctic marine environment by acoustic instruments: a structured analysis". *Antarctic Science*, 17(4), 533-540. doi: 10.1017/S0954102005002956

Bouyoucos, J.V., McLaughlin, J.K., and Selsam, R.L. (1981). "The Hydroshock® water gun". *J. Acoust. Soc. Am*, 70. doi: 10.1121/1.2018893

Burrowes, G. and Khan, J. Y. (2011). "Short-range underwater acoustic communication networks". In *Autonomous Underwater Vehicles*, Cruz N. A. (Ed.), 173-199. doi: 10.5772/24098

Caldwell, J. and Dragoset, W. (2000). "A brief overview of seismic air-gun arrays", *The Leading Edge* 19(8), pp. 898-902. doi: 10.1190/1.1438744

Carr, S.A., Laurinolli, M.H., Tollefsen, C.D.S., and Turner, S.P. (2006). *Cacouna Energy LNG Terminal: assessment of underwater noise impacts*. JASCO Research Ltd. Technical Report.

Casciani-Wood, J. (2015). *An introduction to propeller cavitation*. [online] Available at: www.iims.org.uk/introduction-propeller-cavitation [accessed 28/07/2017]

CEDA (2011). "Underwater sound in relation to dredging". Central Dredging Association (CEDA), Position Paper.

Chitre, M., Shahabudeen, S., Freitag, L. and Stojanovic, M. (2008). "Recent advances in underwater acoustic communications & networking". *OCEANS 2008, 15-18 Sept., Quebec, Canada*. doi: 10.1109/OCEANS.2008.5289428

Cluster Maritime Français (2014). *Underwater noise: economic and environmental challenges in the marine environment*. P. 55

Coates, R. (2006). *Foundation course: basic underwater acoustics. The SONAR course*. Seiche Ltd.

Comyn, M. (1984). "Beaufort Sea caisson retained island". *Journal of Canadian Petroleum Technology*, 23(4), p. 6. doi: 10.2118/84-04-01

Coram, A., Gordon, J., Thompson, D. and Northridge, S. (2014). *Evaluating and assessing the relative effectiveness of Acoustic Deterrent Devices and other non-lethal measures on marine mammals*. Scottish Government

Cybulski, J. (1977). "Probable origin of measured supertanker radiated noise spectra". *OCEANS '77*, 17-19 Oct., Los Angeles, CA., p. 8. doi: 10.1109/OCEANS.1977.1154413

Der, C. Y. (1983). "The Esso caisson-retained island data acquisition system". *Journal of Canadian Petroleum Technology,* 22(4), p. 5. doi: 10.2118/83-04-09

Dickerson, C., Reine, K. J., and Clarke, D. G. (2001). "Characterization of underwater sounds produced by bucket dredging operations," *DOER Technical Notes Collection*, Rep. ERDC TN-DOER-E14. Vicksburg, MS: U.S. Army Engineer Research and Development Center

Dix, J., Bastos, A., Plets, R., Bull, J. and Henstock, T. (n.d.). *High resolution sonar for the archaeological investigation of marine aggregate deposits*. Final project report, University of Southampton, p. 92

DTI (2001). *An Overview of Offshore oil and gas exploration and production activities*, p. 30

Duchesne, M. J. and Bellefleur, G. (2007). *Processing of single-channel, high-resolution seismic data collected in the St. Lawrence estuary, Quebec*. Current Research Rep. 2007-D1. Quebec, Canada: GSC Quebec

Erbe, C. (2013). "International regulation of underwater noise", Acoustics Australia, 41(1), 12-19

Erbe, C., McCauley, R., McPherson, C. and Gavrilov, A. (2013). "Underwater noise from offshore oil production vessels". *J. Acoust. Soc. Am.*, 133(6), *JASA Express Letters*, 465-470. doi: 10.1121/1.4802183

Erbe, C., and McPherson, C. (2017). "Underwater noise from geotechnical drilling and standard penetration testing". *J. Acoust. Soc. Am. Express Letters*, 142(3), 281-285. doi: 10.1121/1.5003328

Erbe, C., Williams, R., Parsons, M., Parsons, S.K., Hendrawan, I.G., I.M. Iwan Dewantama. (2018) "Underwater noise from airplanes: An overlooked source of ocean noise". *Marine Pollution Bulletin*, 137, 656-661. doi: 10.1016/j.marpolbul.2018.10.064

Feltham, A., Mougenot, J., Jenkerson, M., Griswold, S. and Cozzens, A. (2016) "The marine vibrator JIP". *AAPG/SEG International Conference and Exhibition, 6-9 September, Cancun, Mexico*. doi: 10.3997/2214-4609.201801946

Firenze, E. and Valdenazzi, F. (2015). "A method to predict underwater noise form cavitating propellers". *OCEANS 2015, 18-21 May, Genova, Italy*. doi: 10.1109/OCEANS-Genova.2015.7271453

Fisher F. H., Simmons V. P. (1977). "Sound absorption in seawater", *J. Acoust. Soc. of Am*, 62, 558-564. doi: 10.1121/1.381574

Fontana, P., and Boukhanfra, F. (2018). "Near-field measurements versus far-field estimations of air gun array sound pressure levels". Conference Proceedings, *EAGE Annual 80th Conference and Exhibition*, Copenhagen (Denmark), 11-14 June. doi: 10.3997/2214-4609.201800744

Foote, K.G. (2014). "Discriminating between the nearfield and the farfield of acoustic transducers". *J. Acoust. Soc. Am*, 136(4), 1511-1517. doi: 10.1121/1.4895701

Francois R. E., Garrison G. R. (1982a). "Sound absorption based on ocean measurements: Part I:Pure water and magnesium sulfate contributions", *J. Acoust. Soc. of Am.*, 72(3), 896-907. doi: 10.1121/1.388170

Francois R. E., Garrison G. R. (1982b). "Sound absorption based on ocean measurements: Part II:Boric acid contribution and equation for total absorption", *J. Acoust. Soc. of Am*, 72(6), 1879-1890. doi: 10.1121/1.388673

Frisk, G. V. (2012). "Noiseonomics: The relationship between ambient noise levels in the sea and global economic trends". *Scientific Reports*, 2, art. 437. doi: 10.1038/srep00437

Fristedt, T., Morén, P. and Söderberg, P. (2001). *Acoustic and electromagnetic noise induced by wind mills – implications for underwater surveillance systems, Pilot study*. FOI User Report FOI-R-0233-SE, p. 17

Fugro (2008). *Sys09 Specifications.* Fugro Seafloor Surveys, Inc., Technical Specification, p. 3

Funk, D., Hannay, D., Ireland, D., Rodrigues, R. and Koski, W.R. (2008). *Marine mammal monitoring and mitigation during open water seismic exploration by Shell Offshore Inc. in the Chukchi and Beaufort Seas, July-November 2007: 90-day report*. LGL Rep. P961-1, p. 218 + appendices.

Funk, D.W., Ireland, D.S., Rodrigues, R. and Koski, W.R. (2010). *Joint monitoring program in the Chukchi and Beaufort seas, open water seasons, 2006-2008*. LGL Final Report P1050-3, p. 756

Gales, R.S. (1982). *Effects of noise of offshore oil and gas operations on marine mammals – An introductory assessment*. NOSC Technical Report 844 vol. 1. San Diego, CA: Naval Ocean Systems Center

Gallagher, M.L., Brewer, K.D. and Hall, J.D. (1992). *ARCO Alaska, Inc. Cabot prospect/Site specific monitoring plan/Final report*. Rep. from Coastal & Offshore Pacific Corp., Walnut Creek, CA, p.78 + appendices.

Gausland, I. (1998). The Physics of Sound in Water. In chapter 3 of *Proceedings of the Seismic and Marine Mammals Workshop*, Tasker, M.L. and Weir, C. (Eds.). London, England.

Genesis (2011). *Review and assessment of underwater sound produced from oil and gas sound activities and potential reporting requirements under the Marine Strategy Framework*. Genesis Oil and Gas Consultans Ltd., Final Rep. J71656

Götz, T., Hastie, G., Hatch, L.T., Raustein, O., Southall, B. L., Tasker, M., Thomsen, F., Campbell, J. and Fredheim, B. (2009). *Overview of the impacts of anthropogenic underwater sound in the marine environment*. OSPAR Biodiversity Series

Götz, T. and Janik, V. M. (2013). "Acoustic deterrent devices to prevent pinniped depredation: efficiency, conservation concerns and possible solutions". *Marine Ecology Progress Series*, 492, 285-302. doi: 10.3354/meps10482

Graydon L, B., & Delbert W, F. (1969). "Marine vibrator devices". US Patent 3,482,646, December.

Greene, C.R. (1986). *Underwater Sounds from the submersible drill rig SEDCO 708 drilling in the Aleutian Islands*. Polar Research Laboratory, Inc., Santa Barbara, CA.

Greene, C. R. (1987). "Characteristic of oil industry dredge and drilling sound in the Beaufort Sea". *J. Acoust. Soc. Am.*, 82(4), 1315-1324. doi: 10.1121/1.395265

Greene, C. R., and Richardson, W. J. (1988). "Characteristics of marine seismic survey sounds in the Beaufort Sea," J. Acoust. Soc. Am., 83 (6) , 2246-2254. doi: 10.1121/1.396354

Greene, C.R., Blackwell, S.B., and McLennan, M.W. (2008). "Sounds and vibrations in the frozen Beaufort Sea during gravel island construction". *J. Acoust. Soc. Am.*, 123(2), 687-695. doi: 10.1121/1.2821970

Hall, J.D., and Francine, J. (1991). "Measurement of underwater sounds from a concrete island drilling structure located in the Alaskan sector of the Beaufort Sea". *J. Acoust. Soc. Am.*, 90(3), 1665-1667. doi: 10.1121/1.401907

Hall, J.D., Gallagher, M.L., Brewer, K.D., Regos, P.R., and Isert, P.E. (1994). *ARCO Alaska, Inc. 1993 Kuvlum exploration area site specific monitoring program/Final report*. Coastal & Offshore Pacific Corp., Walnut Creek, CA, p. 219.

Hammerstad, E. (2005). Sound levels from Konsberg Multibeams. EM Technical Note, p. 3

Hannay, D., MacGillivary, A., Laurinolli, M., and Racca, R. (2004). *Source Level Measurements from 2004 Acoustics Programme*. Sakhalin Energy, p. 66

Hansen, R. E. (2011). Introduction to sonar. [course material] University of Oslo

Hauser, D.D.W., Moulton, V.D., Christie, K., Lyons, C., Warner, G., O'Neil, C., hannay, D., and Inglis, S. (2008). *Marine mammal and acoustical monitoring of the Eni/PGS open-water seismic program near Thetis, Spy and Levitt Islands, Alaskan Beaufort Sea, 2008: 90-day report*. LGL Rep. P19065-1, p. 194.

Heathershaw, A. D., Ward, P. D., and David, A. M. (2001). "The Environmental Impact of Underwater Sound," Proc. Inst. Acoust., 23(4)

Hermannsen L., Tougaard J., Beedholm K., Nabe-Nielsen J., Madsen P.T. (2015). "Characteristics and Propagation of Airgun Pulses in Shallow Water with Implications for Effects on Small Marine Mammals". *PLoS ONE*, 10(7), 1-17. doi: 10.1371/journal.pone.0133436

Hildebrand, J. A. (2005). "Impacts of anthropogenic sound". In *Marine Mammal Research: Conservation Beyond Crisis*. Baltimore, Maryland: John Hopkins University Press, 101-124

Hildebrand, J. A. (2009). "Anthropogenic and natural sources of ambient noise in the ocean," Mar. Ecol. Prog. Ser., 395, 5–20. doi: 10.3354/meps08353

Hillier, E. (2010). Subsea acoustic positioning. [pdf presentation] Concordia Consultancy Ltd.

Hutchinson, D.R., and Detrick, R.S. (1984). "Water gun vs air gun: a comparison". Marine Geophysical Research, 6(3), 295-310. doi: 10.1007/BF00286531

Hydro International (2007). *Acoustic Modems*. Hydro International Product Survey, p. 4

IACMST (2006). *Underwater Sound and Marine Life*. Inter-Agency Committee on Marine Science and Technology, IACMST Working Group Rep. 6, p. 10

IADC (2014). "Cutter Suction Dredgers". *IADC Facts About,* 2, p. 4

ICES (2005). *Report of the Ad-hoc Group on Impacts of Sonar on Cetaceans and Fish (AGISC).* International Council for Exploration of the Sea, ICES Rep. CM 2005/ACE:06, p. 25

Ireland, D., Hannay, D., Rodrigues, R., Patterson, H., Haley, B., Hunter, A., Jankowski, M., and Funk, D.W. (2007). *Marine mammal monitoring and mitigation during open water seismic exploration by GX Technology in the Chukchi Sea, October—November 2006: 90-day report*. LGL Draft Rep. P891-1, p. 118.

Ireland, D., Rodrigues, R., Funk, D., Koski, W.R., and Hannay, D. (2009). *Marine mammal monitoring and mitigation during open water seismic exploration by Shell Offshore Inc. in the Chukchi and Beaufort Seas, July-October 2008: 90-day report*. LGL Rep. P1049-1, p. 277 + appendices

ISO (2017). Underwater Acoustics – Terminology. ISO 18405:2017

Jenkerson, M.R., Feltham, A.J., Henderson,N., Nechayuk, V.E., Girard, M. and Cozzens, A.J. (2018). "The Marine Vibrator JIP and ongoing Marine Vibroseis development". Conference Proceedings, *80th EAGE Conference & Exhibition 2018 Workshop Programme*, Copenhagen (Denmark), 11-14 June. doi: 10.3997/2214-4609.201801946

Jiménez-Arranz, G., Hedgeland, D., Cook, S., Banda, N., Johnston, P., Oliver, E. (2019). "Acoustic characterisation of a mobile offshore drilling unit". *Proceedings of Meetings on Acoustics (POMA),* 37 (poster 36), 12 pp. Manuscript prepared for the proceedings of the 5th International Conference on the Effects of Noise on Aquatic Life (AN2019), Den Haag (The Netherlands), 7-12 July. doi: 10.1121/2.0001193

Jiménez-Arranz, G., Banda, N., Cook, S. and Wyatt, R. (2020). *Review on existing data of underwater sounds from pile driving activities*. Seiche Ltd.

Johansson, A.T., and Andersson, M.H. (2012). *Ambient underwater noise levels at Norra Midsjöbanken during construction of the Nord Stream Pipeline*. FOI Rep. FOI-R—3469--SE, p. 65

Jones, D., and Marten, K. (2016). "Dredging sound levels, numerical modelling and EIA". *Terra et Aqua*, 144, 21-29

Jong, C. de, Ainslie, M., Dreschler, J., Jansen, E., Heemskerk, E., and Groen, W. (2010). *Underwater noise of Trailing Suction Hopper Dredgers at Maasvlakte 2: Analysis of source levels and background noise*. TNO Rep. TNO-DV 2010 C335, p. 91

Karam, Q. (2015). *Artificial islands construction in offshore areas for oil and gas exploration industry: an environmental perspective*. Kuwait Institute for Scientific Research, Technical Report.

Keen, K.A., Thayre, J., Hildebrand, J.A., and Wiggins, S.M. (2018). "Seismic airgun sound propagation in Arctic Ocean waveguides", *Deep-Sea Research Part I: Oceanographic Research Papers*, 141, 24-32. doi: 10.1016/j.dsr.2018.09.003

Kipple, B. (2002). *Southeast Alaska Cruise Ship Underwater Acoustic Noise/ Underwater acoustic signatures of six cruise ships that sail Southeast Alaska*. NSWC Technical Report NSWCCD-71-TR-2002/574, Naval Surface Warfare Center, p. 92

Kipple, B. and Gabriele, C. (2003). *Glacier Bay watercraft noise*. Bremerton, WA: Naval Surface warfare Center, technical Report NSWCCD-71-TR-2003/522, p. 62

Khodabandeloo, B., and Landrø, M. (2017). "High frequency ghost cavitation – a comparison of two seismic airgun arrays using numerical modelling". *Energy Procedia*, 125, 153-160. doi: 10.1016/ j.egypro.2017.08.158

Konsberg (2003). *MPT 163 Series, Multifuction Positioning Transponder (MPT)*. Konsberg Maritime AS, Technical Specifications, p. 4

Konsberg (2005). *SBP Sub-Bottom Profiler*. Konsberg Maritime AS, Technical Specifications, Doc. 855-164773, Rev. B, p. 4

Konsberg (2014a). *Geopulse, Pinger Sub-Bottom profiler*. Konsberg Geoacoustics Ltd., Technical Specification, p. 2

Konsberg (2014b). *Dual Frequency Side Scan Sonar*. Konsberg Geoacoustics Ltd., p. 2.

Kremser, U., Klemm, P., and Kötz, W.D. (2005). "Estimating the risk of temporary acoustic threshold shift, caused by hydroacoustic devices, in whales in the Southern Ocean". *Antarctic Science*, 17(1), 3-10. doi: 10.1017/S0954102005002361

Kyhn, L. A., Tougaard, J., and Sveegard, S. (2011). *Underwater noise from the drillship Stena Forth in Disko West, Baffin Bay, Greenland*. NERI Technical Rep. 838, National Environmental Research Institute, Aarhus University.

Landrø, M., Zaalberg-Metselaar, G., Owren, B. and Vaage, S. (1993). "Modeling of water-gun signatures". Geophysiscs, 58(1), 101-109. doi: 10.1190/1.1443339

Landrø, M. and Amundsen, L. (2010). "Marine seismic sources. Part I", *Geo ExPro* 7(1)

Landrø, M., Amundsen, L. and Langhammer, J. (2013). "Repeatability issues of high-frequency signals emitted by air-gun arrays", Geophysiscs, 78(6), 19-27. doi: 10.1190/geo2013-0142.1

Landrø, M. (2014) "A practical equation for air gun bubble time period including the effect of varying sea water temperature", 76th EAGE Conference & Exhibition 2014, Amsterdam RAI, the Netherlands, 16-19 June. doi: 10.3997/2214-4609.20141239

LePage, K., Malme, C., Mlawski, R., and Krumhansl, P. (1995). *Exxon SYU Sound Propagation Study*. BBN Acoustic Technologies, Rep. 8120.

Lepper, P. (2007). Anthropogenic noise measurement and impacts for assessment of the marine environment. [pdf presentation] Loughborough University, p. 26

Lepper, P.A., Humphrey, V.F., Theobald, P.D., Robinson, S.P., Wang, L.S., and Hayman, G. (2012). "The contribution to anthropogenic noise from marine aggregate extraction operation in UK waters". In: *Ambient Noise in North-European Seas: Monitoring, Impact and Management, 3rd-5th Oct 2011*, Southampton. Proceedings of the Institute of Acoustics Conference, 33(5), 59-61

Lepper, P.A., Gordon, J., Booth, C., Theobald, P., Robinson, S. P., Northridge, S. & Wang, L. (2014). *Establishing the sensitivity of cetaceans and seals to acoustic deterrent devices in Scotland*. Scottish Natural Heritage Commissioned Report No. 517, p. 121

Lepper, P.A., Turner, V.L.G., Goodson, A.D., and Black, K.D. (2004). "Source levels and spectra emitted by three commercial aquaculture anti-predation devices". *Proceedings of the Seventh European Conference on Underwater Acoustics (ECUA 2004),* Delft (The Netherlands), 5-8 July.

Liu, M., Dong, L., Lin, M. and Li, S. (2017). "Broadband ship noise and its potential impacts on Indo-Pacific humpback dolphins: Implications for conservation and management". *J. Acoust. Soc Am.*, 142(5), 2766-2775. doi: 10.1121/1.5009444

Lurton, X. (2010). *An introduction to underwater acoustics, principles and applications*. Berlin, Heilderberg: Springer-Verlag

MacGillivray, A., and Racca, R. (2006). *Underwater acoustic source level measurements of Castoro and Fu Lai*. Jasco Research Ltd, p. 5

Malme, C.I. and Mlawski, R. (1979). *Measurements of underwater acoustic noise in the Prudhoe Bay area*. BBN Tech. Memo. 513. Cambridge, MA: Bolt Beranek & Newman Inc., p. 74

Malme, C. I., Miller, G. W. and Greene, C. R. (1989). *Analysis and ranking of the acoustic disturbance potential of petroleum industry activities and other sources of noise in the environment of marine mammals in Alaska*. BBN Systems and Technologies Corporation, Rep. No. 6945

Mancini, C.V., Dowse, S.E.W., and Chevalier, J.M. (1983)."Caisson retained island for Canadian Beaufort Sea – Geotechnical design and construction considerations". *Offshore Technology Conference, 2-5 May, Houston, Texas*.

Marine Mammal Commission (2007). *Marine Mammals and Noise: A Sound Approach to Research And Management*, p. 370

McCauley, R. (1998). *Radiated underwater noise measured from the drilling rig Ocean General, rig tenders Pacific Ariki and Pacific Frontier, fishing vessel Reef Venture and natural sources in the Timor Sea, Northern Australia.* CMST Rep. C98-20, Curtin University of Technology, Western Australia.

McDonald, M. A., Hilderbrand, J. A., and Wiggins, S. M. (2006). "Increases in deep ocean ambient noise in the Northeast Pacific west of San Nicolas Island, California," *J. Acoust. Soc. Am.,* 120(2), 711-718. doi: 10.1121/1.2216565

McKenna, M. F., Ross, D., Wiggins, S. M., and Hildebrand, J. A. (2012). "Underwater radiated noise from modern commercial ships". *J. Acoust. Soc. Am.*, 131(1), 92-103. doi: 10.1121/1.3664100

McPherson, C. and Warner, G. (2012). *Sound Sources Characterization for the 2012 Simpson Lagoon OBC Seismic Survey 90-Day Report*. JASCO Technical Rep. P001044-007/00443, ver. 2.0, p. 205

Miksis-Olds, J.L., Nichols, S.M. (2016). "Is low frequency sound increasing globally?" *J. Acoust. Soc. Am.*, 139(1), 501-511. doi: 10.1121/1.4938237

Miles, P.R., Malme, C.I., and Richardson, W.J. (1987). *Prediction of drilling site-specific interaction of industrial acoustic stimuli and endangered whales in the Alaskan Beaufort Sea*. BBN Labs Inc., Rep. 6509; OCS Study MMS 87-0084, p. 341

MMO (2018). *Assessing non-lethal seal deterrent options: literature and data review*. Report prepared by ABPmer Ltd & NFFO for the Marine Management Organisation. MMO Project No. 1131, 45 pp.

Morell, M., Brownlow, A., McGovern, B., Raverty, S. A., Shadwick, R. E. & André, M. (2017). "Implementation of a method to visualize noise-induced hearing loss in mass stranded cetaceans", *Scientific Reports*, 7:41848, 1-8. doi: 10.1038/srep41848

Morton, A. B., and Symonds, H. K. (2002). "Displacement of *Orcinus orca* (L.) by high amplitude sound in British Columbia, Canada". ICES Journal of Marine Science, 59, 71–80. doi: 10.1006/jmsc.2001.1136

Nedwell, J.R. (1994). *Underwater spark sources: some experimental information*. Subacoustech Ltd., Rep. 440R0102, p. 24

Nedwell, J.R, Needham, K., Gordon, J., Rogers, C., and Gordon, T. (2001). *The effects of underwater blast during wellhead severance in the North Sea.* Subacoustech Ltd.

Nedwell, J., Langworthy, J. and Howell, D. (2003). *Assessment of sub-sea acoustic noise and vibration from offshore wind turbines and its impact on marine wildlife; initial measurements of underwater noise during construction of offshore windfarms, and comparison with background noise*. Subacoustech Rep. 544R0424.

Nedwell, J.R. and Edwards, B. (2004). *A review of measurement of underwater man-made noise carried out by Subacoustech Ltd, 1993-2003*. Subacoustech Rep. 534R0109

OGP (2011). "An overview of marine seismic operations", OGP Publications, 448, p. 46

Paganie, D (Ed.) (2015). *Worldwide Seismic Vessel Survey*. Offshore Magazine, March 2015, pp. 53-57.

Patterson, H., Blackwell, S.B., Haley, B., Hunter, A., Jankowski, M., Rodrigues, R., Ireland, D., and Funk, D.W. (2007). *Marine mammal monitoring and mitigation during open water seismic exploration by Shell Offshore Inc. in the Chukchi and Beaufort Seas, July-September 2006: 90-day report*. LGL Rep. P891-1, p. 150

Petras, E. (2003). *A review of marine mammal deterrents and their possible applications to limit killer whale (Orcinus Orca) predation on Steller sea lions (Eumetopias jubatus).* Seattle, WA: AFSC, NMFS, NOAA, p. 53

Ramsay, P. (2017). *Sub-bottom profiling acquisition techniques in HYPACK®*. HYPACK Technical Notes

Reine, K. J, and Clarke, D. (2014). "Characterization of underwater sounds produced by hydraulic and mechanical dredging operations". *J. Acoust. Soc. Am.*, 135(6), 3280-3294. doi: 10.1121/1.4875712

Reine, K. J., Clarke, D., Dickerson, C. and Wikel, G. (2014). *Characterisation of underwater sounds produced by trailing suction hopper dredges during sand mining and pump-out operations*. Environmental Laboratory Rep. ERDC/EL TR-14-3. U.S. Army Engineer Research and Development Center

Reiser, C., Funk, D., Rodrigues, R., and Hannay, D. (2010). *Marine mammal monitoring and mitigation during open water seismic exploration by Shell Offshore, Inc. in the Alaskan Chukchi Sea, July–October 2009: 90-day report*. LGL Rep. P1112-1, p. 268

Richardson, W. J, Greene, C. R., Malme, C. I, and Thomson, D. H. (1995). *Marine Mammals and Noise*. San Diego, CA: Academic Press, p. 581

Richardson, W.J., and Kim, K.H. (2015). *Monitoring of industrial sound, seals, and bowhead whales near BP's Nothstar Oil Development, Alaskan Beaufort Sea, 2014: Annual summary report and comprehensive report*. LGL Alaska Research Associates Inc., and Greeneridge Sciences Inc., LGL Rep. P1259C, p. 96

Robinson, S.P., Theobald, P.D., Hayman, G., Wang, L.S., Lepper, P.A., Humphrey, V., and Mumford, S. (2011). *Measurement of underwater noise arising from marine aggregate dredging operations*. MALSF, Rep. MEPF 09/P108.

Robinson, S. P. (2015). Dredging sound measurements. [pdf presentation] *WODA Workshop, 26th March, Paris*

Rogers, P.H. (1977). "Weak-shock solution for underwater explosive shock waves". *J. Acoust Soc. Am.*, 62(6), 1412-1419. doi: 10.1121/1.381674

Roof, C.J., and Fleming, G.G. (2001). *Hovercraft underwater noise measurements in Alaska*. Volpe Center Acoustics Facility, Cambridge, MA, Draft Letter Report DTS-34-VX015-LR1, p. 16

Ross, D. (1976). *Mechanics of underwater noise*. New York: Pergamon Press

Roth, E.H., Schmidt, V., Hildebrand, J.A., and Wiggins, S.M. (2013). "Underwater radiated noise levels of a research icebreaker in the central Arctic Ocean". *J. Acoust. Soc. Am.*, 133(4), 1971-1980. doi: 10.1121/1.4790356

Roussel E. (2002). "Disturbance to Mediterranean cetaceans caused by noise". In: *Cetaceans of the Mediterranean and Black Seas: state of knowledge and conservation strategies*, Di Sciara, G.N. (ed.) A report to the ACCOBAMS Secretariat, Monaco. Section 13, p. 18

Saucier, R. T. (1970). *Acoustic sub-bottom profiling systems, a state-of-the-art survey*. Vicksburg, MS: U. S. Army Engineer Waterways Experiment Station

Sendra, S. Lloret, J., Jiménez, J. M. and Parra, L. (2016). "Underwater acoustic modems". IEEE Sensors Journal, 16(11), 4063-4071. doi: 10.1109/JSEN.2015.2434890

Sercel (2006). *Marine sources*. Sercel, p. 28

Simard, Y., Roy, N., Gervaise, C., and Giard, S. (2016). "Analysis and modeling of 255 source levels of merchant ships from an acoustic observatory along St. Lawrence Seaway". *J. Acoust. Soc. Am.*, 140(3), 2002-2018. doi: 10.1121/1.4962557

Sman, P. M. van de (1998). "Environmental Aspects of Airguns". Shell EXPRO, p. 25

Sonardyne (2003). *Acoustic Release Transponders*. Sonardyne Oceanographic Systems, Brochure, p. 6

Sonardyne (2007). *Heavy Load DORT Acoustic Release Transponder*. Sonardyne Oceanographic Systems, Technical Specifications, p. 2

Sonardyne (2013). *Coastal Tranponder*. Sonardyne Technical Specifications, p. 3

Sonardyne (2016). *Compatt 6 – USBL/LBL Transponder and Modem*. Sonardyne Technical Specifications, p. 2

Sörnmo, O., Bernhardsson, B., Kröling, O., Gunnarsson, P. and Tenghamn, R. (2016). "Frequency-domain iterative learning control of a marine vibrator". Control Engineering Practice, 47, 70-80. doi: 10.1016/j.conengprac.2015.12.014

Stojanovic, M. and Beaujean, P. P. (2016). "Acoustic Communication". In *Handbook of Ocean Engineering*. Dhanak, M. R. and Xiros, N. I. (Eds.), 359-386

Sub Sea Sonics (2012). Underwater Acoustic Release System/Acoustic Release Model AR-60-E/Acoustic Release Interrogator Model ARI-60. Sub Sea Sonics, San Diego, CA, Technical Note, p. 17

Tashmukhambetov, A. M., Ioup, G. E., Ioup, J. W., Sidorovskaia, N. A., and Newcomb, J. J. (2008). "Three-dimensional seismic array characterization study: experiment and modeling," *J. Acoust. Soc. Am.*, 123(6), 4094-4108. Doi: 10.1121/1.2902185

Tasker, M.L. and Weir, C., Eds. (1998). *Proceedings of the Seismic and Marine Mammals Workshop*. London, England, p. 201

Teledyne (2016). *Source level of Teledyne RD instruments ADCP transducers.* Technical Note no. FST-054, January 2016.

Teledyne (2016). *Benthos Acoustic Releases*. Teledynes Benthos, Brochure, p. 2

Tenghamn, R. (2006). "An electrical marine vibrator with a flextensional shell". Exploration Geophysics, 37(4), 286-291. doi: 10.1071/ASEG2006ab178

Tenghamn, R. (2009). "Driving means for acoustic marine vibrator". US Patent 7,551,518, June.

Theobald, P.D., Robinson, S.P., Lepper, P.A., Hayman, G., Humphrey, V.F., Wang, L., and Mumford, S.E. (2011). "The measurement of underwater noise radiated by dredging vessels during aggregate extraction operations". *Proceedings of the 4th International Conference and Exhibition on "Underwater Acoustic Measurements: Technologies & Results"*, 20-24th June, Kos Island, Greece, 763-769

Thomsen, F., McCully, S., Wood, D., Pace, F. and White, P. (2009). *A generic investigation into noise profiles of marine dredging in relation to acoustic sensitivity of the marine fauna in UK waters with particular emphasis on aggregate dredging: PHASE 1 scoping and review of key issues*. MEPF Rep. MEPF/08/P21

Thomsen, F., and Schack, H.B. (2013). *Danish sustainable offshore decommissioning/Decommissioning of an oil rig in the Ekofisk oil field/ A risk assessment.* DHI, p. 26

Todd, V.L.G., Todd, I.B., Gardiner, J.C., Morrin, E.C., MacPherson, N.A., DiMarzio, N.A. and Thomsen, F. (2015). "A review of impacts of marine dredging activities on marine mammals". *ICES Journal of Marine Science*, 72(2), 328-340. doi: 10.1093/icesjms/fsu187

Tomczak, A. (2011). "Modern methods of underwater positioning applied in subsea mining". Górnictwo i Geoinżynieria, 35:4/1

Trabant, P.K. (1984). *Applied High Resolution Geophysical Methods: Offshore Geoengineering Hazards*. Dordrecht, Netherlands: Springer Science+Business Media Dordrecht, p. 265

UNCTAD (2015). *Review of maritime transport*. New York and Geneva: United Nations, p. 122

USGS (2000). "Seismic survey to map earthquake faults and other subsea stratigraphic information". USGS Seismic Survey Rep. CD-16-00

Urick, R.J. (1972). "Noise signature of an aircraft in level flight over a hydrophone in the sea". *J. Acoust. Soc. Am.*, 52(3), 993-999. doi: 10.1121/1.1913206

Urick, R.J. (1983) *Principles of Underwater Sound*. 3rd Ed., McGraw-Hill, New York.

Vos, E., and Reeves, R. R. (2005). *Report of an International Workshop: Policy on Sound and Marine Mammals*. 28-30 September 2004, London, England. Marine Mammal Commission, Bethesda, Maryland, p. 129.

Wenz, G. M. (1962). "Acoustic ambient noise in the ocean: spectra and sources". *J. Acoust. Soc. Am.*, 34(12), 1936-1956. doi: 10.1121/1.1909155

Willis, H. F. (1941). *Underwater explosions: the time interval between successive explosions*. Technical report, British Report WA-47-21.

Widjiati, E., Djatmiko, E. B., Wardhana, W. and Wirawan (2012). "Measurement of propeller-induced cavitation noise for ship identification". *Acoustics 2012, 14-18 May, Hong Kong, China*. doi: 10.1121/1.4709183

Wyatt, R. (2008). *Joint Industry Programme on Sound and Marine Life/ Review of existing data on underwater sounds produced by the oil and gas industry, issue 1*. Seiche Measurements Ltd., Rep. S186, p. 110

Young, R.W. (1973). "Sound pressure in water from a source in air and vice versa". *J. Acoust. Soc. Am.*, 53(6), 1708-1716. doi: 10.1121/1.1913524

Zykov, M., Deveau, T., and Racca, R. (2013). *South Stream Pipeeline -Bulgarian Sector – Underwater Sound Analysis*. JASCO Technical Report P001226-004/00710, ver. 1.0.

A.I Other Sounds

The current appendix includes three tables with data from measurements made on acoustic sources that are not related to the oil and gas industry. The tables contain information on military, industrial, natural and biological sounds.

Table A.1 Sounds produced by military and industrial acoustic sources

Source (*Model*)	SL [dB re 1µPa@1m]	Signal Characteristics	Description	Reference
Underwater Nuclear Device	328 dB_{rms}	τ = 1000 s	30 kt charge	IACMST, 2006
Ship Shock Trial	304 dB_{rms}	τ = 2 s FR_{-10dB} = 0.5-50 Hz	4.5 t charge	Hildebrand, 2009; IACMST, 2006
Torpedo (*MK-46*)	289 dB_{rms}	FR_{-10dB} = 10-200 Hz	44 kg explosive	Hildebrand, 2009
Military Sonar (*SURTASS/LFA*)	235 dB_{rms} 215 dB_{rms} [a]	τ = 6-100 s DC = 10 % FR_{-10dB} = 100-500 Hz Peak frequency 250 Hz Beam width 30° x 360°	[a] Level emitted by one projector (the system uses a vertical array of typically 18 projectors)	Hildebrand, 2009; IACMST, 2006; ICES, 2005
Military Sonar (*AN/SQS 53A-C*)	235 dB_{rms}	τ = 0.5-2 s DC = 6 % f = 2.6,3.3 kHz	N/A	IACMST, 2006; D'Amico & Pittenger, 2009
Military Sonar (*AN/SQS 56*)	223 dB_{rms}	τ = 1 - 2 s f = 6.8, 7.5, 8.2 kHz	N/A	D'Amico & Pittenger, 2009
Research Sonar (ATOC)	195 dB_{rms}	τ = 1200 s DC = 8 % BW_{-10dB} = 37.5 Hz Peak frequency 75 Hz	N/A	IACMST, 2006; Richardson et al, 1995; D'Amico & Pittenger, 2009
Research Sonar (*RAFOS float*)	195 dB_{rms}	τ = 120 s DC = small BW_{-10dB} = 100 Hz Peak frequency 250 Hz	N/A	IACMST, 2006
Military Sonar (Search and Surveillance)	> 230 dB_{rms}	τ = 4-1000 s Peak frequency 2-57 kHz	N/A	Richardson et al, 1995
Military Sonar (Mine Avoidance)	> 220 dB_{rms}	τ = 1-30 s Peak frequency 25-500 kHz	N/A	Richardson et al, 1995
Tidal Farm	165-175 dB_{rms}	Continuous noise	N/A	Cluster Maritime Français, 2014
Wind Farm	142 dB_{rms}	Continuous noise	Main energy 30-200 Hz	Cluster Maritime Français, 2014
	137 dB_{rms} @ 312 Hz [a]	Continuous noise	[a] TL = $15\log_{10}r$ assumed *by reviewer* (measurement 111 dB_{rms} @ 50 m, 312 Hz)	Fristedt et al., 2001

Table A.2 Sounds produced by natural events

Source	SL [dB re 1µPa@1m]	Description	Reference
Undersea Earthquake	272 dB_{rms}	Magnitude 4.0 on Richter scale Energy integrated over 50 Hz bandwith	Heathershaw et al, 2001
Seafloor Volcanic Eruption	255 dB_{rms}	Massive steam explosion	Heathershaw et al, 2001
Lighning Strike on Sea Surface	250 dB_{rms}	N/A	Heathershaw et al, 2001

Table A.3 Sounds produced by cetaceans

Species (*scientific name*)	Vocalisation	SL [dB re 1µPa@1m]	Frequency Range [Hz]		Reference
			Overall	Dominant	
Bowhead Whale (*Balaena mysticetus*)	tonal moans	128-178 dB_{rms}	25-900	100-400	Richardson et al, 1995
	pulses	152-185 dB_{rms}	25-3.5k	N/A	
	song	158-189 dB_{rms}	20-500	< 4k	
S Right Whale (*Eubalaena australis*)	pulses	172-187 dB_{rms}	30-2.2k	160-500	Richardson et al, 1995
Gray Whale (*Eschrichtius robustus*)	moans	185 dB_{rms}	20-1.2k	20-200, 700-1.2k	Richardson et al, 1995
Humpback Whale (*Megaptera novaeangliae*)	song	144-174 dB_{rms}	30-8k	120-4k	Richardson et al, 1995
	shrieks	179-181 dB_{rms}	N/A	750-1.8k	
	horn blasts	181-185 dB_{rms}	N/A	410-420	
	moans	175 dB_{rms}	20-1.8k	35-360	
	grunts	190 dB_{rms}	25-1.9k	N/A	
	pulse trains	179-181 dB_{rms}	25-1.25k	25-80	
	underwater blows	158 dB_{rms}	100-2k	N/A	
	fluke & flipper slap	183-192 dB_{rms}	30-1.2k	N/A	
Fin Whale (*Balaenoptera physalus*)	moans, downsweeps	160-186 dB_{rms}	14-118	20	Richardson et al, 1995
	moans, tones, upsweeps	155-165 dB_{rms}	30-750	N/A	
Blue Whale (*Balaenoptera musculus*)	moans	188 dB_{rms}	12-390	16-25	Richardson et al, 1995
Bryde's Whale (*Balaenoptera brydei*)	moans	152-174 dB_{rms}	70-245	124-132	Richardson et al, 1995
Minke Whale (*Balaenoptera acutorostrata*)	downsweep	165 dB_{rms}	60-130	N/A	Richardson et al, 1995
	moans, grunts	151-175 dB_{rms}	60-140	60-140	
	moans, grunts	151 dB_{rms}	3.3k-20k	< 12k	
Sperm Whale (*Physeter macrocephalus*)	clicks	160-180 dB_{rms}	100-30k	2k-4k, 10k-16k	Richardson et al, 1995
Killer Whale (*Orcinus orca*)	pulsed calls	160 dB_{rms}	500-25k	1k-6k	Richardson et al, 1995
Bottlenose Dolphin (*Tursiops truncatus*)	whistles	125-173 dB_{rms}	800-24k	3.5k-14.5k	Richardson et al, 1995

A.II Noise & Absorption in Sea Water

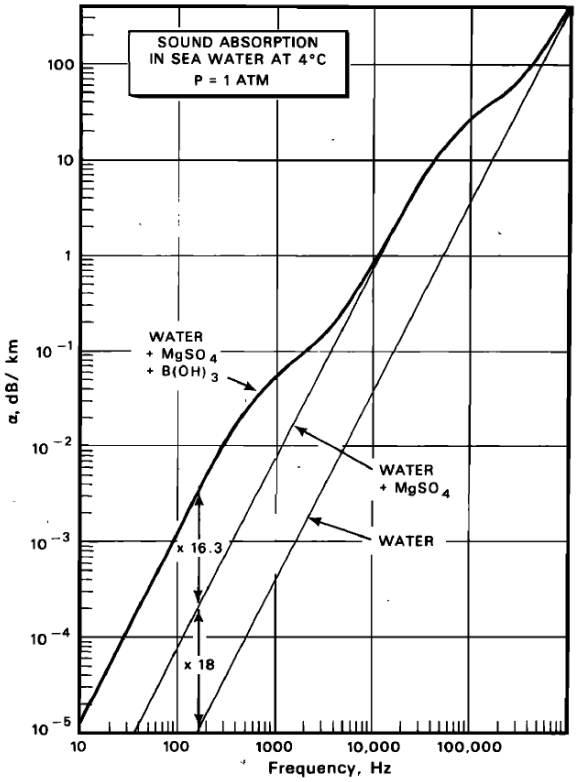

Figure A.1 Absorption coefficient in sea water at 4 °C, 1 atm, salinity 35 ppt and pH 8.0 (from Fisher & Simmons, 1977).

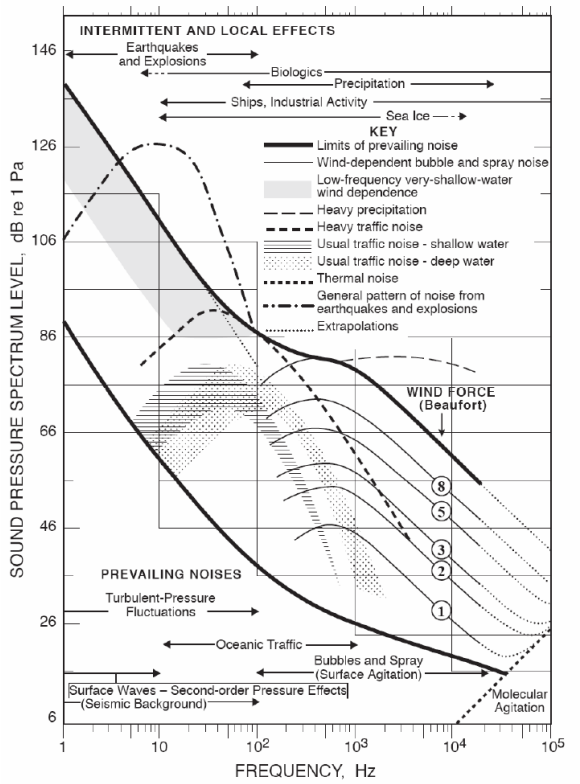

Figure A.2 Composite of ambient noise spectra. An estimate of the expected ambient noise can be obtained by selecting the pertinent combination of ambient noise components (from Wenz, 1962).

A.III Photos from Vessels

Cruise Ships

Figure A.3 Cruise ship *Dawn Princess* (from wikipedia.org)

Figure A.4 Cruise ship *Norwegian Sky* (from wikipedia.org)

Figure A.5 Cruise ship *Holland America Statendam* (from wikipedia.org)

Figure A.6 Cruise ship *Norwegian Wind* (from Kipple, 2000).

Figure A.7 Cruise ship *Crystal Harmony* (from Kipple, 2000).

Figure A.8 Cruise ship *Universe Explorer* (from www.ssmaritime.com).

Bulk Carriers

Figure A.9 Bulk Carrier *Overseas Harriette* (from www.shipspotting.com).

Figure A.10 Bulk Carrier *Peter R. Cresswell* (from www.marinetraffic.com).

Figure A.11 Bulk Carrier *Emerald Bulker* (from www.shipspotting.com).

Figure A.12 Bulk Carrier *Golden Ace*, MMSI 576915000 (from www.shipsnostalgia.com).

Figure A.13 Bulk Carrier *Red Lotus*, MMSI 371978000 (from www.marinetraffic.com).

Figure A.14 Bulk Carrier *Pansolar*, MMSI 240537000 (from www.shipspotting.com).

Figure A.15 Bulk Carrier *Fortune Era*, MMSI 440223000 (from www.marinetraffic.com).

Open Hatch Cargo

Figure A.16 Open hatch cargo *Saga Frontier*, MMSI 477657600 (from www.marinetraffic.com).

Figure A.17 Open hatch cargo *Star Grip*, MMSI 257313000 (from www.marinetraffic.com).

Figure A.18 Open hatch cargo *San Sebastian*, MMSI 477653500 (from www.marinetraffic.com).

Figure A.19 Open hatch cargo *Hardanger*, MMSI 563496000 (from www.marinetraffic.com).

Container Ships

Figure A.20 Container ship *CSL Virginia*, MMSI 636090869 (from www.shipspotting.com).

Figure A.21 Container ship *Ever Reward*, MMSI 352919000 (from www.marinetraffic.com).

Figure A.22 Container ship *Halifax*, MMSI 235007500 (from www.vesselfinder.com).

Figure A.23 Container ship *MOL Express*, MMSI 353287000 (from www.shipspotting.com).

Vehicle Carriers

Figure A.24 Vehicle carrier *Dong Fang Gao Su*, MMSI 413075000 (from www.fleetmon.com).

Figure A.25 Vehicle carrier *Heijin*, MMSI 353788000 (from www.marinetraffic.com).

Figure A.26 Vehicle carrier *Liberty*, MMSI 232872000 (from www.marinetraffic.com).

Figure A.27 Vehicle carrier *United Spirit*, MMSI 636011280 (from www.marinetraffic.com).

Tankers

Figure A.28 Crude oil tanker *NS Century*, MMSI 636012853 (from www.marinetraffic.com).

Figure A.29 Crude oil tanker *Chemtrans Sky*, MMSI 636090885 (from www.marinetraffic.com).

Figure A.30 Oil products tanker *Star Express*, MMSI 371604000 (from www.marinetraffic.com).

Figure A.31 Oil products tanker *Nave Ariadne*, MMSI 319768000 (from www.marinetraffic.com).

Figure A.32 Oil products tanker *Yayoi Express*, MMSI 371924000 (from www.marinetraffic.com).

Figure A.33 Chemical tanker *Theresa Success*, MMSI 636010515 (from www.marinetraffic.com).

Medium-Size Vessels

Figure A.34 Research vessel *Gilavar* (from Funk et al., 2008).

Figure A.35 Survey vessel *Geo Arctic* (from Beland et al., 2013).

Figure A.36 Survey vessel *Mt Mitchell* (from Reiser et al., 2010).

Figure A.37 Survey vessel *Gulf Provider* (from Funk et al., 2008).

Figure A.38 Survey vessel *Mt Mitchell* (from Funk et al., 2008).

Figure A.39 Survey vessel *Alpha Helix* (from Funk et al., 2008).

Figure A.40 Survey vessel *Peregrine* (from Aerts et al., 2008).

Figure A.41 Rig tender ship *Pacific Ariki* (from www.marinetraffic.com).

Figure A.42 Pusher tug *henry Christoffersen* (from Funk et al., 2008).

Figure A.43 Landing craft *Arctic Wolf* (from Aerts et al., 2008).

Figure A.44 Support vessel *Torsvik* (from Funk et al., 2008).

Figure A.45 Support vessel *Norseman II* (from Funk et al., 2008).

Figure A.46 Support vessel *Theresa Marie* (from Funk et al., 2008).

Figure A.47 Bathymetric survey boat *American Islander* (from Funk et al., 2008).

Icebreakers

Figure A.48 Icebreaker *Polar Prince* (from Beland et al., 2013).

Figure A.49 Icebreaker *Jim Kilabuk* (from Funk et al., 2008).

Small Vessels, Boats and Hovercrafts

Figure A.50 Survey vessel *Hook Point* (3rd from left, from Aerts et al., 2008).

Figure A.51 Tug vessel *Alaganik* with *Hook Point* boat (from Aerts et al., 2008).

Figure A.52 Survey vessel *Wiley Gunner* (from Hauser et al., 2008).

Figure A.53 Crew vessel *American Discovery* (from Hauser et al., 2008).

Figure A.54 Landing craft *Maxime* (from Funk et al., 2008).

Figure A.55 Crew vessel *Qayaq Spirit* (from Aerts et al., 2008).

Figure A.56 Crew vessel *Gwydyr Bay* (from Aerts et al., 2008).

Figure A.57 Support vessel *Mariah B* (from Aerts et al., 2008).

Figure A.58 Bow picker *Rumple Minze* (from Aerts et al., 2008).

Figure A.59 Bow picker *Canvasback* (from Aerts et al., 2008).

Figure A.60 From left to right: crew vessel *Qayaq Spirit*, support vessel *Mariah B*, and bowpickers *Cape Fear*, *Rumple* Minze, Canvasback and *Sleep Robber* (from Aerts et al., 2008).

Figure A.61 Bow picker *Sleep Robber* (from Aerts et al., 2008).

Figure A.62 Inflatable boat *DIB* (from Hauser et al., 2008).

Figure A.63 Aluminium boat *Reliance* (from Hauser et al., 2008).

Figure A.64 Jet boat *Storm Warning* (from McPherson & Warner et al., 2012).

Figure A.65 Jet boat *Resolution* (from McPherson & Warner, 2012).

Figure A.66 Propeller boat *Margarita* (from McPherson & Warner, 2012).

Figure A.67 Cabin cruiser *Serac* (from Kipple & Gabriele, 2003).

Figure A.68 Cabin cruiser *Talus* (from Kipple & Gabriele, 2003).

Figure A.69 Landing craft *Capelin* (from Kipple & Gabriele, 2003).

Figure A.70 Cabin workboat *Sigma T* (from Kipple & Gabriele, 2003).

Figure A.71 Cabin cruiser *Arete* (from Kipple & Gabriele, 2003).

Figure A.72 Cabin cruiser *Rebound* (from Kipple & Gabriele, 2003).

Figure A.73 Open skiff *Sand Lance* (from Kipple & Gabriele, 2003).

Figure A.74 Open skiff *Mussel* (from Kipple & Gabriele, 2003).

Figure A.75 Open skiff *Ogive* (from Kipple & Gabriele, 2003).

Figure A.76 Open skiff *Gumboot* (from Kipple & Gabriele, 2003).

Figure A.77 Open skiff *Alaria* (from Kipple & Gabriele, 2003).

Figure A.78 Open skiff *Ursa* (from Kipple & Gabriele, 2003).

Figure A.79 Hovercraft *Griffon 2000TD* (from wikipedia.org).

Contact us

General enquiries

info@soundandmarinelife.org

Media enquiries

press@soundandmarinelife.org
+44 (0) 20 7413 3416

E&P **SOUND & MARINE LIFE** PROGRAMME